FRACTURE OF METALS

ProQuest LLC.
789 East Eisenhower Parkway
P.O. Box 1346
Ann Arbor, MI 48106 – 1346

THESIS

presented to

THE UNIVERSITY OF GLASGOW

for the Degree of

DOCTOR OF PHILOSOPHY

by

ARCHIBALD VETTERS, B.Sc.,A.R.C.S.T.

June, 1961

A C K N O W L E D G E M E N T S

The author wishes to thank Professor E.C.Ellwood for his advice and encouragement while this work was being carried out, and Dr. J. MacLeod for the interest he has shown. He also wishes to acknowledge the generous co-operation of Mr. J.W. Sharpe of the Department of Natural Philosophy with the electron microscope studies.

The work for this thesis was carried out in the Department of Metallurgy and the author would like to express his gratitude for the facilities provided by the members of this Department.

C O N T E N T S

CHAPTER 1

Introduction

Scope of Work 4

Section A A 1 Definition of Internal Friction 5

A 2 Measurement of Internal Friction 6

A 3 Sources of Internal Friction.

(1) The Thermoelastic Effect 10

(2) Grain Boundary Viscosity 11

(3) Stress Induced Ordering 12

(4) Dislocation Internal Friction 15

(5) Magnetoelastic Internal Friction 20

(6) Electron Damping 21

Section B Point Defects of Low Temperature Properties of Metals

B 1 Production of Point Defects 23

B 2 Thermal Annealing of Point Defects 26

Section C. The Effect of Internal Oxidation on the Properties of a Metal 33

Section S. The Effect on the Properties of Iron of Interstitial Elements 38

CHAPTER 2	Apparatus	
	Description of Apparatus	41
	Crystal Arrangement	45
	Calibration of Apparatus	46
	Calibration of Crystals	47
	Calculation of Strain in Specimens	48
	Effect of Support Position	53
	Conclusions	55
	Annealing Process	57
CHAPTER 3	The Effect of Deformation on Oxygen Free High Conductivity Copper	
	(1) Tensile Elongation	60
	(2) Quenching	69
	(3) Discussion	72
CHAPTER 4	The Recovery of Internal Friction in Aluminium after Deformation	78
	Results	
	(1) 99.99% Aluminium	79
	(2) 99.999% Aluminium	81
	(3) Quenching and Elongation	82
	Discussion	83
	Conclusions	86

CHAPTER 5	The Effect of Deformation on Nickel	87
	(1) Recovery after Elongation	88
	(2) Recovery after Fatigue	90
	(3) Recover y after Quenching	91
	Discussion	93
CHAPTER 6	Self Diffusion in Silver	94
	(a) Quenched from 810°C	95
	(b) Quenched from 910°C	95
	Discussion	96
CHAPTER 7	Analysis of Diffusion Results	98
CHAPTER 8	The Effect of Internal Oxidation on Copper Alloys	
	Experimental Methods and Results	104
	Conclusions	112
CHAPTER 9	Movements in Iron	
	(a) Point Defect Movement	113
	(b) Nitrogen Movement	115
	(1) Rate of Decrease of Anelastic Peak	117
	(2) Shift of Peak	119
	(3) Dislocation Internal Friction	120
CHAPTER 10	Torsion Pendulum Results	124
	GENERAL CONCLUSIONS	128

CHAPTER 1

Introduction

Scope of Work

Section A A 1 Definition of Internal Friction

A 2 Measurement of Internal Friction

A 3 Sources of Internal Friction

(1) The Thermoelastic Effect

(2) Grain Boundary Viscosity

(3) Stress Induced Ordering

(4) Dislocation Internal Friction

(5) Magnetoelastic Internal Friction

(6) Electron Damping

Section B Point Defects of Low Temperature Properties of Metals

B 1 Production of Point Defects

B 2 Thermal Annealing of Point Defects

Section C The Effect of Internal Oxidation on the Properties of a Metal

Section D The Effect on the Properties of Iron on Interstitial Elements

INTRODUCTION

Scope of Work.- This thesis was based on the investigation of the initial stages of deformation mainly by an internal friction technique. For this reason it is useful to consider at this stage the nature and scope of internal friction and its measurement. As the deformation of face centred cubic metals gives rise to the diffusion of point defects, it is also of interest to study the effects of point defects on the properties of a metal

In the department in the past, some interest had been shown in internal oxidation as a means of altering the impurity concentration in a solid solution alloy and producing controlled precipitates. It was therefore decided to pursue this field a little further and a brief description of the properties of internally oxidised alloys is included.

As it would be very desirable to extend the field of investigation to body centred cubic metals and as other effects due to impurities intrude, it is convenient to examine the effects of interstitial atoms.

SECTION A

INTERNAL FRICTION

A.1. Internal friction may be defined as that property of a solid which converts its mechanical vibrational energy into heat. Several sources of internal friction are known and some of them which are well understood were described by Zener[1]. At present several different methods of defining internal friction are in use and the main ones are listed below.

(1) The Logarithmic Decrement

The fractional decrease in vibrational amplitude per cycle is called the logarithmic decrement Δ. This is related to the engineering term of damping per cent as

$$D\% = 200\,\Delta$$

If δW is the fractional energy dissipated per cycle then

$$\Delta = \frac{\delta W}{2 W}$$

(2) Resonance Width Factor Q^{-1}

One of the most useful research methods of measuring internal friction is to observe the width of the resonant peak of a specimen in free vibration

$$\frac{1}{Q} = \frac{V_2 - V_1}{Vr}$$

Where Vr = resonant frequency and V_1 and V_2 the frequencies at

which the amplitude has fallen to $1/\sqrt{2}$ of the amplitude at Vr. Often the more convenient method is to measure the frequencies V_3 and V_4 at which the amplitude has fallen to one half that at Vr, and then

$$\frac{1}{Q} = \frac{\pi}{\sqrt{3}} \frac{V_4 - V_3}{Vr}$$

(3) Ultrasonic Attenuation

The attenuation of an ultrasonic wave passing through a solid can be measured and is a measure of the internal friction of that solid. If A is the attenuation and V the velocity of the wave in the solid, F being its frequency then

$$\Delta = \frac{AV}{F}$$

The full relationships may be listed as.

$$= \frac{1}{\sqrt{3}} \quad \frac{V_4 - V_3}{Vr} = \frac{\delta W}{2W} = \frac{AV}{F} = \frac{\text{Damp. Cap.}\%}{200} = \frac{\pi}{Q}$$

A.2. Methods of Measurement

The method used in the measurement of internal friction depends largely on the frequency at which one wishes to make the measurement.

(1) $1 - 10^2$ cycles/second

In this range a torsion pendulum is normally used of the type described by Ke[2]. In this apparatus the specimen is in the form of a suspended wire with a cross beam inertia member

attached to its bottom end. The vibrations are initially induced by a magnetic method. Recording is normally achieved by an optical method either photographically or photo-electrically. The maximum strain amplitude induced in the apparatus is usually of the order of 10^{-5} and as the specimen is in torsion the stress varies from zero at the centre of the wire to a maximum at the surface. A static tensile stress is produced on the specimen due to the weight of the cross beam. While this is not normally considered very important it is possible to invert the apparatus and suspend the beam from an inertia free support, Norton[3].

The torsion pendulum tends to have a rather high apparatus damping often of the order of 10^{-4} and thus may be unsuitable for measurements of low internal friction materials. It is quite possible to arrange the apparatus to work under vacuum and this reduces its apparatus damping. The strain amplitude used cannot easily be varied over a useful range and this tends to limit the usefulness of the apparatus. The frequency of measurement is however easily changed by altering the inertia of the cross beam and the apparatus finds its main application where frequency dependent rather than amplitude dependent phenomena are studied.

(2) 10^2 - 10^4 cycles/second.

This is probably the most used frequency range and normally the specimen is in the form of a rod or bar which is induced to vibrate in one of its normal modes of vibration without the use of an inertia member. The specimen may be driven in several different ways. Quimby[21] introduced the piezoelectric method which used quartz crystal cemented to the specimen. The crystal is usually matched to the frequency of the specimen. A second crystal is often fitted to the other end of the specimen to act as a gauge. An electrostatic method[22] has been used to excite and detect the vibrations in the specimen by using its end as one plate of a capacitor. Vibration can also be induced by eddy current methods or by placing a small magnet[23] at the end of the specimen. A nickel transducer may also be used, one end of a nickel wire being attached to the specimen.

Förster[24] introduced a method in which a bar specimen was supported horizontally by threads or wires at points a little removed from the nodes. The specimen is excited in transverse vibration by electromagnetic or piezoelectric devices at the top of one of the support threads. The other thread is connected to a similar device which serves to detect the vibration of the

specimen. By suitable choice of driving devices a very wide range of strain amplitudes can easily be obtained (for example 10^{-10} to 10^{-3} from a piezoelectric driver). It is important to note that damping can arise from the fact that the support threads are not placed at the nodes but these losses can easily be calculated and are normally of little importance.

If it is intended to study amplitude dependent phenomena it is most important to consider the stress systems in the various modes of vibration. With longitudinal vibrations the specimen is stressed evenly across its diameter but not along its length. In transverse vibration the stress system is rather involved and varies along the length as well as across the diameter of the specimen. A point to note however is that the strain in transverse vibration can be measured by a microscopic technique while this may not be possible for longitudinal vibrations. A disadvantage of the above methods is that the frequency used is generally restricted to the fundamental resonant frequency and to one or two harmonics.

(3) 10^{6} - 10^{8} cycles/second.

In this range ultrasonic pulse methods are used. A pulse is introduced at the end of the specimen by a crystal and the internal friction measured by observing its attenuation as it passes through

the material. Stresses achieved are very low and no useful amplitude dependent measurements can be made but the frequency is readily changed. Difficulties arise in interpretation because of the curvature of the wave front and this has to be accounted for.

(4) 10^{12} cycle/second

It is possible that measurements could be made by means of thermal conductivity or diffuse X-ray measurements at this frequency but this does not appear to have been done yet.

A.3. Sources of Internal Friction

In a metal internal friction can arise from a number of largely independent sources. The common ones are listed below.

(1) The thermoelastic effect

(2) Grain boundary viscosity

(3) Stress induced ordering

(4) Internal friction due to dislocations

(5) Magnetoelastic effects

(6) Electronic damping

(1) The Thermoelastic Effect

When a metal is stressed its temperature changes and if it is stressed unevenly there will tend to be a flow of heat. Under a vibrational stress there tends to be a flow of heat back and forth

across the specimen. At very high frequencies of vibration there is insufficient time for appreciable heat to flow and the process is adiabatic and does not give rise to internal friction. At very low frequencies on the other hand complete thermal equilibrium is established and the process is isothermal and does not cause any internal friction. At one intermediate frequency however the period of the applied stress is comparable with the time required for heat flow. Zener[1] calculated the effect to give a relaxation time

$$\tau = \frac{d^2}{DC}$$

where d = thickness of specimen
and DC = $\frac{\text{thermal conductivity}}{(\text{spec. heat})\ (\text{density})}$

Thermoelastic internal friction can arise from both specimen dimensions and in a polycrystalline material from relaxation across the grains.

The internal friction from this source can be quite high and it is important that it should be considered. Very often it is desirable to adjust the grain size of the material to avoid internal friction from this source.

(2) Grain boundary viscosity

At relatively high temperatures in a polycrystalline material a viscous-like dissipation of energy can occur at the grain boundaries. Ke showed that the internal friction could be expressed as a function

$$\text{grain size} \times \text{frequency} \times e^{E/RT}$$

where E was about 1·5 ev.

Grain boundary relaxation peaks have been found in a large number of metals[25]. The exact shape of the relaxation peak depends on the grain size distribution.

(3) Stress Induced Ordering.

A metal may contain interstitial impurity atoms in ordered or random positions when it is unstrained. If when it is strained the interstitial atoms become either disordered or ordered, then an internal friction peak may be found. Zener showed that the relaxation time τ for the internal friction peak was related to the frequency f by the relationship

$$\frac{1}{\tau} = \alpha f \quad \text{where } \alpha \text{ is a constant}$$

The internal frequency peak is found when

$$\omega\tau = 1 \quad \text{where } \omega \text{ is the angular frequency of vibration } (2\pi f)$$

The diffusion coefficient D for the movement of the interstitial atoms in the purest metal is given by

$$D = \beta a^2 f \qquad \begin{array}{l} a \text{ is the lattice parameter} \\ \beta \text{ is a constant} \end{array}$$

Thus it is possible by determining the temperature and frequency of the internal friction peak to calculate the diffusion coefficient

$$D = Do\ e^{-E/RT} \quad \text{where E is the activation energy}$$

The ease with which diffusion data can be obtained at low temperature is the great advantage in using this type of internal friction.

The most extensive study of stress induced ordering has

been carried out in the B.C.C. metals and the diffusion of carbon and nitrogen in α iron has been widely investigated. Snoek[4] showed that the interstitial atoms took up positions at the cell edges and at the face centres. Under zero stress a random distribution of interstitial atoms occurs but on the application of a stress they go to ordered positions. The height of the internal friction peak is proportional to the quantity of interstitial in solution[26]. The height of the peak is also dependent upon the crystallographic axis along which the stress is applied. If, as is the case with carbon and nitrogen in iron, the metal can be made supersaturated with an interstitial, an ageing process can be followed. If the internal friction is measured in a torsion pendulum at about 1 c/s then the internal friction peaks due to carbon and nitrogen occur at 20 - 30°C. Little or no precipitation takes place at these temperatures and internal friction measurements may be made after successive temperings. If on the other hand the internal friction is measured at 1000 - 3000 c/s then the peak temperatures are about 100 - 150°C and at these temperatures it is possible that the ageing will proceed too quickly to be followed.

The equation relating peak temperature and frequency is

$\tau = \tau_0 e^{-E/RT}$, τ_0 being a constant

Wert and Zener[5] gave the constants for this equation for carbon and nitrogen in α iron

	C.	N
γ_0^{-1} (10^{13} cm^{-1})	23	3·7
E cals/mol	19,800	17,700

From the above equation it is possible, if the values of γ (or peak frequency) are known at different temperatures, to calculate E. However it is not always convenient to change the frequency and there is an alternative method of calculation using the decrease of the peak height with time. Cottrell and Beilby[6] showed that

$$Nt = 3\left(\frac{\pi}{2}\right)^{1/3} No \; L\left(\frac{A\,Dt}{KT}\right)^{3/3}$$

where Nc = number of solute atoms per unit volume which have migrated to the dislocations after time t

No = original concentration of solute atoms

D = diffusion coefficient

L = length of edge dislocation per unit volume.

Harper modified this expression to account for the mutual interaction of the solute atoms and gave

$$\ln(1 - \varphi) = 3\left(\frac{\pi}{2}\right)^{1/3} \; L\left(\frac{ADt}{KT}\right)^{3/3}$$

where φ is the fraction of solute precipitated after time t. This equation was shown to hold for large amounts of precipitation. One important feature of this equation is that it allows a calculation of the dislocation density. The calculations which

have been done are in fair agreement with other work.

(4) Internal friction due to dislocations.

In a pure metal the internal friction due to dislocations is amplitude dependant above a certain stress. Below this stress it is amplitude independent and it is usual to separate the dislocation internal friction into two parts as

$$\Delta = \Delta_I + \Delta_H$$

where Δ_I is the amplitude independent internal friction and Δ_H is the amplitude dependent internal friction.

Theories of dislocation internal friction.

It is generally agreed that the internal friction arises from the movement of dislocations and the problem resolves to finding a mechanism to explain the impedance of the dislocation lines. Mason[7] used a Peierl's valley mechanism and Seeger modified this but has not worked out completely his theory. Interaction with other dislocations is a possible explanation and was discussed by Weertman and Koehler[8]. Impurity atoms have been used in two explanations. Weertman and Salkovitz[9] used the Mott-Nabarro theory of dislocation movement in a solid solution. Foreign atoms cause a stress field of wavelength $\lambda = \frac{a}{\sqrt{c}}$ where a is the atomic spacing and c the concentration of impurity atoms. When the stress peak was overcome the dislocation moved forward a distance λ. However this theory does not appear to agree with the experimental results.

Koehler proposed that the dislocations vibrate in loops between the pinning points of the impurity atoms rather as a stretched string would do. It is possible to explain amplitude dependent damping as the tearing away from the pinning points in this thoery. Granato and Luke[10] expanded this theory, and gave as a model a dislocation pinned at its ends by the network dislocations and at various points along its length by impurity atoms.

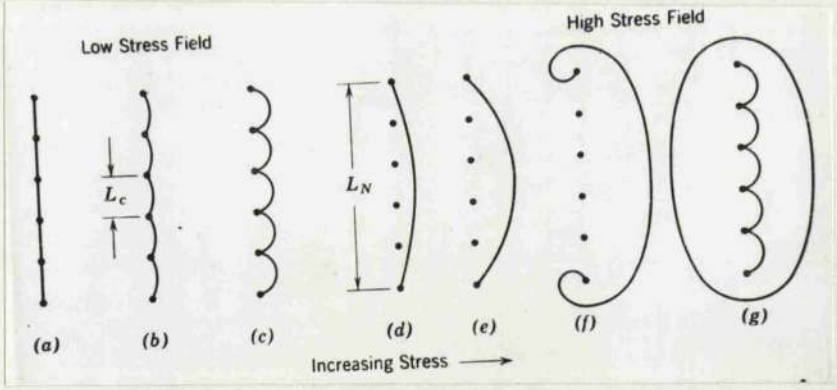

The number of impurity pinning points is governed by

$$\frac{a}{L_c} = C_0 e^{\frac{Q}{KT}}$$

Q = Cottrell interaction energy

C_0= concentration of impurity atoms

They showed that

$$\Delta_I = \frac{\Omega \Lambda L^4 \beta \omega \tau_1}{\pi^3 C}$$

where Ω is a concentration factor

$t_1 = 120$

This describes the amplitude independent loss due to the dislocations and assumes that the dislocation line does not tearaway from the pinning points. Under a sufficiently high stress the tear

away takes place as in the above diagram and leads to an amplitude dependent loss. The description of this loss was given by Granato and Luke[10].

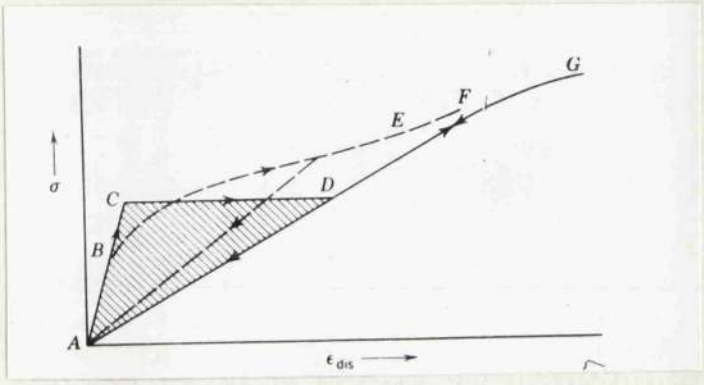

The argument was of the form that the critical stress for tearing away depended upon the loop length

$$\varepsilon_c = \frac{Q}{\omega^2 l} \qquad \varepsilon_c = \text{critical stress}$$

After breaking away from the pinning point the dislocation returned by a different path and the energy loss was given by the shaded area in the diagram

$$\Delta_H = \frac{\Omega \, l \, L n^3 K \eta a}{\pi^2 L_c^2 \varepsilon_0} \, e^{\frac{-K\eta a}{L_c \varepsilon_0}}$$

It is convenient to note that from the above relationship s

$$\Delta_I \propto L_c^4 \;, \quad \Delta_H \propto \frac{1}{L_c^2} \quad \text{and} \quad \varepsilon_c \propto \frac{1}{L_c}$$

Experimental evidence has shown that the above theory is sound with regard to most of the parameters. It is much easier to examine the amplitude dependent part as it may easily be

separated from the other types of internal friction in experimental results.

A plot of $\log \Delta_H \varepsilon_0 / \frac{1}{\varepsilon_0}$ (ε_0 is the measuring stress) should be a straight line and very often this is in fact the case. However, as mentioned above, many types of apparatus do not strain the specimen evenly and amplitude dependant results are difficult to assess.

The effect of impurity concentration has been measured by Wiertman and Salkovitz[9] for lead containing bismuth, and by Besters[11] for copper containing gold. The effect of impurities in α iron was measured by Robertson and Rawlings[12]. The influence of dislocation density was measured in copper by Read[13] and the results are taken to be in agreement with the theory.

The amplitude independant internal friction is rather difficult to assess. This is due to the fact that other types of internal friction in the material are also independant of amplitude and may be difficult to estimate. The main confirmation of the Granato and Luke theory for ΔI comes from the irradiation results of Thomson and Holmes,[14] who showed that the decrement was proportional to L^4.

One of the more useful derivations of the Granato and Luke theory concerns the time dependant effects when the number

of point defects becomes out of equilibrium with the dislocation line. This situation arises after almost any cold working process or after quenching from near the melting point. The analysis of this process was again done by Granato and Luke[15] who showed that the average loop length L is given by

$$\frac{1}{L} = \frac{1}{L_n} + \sum_{i=1}^{k} \frac{c_i}{a}$$

c_i = concentration of defects of the ith type
k = no defects types

Now if C_{10} is the number of vacancies and C_{20} the number of impurity atoms which are assumed not to be mobile at the temperature used.

In a F.C.C. metal

$$\Delta_H = A_1 \exp\left[-A_2 (C_{10}+C_{20})\{1+\beta t^{2/3}\}\right]$$

and $$\Delta_I = \frac{A_3 a^4}{C_{10}+C_{20}} \cdot \frac{1}{(1+\beta t^{2/3})^4}$$

where $$\beta = \frac{C_{10}}{C_{10}+C_{20}} \cdot \frac{4\alpha}{a^2} \left(\frac{AD}{kT}\right)^{2/3}$$

$$A_1 = \frac{2.5 \Omega L_n^3}{\pi^2 L} \cdot \frac{K \eta a}{L \varepsilon_0} \left[1 - \frac{\pi \omega L_n^3}{a^2}\right]$$

$$A_2 = \frac{K \eta a}{30}$$

$$A_3 = \frac{120 \Omega \Lambda \beta \omega}{\pi^3 C}$$

Ω is an orientation factor Λ dislocation density

L_n network loop length L average loop length

K a parameter η Cotterell's misfit parameter

a lattice parameter ε_0 the strain amplitude

ω angular frequency A a parameter D Diffusion coefficient

It is possible from the above equations to calculate the activation energy for the movement of a point defect if the time and temperature variations of the A_{14} value can be measured. The above equations were extensively checked by the authors against independently obtained data[27,28] with very satisfactory results. However it was stated by Granato and Luke that the theory should only be applicable to high frequencies but there is now little doubt that it may be applied to quite low frequencies.

In conclusion it may be said that the above theories are by far the most satisfactory interpretation of dislocation damping in metals. However it should be recognised that they are not completely in agreement with all the experimental facts and possibly some slight modification is required.

(5) Magnetoelastic Internal Friction

It is well known that when a material is magnetised its length changes. Conversely, when it is stressed its magnetic properties change. There are three types of magnetoelastic internal friction.

(1) Macro-eddy currents.- This is very similar to thermoelastic internal friction because after stressing a diffusion of eddy currents takes place from the surface of the specimen. The process has a peak of the normal type but does not have a true relaxation time.

(2) Micro-eddy currents.- This arises from local

differences in domain magnetism and is in other respects similar to macro-eddy current damping.

(3) Magnetoelastic static hysteresis:- At low frequencies eddy current losses disappear as the rate of change of magnetisation is very small but a hysteresis loss can be set up. This loss is frequency independent but amplitude dependent. Boulanger[16] discussed this type of damping in detail.

(6) Electronic Damping:- At temperatures below 20°K the internal friction of a metal increases rapidly with falling temperature when the metal is in the normal condition. If, on the other hand, the metal becomes superconducting, the internal friction falls rapidly. Mason[17] gave as the explanation that the electron gas obtained some energy from the lattice vibrations in a viscous manner. Morse gave the explanation as a distortion of the Ferni surface by a sound wave.

In conclusion it can be said that internal friction measurements have several advantages in fundamental research on metals. ~~It is~~ THEY ARE more directly connected with the basic atomic process than other forms of examination. As described above many of the species of internal friction have been more or less convincingly explained and may be used as a tool in obtaining information on the basic physical properties of metals. The study of ageing and precipitation is by far the most rewarding

field for internal friction research as no other properties are so completely determined by the quantity of precipitation. Excellent reviews of the subject were given by Nowick[19] and Niblett and Wilks[20].

In the field of testing mechanical components internal friction measurements have been rather disappointing. Cracks and inclusions are very often only detected if they lie in certain positions in the specimen. It had at one time been hoped to determine the extent of fatigue damage by internal friction measurements but it was found that it did not change till immediately before failure.

SECTION B

Point Defects and the Low Temperature Properties of Metals

B.1 It is now generally agreed that many low temperature effects may be attributed to point defects. The most notable of these are changes in resistivity, yield point, the Koster effect, i.e. decrease with time of internal friction and the ageing of certain materials.

There are several methods of introducing point defects into a metal and it is convenient to discuss them separately.

(1) Point defects introduced by quenching: The equilibrium concentration of any type of point defect at any temperature T is given by

$$C = \exp \frac{-(\Delta H_f - T \Delta S_f)}{KT}$$ - Zener[29]

where ΔH_f = Heat of formation of defect

ΔS_f = Change in entropy

It is usual to assume that $\frac{\Delta S_f}{K}$ is of the order of unity and and by using the values of ΔH (obtained by calometric experiments usually) to calculate the defect concentration. Broom and Ham[30] gave the following table for copper:

	ΔH (ev)	300°K	800°K	1300°K
Vacancy	~1	10^{-17}	$10^{-6\cdot2}$	$10^{-3.9}$
Vacancy pair	~1·6	10^{-27}	10^{-10}	$10^{-6\cdot2}$
Interstitial	~4	10^{-67}	10^{-25}	10^{-15}

If the metal is annealed at high temperature and then rapidly quenched,most of the defects may be retained at room temperature. As the metal now contains a concentration of defects far in excess of the equilibrium concentration, migration effects are to be expected. Naturally the number of defects retained at low temperature will depend upon the severity of the quench. This depends both upon the quenching medium and the size and shape of the specimen. Both gas and liquid quenches are used and the specimen is often in the form of a thin wire or foil.

(2) Irradiation by atomic particles. The mechanism of vacancy introduction in a metal by neutron bombardment is thought to be that, when an atom is struck it obtains a very large q uantity of energy. This atom is displaced violently from its lattice position and displaces further atoms. The result of each such neutron collision is that 100 - 200 vacancy and interstitial pairs are formed in the area around the position of the neutron hit. The vacancies and interstitials will be formed in approximately equal numbers.

It has been known for some time that irradiation will considerably alter the properties of a metal. For example, a yield point is introduced into a F.C.C. metal and the deformation characteristics are altered. The ductile brittle transition temperature in steel is raised by bombardment.

(3) Formation of Point Defects by Cold Work.

Since the original experiments of Molenaar and Aarts, more data indicating that cold work can form point defects has become available. The mechanism of the point defect formation is not clear at present. The earlier theory was that two intersecting screw dislocations were capable of producing vacancies. However, Friedel[31] has pointed out that this is not likely. An alternative system has been proposed making use of a dislocation loop containing two jog components.

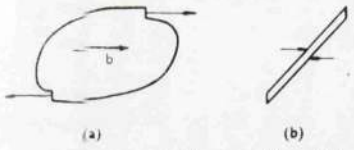

Fig. 10.—Jogs on a Dislocation Ring with a Burgers Vector b. If the ring is expanding, diagram (*a*), the jogs can glide in the direction shown without making point defects. But if the ring is contracting, a stage is reached, diagram (*b*), at which a line of point defects can form.

In the expanding condition no point defects are formed but during unloading when the ring gets to stage (b) it will disappear leaving a line of point defects between the two jogs.

Friedel[31] postulated a process using two Frank-Reid sources in adjacent planes. These are thought to coalesce at the end of each cycle of operation to form a line of point

defects. He calculated that

$$C \simeq 10^{-5}\varepsilon$$ (C = concentration of defects and ε = strain)

This result is comparable with the values of

$$C = 10^{-4}\varepsilon$$

given by Seitz[32] and Mott[33]. On the other hand, Von Buren and Jongenburger[34] gave

$$C \propto \varepsilon^{\frac{2}{3}}$$

and Blewitt[35] observed a parabolic increase in single crystals.

(4) Introduction of Vacancies by Non-Stoichiometry:

In certain intermetallic compounds vacancies are sometimes formed in order that the electron/unit cell ratio may be maintained. The properties of these alloys are not really understood at present.

B.2 Thermal Annealing of Point Defects

The vacancies and other point defects are normally formed in the metal in a more or less random manner. There is reason to believe that in random distribution they do not harden the material. It is as well to note that the electrical resistivity is increased by randomly dispersed defects.

The defects in excess of the equilibrium concentration will, if the thermal conditions are satisfactory, diffuse to the sinks available to them. These sinks can be either free surfaces grain boundaries, or dislocations. Naturally in a fairly coarse

grained material the vast majority of the defects will reach the dislocations and it is these which cause most of the observed changes in properties during annealing.

It was suggested by Friedel[31] that the vacancies were not annihilated at the dislocations but are retained there in the area round the dislocation line. However, this theory does not appear to be fully acceptable as some work on quenched wires has shown that the length decreases with its electrical resistivity[36]. This indicates that there was in fact a loss of vacancies in the process. Maddin and Cottrell[37] gave as a more probable interpretation that the dislocation line was in fact broken up by jog formation and this leads to hardening.

The mechanism of the movement of the defect is of the utmost importance in the interpretation of the phenomenon. It is generally accepted that

$$E_D = E_F + E_M$$

where E_F = energy of formation of vacancy
E_D = energy of diffusion of vacancy.

It is normal to measure the life of a defect in terms of the number of jumps it can make in its life. The time this will take naturally depends upon the temperature. It is generally accepted that the vacancy can make above 10^9 jumps in its lifetime, and this is equivalent to about an average travel of 10^{-3} cm. As pointed out above, more than one type of defect will be present in the material at any one time. The main

type of defect will naturally be the single vacancy but an appreciable number of divacancies will also exist. Koehler[38] suggested that the vacancy existed for part of its life as a divacancy but Kimara and Maddin[39] showed that this was most unlikely.

The various species of point defects have different diffusion characteristics and due to the different values of E_M of the diffusion activation energies, anneal out at different temperatures. This leads to a recovery spectrum for the annealing of point defects; Koehler[40] et al discussed the various stages. There are generally six stages in the annealing of point defects in noble metals.

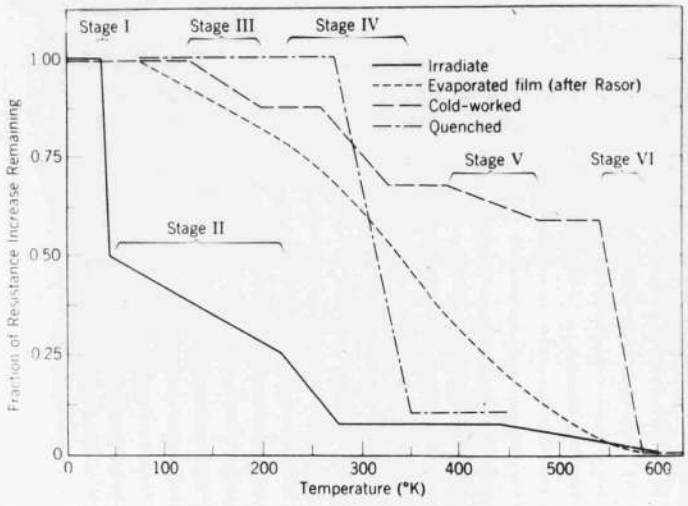

Fig. 7. Showing the various stages in the annealing out of imperfections produced in copper by various methods.

Stages (1) and (2) are reported only in irradiated specimens. Stage (1) is said to be due to the motion of interstitial atoms and stage (2) to the movement of interstitial GROUPS Stage (3) is thought to be due to the diffusion of divacancies and stage (4) is due almost certainly to the diffusion of single vacancies. Stage (5) is at present rather vague, but stage (6) is probably due to recrystallisation.

The activation energies for the various stages are known approximately and it is of some interest to note these for the noble metals. Huntingdon[41] gave the E_M for the copper interstitial atom as 0·07 ~ 0·27 e v. The E_M for a single vacancy in copper is, according to most of the reported results, about 1·0 e v. Bartlett and Dienes[42] calculated that the energy to move a divacancy would be 1/3 to 1/2 of that for a single vacancy.

When vacancies are quenched into a metal there is another mechanism by which they can leave the lattice and this is to form a vacancy ring which may collapse into a sessile dislocation. The periphery of the ring can then act as a sink for vacancies just as a dislocation line does. Kimura, Maddin[39] et al calculated the decay laws for this type of system. The complication of this type of vacancy sink is that it increases in size and vacancy capturing area as more vacancies reach it. Dislocations on the other hand are regarded as being essentially fixed sinks.

It was also shown that the quenching temperatures could influence the type of hardening produced[39]. When the metal (copper) was quenched from below 800°C normal vacancy recovery was found. On quenching from above 800°C two stages of recovery occurred, the first and faster was due to divacancies and the second and slower stage to vacancies.

Silcox and Whelan[43] showed by electron microscopy measurements in a quenched aluminium foil the movement of the quenched-in dislocatipn loops. The activation energy for the movement of the ring was found to be the same as that for a single vacancy. Washburn[44] showed that the cluster could be removed by 5 % deformation. This indicates that small amounts of plastic work could actually reduce the dislocation density.

In conclusion it may be said that most of the irradiation and time dependent effects noted after deformation may with confidence be related to migration of point defects. It has been shown that the annealing of radiation damage proceeds with the same activation energy as self diffusion.

Quenching gives rise in time to quench hardening which appears with the same activation energy as that expected for the movement of vacancies and divacancies. Levy and Metzgen[45] measured the internal friction of aluminium after various rates of cooling. They found that at slow rates of cooling the specimen retained its amplitude dependent internal friction as might be

expected. An air cool left less of the amplitude dependent effect and a quench removed it entirely.

As was mentioned previously Granato and Luke[15] proposed that the Koster effect was due to the diffusion of lattice defects to the dislocations causing the internal friction to decrease. As the above theory is fairly well established it is now possible to get at least quantitative measurements of the numbers of point defects introduced by different types of deformation and quenching processes. The direct comparison of internal friction results with those obtained by yield point, hardness, and electrical conductivity presents little difficulty.

As can be seen from the above equations of Granato and Luke[10], very little dislocation internal friction is to be expected when the loop length of the dislocation is reduced to about one atomic spacing between pinning points. However, it is readily calculated that in most types of deformation which have been studied up to date, the number of vacancies produced is more than enough to saturate the available dislocation lines. It would then appear that dislocation internal friction could only usefully study the earlier stages of deformation. Internal friction measurement will probably give useful data in the diffusion activation energies for the various species of point defects encountered. It should however be remembered that the theories of Granato and Luke[15] apply only to a dislocation sink for vacancies and it is known that vacancy clusters can form an

alternative trap for excess vacancies. This will probably become significant in quenching experiments where the vacancy clusters appear to be most common.

SECTION C

The Effect of Internal Oxidation on the Properties of a Metal

If a noble metal contains a small percentage of a baser solute, then it is possible by annealing the alloy in a dilute oxygen atmosphere to oxidise the solute without oxidising the solvent. Rhines[46] showed that the rate of internal oxidation could be expressed by the formula

$$\log \frac{x^2}{t} = \frac{a}{T} + b$$

where x is the penetration in cms.
t the time in seconds
a and b are constants

This equation was shown to hold in copper alloys for temperatures between 750°C and 1000°C and the constants a and b were given for a large range of solutes.

It is easily shown that oxide precipitation takes place on the grain boundaries preferentially because the rate of oxygen diffusion is greatest at the boundary. Wood[47] showed that the size of the precipitated oxide increased as the distance from the surface of the specimen increased. The hardness was also shown to decrease as the distance from the surface increased and the grain size was larger at the centre.

The present interest in internally oxidised material is stimulated by the fact that unlike many other types of dispersion hardened alloys, they retain their strength at higher temperatures.

Another important point is that the reduction in thermal and electrical conductivities is not as severe as is the case with solid solutions. The only really serious handicap is that the precipitate of oxide at the grain boundaries can reduce the properties of the alloy. Various methods of avoiding this are used successfully.

Oxide dispersions can be produced in a number of ways. The most obvious and widely used is to sinter the metal and oxide together in the form of powders which avoids the grain boundary effect mentioned above. An alternative method is to make up a solid solution alloy and oxidise it in a dilute atmosphere of oxygen at elevated temperature. This can be done in copper alloys by passing a stream of argon containing a little oxygen over the specimens. The more usual method is to seal the specimens up in an argon atmosphere over a mixture of copper and cuprous oxide powders.

Various theories have, from time to time, been put forward to explain the process of dispersion hardening and it is convenient to consider these in relation to internally oxidised specimens. Mott and Nabarro[48] postulated that the solute caused internal stresses in the matrix due to the misfit of the particle. They gave τ the yield strength in sheer as

$$\tau = 2G\epsilon F$$

G = modulus of rigidity
ϵ = strain in precipitate
F = volume fraction of solute atoms

When the flexibility of the dislocation line was taken into account[49] the critical distance between the particles was shown to be

$$\lambda_c = \frac{b}{\varepsilon F} \qquad \text{where } b \text{ is the Burgers vector}$$

This equation gave λ_c for the critical spacing as about 50 atomic spacings which is of the correct order.

Orowan[50] proposed that dislocation loops were left encircling the precipitated particles causing the hardening effect. He showed that

$$\tau = \frac{G\,b}{\lambda}$$

This equation has the advantage that it illustrates that in averaging as λ increases τ decreases. Possibly a slight modification to this theory to compensate for the particle size is required.

$$\tau = \frac{G\,b}{\lambda - a} \qquad \text{where } a \text{ is the particle radius}$$

Geisler[53] suggested that coherency strains in the lattice round the precipitate gave it a larger effective radius and this reduces λ.

As mentioned above the hardness and tensile strength of a dispersion hardened alloy is found to be more or less inversely proportional to the size of the precipitated particles. The creep properties of internally oxidised copper/aluminium/silicon alloys were shown by Martin and Smith[52] to be much superior to the unoxidised alloys. On the other hand the fatigue properties

were poorer in a polycrystalline specimen. In a single crystal however the fatigue properties had improved. In every case the finer particle gave the best properties. The weakness in fatigue in the polycrystalline material brings out the deleterious effect of the preferential deposition of oxide at the grain boundaries.

Internal friction measurements are of considerable interest. In the solid solution alloy the solute atoms will be firmly attached to the dislocation lines and not amplitude dependant, and very little independant damping will be found. On internal oxidation the solute atoms are removed from the lattice and are precipitated as oxide particles. This will have the effect of unpinning the dislocation.lines. This will allow amplitude dependant internal friction to be observed. However, this argument does not allow for the hardening by the particles. O'Hara and Gibbons[53] showed for Cu/0·2% that when the alloy was externally oxidised its internal friction became higher even than that of pure annealed copper. The reason given for this was that the silica particles which were spherical gave rise to strain in the lattice on cooling from the oxidising temperature and ca used the creation of loosely pinned dislocations. There seems little doubt that such particles can in fact cause such effects as dislocations have been seen in silver chloride[54] and iron alloys[55] round precipitates.

The increase in internal friction after internal oxidation, where it should be remembered that the metal still contained some oxygen, indicates an apparent increase in the loop length of the dislocations. This seems rather strange in view of the fact that the metal had been hardened. Possibly an explanation can be found in the fact that dislocation damping is measured on only a few atomic spacings of dislocation movement, while the yield point measurements require quite extensive movement for their measurement. Thus it may be that the precipitation barriers do not interfere greatly with the vibration of the dislocation lines.

SECTION D

The Effect on the Properties of Iron of Interstitial Elements

The common interstitial elements which dissolve in iron, i.e., carbon, nitrogen and perhaps hydrogen, are thought to give rise to two types of effect. The first is the diffusion of the interstitial atoms to the dislocation which they then impede in motion. The second effect is the formation and precipitation of carbides and nitrides which have varied effects on the mechanical properties depending on their distribution and size.

As previously described, Cottrell and Beilby[6] and later Harper[56] gave the laws for the segregation of interstitial atoms to the dislocations

$$\log_e (1 - q) = - \alpha \left(\frac{A\,Dt}{KT}\right)^{3/3}$$

A is a constant
a fraction of atoms moved to dislocations

This equation has been shown to hold up to almost total precipitation at least as far as internal friction results are concerned. The effects of ageing on the other physical properties are rather more complex. Wilson and Russell[57] measured the effects on various mechanical properties. They showed that the yield point returned when the segregation had reached about one atom per PLANE in the dislocation lines. The yield point rose quite rapidly during this stage of ageing as did the Lüdders Band energy.

A second stage then started which was rather less effective in raising the yield point. This was taken as representing the formation of an outer envelope of interstitial atoms. Up to the end of this second stage the 'precipitates' are easily redissolved by straining.

When the segregation reaches more than about two atoms over the unit length of the dislocation line the segregation becomes more stable and reduces the ductility and affects the work hardening properties of the material.

As mentioned earlier, the height of the internal friction peak was a measurement of the quantity of carbon or nitrogen left in the lattice. It is thus possible to follow the ageing of an iron alloy containing either carbon or nitrogen by an internal friction method. Unfortunately the more realistic experiment with both carbon and nitrogen is complicated by the fact that interaction takes place between the relaxation processes. The carbon and nitrogen relaxation peaks lie close together and must overlap in measurement and their resolution is rather difficult. It is also known that the presence of carbon influences the position of the nitrogen peak. Other alloying elements are thought to have similar effects.

It may well be possible to use the measurement of dislocation internal friction to follow the ageing process. On quenching the dislocation line will contain fewer interstitial atoms than it would on equilibrium and its loop length will be longer. As ageing proceeds the loop length will be reduced

and with it the dislocation damping. As described earlier, there is a theory which allows a connection to be made between diffusion of point defects and dislocation damping. It is felt that this type of measurement would be a more direct measure of the state of ageing of a material than the previous method at least in the first stages of ageing.

CHAPTER 2

APPARATUS

Description of Apparatus

Crystal Arrangement

Calibration of Apparatus

Calibration of Crystals

Calculation of Strain in Specimens

Effect of Support Position

Conclusions

Annealing Process

APPARATUS

The apparatus used was of the type first described by Forster. In this type of apparatus the specimen, in the form of a rod or bar, vibrates in a free-free transverse manner. The frequency of vibration is decided purely by the shape of the specimen. The specimen is supported horizontally by two threads at positions just outside the nodes of vibration. The upper ends of the threads were attached to Rochelle salt piezo electric crystals. These crystals were used to excite and detect the vibration of the specimen. The crystals were attached by means of rubber faced clamps at their mid-points to heavy pieces of steel which were supported by a three spring arrangement. This system was designed to reduce as far as possible the effects of external vibration. The general arrangement is shown in Fig.1,2 The crystals were of the parallel bender type 1" x ·06" x ·25" manufactured by Messrs. Cosmocord, Ltd. Connection to the crystals was made by coiled varnished wires. The driver crystal was powered by a Muirhead Wigan D - 650 decade oscillator which could supply up to 2 watts into a 7000 impedance at any frequency between 1 c/s and 10 K c/s. It had a specified accuracy of ± 0·2% and on servicing checks was generally found to be much more accurate than this.

The receiver crystal was connected to a Muirhead D-690- A analyser. This is in effect a tunable amplifier with a self-contained

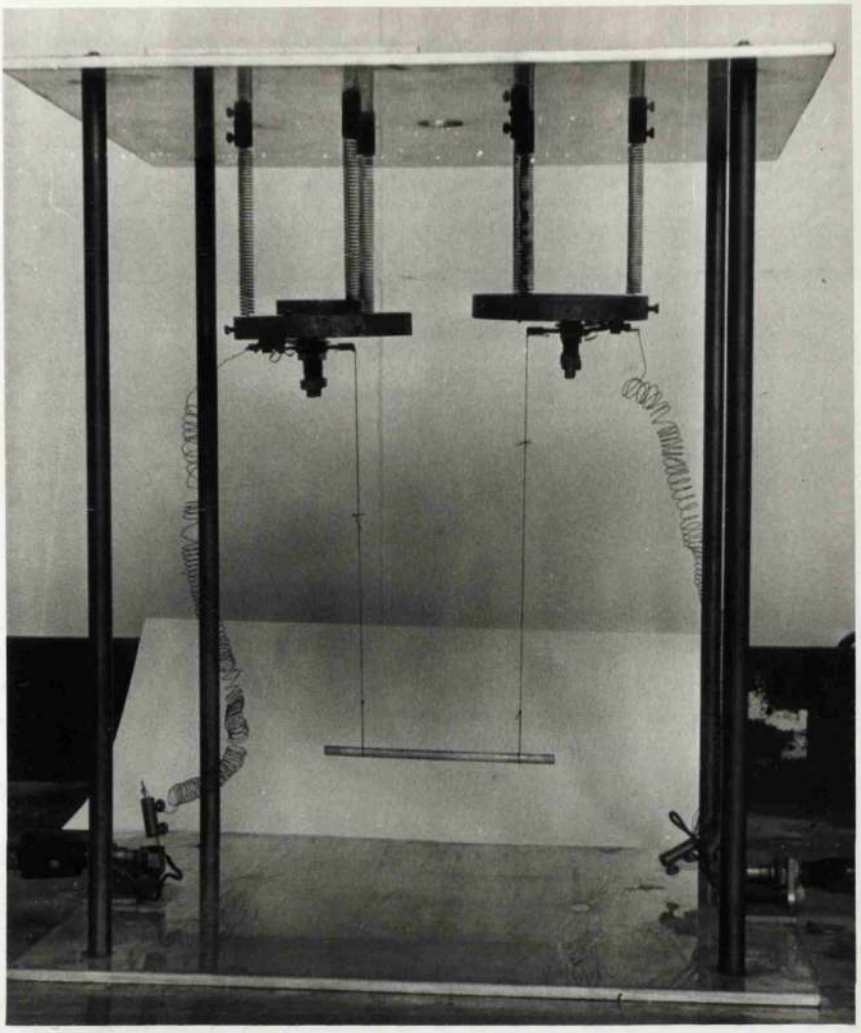

Fig. 1 General View of Suspension Arrangement.

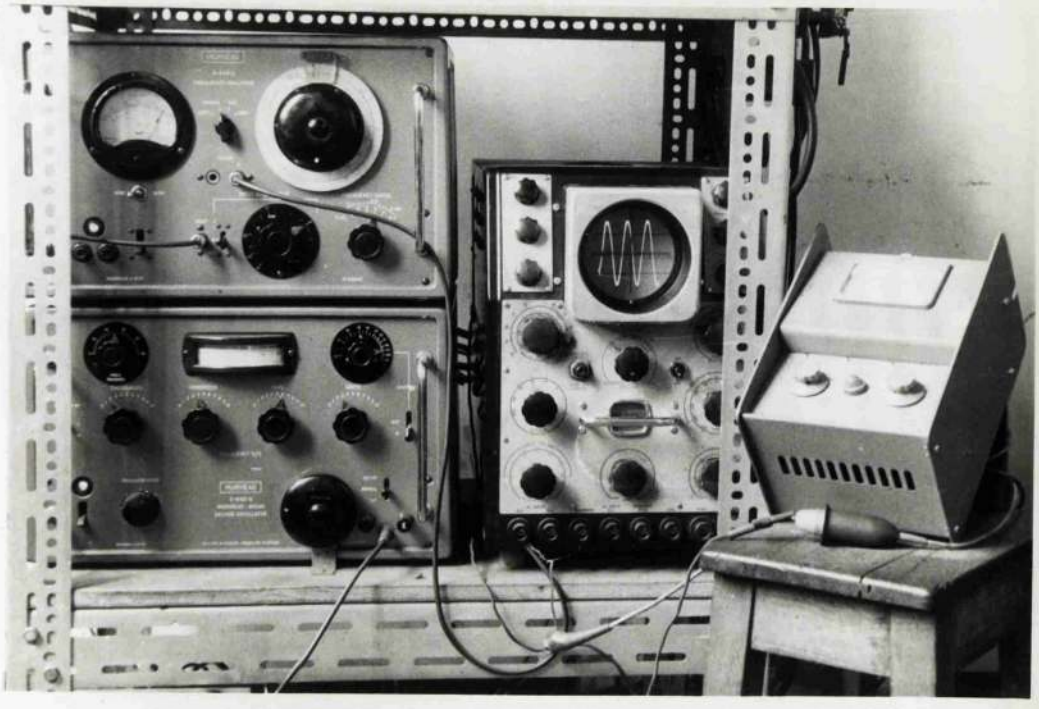

Fig. 2 Electronic Apparatus.

voltmeter. Previous experience had shown that in order to make accurate measurement at small amplitudes, it was essential to eliminate any spurious signal or hum in the apparatus, and this can best be done by using a tuneable amplifier. This amplifier was fitted with a standard attenuator, which allowed measurements at full scale deflection of from 300μV to 3V to be made at any frequency between 30 c/s and 30 Kc/s.

A Cossor 1049 M III oscilloscope was used to display the wave form from the analyser. This instrument had originally been chosen as it usedD.C. amplifiers which have a better frequency response than the A.C. amplifiers in the other instruments available. The main amplifier in the oscilloscope had a gain of approximately 900 times and in order to extend measurements to lower amplitudes it was used to feed a valve-voltmeter. The valve voltmeter was a Marconi TF 1300. This is quite a normal valve voltmeter. The circuit arrangement is shown below.

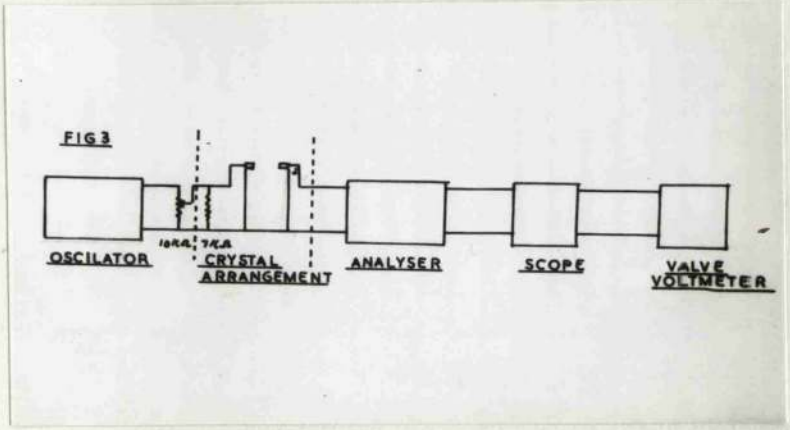

FIG 4

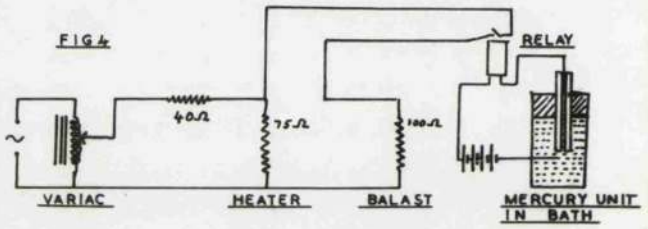
RELAY
40Ω
75Ω
100Ω
VARIAC
HEATER
BALAST
MERCURY UNIT
IN BATH

FIG 5

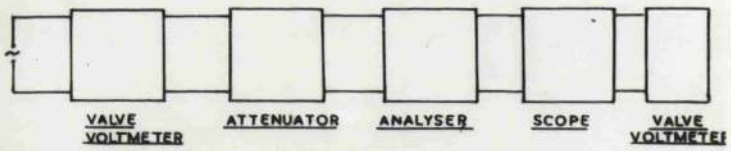
VALVE
VOLTMETER
ATTENUATOR
ANALYSER
SCOPE
VALVE
VOLTMETER

The two resistors between the oscillator and the driver crystal require some explanation. The 10 KΩ potentiometer was simply to allow finer control of the output of the oscillator. The 7 KΩ resistor was put in the circuit in order that the oscillator would be correctly loaded. This was thought necessary as the oscillator was designed to feed into a 7 KΩ impedance and the crystal was found to have an impedance of about 50 KΩ at the frequencies used.

Throughout the apparatus the greatest possible care was taken to shield the electrical system from interference. It was quite evident that a great deal of external electrical interference could be expected in the laboratory. Allconnecting wires were of co-axial cable and connections made by jack-plugs in order to reduce the pick up of interference. It was found that under certain conditions electrical coupling could occur between the coiled wires of the exciting and detecting systems. This was largely avoided by placing a sheet steel baffle round the wires to the receiver crystal. Three sets of crystals were used, and while they differed in actual construction, they were made as far as possible functionally identical. Each of the sets of apparatus had its own 7000Ω resistors and it was felt that this was better than a single resistor at the oscillator. Only one set of flexible leads was used and connections made by jack-plugs at each of the three sets of crystals.

Even with a tuneable amplifier it was felt that the 50 c/s pick up by the apparatus from the main should be reduced to a minimum. The normal trial and error procedure with earthing wire positions, etc., was carried out. As every apparatus operates under unique conditions it is pointless to describe these in detail. A point worth noting is that an earthed steel sheet beneath the apparatus was of the greatest value in reducing mains frequency interference.

The electronic apparatus required some hours to stabilise sufficiently for accurate use and for convenience a contactor clock was used to switch the apparatus on in the morning.

As it was felt that it would be useful to measure the internal friction at temperatures above and below room temperature, two baths were constructed. The low temperature bath was simply a lagged glass container. The specimen was suspended in a small copper container whose cross-section was like an inverted keyhole. This container was surrounded by the liquid cooling medium, i.e. acetone or methylated spirits and dricold or liquid air. The higher temperature bath was a lagged copper tank which was heated by an electric kettle element. Figure 6 . For temperatures up to 200°C an oil heating medium was used with the copper container described above. A simple controller was constructed for this bath and is shown in Figure . The apparatus functioned fairly well and gave reasonable control $\pm\frac{1}{2}$°C over the working range. It was constructed to take up as little room as possible in the heating space.

Fig. 5A Clamping of Crystal

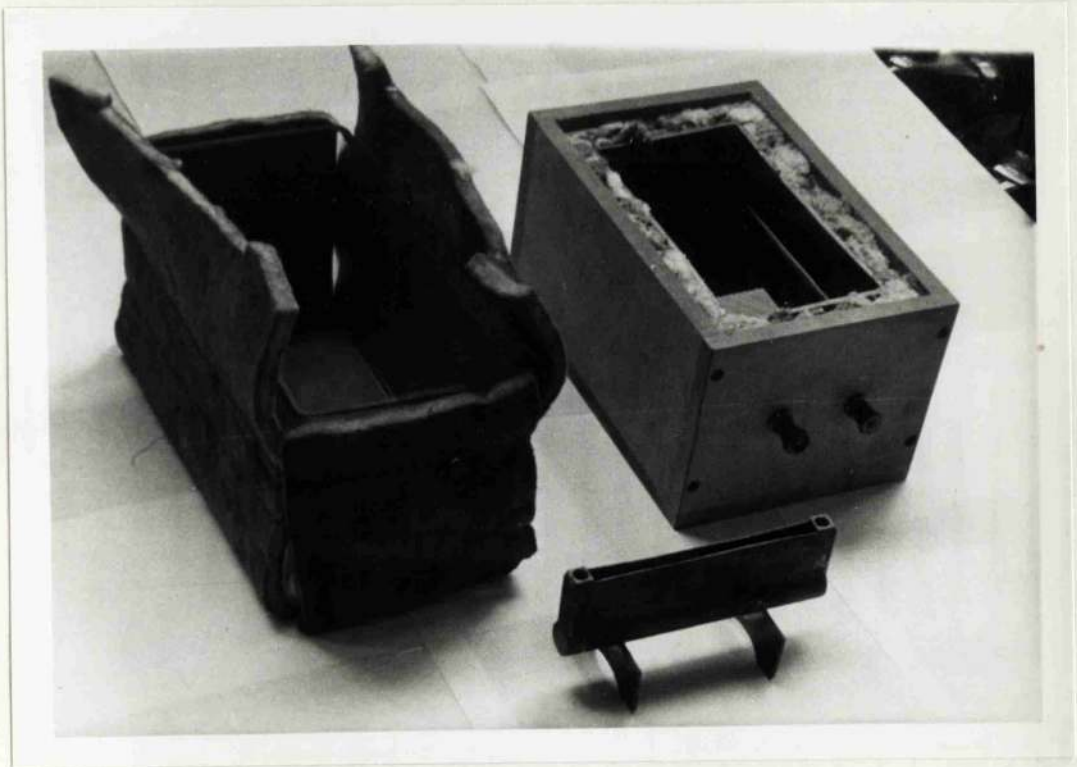

Fig. 6 Low and High Temperature Baths with Specimen Container.

Crystal Arrangement. From a considerable amount of past experience, it was found necessary to adjust the clamping pressure on the crystals very carefully. Fig 5A In the receiver crystal especially it was found that the output voltage for a given amplitude of vibration was very sensitive to the clamping pressure. In practice the clamping on the crystal was adjusted to give 80 - 90% of its maximum possible output voltage. This allowed all the crystals to be made as far as possible similar. It was necessary to check the output of a crystal a few days after setting as it tended to change as the rubber bedded in. The exciter crystal was simply adjusted to give the best driving effect. It was found that these crystals tended to fracture if the voltage applied exceeded 30 volts and this limited the maximum permissible power applied.

As the crystals were cut from Rochelle salt, i.e. sodium-potassium tartrate hydrated, they will tend to decompose under vacuum and the apparatus was used in air at atmospheric pressure. Replacement with a non-hydrated crystal was not considered possible as the available materials were not sufficiently sensitive.

As mentioned above, the power efficiency of the oscillator - piezo-electric system was rather poor due to the difference in impedance of the oscillator and crystal and this is also a factor which reduces the maximum power available. An attempt was made to increase the power to the specimen by REPLACING the exciter crystal by an electromagnetic driver (Goodman). However it transpired that the small Goodman available (½ W) did not even

with a matching amplifier drive as efficiently as a crystal. No larger drives were manufactured apart from very large sizes indeed. The electromagnetic drive method was then abandoned after it had been found that the vibrator was too sensitive to a small low frequency signal in the amplifier system.

For reasons which will be more fully discussed later, it would be useful to support the specimen at the nodes and drive and detach by magnetic forces alone. A magneto-striction drive was constructed but did not prove sufficiently sensitive and the method was abandoned.

Calibration of Apparatus

The frequency accuracy of the oscillator was checked by the manufacturers from time to time and was accepted as accurate to the specified limits.

The accuracy and linearity of the analyser, oscilloscope and meter are of paramount importance. The method of calibration is shown in Figure 5 . The voltage from the oscillator was kept constant from the reading on the valve voltmeter. The detecting system was supplied from the standard attenuator which passed an accurate fraction of the voltage supplied to it. A series of readings were taken on the analyser and second valve voltmeter as the standard attenuator was varied. Graph (1). The supply frequency used in these experiments was 1700 c/s which was close to the frequencies to be used. The analyser was found to be quite linear and perfectly reliable. The analyser

attenuator was checked and found to be standard. The analyser had a self-contained calibration method and could be checked and adjusted very quickly and easily. The oscilloscope - valve voltmeter system was much less linear and would require a calibration chart if it were to be used. However, using the standard attenuator on the analyser at any time the required calibration could be obtained in seconds.

Calibration of Crystals

The deflection of the receiver crystal caused a voltage to be transmitted to the analyser. In order to calculate the amplitude of vibration and the strain in the specimen it was necessary to know the voltage/amplitude relationship for specimen vibration.

A proximity meter method was tried, but did not prove sufficiently sensitive. A microscopic method was then adopted. The centre of a specimen was coated with black cellulose and while this was still sticky some 700 mesh Carborundum powder was blown into it. This gives small angular particles which show up well against a dark background. A metallurgical microscope was mounted horizontally at the centre(antinode) of the specimen at its maximum magnification. A graticule eyepiece was used to measure the size of a particle in the centre of the field. The specimen was then made to vibrate to give a certain voltage on the receiver crystal and its apparent vertical size was noted from the microscope. As it was only

possible to use the above method at relatively high amplitudes it was necessary to assume that the amplitude/voltage relationship was linear and could be extrapolated to low amplitudes. Several amplitude/voltage measurements using different particles were made. Graph (2). Each set of crystals was adjusted by means of the clamping screws to be as close as possible to each other. The accuracy of these measurements was not better than ± 10%.

Calculation of Strain in Specimen

In order to arrive at the strain in the specimen from the above microscopic results it was necessary to consider the nature of free-free vibration of a rod.

For a small deflection the curvature is given by

$$\frac{1}{R} = \frac{d^2y}{dx^2}$$

R = radius of curvature
y = vertical displacement
x = distance from centre

The bending moment M is given by

$$M = \frac{B}{R}$$

B is a constant

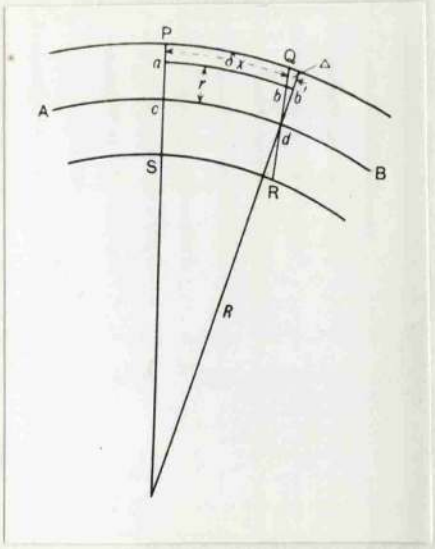

A B is the neutral axis
Consider a b at distance r from A B of length δ x
Area ω

a Eb' after bending = $\delta x + \Delta$

Now if E = Young's modulus

$$F \text{ (force)} = \frac{E \omega \Delta}{\delta x}$$

Now $\frac{\delta x + \Delta}{R + r} = \frac{\delta x}{R}$ where $\frac{\Delta}{\delta x} = \frac{r}{R}$ (Strain)

$$F = \frac{E \omega r}{R}$$

$$\text{Moment} = \frac{E \omega r^2}{R}$$

Total moment PS on arc S

$$= \frac{F}{R} \Sigma \omega r^2 = \frac{E \, SK^2}{R}$$

where K^2 = radius of gyration = $\frac{a^2}{4}$ or $\frac{\tau^2}{12}$

if a is the radius of a circular specimen and

t the thickness of a rectangular one

as $\frac{1}{R} = \frac{d^2 y}{dx^2}$

$$M = E \, S \, K^2 \frac{d^2 y}{dx^2}$$

If F is transverse shear force, ρ is density

S is area

$$\frac{d^2 y}{dt^2} = \text{acceleration of } \delta x$$

$$\delta F = \rho S \, \delta x \frac{d^2 y}{dx^2}$$

OR $$\rho S = \frac{d^2 y}{dt^2} = \frac{dF}{dx}$$

As the area S is rotated by a small angle $\theta = \frac{dy}{dx}$

$$I \frac{d\theta}{dt^2} = \delta x + F \delta x$$

This gives $$\rho S\left(\frac{d^2y}{dt^2} - K^2 \frac{d^4y}{dx^2 dt^2}\right) = -\frac{d^2y}{dx^2}$$

for small deflections we get

$$\frac{d^2y}{dt^2} = K^2 C^2 \frac{d^2y}{dy^2}$$

where $C = \sqrt{\frac{E}{\rho}}$ the velocity of the longitudinal wave

$z = a \cos n t$ assumed

$$\frac{d^2y}{dx^2} = \frac{\rho m^2}{E K^2}$$

$$y = m^4 y$$

$$m^4 = \frac{n^2}{E K^2}$$

$$y = (A \cosh m x + B \text{ shin } m x + (\cos m x + D \sin m x) \cos n t$$

By applying the end conditions of a bar of length l and mid point x

$$\frac{d^2y}{dx^2} = \frac{d^3y}{dx^3} = 0 \quad \text{at } x = \pm \tfrac{1}{2} l$$

This gives

$$y = (A \cosh m x + C \cos m x) \cos n t$$

$$x = \frac{m l}{2} = (S - \tfrac{1}{2})\pi + B$$

where $S = 1, 2, 3 -$

B is small except when $S = 1$

Thus $m = \frac{2\pi (S - \frac{1}{4})}{l}$

$= \sqrt[4]{\frac{\rho n^2}{E k^2}}$

$N = \frac{n}{2\pi} = \frac{(4S - 1)}{8} \frac{K}{l^2} \sqrt{\frac{E}{\rho}}$

Where N is the frequency in cycles per second.

This is the equation for transverse vibration

when S = 1, (4S - 1) = 3·0112 (due the factor B)

This leads to the results (Wood)

Number of Zone	Number of Nodes	Position of Nodes	Ratio of Frequency
1	2	0·2242, 0·7758	1
2	3	0·132, 0·50, 0·8679	2·756
3	4	0·094, 0·356, 0·644, 0·905	5·404
4 4	5	0·073, 0·277,0·50, 0·72, 0·926	9·33

Now using $y = (A \cosh m x + C \cos m x) \cos n t$ at the maximum deflection of the bar (centre) amd $\cos n t = 1$

The radius of the bent bar is given by

$$R = \frac{1}{\frac{d^2 y}{d x^2}}$$

$\frac{d y}{d x} = A m \sinh m x - C m \sin m x$

$\frac{d^2 y}{d x^2} = A m^2 \cosh m x - C m^2 \cos m x$

$R = \frac{1}{m^2(A \cosh m x - C \cos m x)}$

At the centre of the bar $x = 0$

$R = \frac{1}{m^2(A - C)}$

Now consider the nodes at the same time

$y = 0$ (by definition of 1st harmonic node)

For a 10 cm bar $m = 0 \cdot 473$

$$0 = A \cosh m x + C \cos m x$$

$$= A \cosh 0 \cdot 473 \times 2 \cdot 758 + C \cosh 0 \cdot 473 \times 2 \cdot 753$$

$$= A \cosh 1 \cdot 3 + C \cos 1 \cdot 3$$

$$= A\ 1 \cdot 9709 + C \cos 74 \cdot 50$$

$$\frac{A}{C} = -0 \cdot 1324$$

$$y = C\ (-0 \cdot 1324 \cosh m x + \cos m x)$$

at $x = 0$

$$y = 0 \cdot 8676\ C$$

This gives the required correlation between the values of A and C for fundamental deflections

$$A = -0 \cdot 1324\ C$$

$$= 0 \cdot 8676\ C$$

$$A - C = 1 \cdot 3y$$

$$R = \frac{1}{m^2(A - C)} = \frac{1}{0 \cdot 223 \times 1 \cdot 3y}$$

Strain $\varepsilon = \frac{r}{R}$ $= 0 \cdot 231 \times 0 \cdot 223 \times 1 \cdot 3y$ for 3/16" dia. bar

$$\varepsilon m = 0 \cdot 067y$$

From the relationship of y obtained microscopically and the voltage the εm/voltage relation is deduced

This gives

$$1V = 16 \times 10^{-4}\ y$$

$$\varepsilon m = 0 \cdot 067 \times 16 \times 10^{-4} \doteq 1 \times 10^{-4}$$

While the relative values of amplitude can be given with some accuracy the absolute amplitude is not known to better than ± 10%

Higher Harmonics

A bar in free-free motion can only vibrate in a node which is symmetrical about its centre (Wood). This means that S = 2 is not a possible harmonic in this apparatus. This was shown experimentally to be the case.

When S = 3 vibration is possible, but from the equation

$$= a \cosh m x + C \cos m x$$

it can be seen that when x is greater than one centimetre, the exponential part is greater than the cosine. This considerably complicates the problem and as little advantage would be obtained by a five fold increase in frequency, it was decided not to use higher harmonics at least where the amplitude was of importance.

The Effect of Support Position

In the Forster apparatus the specimen is supported at a point other than the node of vibration. This is of course necessary if any exciting or detecting of the specimen is required. The threads used for supporting have unfortunately a damping effect on the specimen and it was noted by Forster than this increased as the distance of the support from the node increased.

Wachtman and Tefft[67] gave the following analysis of the system :

If Q_a^{-1} is damping due to apparatus

Q_s^{-1} is damping of specimen

Q_m^{-1} is total (apparent) damping

Then if y is the movement of the thread and y_0 the movement of the end of the specimen

$$Q_a^{-1} \propto k_a \; y^2$$

$$Q_s^{-1} \propto k_s \; y_0^2$$

and $$\frac{k_a}{k_s} = k$$

$$Q_m^{-1} = \frac{Q_s^{-1} + k\, Q_a^{-1} \left(\frac{y}{y_0}\right)^2}{1 + k \frac{y}{y_0}}$$

Rayleigh gave the value of $\frac{y}{y_0}$ as

$$= \frac{1{\cdot}018\,(\cosh 4{\cdot}73\frac{x}{\ell} + \cos 4{\cdot}73\frac{x}{\ell}) - (\sinh 4{\cdot}73\frac{x}{\ell} + \sin 4{\cdot}73\frac{x}{\ell})}{2{\cdot}036}$$

Where x is the distance from the end of the specimen, length ℓ

By measuring Q_m^{-1} for various positions of $\frac{y}{y_0}$ it is possible to calculate the values of k and Q_a^{-1}. If as is normally the case the specimens are amplitude dependant, it is necessary to keep the amplitude constant to maintain Q_s^{-1}. This was done by O'Hara, who calculated the voltage to be expected on the receiver crystal with the supports in various positions assuming constant amplitude of specimen vibration. As it was extremely difficult to place the threads accurately on the specimen the method was rather inaccurate due to errors in specimen amplitude.

The present apparatus was constructed to allow measurements at low amplitudes of vibration ($\varepsilon_o = 1 \times 10^{-8}$) where no amplitude dependance is found in the specimens used. The damping of the specimen was measured at low amplitude for the threads in a series of positions and a graph drawn of distance from node/ Δ Graph (3). This was extrapolated to the node to give the true damping of the specimen. It was felt that this method was sufficiently accurate for the present work.

It will be noted from the results shown that each of the suspension sets gave a different value of apparatus damping. This could be explained by the different types of threads used in each suspension set.

Conclusions.

An apparatus had been developed which was capable of making measurements of internal friction over quite a wide range of strain amplitudes. While the relative amplitudes are known with some accuracy, the absolute values are only approximately known. The different sets of apparatus while similar are not identical and it is important that all measurements in one set of experiments should be made on the same receiver crystal method of measuring internal friction.

The width of the resonant peak was used to measure the

internal friction. The specimen after being placed in the apparatus was vibratedand its resonant frequency found by experiment The voltage fed to the exciter crystal was then altered until the output voltage from the detector crystal had reached a chosen value. This frequency Vr was then noted and the frequency of the oscillator raised until the voltage output was exactly half that of the resonant frequency V_2. The frequency was then lowered until the voltage was again half V_1. The internal friction is then given by

$$\delta = \frac{\pi}{\sqrt{3}} \frac{V_2 - V_1}{Vr}$$

The amplitude of vibration at the resonant frequency was chosen so that normally a full scale deflection was obtained on the analyser and alterations in amplitude were obtained by varying the attenuator on the analyser. As this was calibrated in decibels, it was normal to increase the amplitude by a factor of 10 d.b., which corresponds to an increase of about 7·6 times. Occasionally 6 d.b. increases were used and this corresponded to doubling the amplitude. As described above, it was necessary on occasion to use the amplifier oscillator and a valve voltmeter to make measurements at lower amplitudes. The process was similar but a calibration of the system was needed.

Annealing Process

Most of the specimens used were vacuum annealed to remove gases and internal stresses as well as to obtain a suitable grain size. The furnace used was a horizontal crucilite furnace with a 2.1/4" mullite tube The vacuum system was a normal two stage oil diffusion pump backed by a two stage rotary pump. The vacuum obtained was of the order of 5×10^{-5} m.m. Hg. No cold trap was used and a Sanders type valve was used in place of the normal flap type.

Copper specimens were annealed in spectrographically pure graphite rods. All other metals used were annealed on open alumina plaques grooved to hold the specimens.

The furnace was arranged to give an even temperature over about six inches at its centre and was controlled by a Kelvin-Hughes controller working from a chromel-alumel couple. Quenching was done either from argon or under vacuum. The argon quench was done from a 2" vertical nichrome furnace, the specimen being held by a 40 gauge nichrome wire with a slip knot at its end. The quenching medium was water at room temperature. The water contained a cushion of glass wool to prevent jarring of the specimen. The vacuum quench was arranged so that all necessary operations were done under vacuum. The furnace was vertical and pumped by a rotary/oil diffusion system. The vacuum system was attached

to the furnace by a T junction at its lower end. A 1.1/2" dia Saunders valve was used to seal the diffusion pump. A by-pass system was also included. The top of the furnace tube was sealed by a copper cap through which an insulated electrode passed. The specimen was supported by a wire with a slip knot at the top of which was a small brass washer. This washer was supported from an iron wire stretched between the terminals in the top cap. The specimen was quenched by fusing the iron wire by a heavy electrical current. The brass washer was found to be essential in order to ensure that the iron wire did not weld to the wire which supported the specimen. The specimen support wire depended upon the temperature and specimen used. Platinum wire was used for nickel specimens quenched from about 1200°C., iron wire for iron specimens and nichrome wire for silver specimens.

The quenching medium was diffusion pump oil in the lower leg of the T junction. Again glass wool was used to prevent jarring.

Internal oxidation was done in a horizontal closed end furnace with a 2.1/4" dia. aluminous porcelain tube. A static atmosphere of argon was used and the pressure of this was increased from day to day as required. The furnace which was controlled by a Kelvin-Hughes controller was wound with a graded element to obtain a very even heating zone. Wet hydrogen treatment was also done in this furnace. A few cubic centimeters of hydrogen per minute were bubbled through water at room temperature

before being admitted to the furnace.

Nitriding was done ina 3" dia. nichrome furnace. Hydrogen and ammonia were passed through separate flow gauges, mixed and passed into the furnace. A cracking furnace was used to dispose of any remaining ammonia.

GRAPH NO 1 CALIBRATION OF ANALYSER AND VALVE VOLTMETER

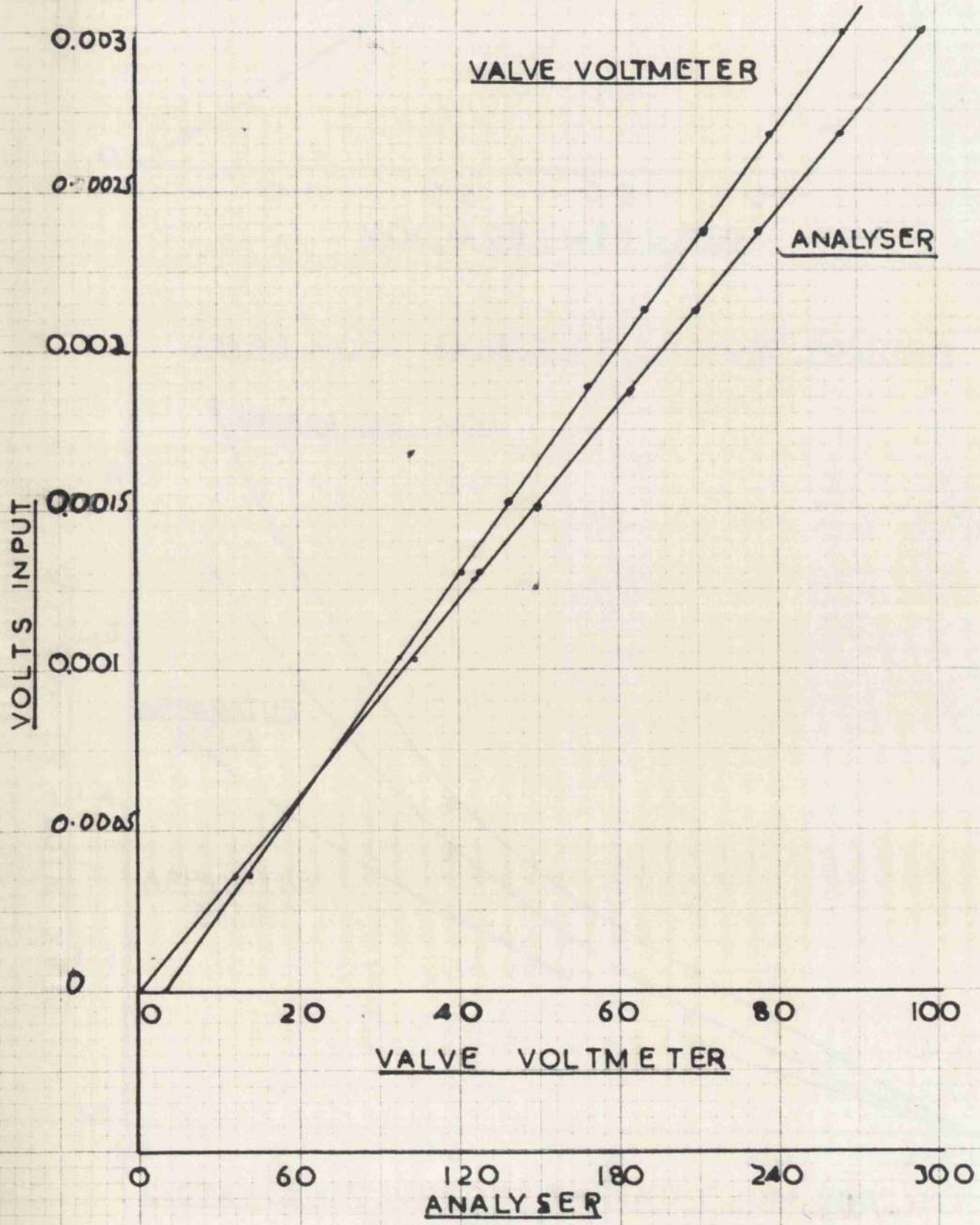

GRAPH NO 2 OBSERVED MOVEMENT / VOLTAGE

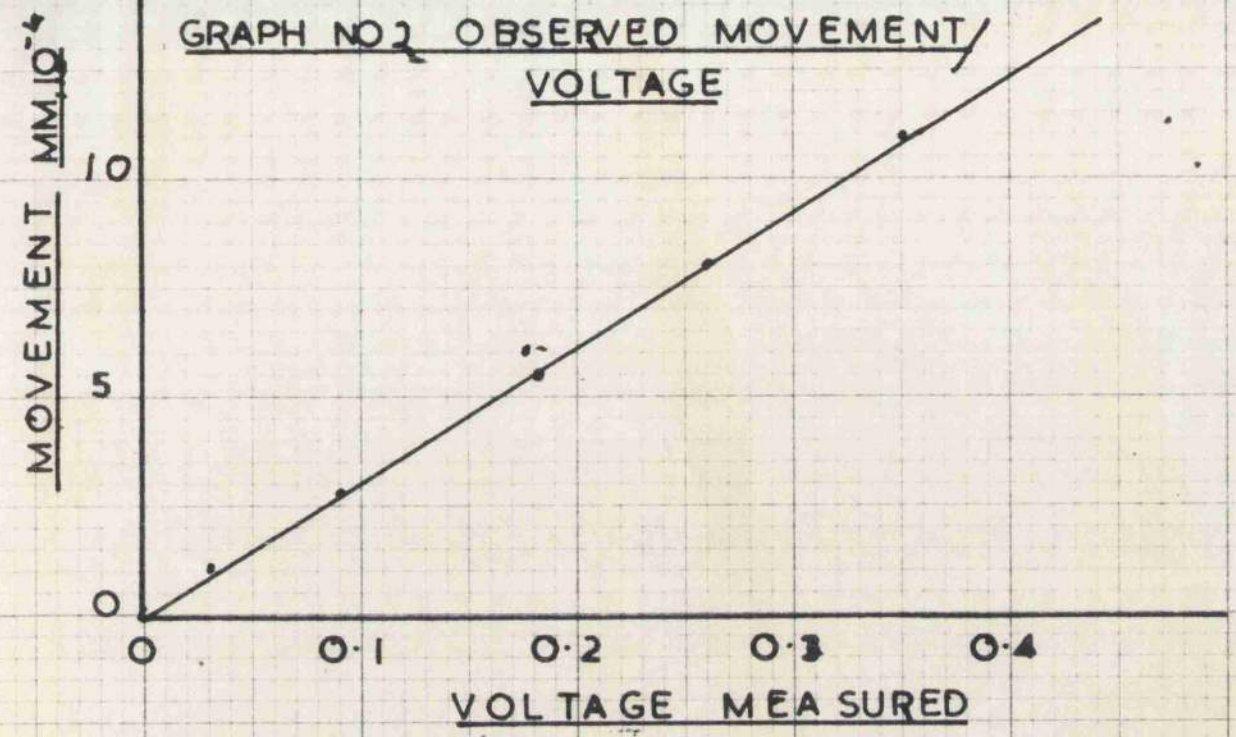

GRAPH NO 3 EFFECT OF SUPPORT POSITION

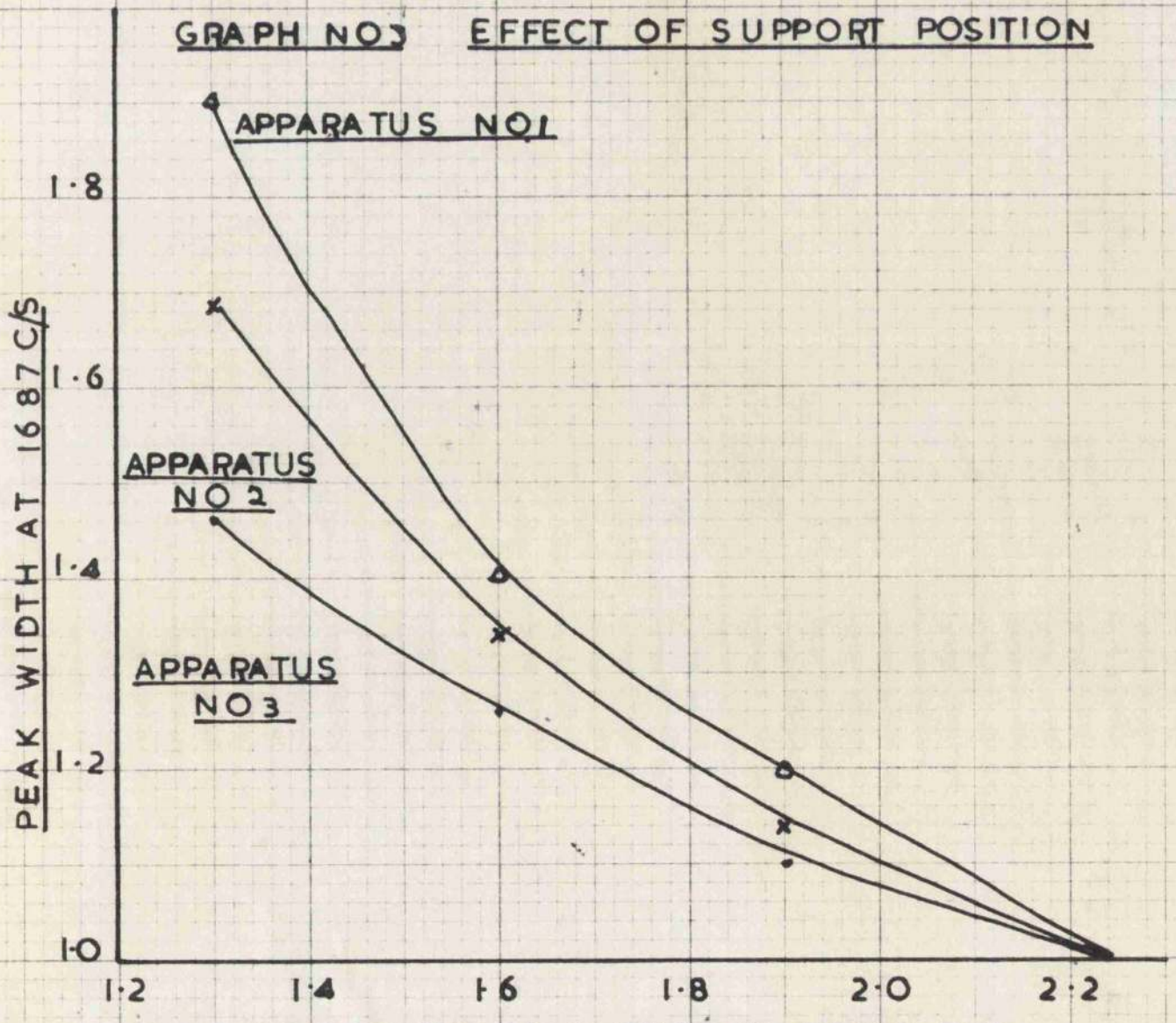

CHAPTER 3

THE EFFECT OF DEFORMATION ON OXYGEN FREE HIGH CONDUCTIVITY COPPER

(1) Tensile Elongation

(2) Quenching

(3) Discussion

The Effect of Deformation on Oxygen Free High Conductivity Copper

(1) Tensile Elongation

It was known from the literature that deformation would either increase or decrease the internal friction of an annealed material and that certain time dependant processes were at work. However, no complete range of data was available for different amounts of deformation. As some work had already been done in the department on copper it was decided to use the same material, as far as possible under the same conditions. The specimens were in the form of 3/16" dia. rod made to B.S.S. 1861. The rods were annealed under vacuum at 920° for 1.1/2 hours in hollow graphite rods. This resulted in a uniform and convenient grain size.After annealing the specimens were always handled with the utmost care to prevent accidental deformation. The specimens were annealed in 15 cm lengths and were cut to 10 c.m. after deformation, thus removing the rather distorted ends which had been gripped by the jaws of the tensile machine.

The tensile machine used was a 25 ton Avery testing machine but as it was necessary to remove the unbroken specimen without bending a modification was necessary. The upper end of the specimen was secured by a Hounsfield wire testing jaw which was suspended from the upper jaw of the Avery machine by a chain. The lower end of the specimen was simply held by the normal sheet jaw for the Avery machine. The specimen was first fitted into the Hounsfield grip which was then placed on

the chain in the tensile machine. The height of the machine was adjusted until the lower part of the specimen could be held in the lower jaw. The specimen was then elongated in the normal way and the load released. The lower jaw of the tensile machine would then either drop free by itself or fall if lightly tapped. The specimen and the Hounsfield grip were then removed. The Hounsfield grip was unscrewed and the jaws knocked back by a tube placed round the specimen. The specimen was then sawn to length by a fine jeweller's saw. Only the ends to be discarded were held in the vice. The specimen was then placed in the apparatus and measured in the usual way.

It was shown by experiment that the clamping and sawing carried out had virtually no effect on the internal friction of the specimen if done carefully. The probable reason for this is that the ends of the specimen do not contribute to the internal friction in the Forster apparatus and hence the slight deformation inevitable in sawing is of no significance.

A normal stress/strain curve for the material was determined and this is shown in Graph (4). The extensometer used was a 2" gauge Hounsfield on a six inch specimen for the lower range and a pair of callipers for the larger extensions.

The following results were obtained before the analyser was put into the system and this meant that no amplitude independent (Δ_I) measurements could be made directly. To make such amplitude

independent measurements it was necessary to obtain a series of internal friction measurements at various amplitudes and extrapolate to zero stress. While this could be done, some time was required and little useful data on recovery could be obtained.

The results shown in Graph No. (5) are the measurments of internal friction determined 1 and 24 hours after deformation at a maximum strain amplitude of $2 \cdot 5 \times 10^{-5}$. It will be noted that the internal friction increases rapidly up to about 1/2% elongation and then decreases more slowly until it is almost constant at about 7% elongation. It will be clear that at the higher internal friction range a considerable scatter is found in the results while the lower internal friction results are more reproducible. The extent of the recovery with time will be seen to be greatest where the internal friction is highest. This is in complete agreement with most of the reported investigations. The actual rate of recovery was thought to be of some interest and it was decided to measure it.

As recovery rates can only be compared if the specimens used are equally stressed in measurement, it is necessary to adopt two standard amplitudes of measurement. The lower of these was chosen so that the specimen was not stressed into the amplitude dependent region. This measured not only the amplitude independent dislocation internal friction but also all the other types of internal friction acting in the specimen. The apparatus

damping was also included in this measurement. The second measurement was made at a very much higher amplitude and included the amplitude dependant internal frication. The Δ_H part of the internal friction could then be obtained by simply subtracting the two above values. The advantage of the analyser in the circuit is that direct measurement of the independent part of the internal friction is easily made.

As the driving power of the apparatus was rather limited it was necessary to select some amplitude of vibration which could be reached with the specimens used. Naturally specimens of high internal friction were more difficult to excite and thus the higher damping of the specimens which had been subjected to small amounts of deformation governed the maximum amplitude permissible. After some experiment it was decided to use strain amplitudes of 5×10^{-9} and 1×10^{-6} as these appeared to be the best for the elongations used, i.e. 2%, 3%, 4·2%, and 5·6% measurements were made only for about the first 30 minutes after deformation as most of the recovery appeared to take place during this time. The results are shown in Graphs 6, 7, 8 and 9 plotted by $\log \Delta H/t^{\frac{1}{3}}$. The reason for this rather peculiar plot is that from the results of O'Hara and the theories of Granato and Luke a straight line should be obtained. As is obvious there is a great deal of scatter in the results. This may be explained from a shortcoming in the oscillator used. As it was a decade instrument slight inaccuracies were inevitable

between the scale settings and the frequency supplied. Unfortunately these slight differences, while proportionally very small, were enough to scatter the recovery results. It was felt that as the $t^{2/3}$ law was known to hold rigidly, for this type of recovery parallel lines could be drawn through the experimental results and give the correct recovery line. The vertical displacement between the lines was taken to be due to frequency errors in the apparatus. Naturally this error will be much less severe with high ΔH values and at all times it was necessary to use amplitudes which gave a reasonably high ΔH if this effect was to be reduced. However, at all times it was necessary to allow for this effect in interpreting any recovery data.

The results while rather unsatisfactory show that the rate of recovery is greater for the greatest elongation.

Granato and Luke[15] gave

$$= \frac{2\cdot5\,\Omega\Lambda\,l^3 n^3 K\eta a}{\pi^2 L \varepsilon_0}\left[\frac{1+\pi\omega a l n^3}{a^2}\right] \cdot$$

$$\times e^{-\frac{K\eta a}{\varepsilon_0}(C_{10}+C_{20})(1+\beta t^{2/3})^4}$$

Thus $\log \Delta H$

$$= C - \frac{K\eta a}{\varepsilon_0}\left(C_{10}+C_{20}\right)\left(1+\frac{C_{10}}{C_{10}+C_{20}}\right)\frac{4a}{a^2}\left(\frac{AD}{KT}\right)^{2/3} t^{2/3}$$

Thus the gradient of $\log \Delta H/t^{2/3}$ = R os given by

$$R = \frac{K n a}{\varepsilon_0}\left(C_{10}\right)\frac{4}{a^2}\left(\frac{AD}{KT}\right)^{2/3}$$

$$= E\ C_{10}\left(\frac{AD}{KT}\right)^{2/3}$$

Where C and E are constants.

Thus if the diffusion coefficient D is a constant, then a plot of R/C_{1o} should be a straight line. Cottrell gave the concentration of vacancies to be proportional to the elongation. The values of R obtained were plotted against elongation and are shown in Graph (10). This shows quite a regular curve and thus it seems that the value of the diffusion coefficient D varies with the amount of elongation.

The activation energy of the recovery process is likely to be of more significance than the diffusion coefficient. The activation energy is also obtained from the Granato and Luke equation

$$\Delta H = A \exp\left[-A_1 (C_{1o} + C_{2o})(1 + B t^{\frac{2}{3}})\right]$$

$$\log \Delta H = -A_1 (C_{1o} + C_{2o})(1 + B t^{\frac{2}{3}})$$

Gradient of $\log \Delta H / t^{\frac{2}{3}} = R = -A_1 (C_{1o} + C_{2o}) B$

Substituting for B

$$R = A_1 C_{1o} - \frac{4\alpha}{a^2} \left(\frac{AD}{KT}\right)^{\frac{3}{3}}$$

$$\log R \cdot T^{\frac{2}{3}} = K - \frac{2}{3} \log_e T - \frac{2}{3} \frac{Q}{KT}$$

$$\log R \cdot T^{\frac{2}{3}} = \frac{2}{3} \frac{Q}{KT}$$

Gradient of $\log R \cdot T^{\frac{2}{3}} / \frac{1}{T}$ is $\frac{2}{3} \frac{Q}{K}$

Thus when the temperature dependance of gradient of $\log \Delta H / t^{\frac{2}{3}}$ is determined the activation energy for the process may be calculated.

The experimental results obtained using the method previously described suffer from a rather serious drawback. As previously mentioned the slight inaccuracies when changing from scale to scale in the oscillator lead to an apparent scattering of the results. The oscillator used was a decade instrument and while very accurate and stable when compared with other commercial instruments, the small margin of error became quite important. The spread of the peak at half width was of the order of units of cycles on a resonant frequency of about 1500 c/s.

With the decade instrument used a frequency variation of 0 - 1 c/s could be obtained by the rotation of a control which gave continuous variations over the range 0 - 1·2 c/s. However, if as normally was the case a frequency variation of more than 1 c/s was required then a control giving a variation of 0 - 10 c/s in 1 c/s increments was used. It was found that the increments obtained in this way were not exactly 1 c/s but included a small error due to the apparatus. The total instrument error was quoted by the manufacturers to be ± 0·2% of the frequency. Naturally this error did not occur altogether in one control but this figure may be taken as the maximum frequency error. While small compared with the actual working frequency (approximately 1500 c/s), it is rather large when measuring the width of the resonant peak, over say 5 c/s. In actual fact the total instrument error was found

to be much less than the figure quoted above. Naturally if for any reason it was necessary to change either the 10 - 100 c/s ot the 100-1000 c/s ranges a more serious error was likely to be introduced. When a measurement of internal friction was being made the frequency difference at the half peak height was determined normally by moving both the 0 - 1 and 1 - 10 c/s controls though occasionally it was necessary to change the 10 - 100 c/s control. While the frequency difference and hence the internal friction thus determined was not absolutely accurate, this is not of prime importance so long as the rest of the readings in the set were made by moving the 1 - 10 and 10 - 100 c/s controls by exactly the same increments for each reading time. However, as the internal friction changed with time this was not always possible. It must also be remembered that during a recovery process the resonant frequency of the specimen may be expected to increase. Thus during an experiment there will be a steady change in resonant frequency and hence a change in the particular settings required to measure the internal friction and the errors introduced will also tend to change. Thus a number of successive recovery measurements were often made with the same digits used and hence with a constant error and the next one or two readings may be made with perhaps only one digit changed but with a different error. When these results are

plotted there will be a sudden interruption of the recovery line but both portions of the line will be parallel. Since the activation energy depends only on the slope of the line these interruptions are not important so long as the slopes can be found with certainty.

As the final plot of LogΔH depends on two separate internal friction measurements, it is to be expected that these variations would be quite frequent. However, if the Δ F value is of the order of 3 - 4 c/s it was found that the only error which was appreciable was that due to the change of the 10 - 100 c/s control. If on the other hand the Δ F value was only of the order of 1 c/s or less then appreciable errors were introduced by the 1 - 10 c/s range.

For these reasons it was necessary when examining a set of experimental results to plot a series of parallel lines rather than a single line which might appear to be the best for the available points. When there was doubt as to which were the correct lines to draw it was necessary to examine the original readings to determine at which points discontinuities may be expected. It was often the case that two or three points fell on one line, the next two or so on another parallel line, and then perhaps some more near the first line. This comes about simply because succeeding errors must cancel if they are not to become cumulative. Naturally some trepidation was felt with regard to a single set of results of this nature and it was necessary to

obtain confirmation from replicate experiments. In the following results, while often only one or two sets of results are shown, in each case confirmatory results were obtained but not plotted for the sake of clarity.

The method used is best appreciated by considering two typical graphs chosen at random from the following results. Graph 8 shows the recovery of copper after 4·4% elongation. The points at 4, 8, 13 minutes are on one line, while the points at 12 and 22 minutes are on another parallel line.

This interpretation arises from the fact that at 4 and 8 minutes all the readings were made in the range 1630-1640 c/s. The readings at 13 and 22 minutes were made with the lower readings in the 1630 - 1640 c/s range and the upper frequency readings in the range 1640 - 50 c/s. At the 18 minute reading the frequencies used were wholly in the 1640 - 50 c/s range. As the internal friction was quite high in this experiment only the change of the 10 - 100 c/s range gave an appreciable error.

In graph 9 on the other hand the internal friction was rather low. The actual experimental readings were:

Time Mins		Resonant Frequency c/s	Upper Frequency	Lower Frequency	
4	I	1625·75	1625·22	1621·54	3·68
I +	II	1624·39	1627·10	1622·90	4·20
8	I	1626·80	1628·70	1625·30	3·40
I +	II	1627·10	1629·29	1625·44	3·85
11	I	1628·11	1629·80	1626·70	3·10
I +	II	1628·27	1630·36	1626·60	3·76
15	I	1629·66	1631·26	1626·24	3·02
I +	II	1629·90	1631·36	1628·01	3·55
20	I	1631·03	1632·75	1629·69	3·06
I +	II	1630·98	1632·97	1629·45	3·51
26	I	1631·66	1633·22	1630·26	2·96
I +	II	1631·46	1633·42	1630·01	3·41

For the first point (4 mins) 4 and 5 digits were changed to obtain the readings, while for the next two points (8 and 11 minutes) the 3 and 4 digits were changed and it was these two points, which were obtained on the same setting, which were used to obtain the slope of the line. After 15 minutes the 10 - 100 c/s range was changed and the point is not near the line. At 20 minutes it was also changed but different settings on the units scale were used.

Taken in isolation this set of results is obviously very suspect but provides the last point on graph 10 from which

Time		Resonant Frequency c/s	Upper Frequency	Lower Frequency	
4	I	1622·75	1625·22	1621·54	3·68
I+	H	1624·39	1627·10	1622·90	4·20
8	I	1626·80	1628·70	1625·30	3·40
I +	H	1627·10	1629·29	1625·44	3·85
11	I	1628·11	1629·80	1626·70	3·10
I +	H	1628·27	1630·36	1626·60	3·76
15	I	1629·66	1631·26	1628·24	3·02
I +	H	1629·80	1631·36	1628·01	3·55
20	I	1631·03	1632·75	1629·69	3·06
I +	H	1630·98	1632·97	1629·45	3·51
26	I	1631·66	1633·22	1630·26	2·96
I +	H	1631·46	1633·42	1630·01	3·41

For the first point (4 mins) 4 and 5 digits were changed to obtain the readings, while for the next two points (8 and 11 minutes) the 3 and 4 digits were changed and it was these two points, which were obtained on the same setting, which were used to obtain the slope of the line. After 15 minutes the 10 - 100 c/s range was changed and the point is not near the line. At 20 minutes the ten cycle per second scale was altered and at 26 minutes it was also changed but different settings on the units scale were used.

Taken in isolation this set of results are obviously very suspect but they provide the last point on graph 10 from which

it will be seen that they form a consistent extension of the remaining results.

It will also be noted in succeeding sections of this work that two stages of recovery are sometimes involved and it is possible, for example, that the points for 20 and 26 minutes in Fig. 9 may be affected by the second stage of recovery in addition to the other factors concerning measurement discussed above.

The method was used first on the recovery after 4·2% elongation, as it appeared to have a reasonable amount of amplitude dependant internal friction with a suitable rate of recovery. Recovery was measured after deformation at 20, 42·5 and 59°C and the results are shown in graphs 11, 12 and 13. It can be seen that apparently two stages of recovery are active. The first stage occurred during the first 15 minutes or thereabouts, and as only a few points were obtained in this range, the second was plotted. The data obtained for this second stage may be summarised in Table I.

Table I - Copper 4·2% Elongation

°C.	°K	$\frac{1}{T}$ x 1000	$T^{2/3}$	R/2.303	R	$T^{2/3}$ R	log[$T^{2/3}$ R]
20	293	3·41	44·1	0·00428	0·0116	0·51	-0·29
42·5	315	3·18	46·1	0·0216	0·05	2·3	0·36
59	332	3·02	48·0	0·168	0·156	7·8	0·88

The values of log [$T^{2/3}$ R] were plotted against 1/T in graph (14) and the activation energy for the process calculated as 20·08Kcals/mole.

As the apparatus could now be used to obtain results at some speed it was felt that an attempt should be made to measure the activation energy for the first stage of the recovery. The specimen could be placed in the apparatus two minutes after deformation and a bout a further one minute was required to find its resonant frequency, and if necessary adjust the specimen.

Measurements could then be made at the rate of one complete Δr and Δ_μ measurement every two minutes.

The specimens were elongated as before and measured at the same strain amplitudes as above, i.e. $1{\cdot}6 \times 10^{-9}$ and 3×10^{-6} at temperatures of 5·0, 19·4, and 27·4°C. The rather lower temperatures used in this case were made necessary by the faster rate of recovery of the specimen in this first stage.

The results in graphs 15, 16 and 17 are much more satisfactory than the previous set and show the linear recovery rather well. The data obtained may be summarised in Table 2.

Table 2 - Copper 4·2% Elongation Rapid Recovery

°C	°K	$\frac{1}{T}$ x 1000	$T^{\frac{2}{3}}$	R/2·303	R	$T^{\frac{2}{3}}R$	$\log[T^{\frac{2}{3}}R]$
5·0	278	3·60	42·1	0·019	0·0437	1·84	0·265
19·4	292·4	3·43	43·8	0·035	0·0805	3·40	0·537
27·4	300·8	3·33	44·6	0·049	0·113	4·75	0·677

The values of $\log T^{\frac{2}{3}} R/\frac{1}{T}$ were plotted in Graph (18) and gave an activation energy for the recovery process of 10·35 Kcals/mole. This result is comparable with O'Hara's result of 9·4 Kcals/mole for fatigued copper.

As the results above were thought to be fairly satisfactory, it was decided to try to obtain activation energies for recovery after more and less elongation. The previous results on extension of 3 and 5·5% were thought to be

unsatisfactory owing to the measuring stresses used and it was decided to repeat the entire estimations. The material was elongated as before and measured at stresses of $9 \cdot 5 \times 10^{-8}$ and 3×10^{-6}. The 3% elongation was measured at 5·6, 17·8 and 27·2°C and is shown in graphs 19, 20 and 21. The results while not entirely satisfactory are adequate for the purpose required and the data obtained is shown in Table 3.

Table 3 - Copper 3% Elongation

°C	°K	$\frac{1}{T} \times 1000$	$T^{\frac{2}{3}}$	$R/2 \cdot 303$	R	$T^{\frac{2}{3}} R$	$\log[T^{\frac{2}{3}} R]$
5·6	278·6	3·59	42·5	0·014	0·0232	1·38	0·14
17·8	290·8	3·44	43·8	0·024	0·0552	2·93	0·38
27·2	300·2	3·33	44·6	0·036	0·0828	3·69	0·57

These results plotted in Graph 22 give an activation energy for the process of 11·55 Kcals/mole.

The material elongated 5·5% was measured at 0, 5·6 and 17·2°C and is shown in Graphs 23, 24 and 25. The results are much less satisfactory than before but again the gradients of the lines were deduced and the results are shown in Table 4.

Table 4 - Copper Elongated 5·5%

°C	°K	$\frac{1}{T} \times 1000$	$T^{\frac{2}{3}}$	$R/2 \cdot 303$	R	$T^{\frac{2}{3}} R$	$\log [T^{\frac{2}{3}} R]$
0	273	3·66	42·0	0·015	0·0345	1·45	0·161
5·6	278·2	3·59	42·2	0·017	0·039	1·72	0·236
17·2	290·2	3·45	43·8	0·0285	0·0656	2·8	0·462

These results plotted in Graph 26 give the activation energy for the process as 9·4 Kcals/mole.

As can be seen from the graphs the results from the above experiments are not as satisfactory as could have been hoped. However it is felt that the activation energies obtained are at least of the correct order. No attempt was made to measure the slower recovery of the second stage.

It is of some interest to note that the rates of recovery (R) at comparative temperatures are higher for the 5·5% elongation. This is as would have been expected from the theory if the number of point defects was higher as indeed it must be.

(2) Quenching Experiments

From the above results it appeared that the activation energy was controlled either by the dislocation density or the point defect concentration, perhaps even both. It was decided to quench the metal from near the melting point which should introduce point defec ts without appreciably allowing the dislocation density. The quenched-in point defects would diffuse to the dislocation lines exactly as the defects produced by deformation had done in the previous experiments.

The material was cut to 10 c.m. length and annealed in argon at 1020°C for twenty minutes before quenching into water at room temperature. As mentioned above the shock of the fall was reduced by glass wool in the quenching tank. The strain amplitudes of measurement used were $1{\cdot}6 \times 10^{-9}$ and $9{\cdot}5 \times 10^{-7}$ readings being taken at 18, 23·3 and 45°C. The results are

shown in Graphs 27, 28 and 29, and are fairly satisfactory. The data in Table 5 were deduced for the first stage of the recovery.

Table 5 - Copper Quenched from 1020°C

°C	°K	$\frac{1}{T}$ x 1000	$T^{\frac{3}{2}}$	R	$T^{\frac{3}{2}}R$	log $[T^{\frac{3}{2}}R]$
18	291	3·433	44·0	0·0448	1·97	0·295
23·3	296·3	3·37	44·1	0·064	2·84	0·453
45	318	3·4	46·1	0·167	7·75	0·8[illegible]

From graph No. 30 the activation energy for the first stage in the recovery was found to be 12·2 Kcals/mole.

The above results represents a fairly low concentration of both dislocations and point defects. To complete the range it was thought that if the dislocation concentrations could be kept about the same as the 4·2% elongated specimens while the vacancy concentration was increased some interesting conclusions might be drawn.

In order to achieve this the specimens were quenched 15 c.m. in length and allowed to age for 24 hours at room temperature. This resulted in the vacancies and other point defects being attached to the dislocation lines. An elongation of 4·2% was then applied and the specimen measured as before. This it was hoped would result in an increased vacancy concentration while the dislocation density remained about the same as in simple elongation.

Measurements were first made at strain amplitudes of $9·5 \times 10^{-6}$ and 3×10^{-6} and a reasonably satisfactory set of results were obtained, when an allowance was made for the instrument errors mentioned above, Graphs 31 - 34.

However it was later found that the strain amplitude of $9 \cdot 5 \times 10^{-8}$ was just above the critical stress and the specimen was amplitude dependent. The series was repeated using a strain amplitude of $1 \cdot 6 \times 10^{-9}$ for the independant internal friction Graphs 35 - 37. As the first set of results appear to have been only slightly in error the data from both sets of extensions is shown in Table 6.

Table 6 - Copper Quenched 1020°C Elongated 4·2%

°C	°K	x1000	T	R	T R	log [T R]
			Strain Amplitude $1 \cdot 6 \times 10^{-9}$			
19·9	292·2	3·42	44·0	0·0806	3·00	0·58
46	313	3·2	46·0	0·126	5·8	0·76
55·5	328·5	3·02	47·2	0·32	1·51	1·178
			Strain Amplitude $9 \cdot 5 \times 10^{-8}$			
16·7	289·2	3·45	43·5	0·0736	3·2	0·507
29	302	3·31	45·0	0·11	6·95	0·695
42	315	3·18	46·0	0·119	5·481	0·74
53·5	326·5	3·06	47·0	0·129	6·07	0·783

These results were all plotted on Graph (38) and gave the activation energy for the process as 5·5 Kcals/mole. While this result is very different from the previous ones there can be little doubt that it is correct because of the good agreement of the seven results shown.

Discussion

The above results appear to fall into two groups. The first stage of recovery gives an activation energy of about half that for the second and slower stage. The first stage which was most intensively investigated has an activation energy which appears to be dependant on the severity of deformation prior to measurement. The results are group ed in order of working in Table 7.

Table 7

(1) Quenched 1040°C	Q = 12·2 Kcals/mole
(2) 3% elongation	Q = 11·55 Kcals/mole
(3) 4·2% elongation	Q = 10·35 Kcals/mole
(4) Fatigue 10^5 cycles at ± 10,680 lb/in^2	Q = 9·82 Kcals/mole (O'Hara[58])
(5) 5·5% elongation	Q = 9·4 Kcals/mole
(6) Quenched 1040°C - 4% elongation	Q = 5·5 Kcals/mole

From this table it is clear that the activation energy for the process does in fact decrease with the severity of working as had been predicted from the previous results.

The disparity in the result for the long term recovery of the 4·2% elongation indicates that a different process is operating in that part of the spectrum. The activation energy of 20 Kcals/mole (0·87 e.v.) is very close to the value of 0·82 e.v. in the literature for the movement of vacancies and this is strong

proof that the slower stage in the recovery is due to single vacancies.

The first and faster recovery process, having activation energies from 0·53 - 0·25 e.v., indicates the movement of divacancies which from the literature are expected to move with an activation energy of about 0·60 e.v. However, the above results are closer to the estimated values of Bartlett Diens[59] than the result of Kimura and Maddin[39] mentioned above. Manhfelt showed that in copper after 7 - 10% elongation two recovery processes of activation energies, 0·20 and 0·88 e.v., were operative. These results are very close to those found in this investigation.

The results obtained by electrical resistivity measurements of Kimura and Maddin showed two stages in the decay after quenching noble metals. When the metal was quenched from above 850°C a large part of the recovery would be due to divacancies. Quenched from below 850°C most of the recovery was due to single vacancies. Two types of point defect sinks were postulated.

(1) Dislocation networks

(2) Formation of sessile dislocation rings (mainly by divacancies)

It is interesting to note that when a 0·25 mm. wire was quenched from 1030°C the activation energy was 0·6 ± 0·05 e.v., while a 0·64 mm. wire gave 0·72 ± 0·10 e.v. Naturally, the thicker wire suffered the less severe quench and thus, it also appears in these results that the activation energy is reduced by an

increase in the number of point defects.

As mentioned in the introduction, as the material is heated the concentration of divacancies increases. However, it appears that on quenching from the higher temperature, even more of the defects are retained in the form of divacancies than would be expected.

From the results obtained in this investigation and those of Manhfeld, there is little doubt that divacancies are also present after mechanical deformation. It is thought that after both quenching and tensile deformation the recovery process is largely similar.

After either quenching or deformation, a high concentration of free vacancies and divacancies exists in the lattice. These point defects will diffuse to the dislocations to form sessile dislocation rings or collapsed vacancy clusters. As the divacancies will diffuse rather faster than the single vacancies, it is feasible that the first stage in the recovery is due to the divacancies. After a time this recovery will give way to the slower single vacancy recovery stage as the supply of divacancies becomes exhausted. The transition between the two recovery stages will probably be quite complex due to the alteration of the diffusion conditions.

From the results quoted above it appears that the activation energy for divacancy movement is decreased as the point defect concentration increases. While in the literature

there is not a great deal of reliable data, what little exists is not incompatible with the data obtained here. O'Hara's fatigue result seems to indicate that the fatigue damage he introduced was equivalent to that introduced by 4 - 5% elongation. This persistance of divacancies after fatigue is rather strange in view of the speed with which they diffuse. It might have been expected that excess divacancies would have continuously diffused to the dislocation lines during fatigue. However, there can be little doubt of their existence from the activation energy obtained.

The results obtained from the quenching experiments were only partially satisfactory. With the rather large specimens (3/16" dia.) used the rate of cooling would not be very great. It would, for example, be less severe than most of the quenches used by other workers. It must be remembered that the quench would be most severe at the surface of the specimen. The surface, it will be remembered, is the part of the specimen most significant in measurement in the Forster apparatus. The quenching process must then be taken, from both the rate of recovery and the activation energy obtained, to have been the least severe of the processes used.

The quenched-aged-elongated specimens are thought to be somewhat different. When the metal was quenched the usual divacancy and vacancy ageing would take place. The point

defects would either go to the dislocations or form sessile rings. After twenty-four hours at room temperature equilibrium conditions would be approached. Subsequent deformation would release the vacancies and divacancies from the dislocation lines and also sweep the material free of the sessile rings. The process was shown to hold in aluminium by Washburn[44]. Immediately after deformation the dislocation density would be about the same as in simple elongation but with a much higher vacancy concentration. The recovery will then proceed as above. The activation energy obtained is very low compared with the other results above but is well supported by experimental data. It is as well in this case to examine the possibility that the recovery here is due not simply to divacancy movement but to some other mechanism. The activation energy obtained is close to that for interstitial movement given by Huntington[60]. However, as it was calculated by Seitz[61] that the formation of an interstitial atom in copper required 25 e v, this explanation is rather unlikely. Another possibility is the movement of defects along the dislocation lines but this is thought to proceed quite quickly and might well have a lower activation energy than that obtained here.

In conclusion it can be said that there are two stages in the recovery. The first is probably due to divacancies and the second to single vacancies. The actual values of activation energies obtained are only fairly close to those in the literature but as it appears that the value is dependant in some way upon

the concentration of point defects this is not surprising. It should be remembered that superimposed in the divacancy measurement was the normal vacancy recovery and as no attempt was made to separate these the result obtained is not an absolute measurment of divacancies. However, it is quite close to the actual value as the vacancy recovery is quite slow and it is comparable with the other results mentioned where no separation was done either.

GRAPH 4

O.F.H.C. COPPER

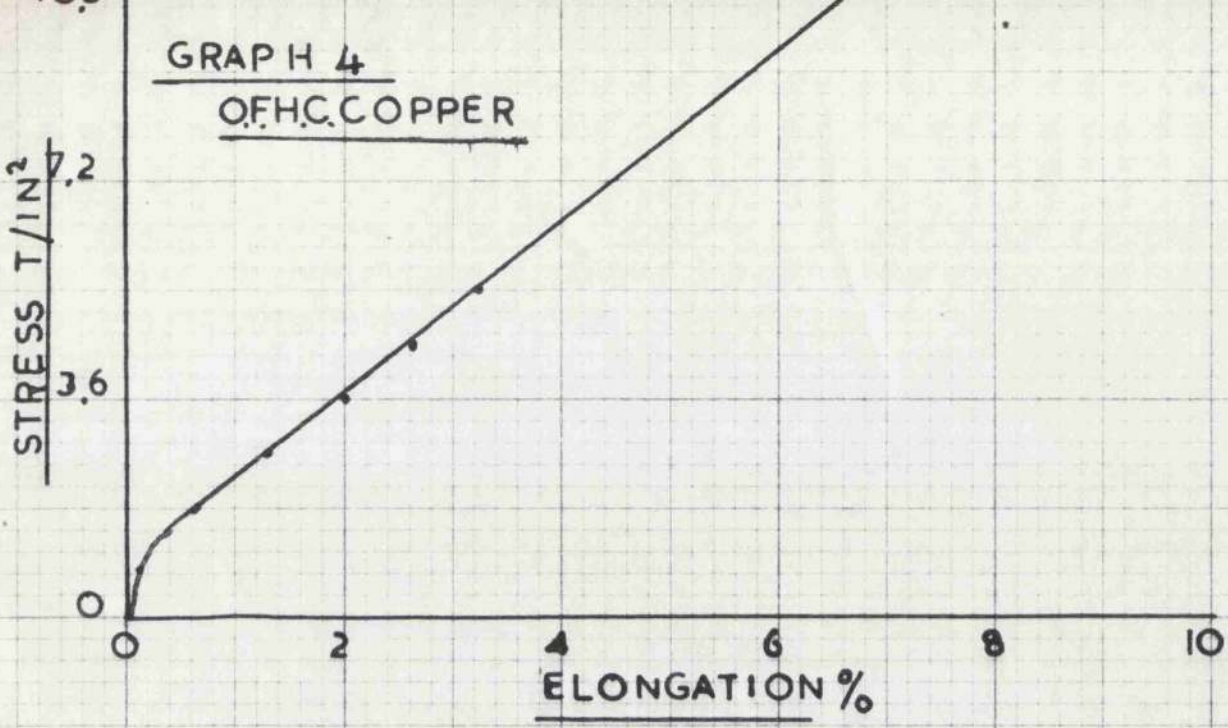

GRAPH 5 INTENAL FRICTION / ELONGATION

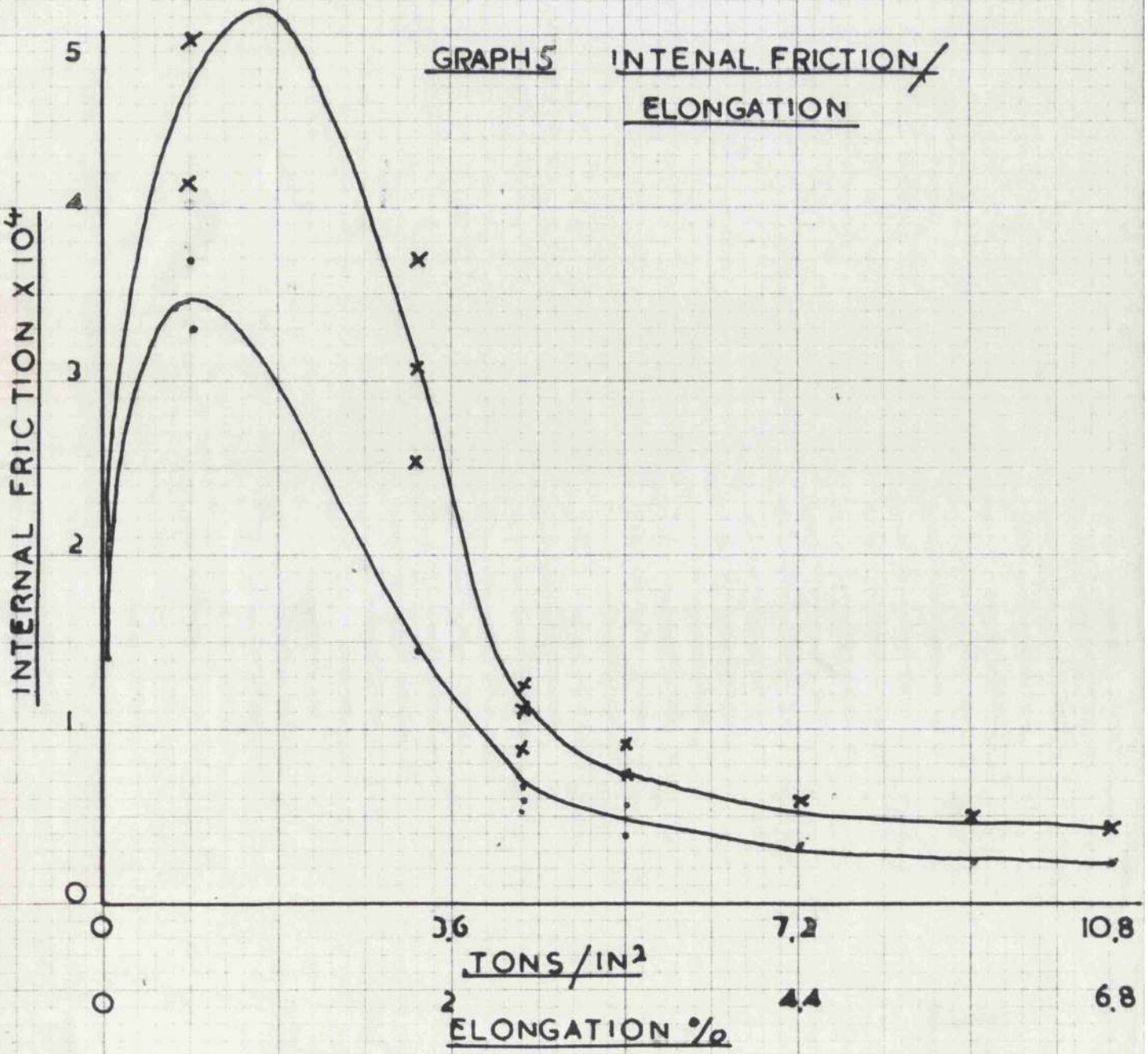

GRAPH 6 COPPER 2% ELONGATION

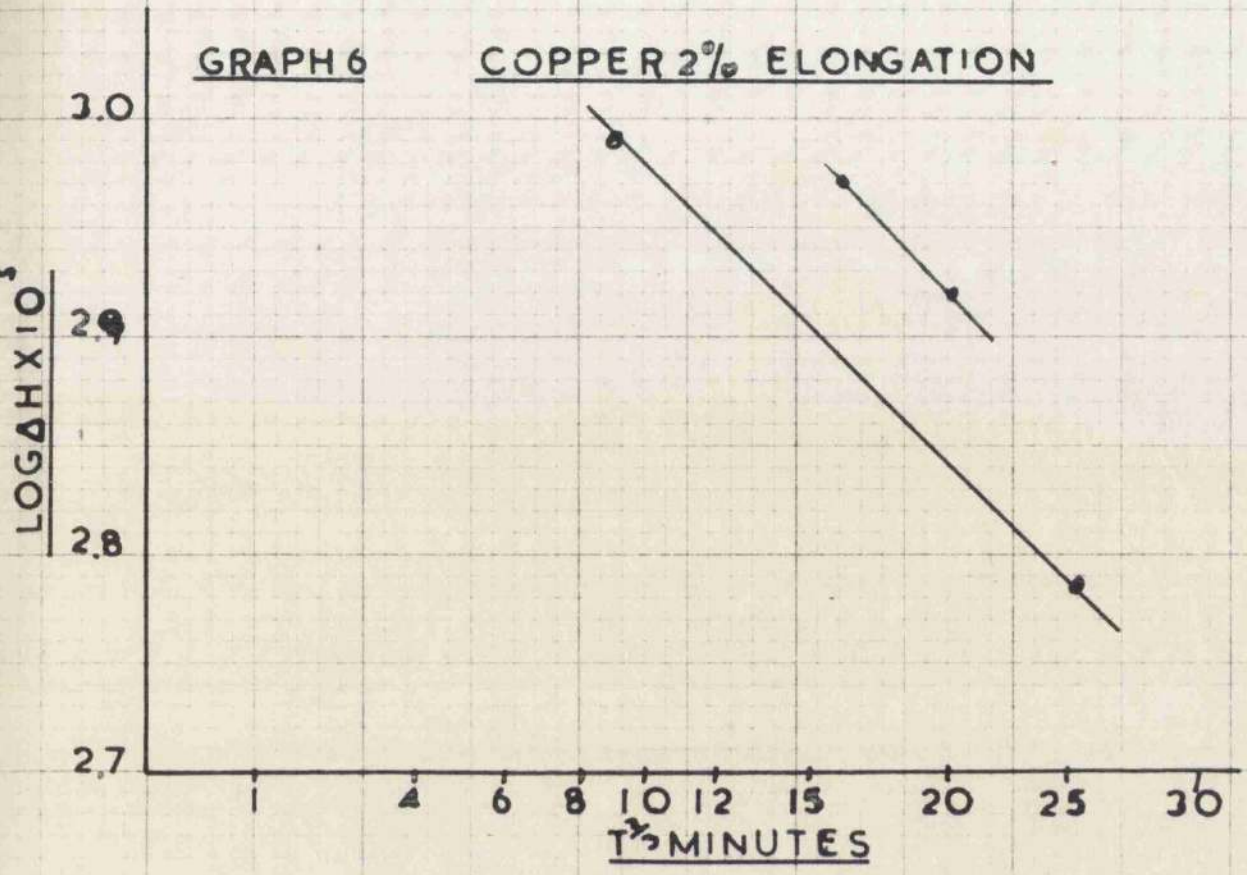

GRAPH 7 COPPER 3% ELONGATION

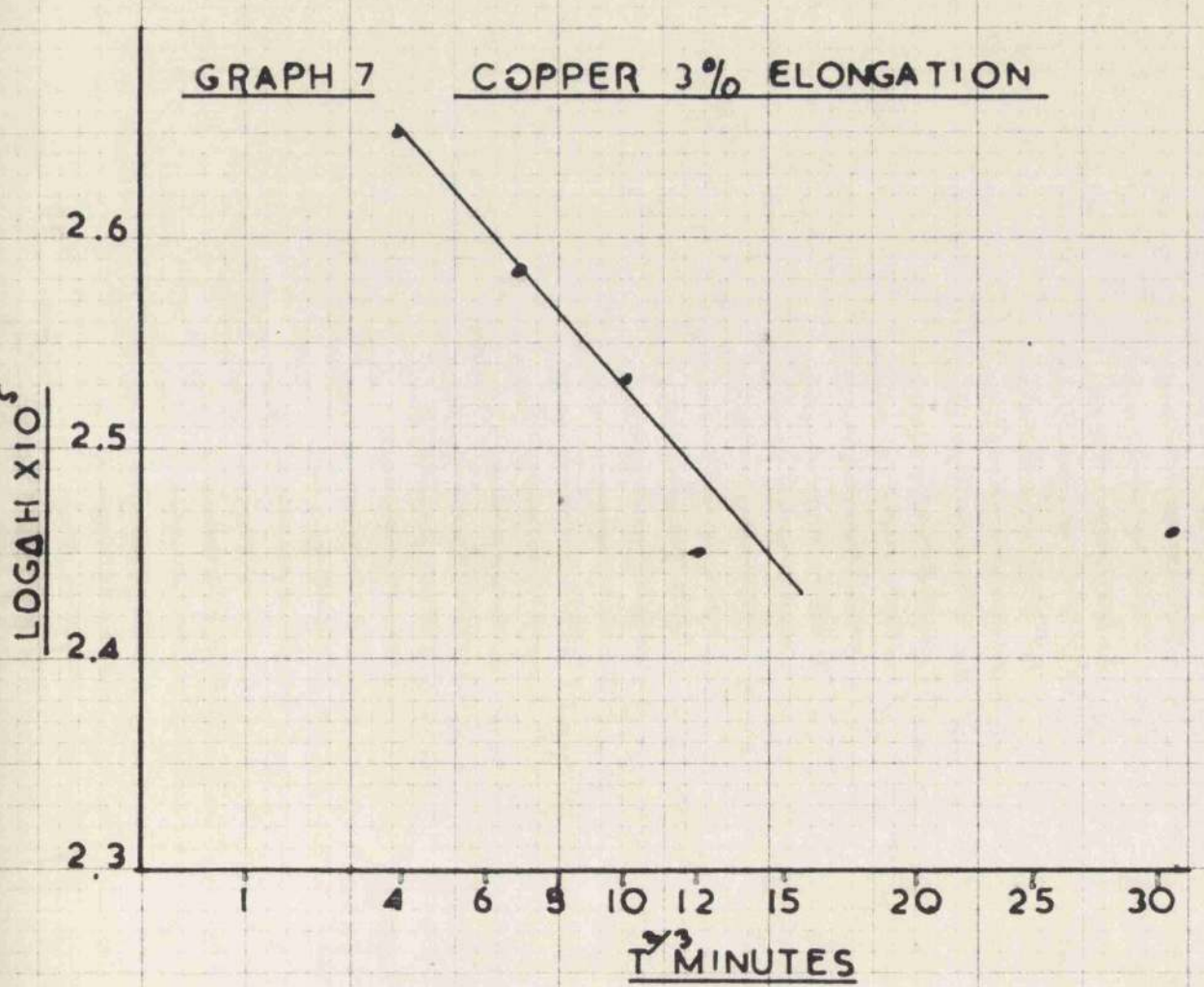

GRAPH 8 COPPER 4.4% ELONGATION

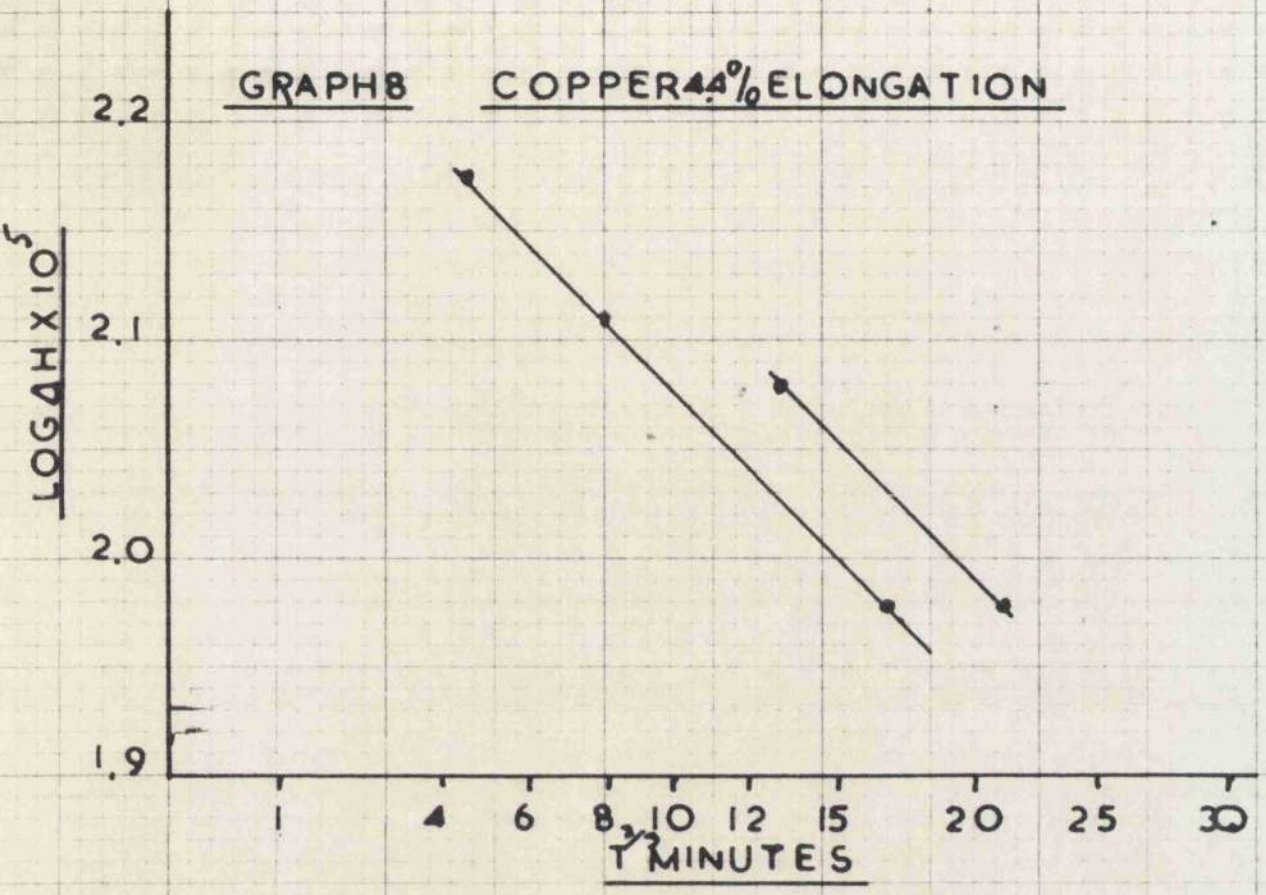

GRAPH 9 COPPER 5.6% ELONGATION

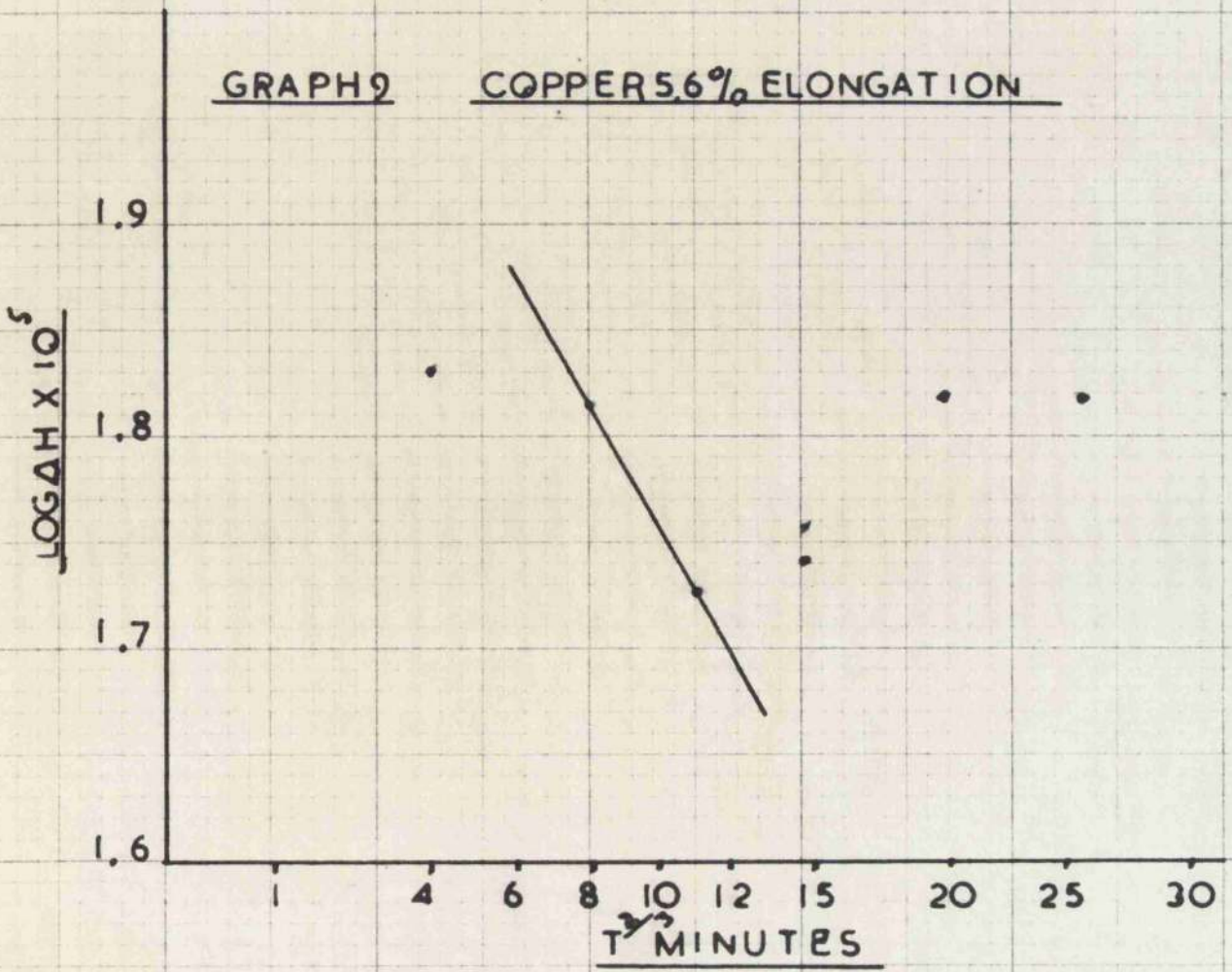

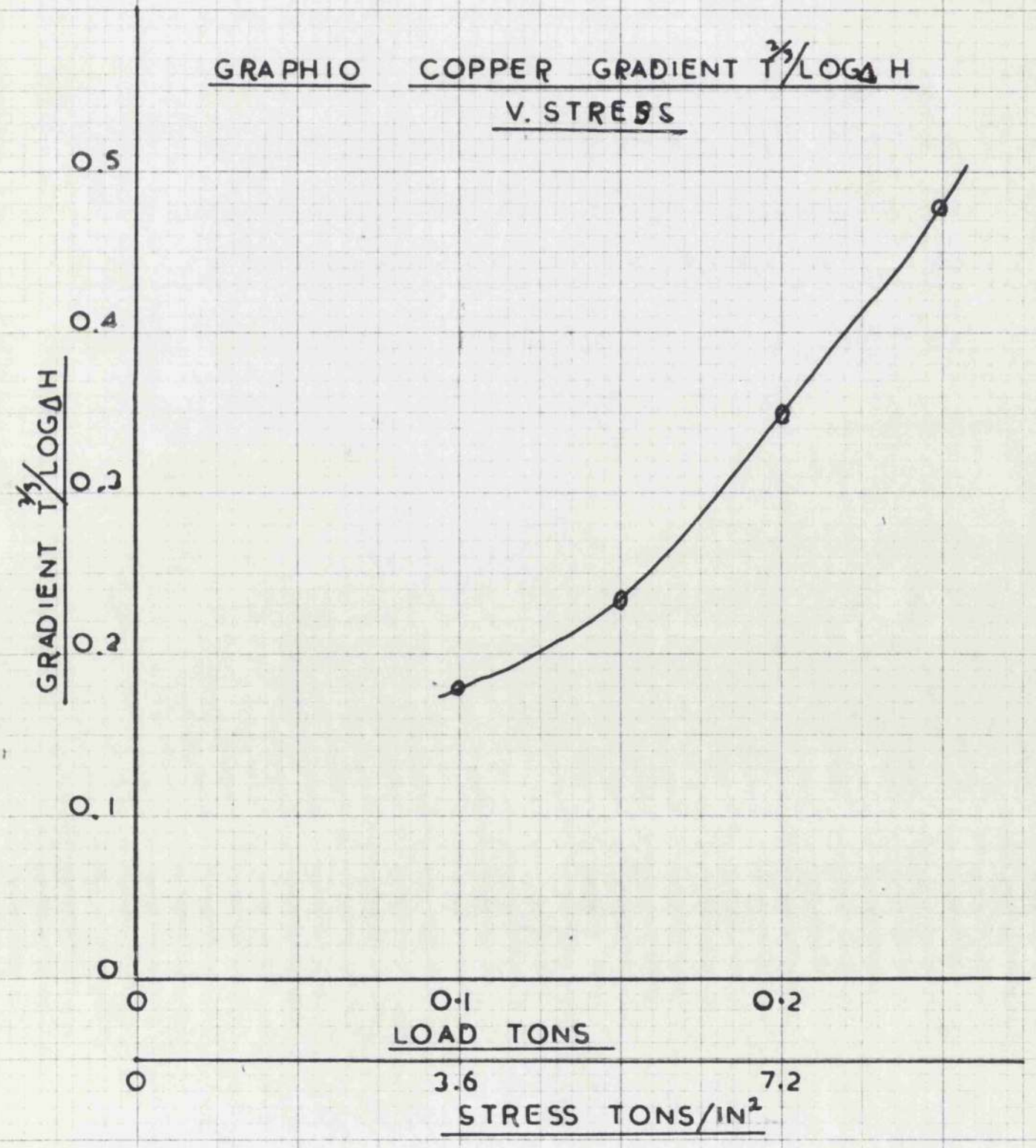
GRAPHIO COPPER GRADIENT T^2/3/LOGΔH V. STRESS
GRADIENT T^2/3/LOGΔH
0.5
0.4
0.3
0.2
0.1
0
0
0·1
0·2
LOAD TONS
0
3.6
7.2
STRESS TONS/IN²

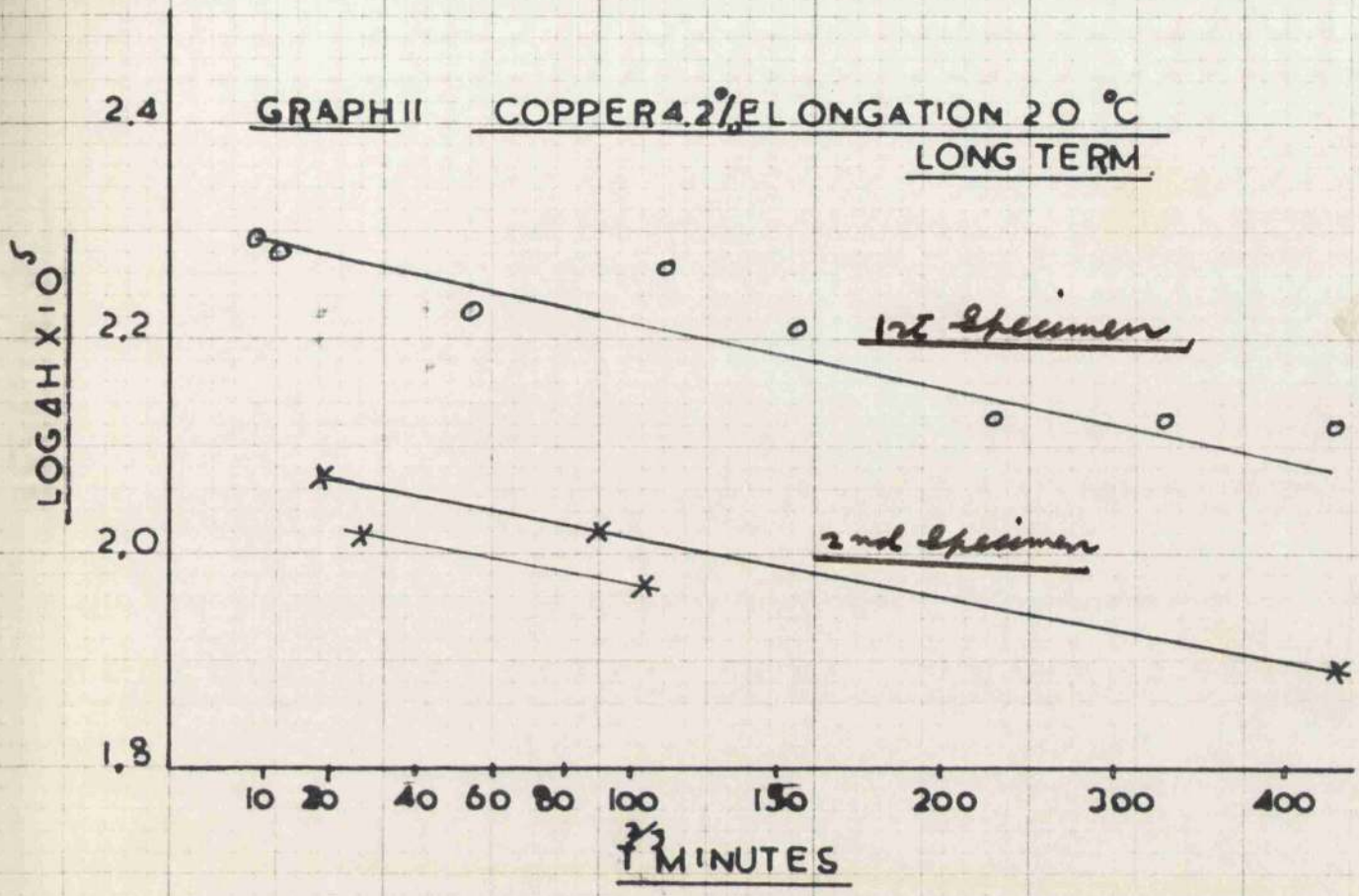
GRAPH II COPPER 4.2% ELONGATION 20 °C
LONG TERM
LOG ΔH X 10^5
2.4
2.2
2.0
1.8
1st Specimen
2nd Specimen
10 20 40 60 80 100 150 200 300 400
T^2/3 MINUTES

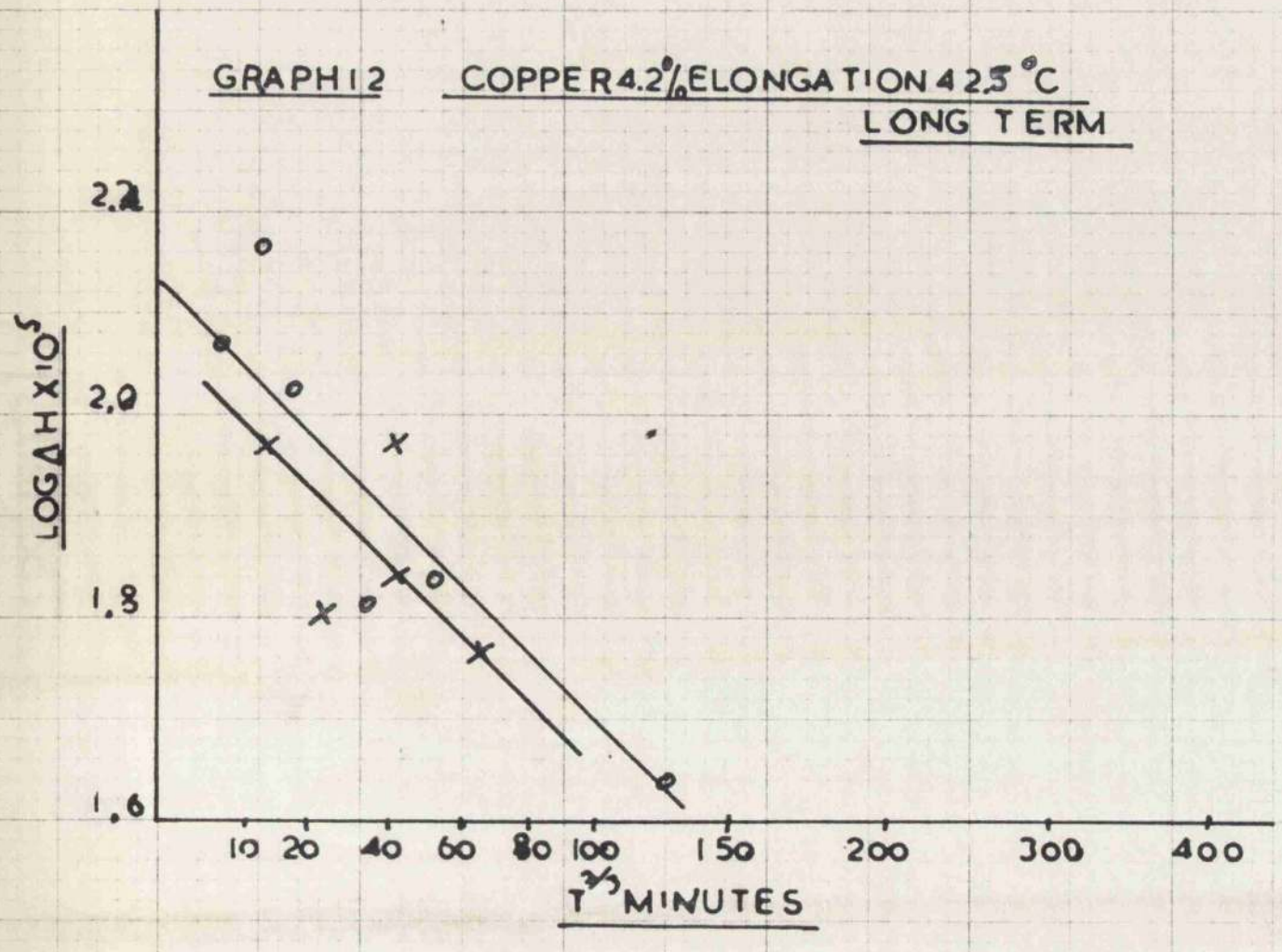
GRAPH 12 COPPER 4.2% ELONGATION 425 °C
LONG TERM
LOG ΔH X 10^5
2.2
2.0
1.8
1.6
10 20 40 60 80 100 150 200 300 400
T^2/3 MINUTES

GRAPH 13 COPPER 4.2% ELONGATION 59 °C
LONG TERM

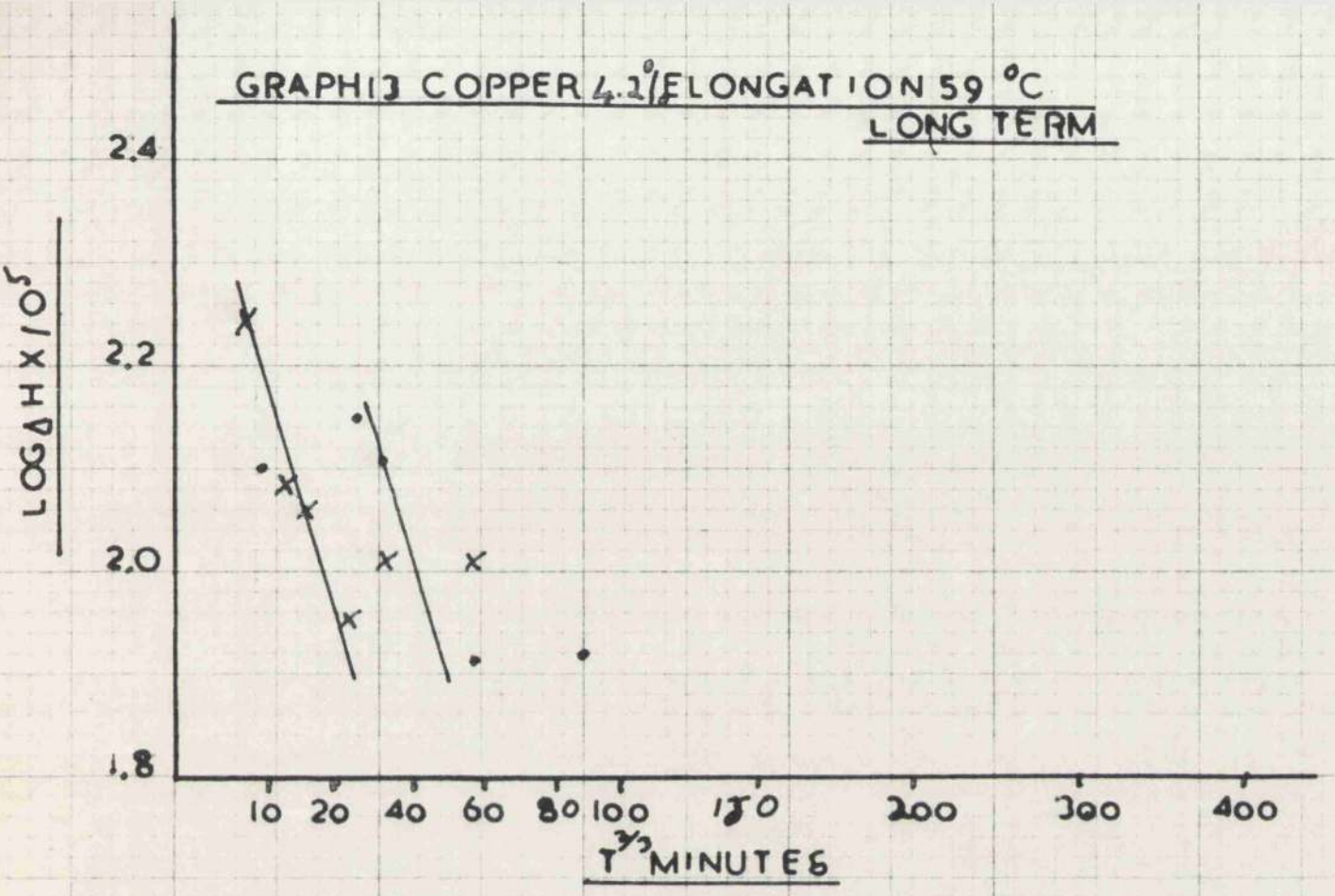

GRAPH 14 COPPER 4.2% ELONGATION LONG TERM

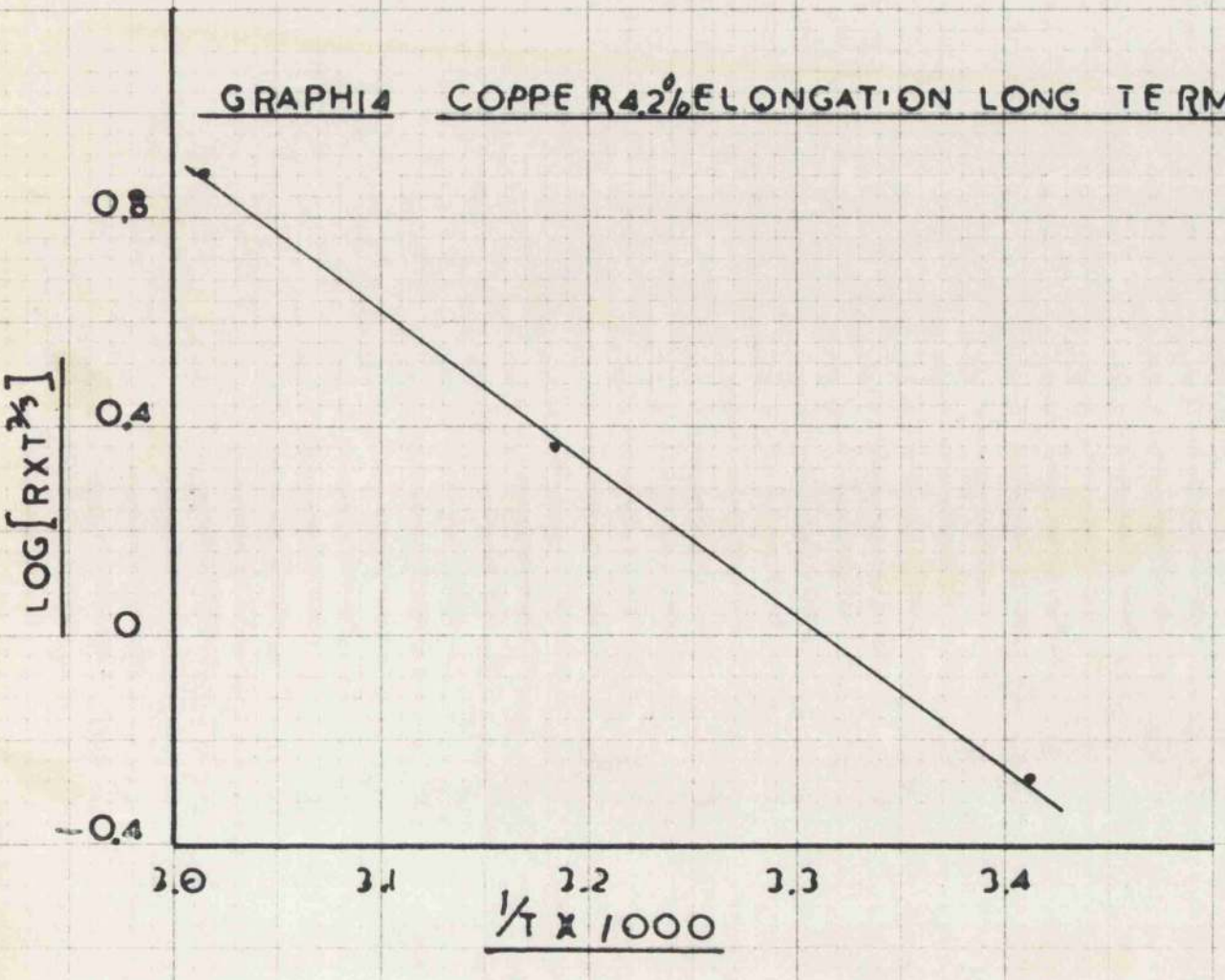

GRAPH 15 COPPER 4·2% ELONGATION 5 °C
SHORT TERM

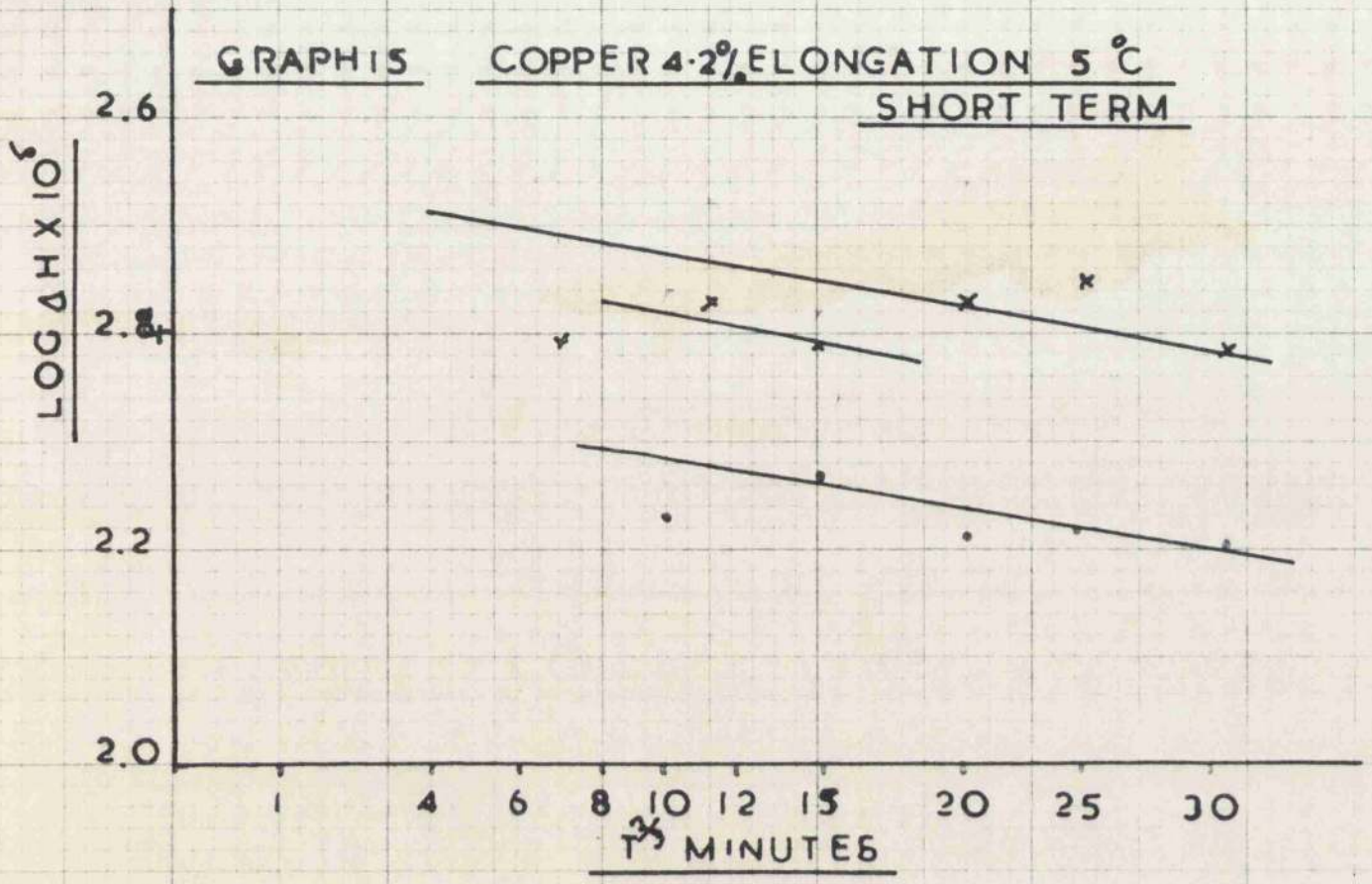

GRAPH 16 COPPER 4·2% ELONGATION 194 °C
SHORT TERM

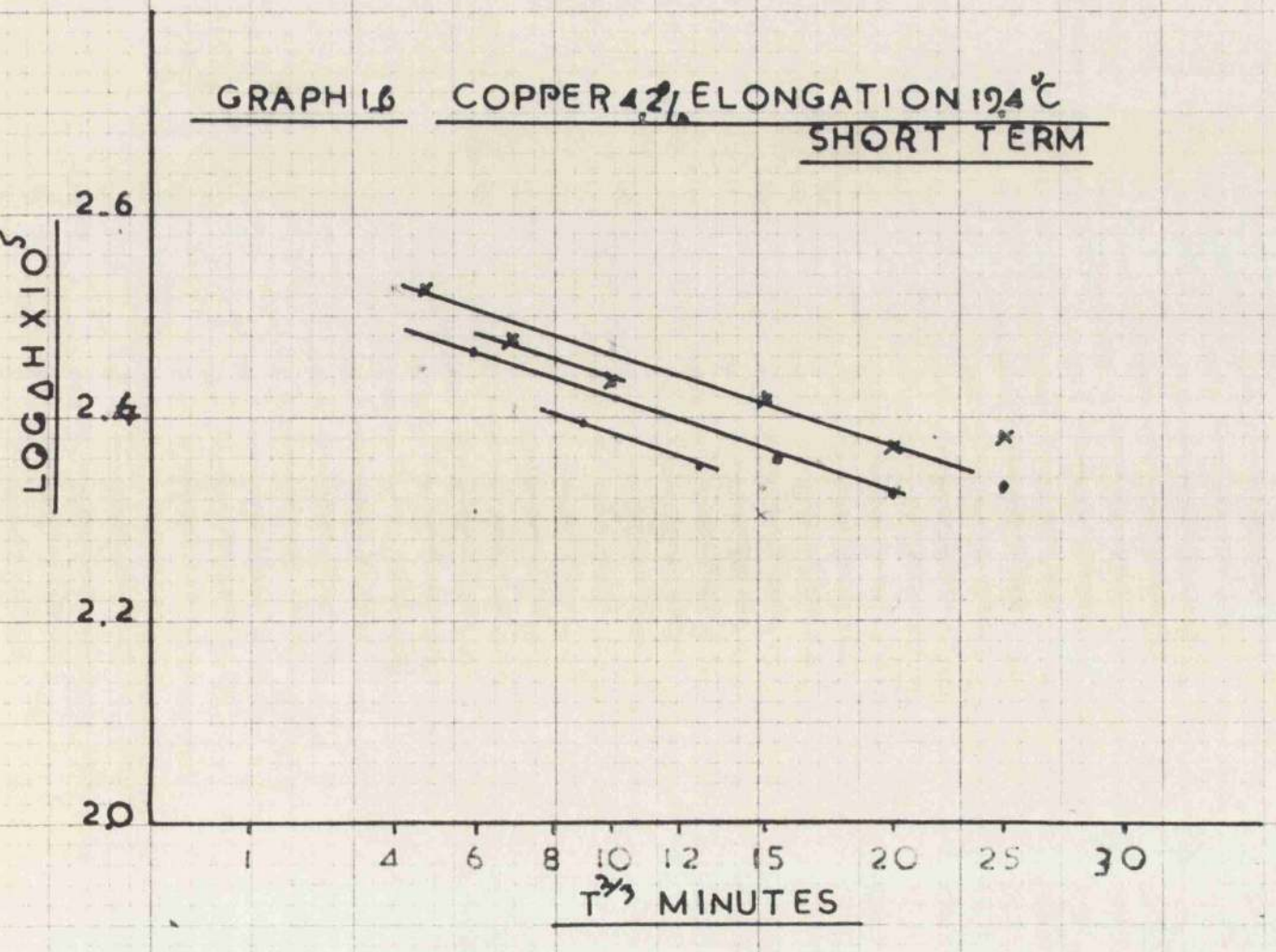

GRAPH 17 COPPER 4.2% ELONGATION 27.8 °C
SHORT TERM

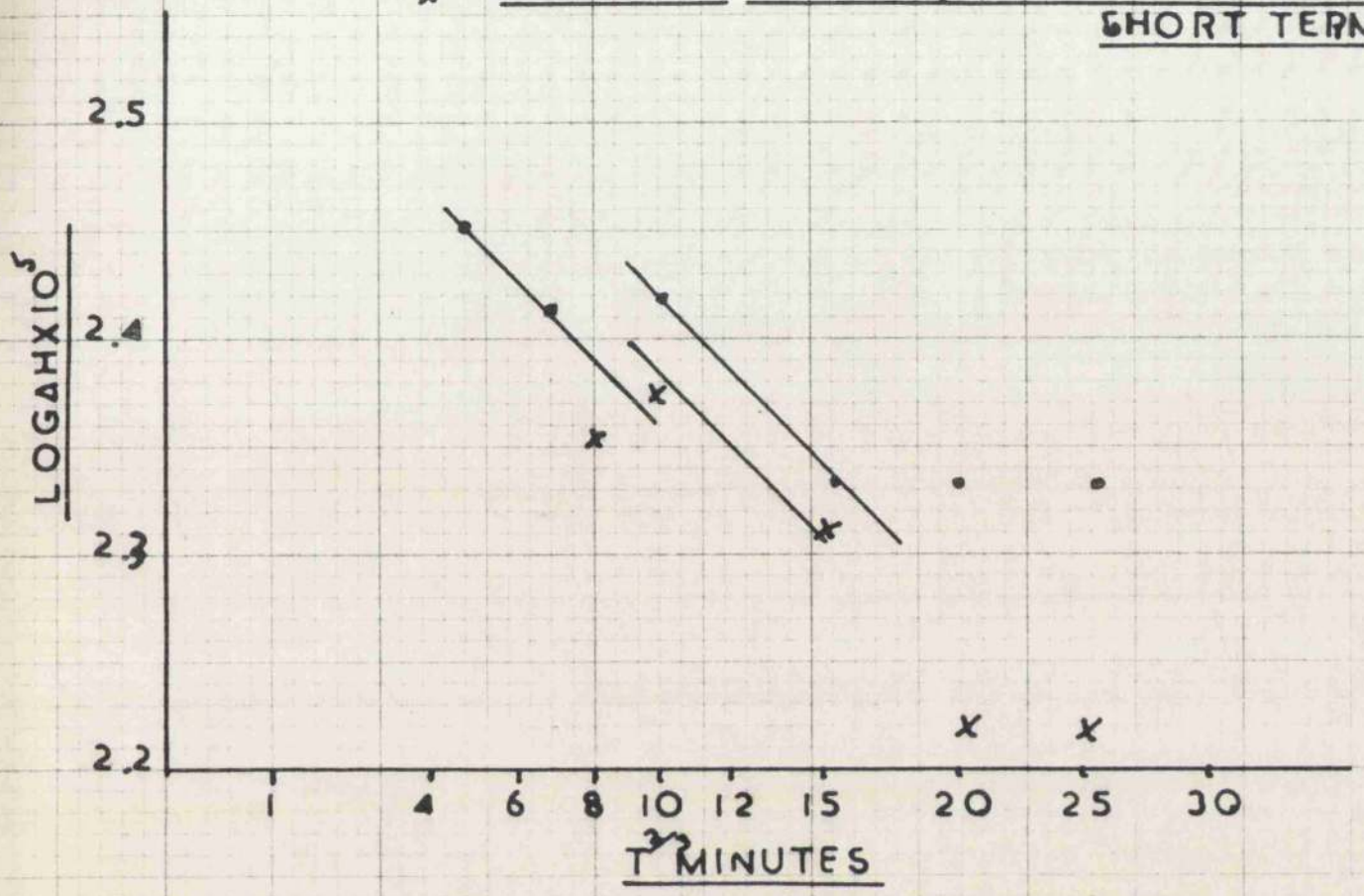

GRAPH 18 COPPER 4.2% ELONGATION
SHORT TERM

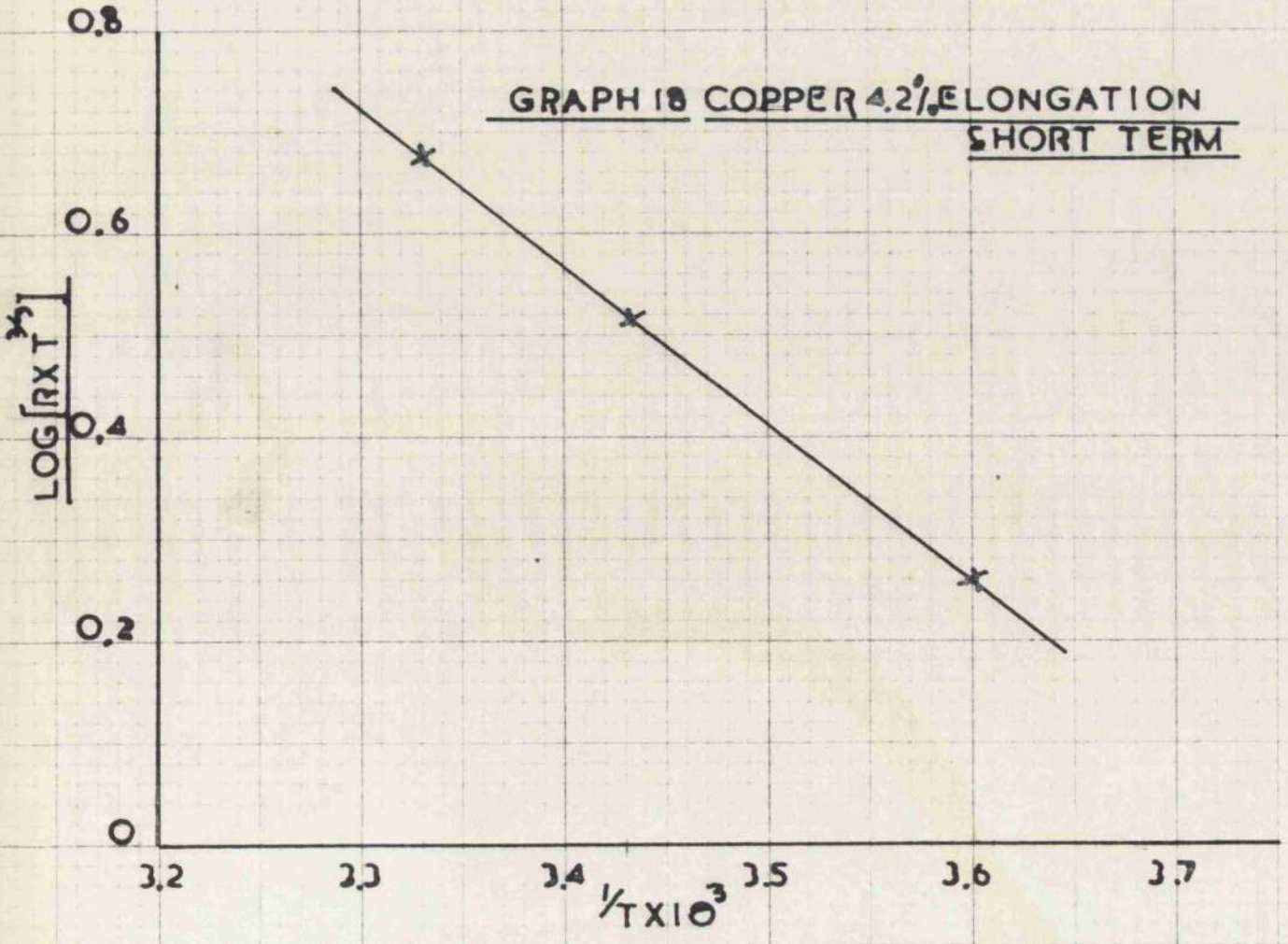

GRAPH 19 COPPER 3% ELONGATION 5.6 °C

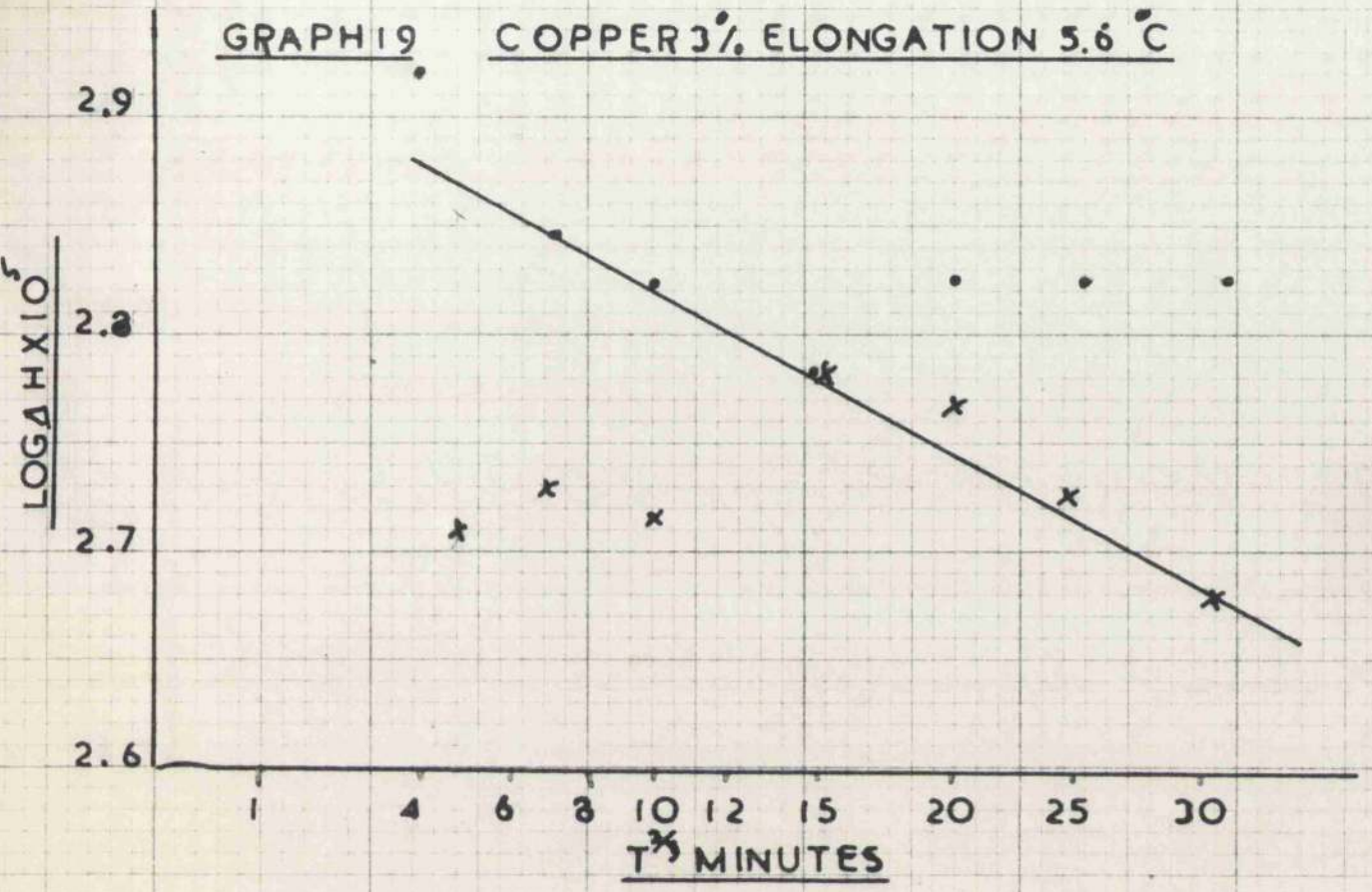

GRAPH 20 COPPER 3% ELONGATION 17.8 °C

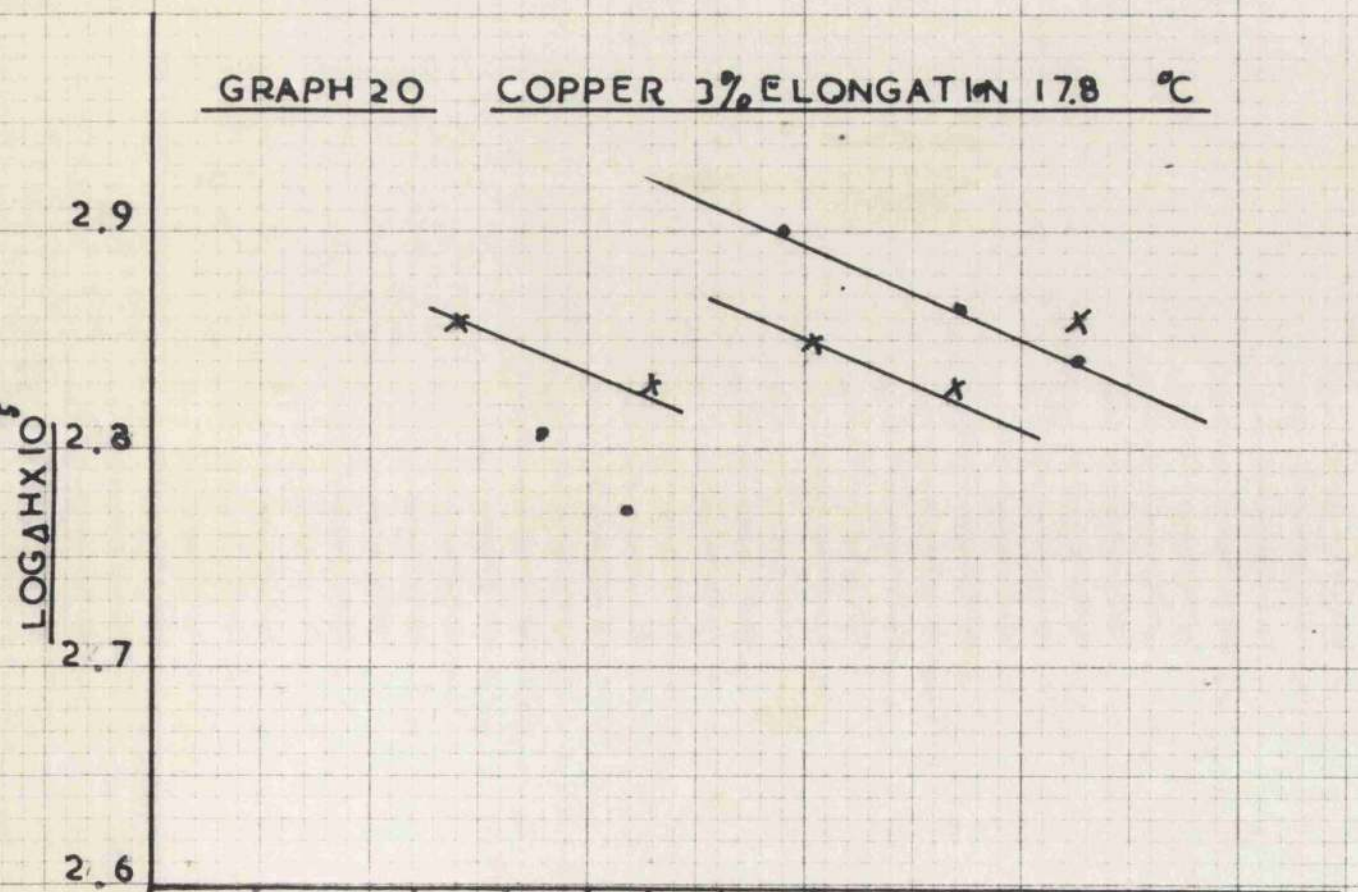

GRAPH 21 COPPER 3% ELONGATED 27.2 °C

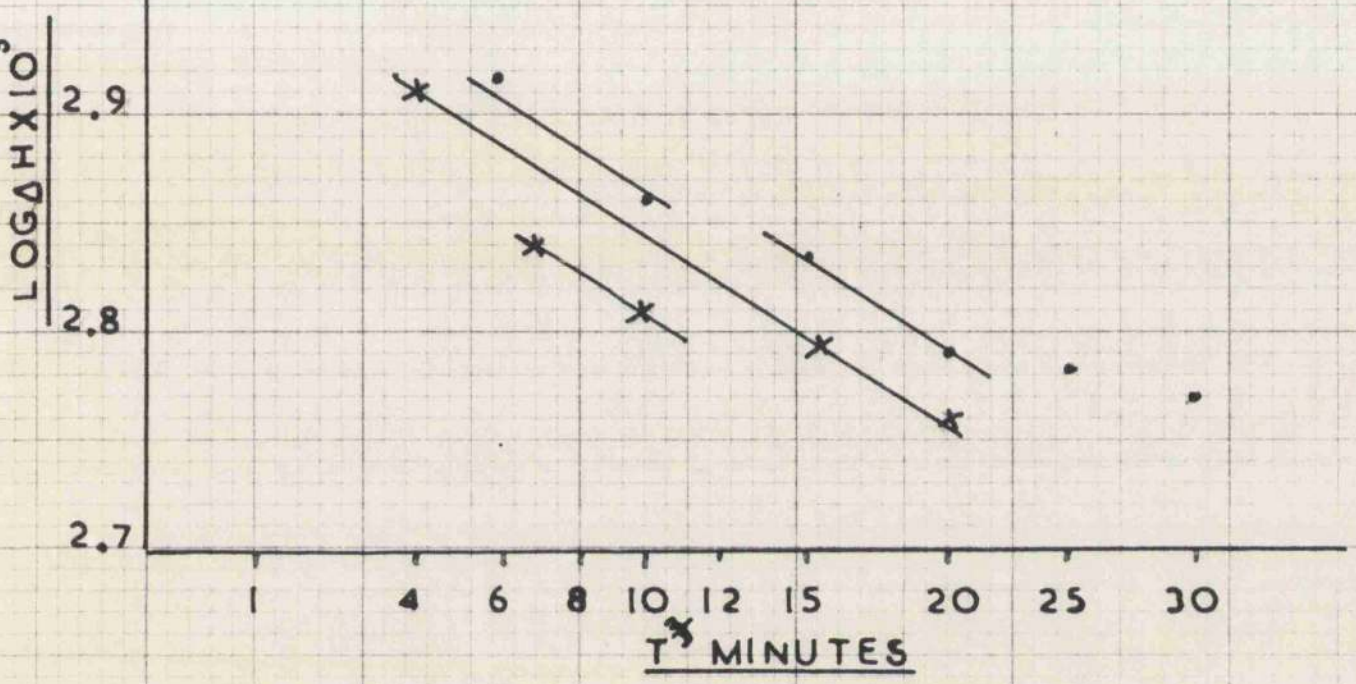

GRAPH 22 COPPER 3% ELONGATION

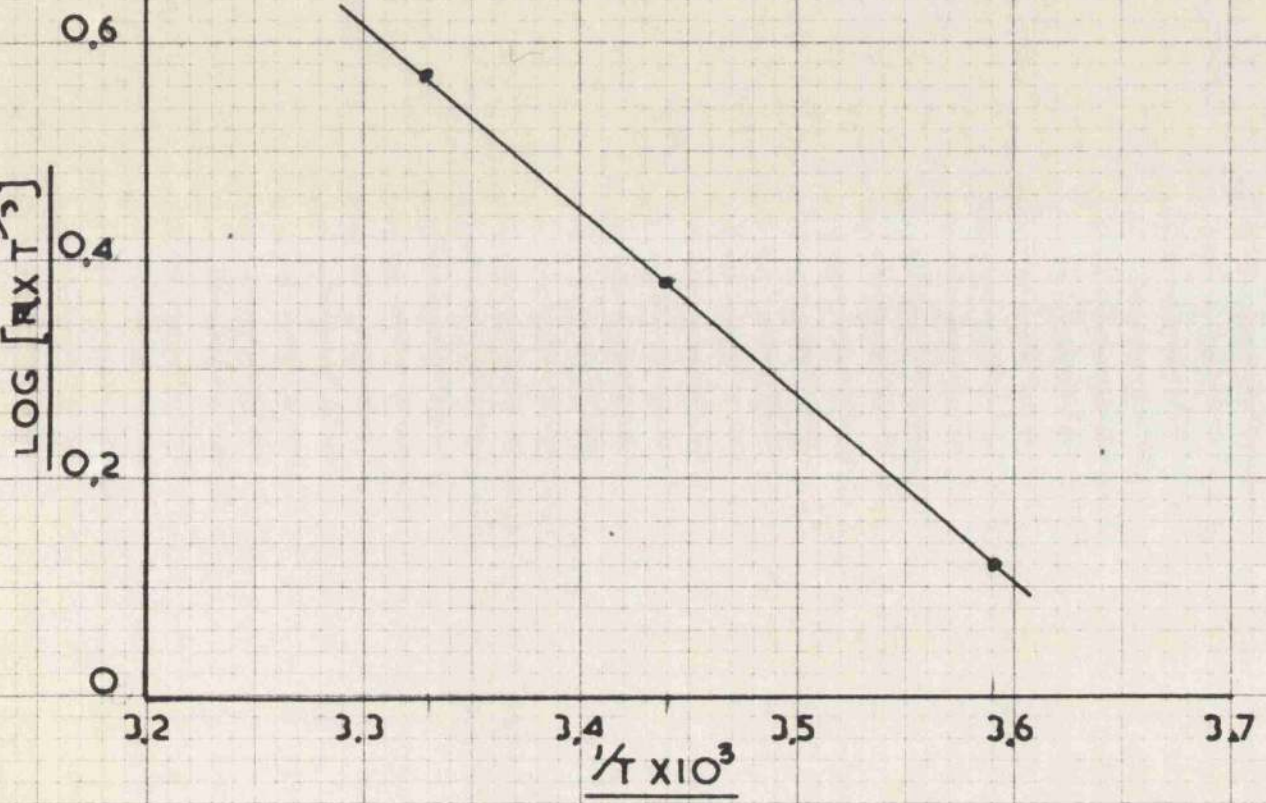

GRAPH 23 COPPER 5.5% ELONGATION 0 °C

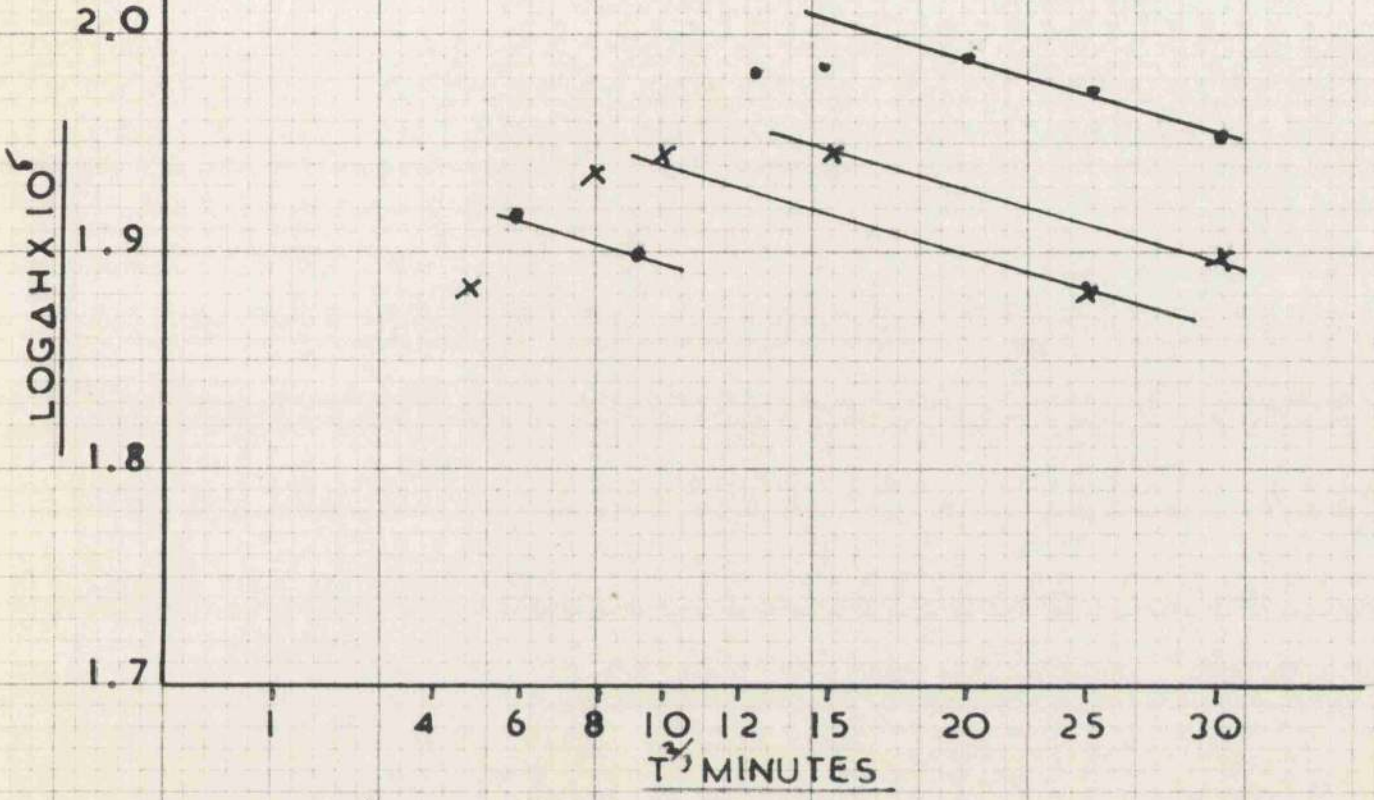

GRAPH 24 COPPER 5.5% ELONGATION 5.6 °C

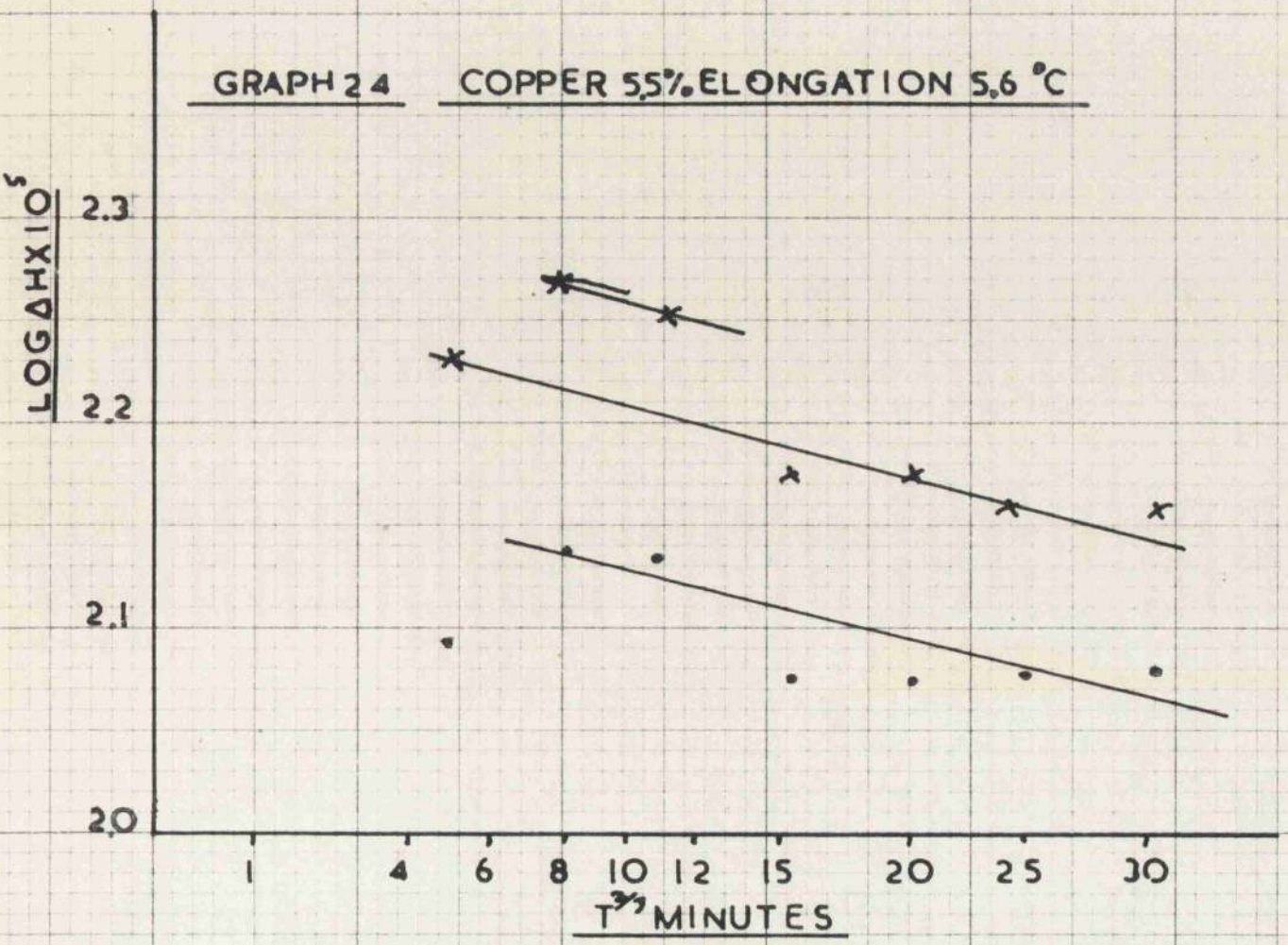

GRAPH 25 COPPER 5.5% ELONGATION 17.2 °C

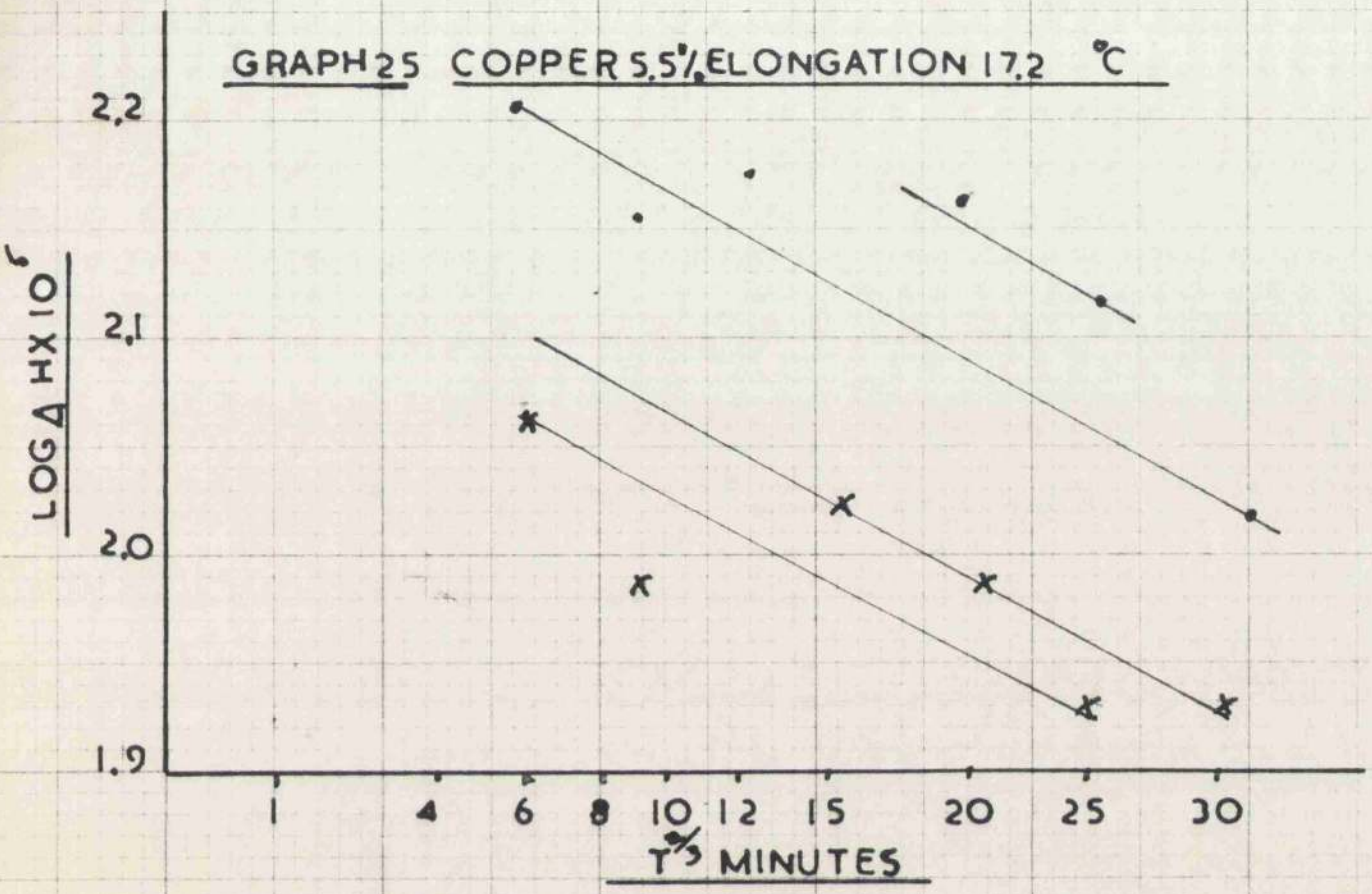

GRAPH 26 COPPER 5.5% ELONGATION

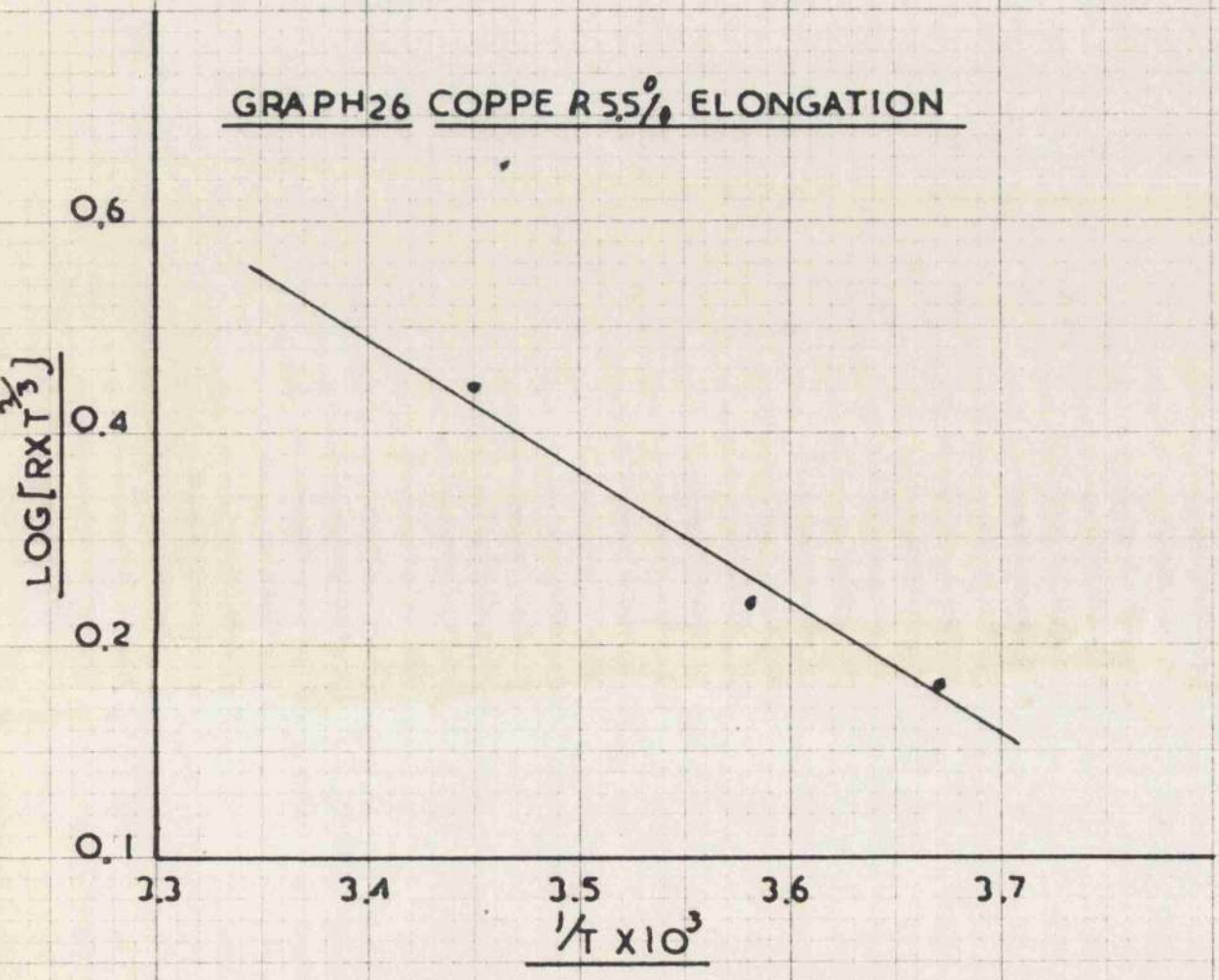

GRAPH 27 COPPER QUENCHED 1020 °C
18 °C

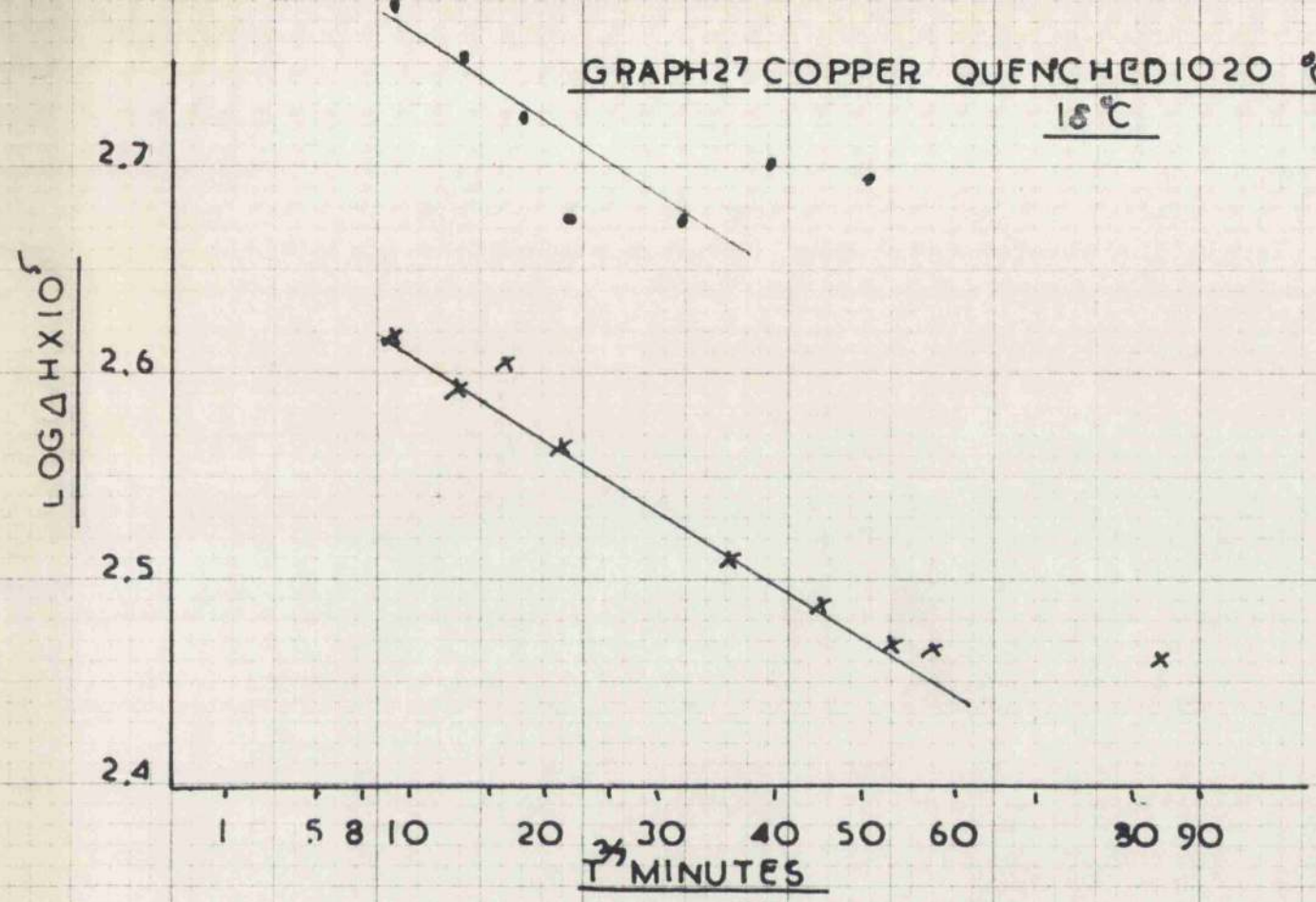

GRAPH 28 COPPER QUENCHED 1020 °C
23 °C

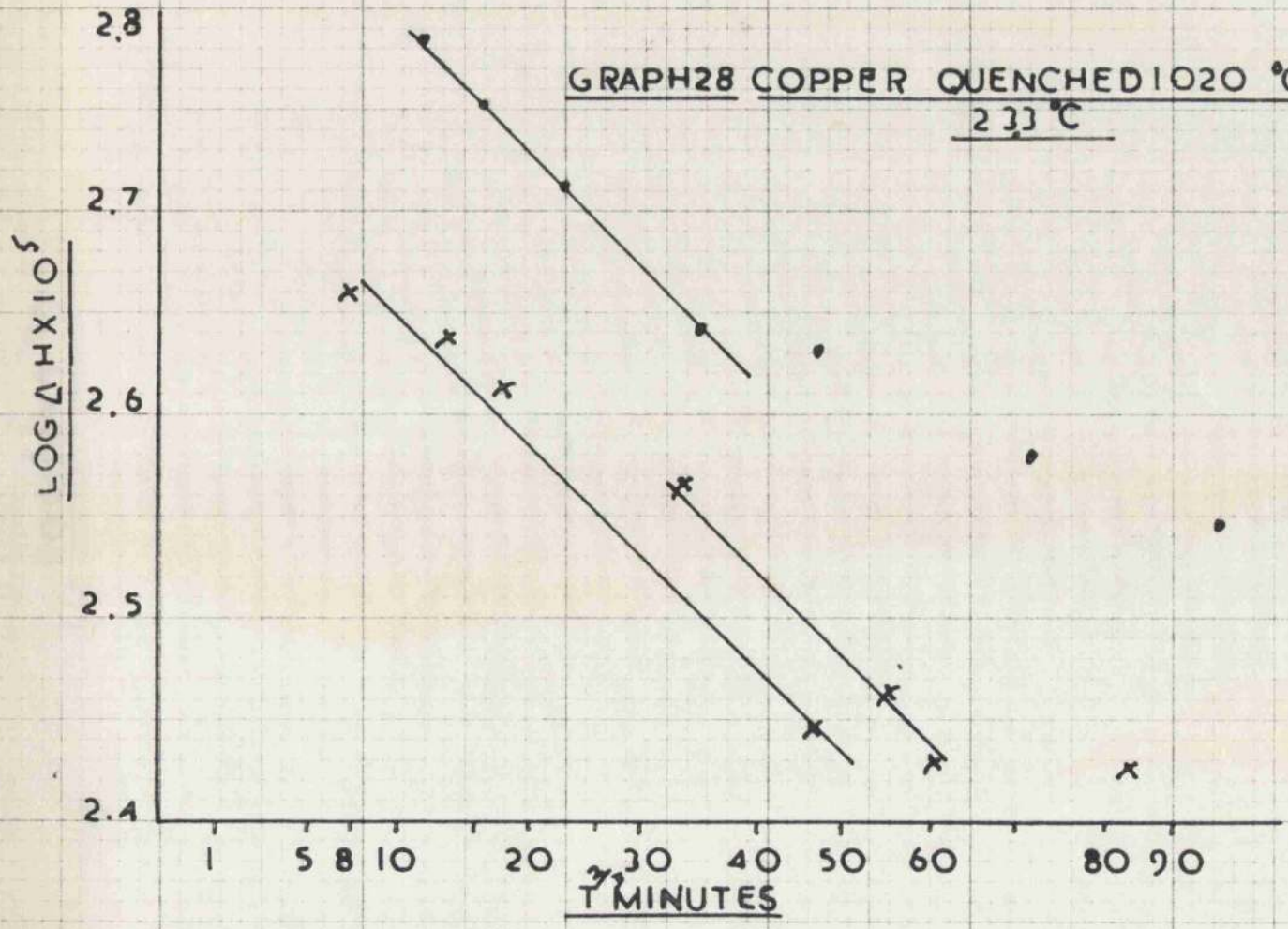

GRAPH 29 COPPER QUENCHED 1020 °C
45 °C

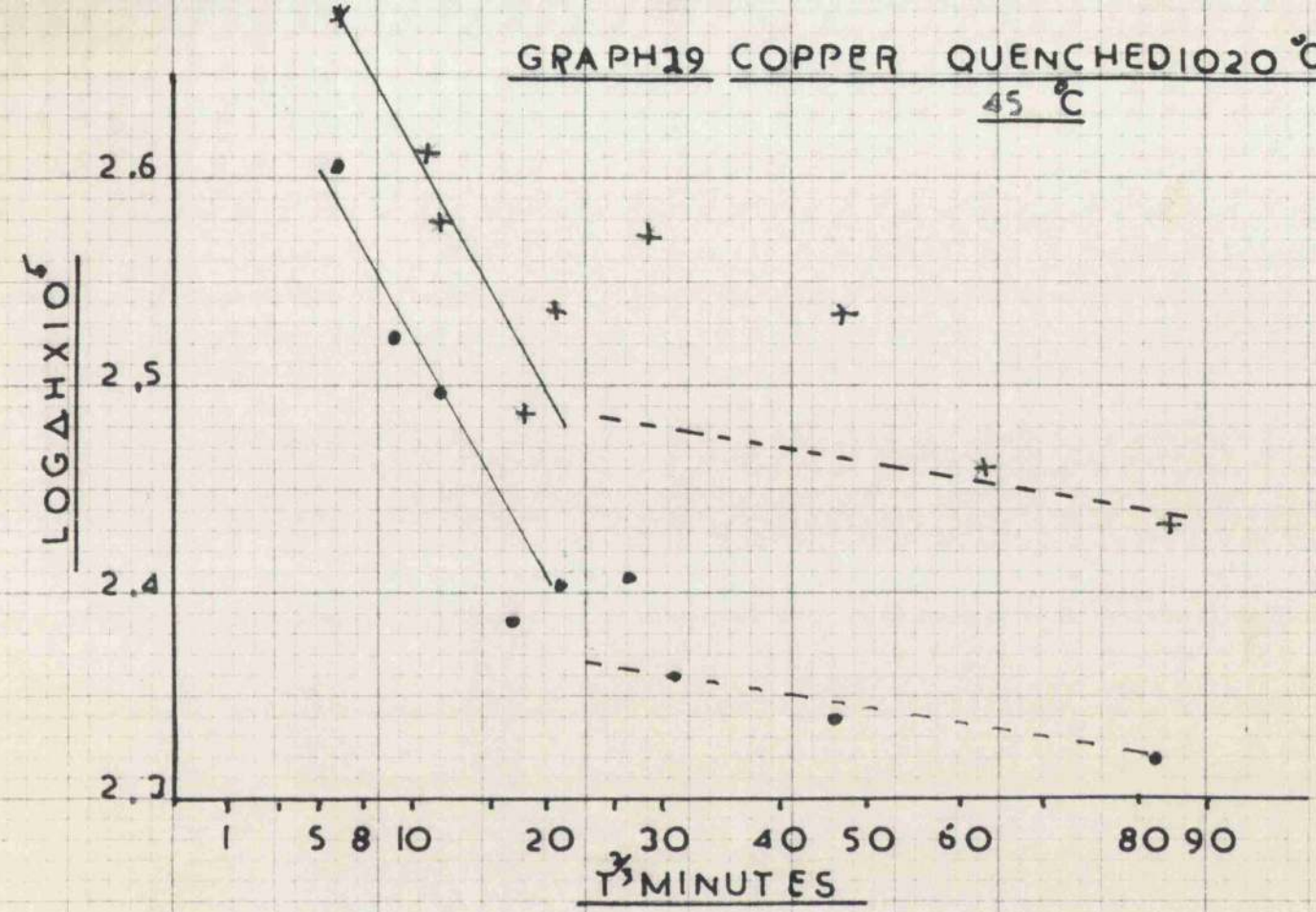

GRAPH 30 COPPER QUENCHED 1020°C

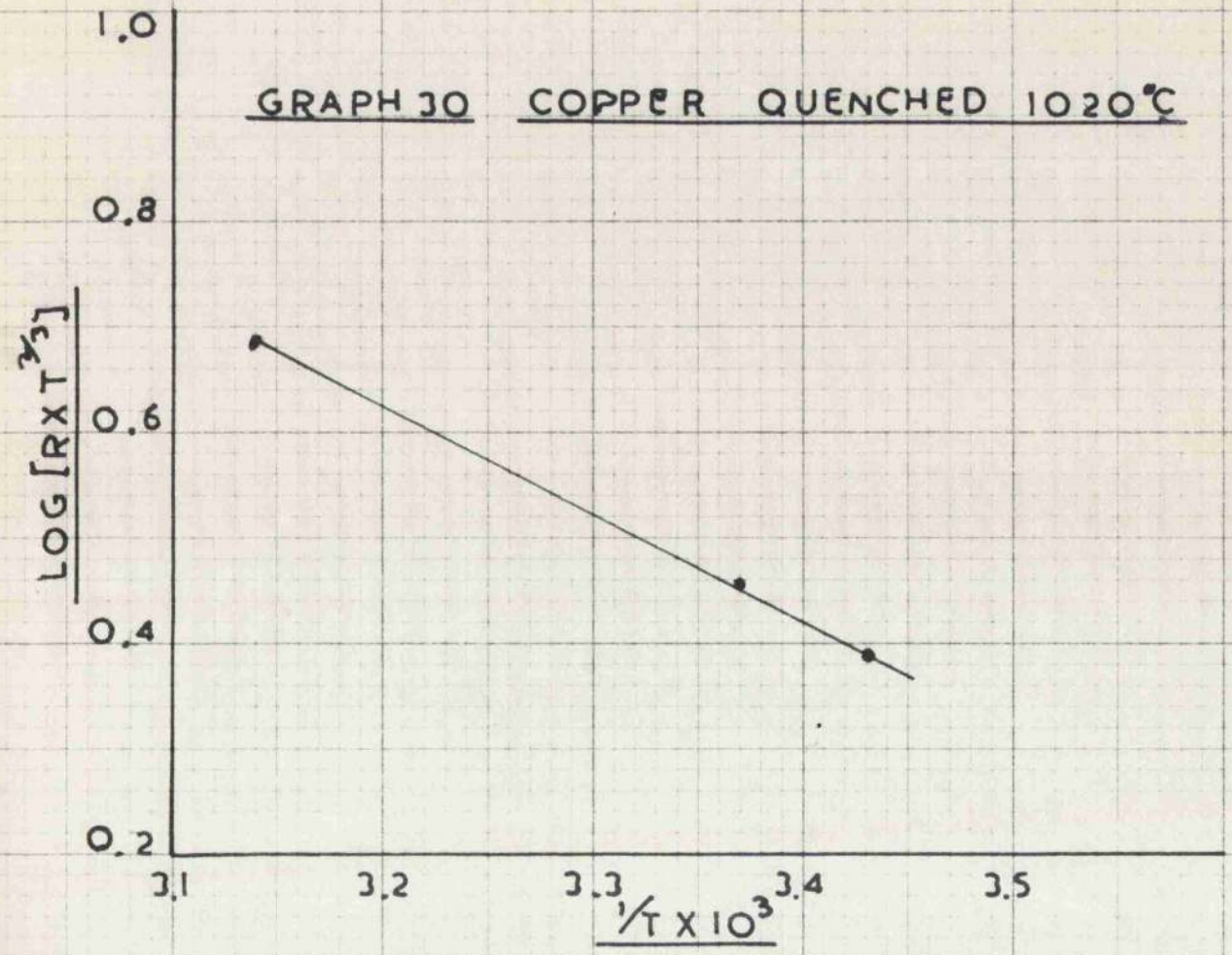

GRAPH 31 COPPER QUENCHED 1020°C 4·2% ELONGATION
STRAIN AMPLITUDE 10^{-7}, 199°C

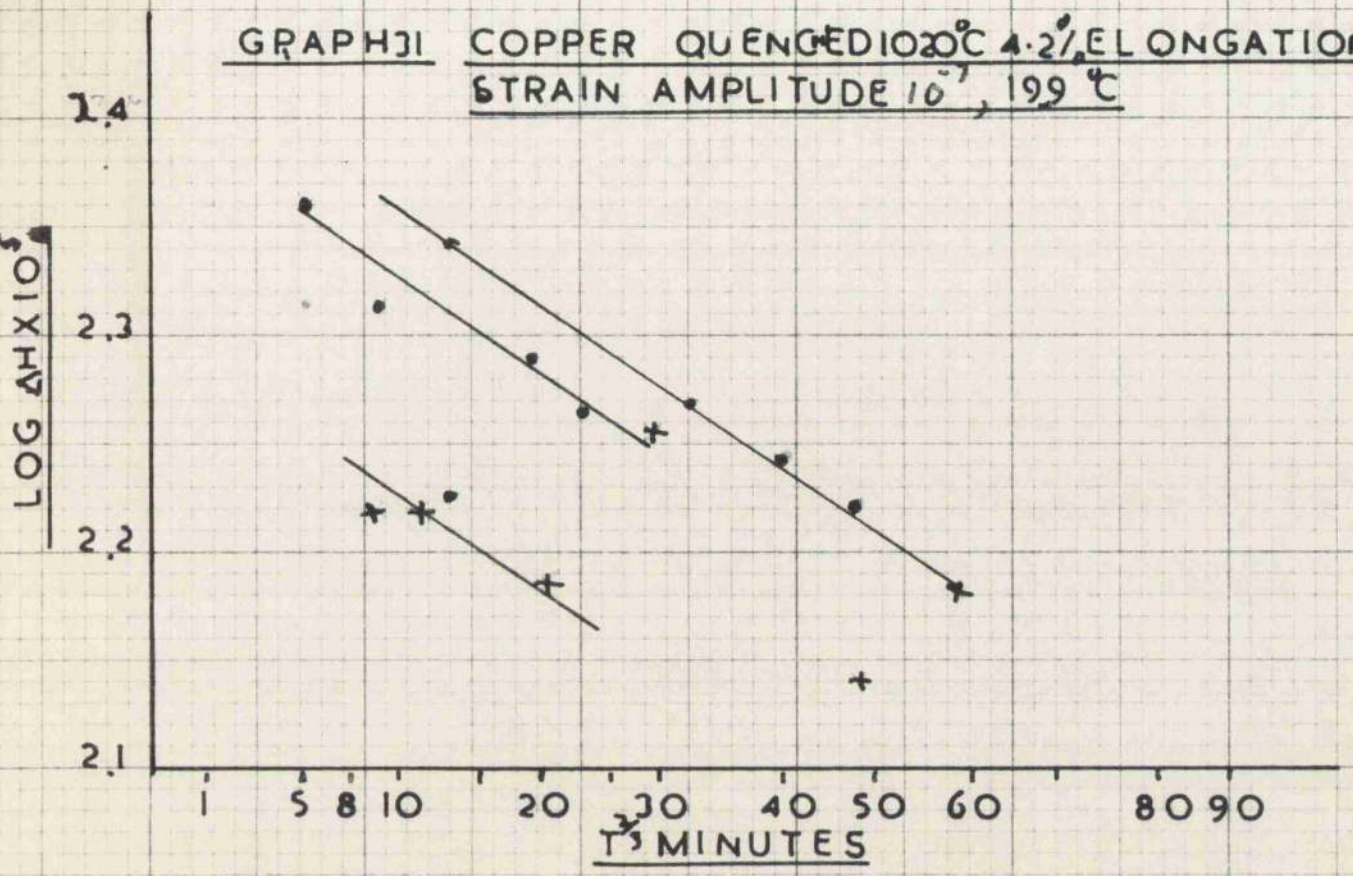

GRAPH 32 COPPER Q. 1020°C EL. 4% 26°C
$\varepsilon_0 = 10^{-7}$

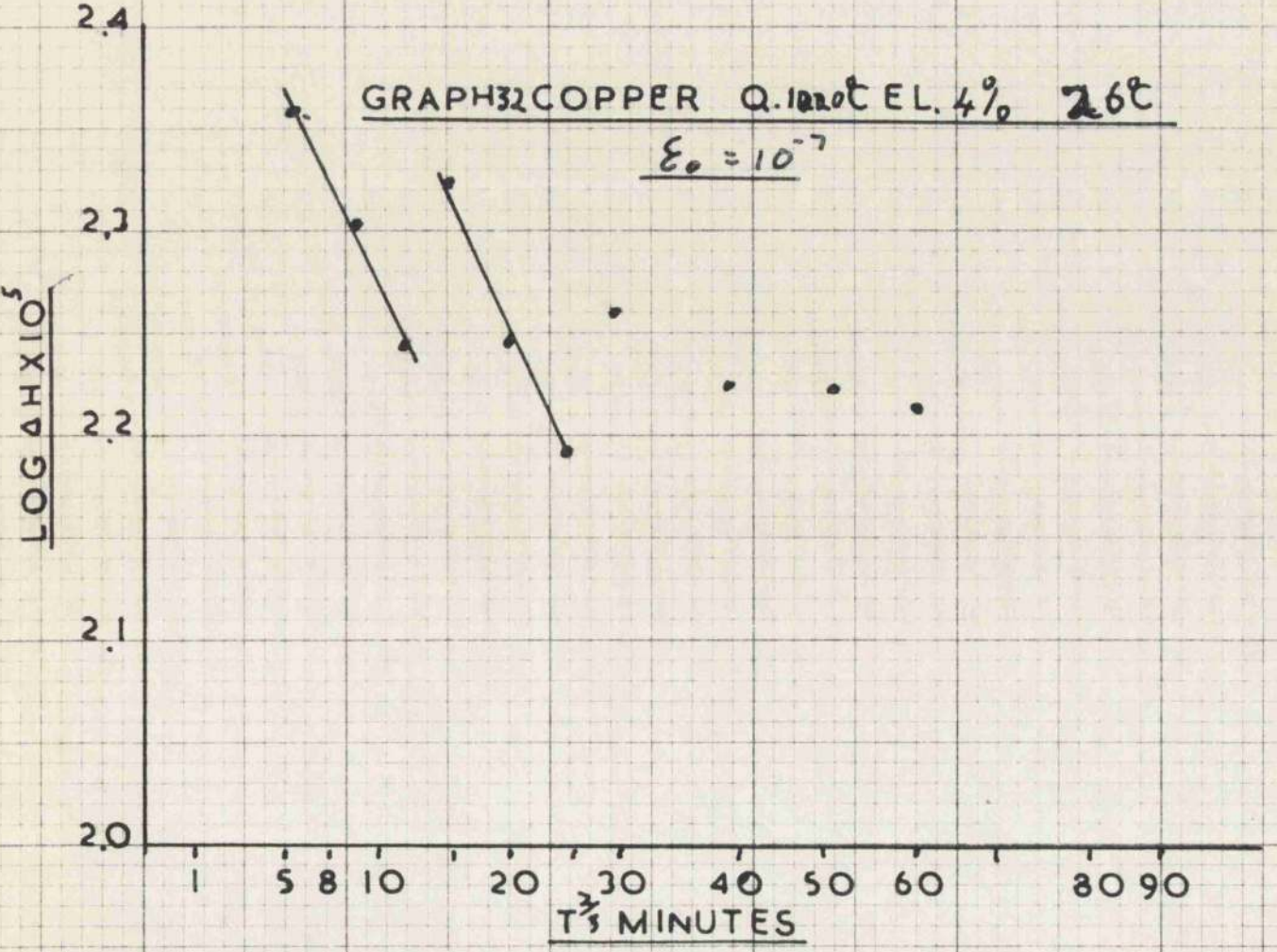

GRAPH 33 COPPER Q 1020°C EL 4.2% 42°C

$\varepsilon_0 = 10^{-7}$

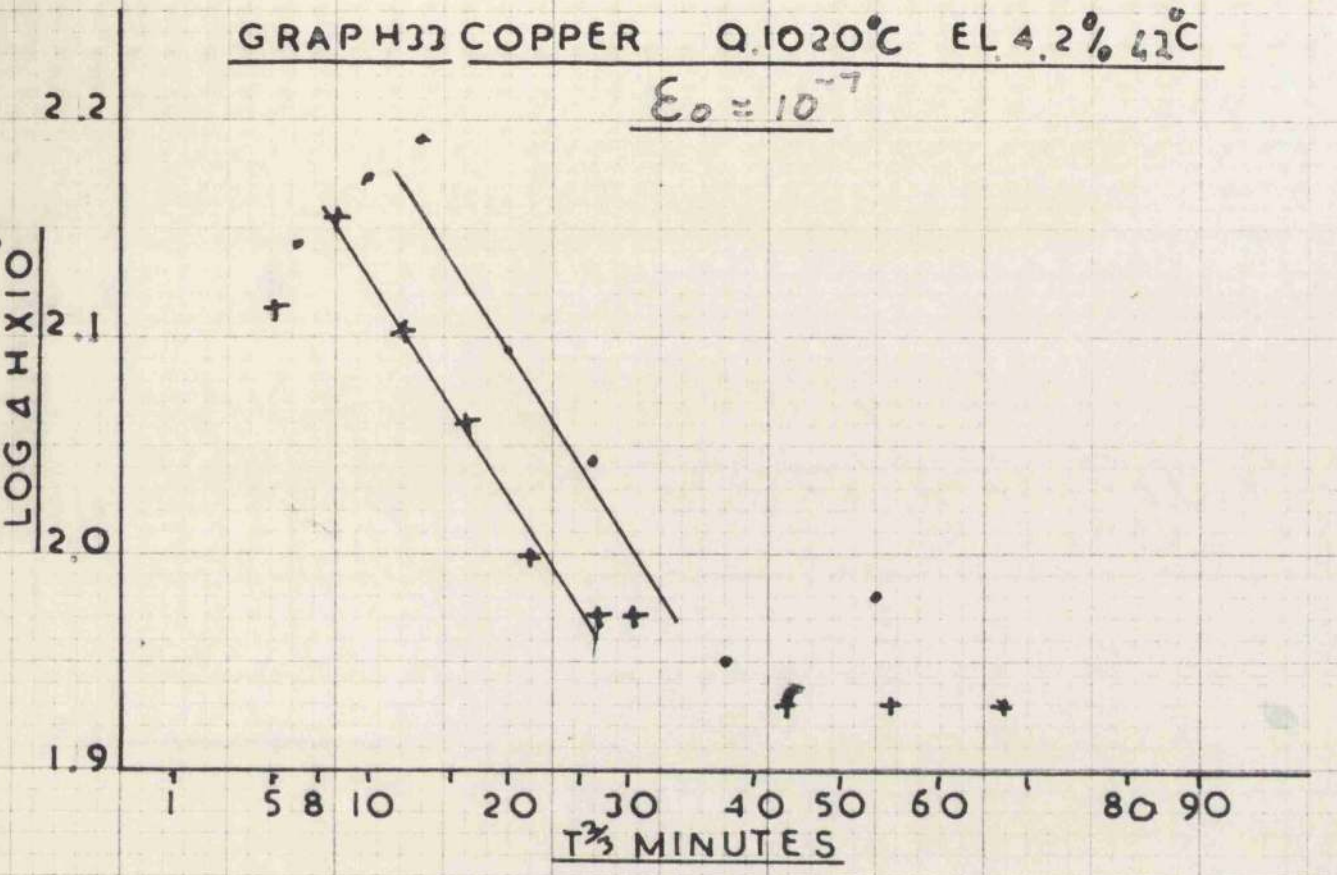

GRAPH 34 COPPER Q 1020°C EL 4.2%, 53.3°C

$\varepsilon_0 = 10^{-7}$

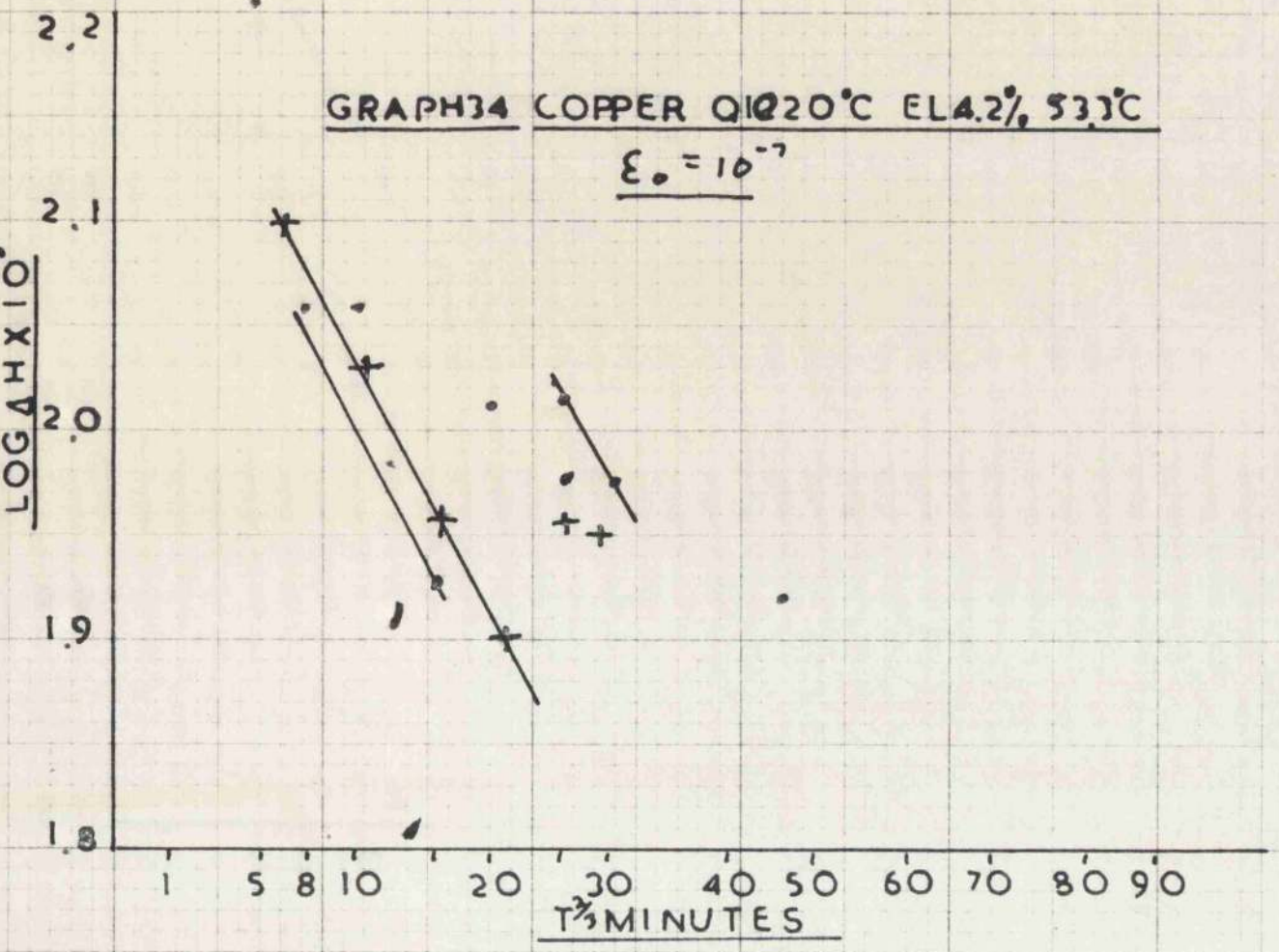

GRAPH 35 COPPER Q. 1020°C EL. 4.2% 19°C

$\varepsilon_0 = 10^{-9}$

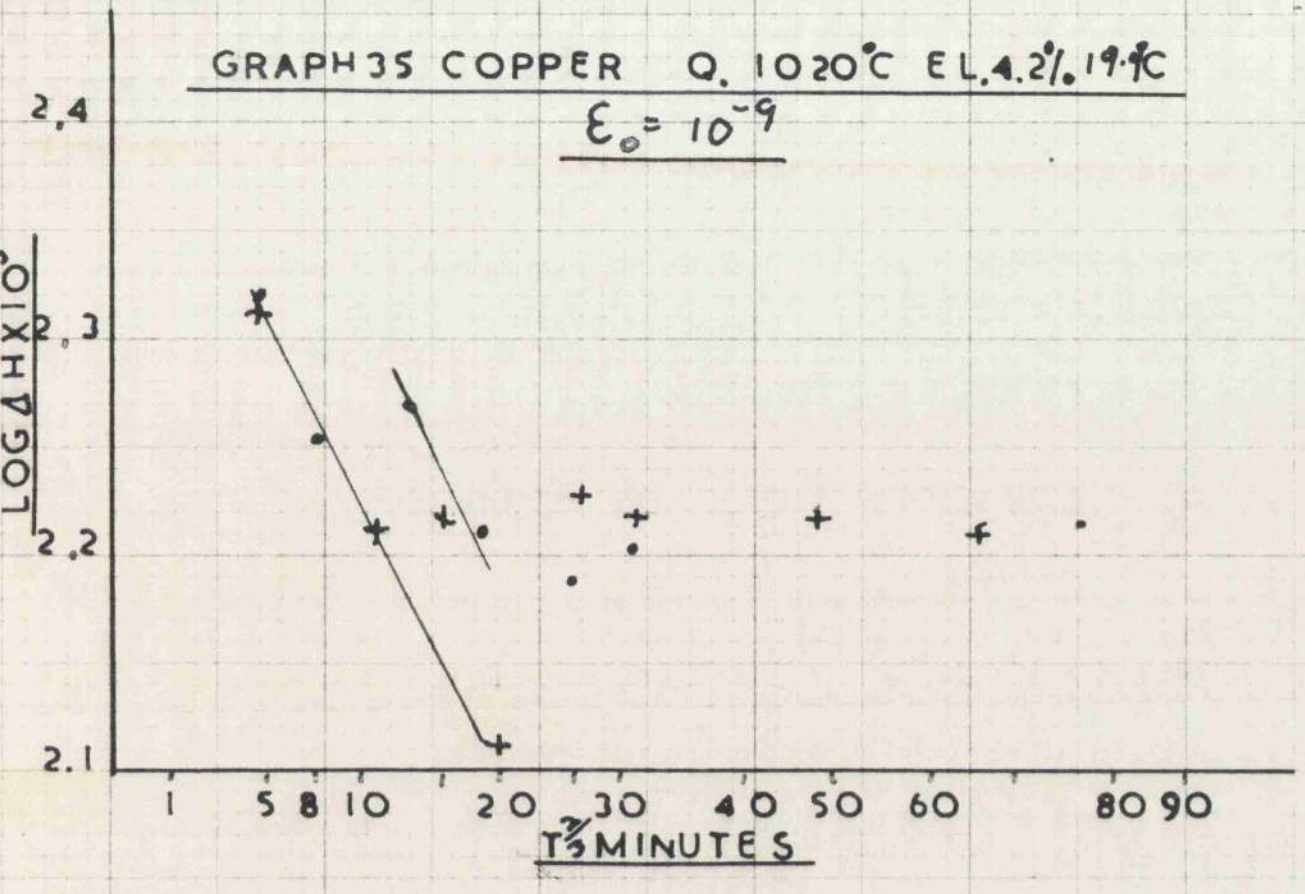

GRAPH 36 COPPER Q 1020°C EL 4.2% 29°C

$\varepsilon_0 = 10^{-9}$

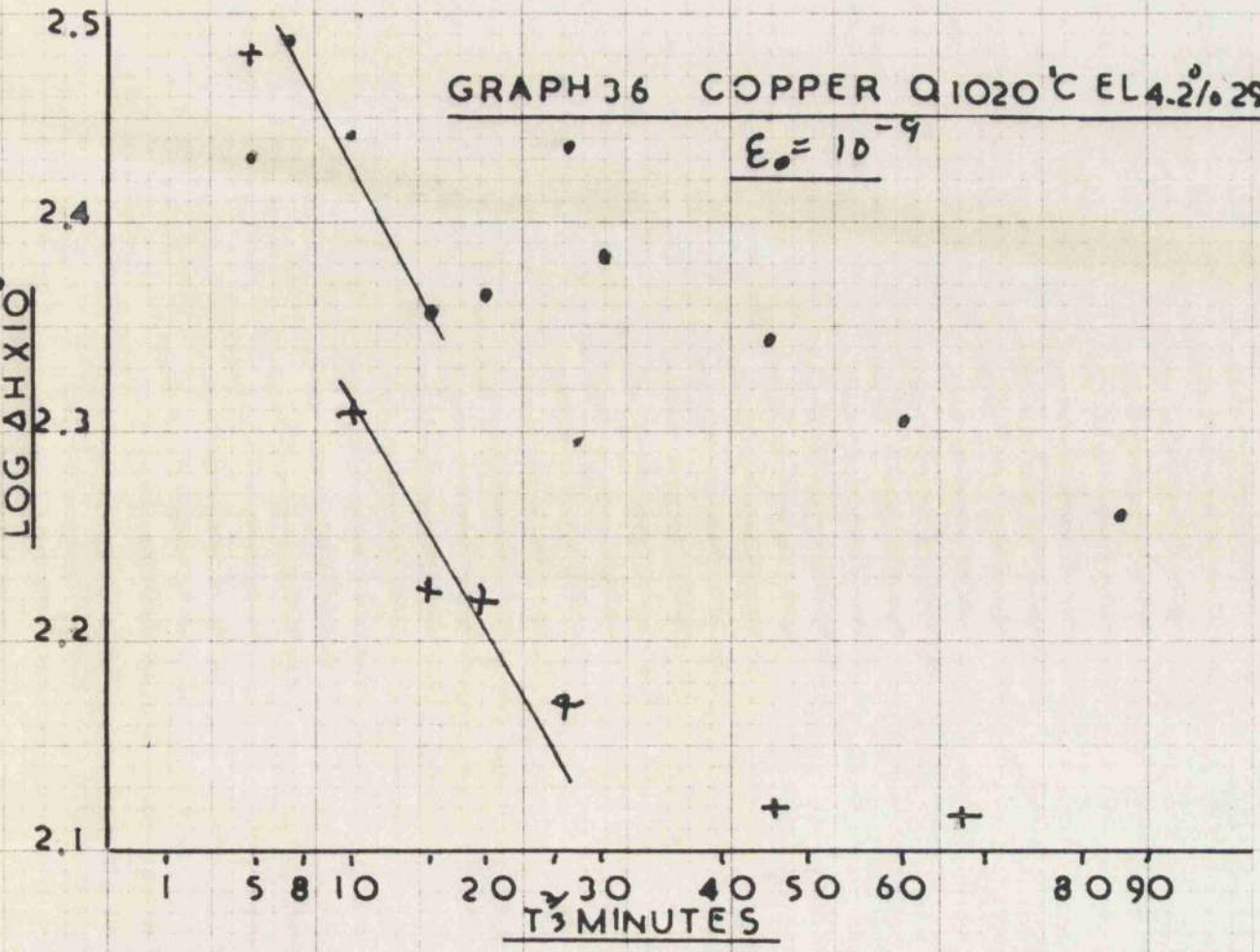

GRAPH 37 COPPER Q1020°C EL 4.2% 56°C

$\varepsilon = 10^{-9}$

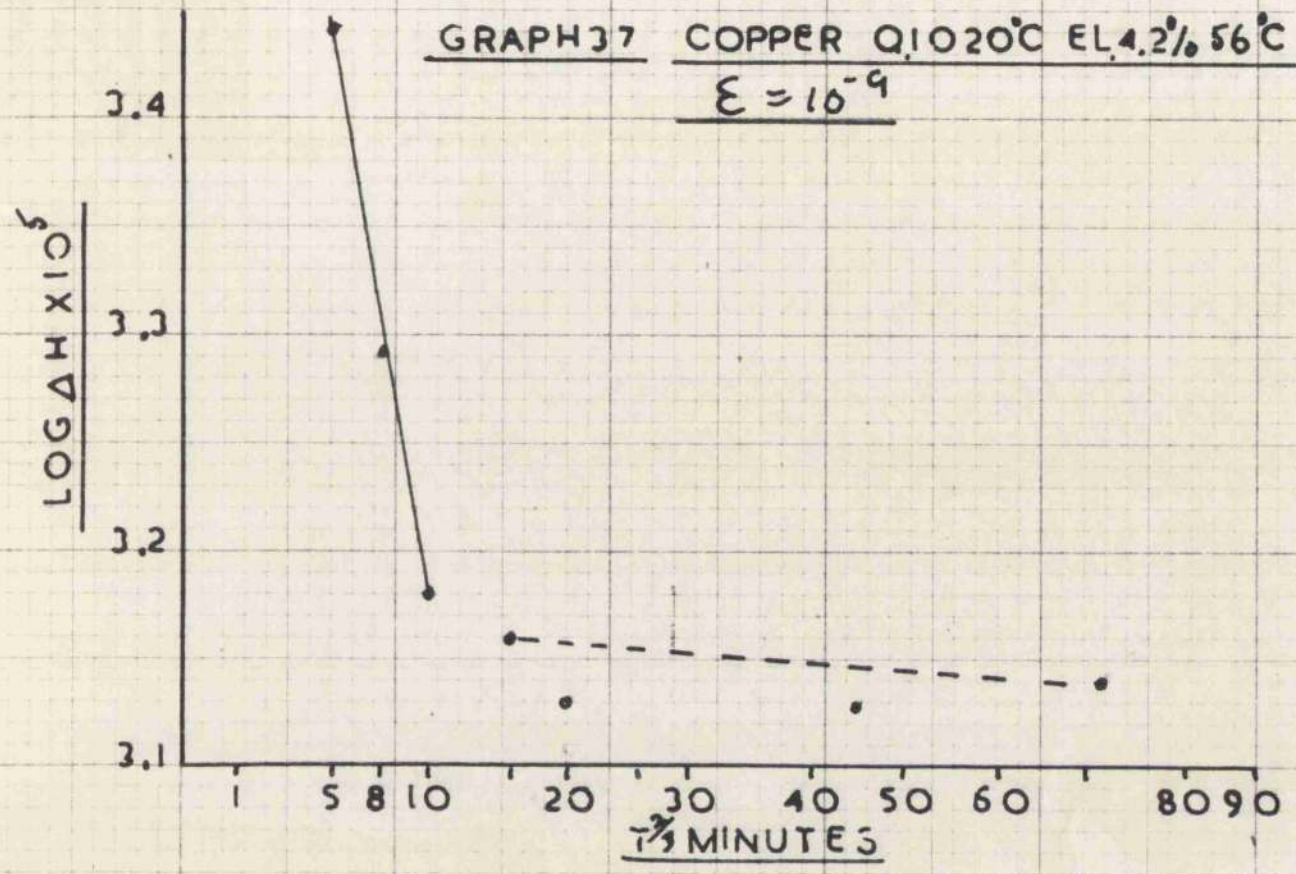

GRAPH 38 COPPER Q1020°C EL 4.2% t

o $\varepsilon = 10^{-9}$

Δ $\varepsilon = 10^{-7}$

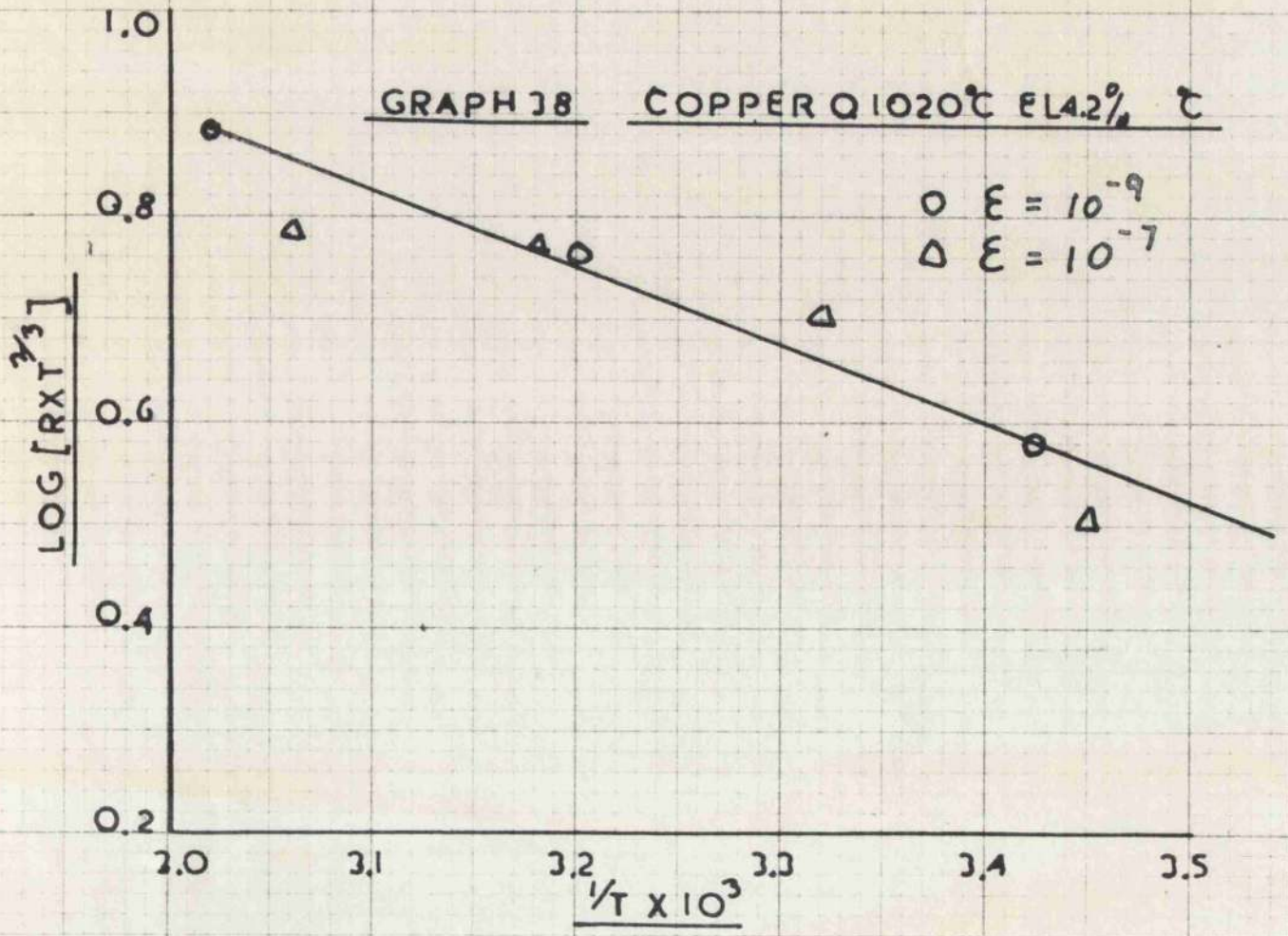

CHAPTER 4

THE RECOVERY OF INTERNAL FRICTION IN ALUMINIUM AFTER DEFORMATION

Results

(1) 99·9% Aluminium

(2) 99·999% Aluminium

(3) Quenching and Elongation

Discussion

Conclusions

The Recovery of Internal Friction in Aluminium after Deformation

Following the experiments on copper a similar set of measurements were made in aluminium. The metal was obtained in three grades: 99·8% al., 9999% al. and one of better than 99·999% al. The 99·8 and 99·99% metals were in the form of 3/16" dia. rod, and the higher purity grade was 3/16" square bar. The material was annealed at 550°C for 1.1/2 hours under vacuum. This resulted in a mean grain size of greater than 0·5 m.m., which was sufficiently large to avoid the grain thermoelastic relaxation peak at the frequency used (2100 c/s). This rather large grain size was also large enough to reduce vacancy loss to the grain boundaries to an acceptable value. The specimens were annealed on alumina plaques in the furnace previously described.

As before, the specimens were annealed in 15 cm. lengths and cut to 10 cm. by a fine saw after deformation. It was shown experimentally that the clamping and sawing of the specimens did not significantly alter their internal friction from the annealed state. The apparatus and technique for deformation was used exactly as before. Unfortunately the tensile machine was such that the load required (0·03T) represented only a very small part of the scale and no useful variation of load was possible

No other suitable machine was available. A series of experiments were carried out in order to determine the optimum elongation for recovery measurements and it was decided that 4% elongation was the most suitable and also had the advantage of being comparable with the results obtained in copper. However, the load required for this elongation was only about one ton per square inch and corresponded to only 0·03 tons stress from the tensile machine. For this reason it was felt that the elongation could not be usefully altered as any measurable change in the applied stress would produce too large a variation in the elongation.

Preliminary experiments also showed that the 99·8% purity aluminium was unsuitable for this work. It was found that even in the annealed state no significant amount of amplitude dependant internal friction could be measured. Clearly, the reason for this was that the small percentage of impurity in the metal was sufficient to pin the dislocation loops and prevent them vibrating.

Experimental Results

(1) 99·8% Purity Aluminium:

The specimens were elongated 4% by a stress of 1·08 T/in^2 in the apparatus described previously. Measurements were made at maximum strain amplitudes of $9·5 \times 10^{-8}$ and 3×10^{-6} at temperatures of 2·2, 14·4 and 33·3°C and the results are shown in graphs Nos. 39,

40 and 41. It can be seen from the graphs that at the lower temperature only is the recovery a steady process over the full 90 minutes recorded. At the two higher temperatures it can be seen that the initial recovery process gives way after a time to a slower rate of recovery. It is of some interest to note that the time required for this transition became less as the temperature of the experiment was raised.

The actual experimental results show, as was the case with the previous results, the shift in the points as the oscillator range was changed resulting in the appearance of a set of parallel lines rather than a single recovery line. The results shown in the above graphs gave the following data.

Table 8 - 99·99% Aluminium 4% Elongation

°C	°K	$\frac{1}{T}\times 1000$	$T^{\frac{2}{3}}$	R/2·303	R	$T^{\frac{2}{3}}$ R	log $[T^{\frac{2}{3}}$ R]
2·2	275·2	3·68	42·1	0·0396	0·049	3·74	0·573
14·4	287	3·48	43·2	0·081	0·180	7·75	0·89
33·3	306	3·26	45·2	0·163	0·376	17·0	1·246

These results from Graph No. 42 gave the activation energy for the process as 13·35 Kcals/mole. The second and slower stage in the recovery process did not yield an activation energy from the above results and it is thought that it is not a true diffusion process.

(2) 99·999% Purity Aluminium.

These specimens were 3/16" rectangular bars and were elongated 4% by a stress of 0·852 T/in^2. This lower stress indicates the purer and softer nature of this material as compared with the previous one. Another indication of the higher purity is seen in the recovery graphs, Nos. 42, 43 and 44, where the amplitude dependant damping is higher than in the previous results. While the influence of the errors due to frequency variations in the oscillation are still present they are much less serious due to the higher internal friction.

As before, the continuous rate of recovery was only found in the lower temperature. In the higher temperatures after a time the fast recovery gives way to a slower rate. Measurements were made at strains of $9·5 \times 10^{-6}$ and 3×10^{-6} and are given in Table 9.

Table 9 - 99·999% Aluminium 4% Extension

°C	°K	$\frac{1}{T} \times 1000$	$T^{\frac{2}{3}}$	$R/2·303$	R	$T^{\frac{2}{3}} R$	$\log [T^{\frac{2}{3}} R]$
-5·6	267·6	3·74	41·1	0·043	0·099	4·06	0·609
2·2	275·2	3·64	42·0	0·080	0·154	7·74	0·859
13·3	286	3·5	43·1	0·152	0·35	15·1	1·179

From graph No. 45 the activation energy of 14·0 Kcals/mole.

(3) It had been hoped to obtain additional data from material which had been quenched from near its melting point. However it was found that after quenching the amplitude dependant internal friction was very small and could not be used to obtain recovery data. This is very similar to the results obtained by Levy and Metzger[55] who showed complete amplitude independance after a water quench in aluminium. For this reason it was decided to strain the metal after it had been fully quench aged.

The specimen 99·99% purity aluminium, 15 cm. in length, was suspended in a vertical furnace at 570°C for 30 minutes in an argon atmosphere. The suspension wire was 40 gauge nichrome and was attached to the specimen by a simple slip knot. Quenching was achieved by dropping the specimen into water at room temperature. The specimen was allowed to age for 24 hours at room temperature and then elongated 4% in the same manner as before. The stress required was 1·08 T/in^2 and the specimen was then cut to 10 cm. in the usual way.

Measurements were made at strain amplitudes of $9·5 \times 10^{-6}$ and $9·5 \times 10^{-6}$ in order to obtain a reasonable amount of amplitude dependant internal friction. The results are shown in Graphs No.46, 47 and 48. The rather lower amplitude dependant part of the internal friction has made the apparatus errors rather obvious but the data in Table 10 was deduced.

Table 10 - 99·99% Purity Aluminium Quenched 570°C Elongated 4%

°C.	°K	$\frac{1}{T}$x1000	$T^{\frac{2}{3}}$	$R/_{2·303}$	R	$T^{\frac{2}{3}}$ R	[log $T^{\frac{2}{3}}$ R]
-6·7	266	3·78	41·2	0·0161	0·0373	1·52	0·183
-1·1	272	3·68	41·9	0·0217	0·05	2·09	0·320
13·3	286	3·5	43·1	0·05	0·115	4·96	0·696

This from Graph No. 49 gives the activation energy for the process at 13·6 Kcals/mole. In other repsects these results seem very similar to the two previous sets obtained.

Discussion:

The results obtained are in good agreement with those obtained by Federghi by electrical resistivity and Silcox and Whelan[43] by electron microscopy on quenched material. There seems to be no doubt that the recovery measured is due to the migration of single vacancies. The activation energy formed is identical with that expected for the movement (Em) of vacancies in aluminium. This does not necessarily preclude the presence of divacancies in the material after deformation but it seems that they would have fully decayed before measurements were started. As about four minutes were required before any measurements could be made it seems quite probable that the divacancies formed could have fully condensed on to the dislocation lines in this time.

A possible explanation for the deviation from linearity of the graphs may be found in the presence of vacancy clusters or

sessile dislocation loops. After deformation some of the excess vacancies are condensed to form ~~of~~ clusters or sessile dislocation loops. This can act as a sink for vacancies and it is of some interest to note that it increases in capturing efficiency as it grows larger.

Federinghi showed that at about 170°C a second stage occurred in the recovery of electricial resistivity and Silcox and Whelan [43] showed that this was probably due to the migration of the vacancy clusters. It was calculated that the migration of the clusters resulted in the generation of vacancies. It seems possible that some movement of this type is possible at much lower temperatures than 170°C, indeed from Fedringhi's paper it seems that it may occur at 50°C. Thus it appears that the formation of the vacancy cluster could reduce the rate of recovery of internal friction by removing the vacancies from the lattice and this will be a rather complex effect owing to the increase in size of the sink as more vacancies are captured. A second effect may be the migration of the clusters which is thought to lead to the loss of vacancies to the lattice and some of these would presumably reach the dislocation lines.

The recovery of aluminium after deformation is then visualised as follows. After deformation a high concentration of vacancies will be free in the lattice. These will if the temperature is high enough (above -30°C) diffuse either to the

dislocation network or condense to form vacancy clusters or sessile dislocation rings. The vacancies which reach the network dislocations reduce the internal friction and lead to the increased recovery. If the clusters migrate, it seems probable that a further slower rate of recovery will be due to the vacancies produced in this way.

After quench ageing and then elongating a somewhat different process occurs. The quench results in a high concentration of vacancies which either coalesce to clusters or diffuse to the dislocation lines. Subsequent deformation was shown by Vandervoort and Washburn[44] to remove these clusters. It seems probable that the dislocation density will be very similar to that of the previous specimens but that the vacancy concentration will be increased. The recovery is then thought to proceed as before.

The activation energy obtained for the process of 0·58 ± 0·025 ev is in very good agreement with both results of quenching and tracer methods. It seems quite certain that the recovery is due purely to vacancy movement. No divacancy movement has been noted but it is not suggested that none exists. As a divacancy is expected to move with about one half the energy for a single vacancy, it will have condensed before measurements could be started. The PRESENCE of divacancies is indicated by the fact that no amplitude dependant internal friction could be found after quenching. As a quench would be very prolific in producing divacancies it could be expected to harden the metal very quickly.

Conclusions.

The activation energy for the movement of a vacancy in aluminium at near 300°K is 0·58 ± 0·025 ev which is in agreement with previous results. It appears that within the ranges used vacancy and impurity concentration do not noticeably alter the value of Em.

GRAPH 39 99.99% ALUMINIUM
4% ELONGATION 22°C

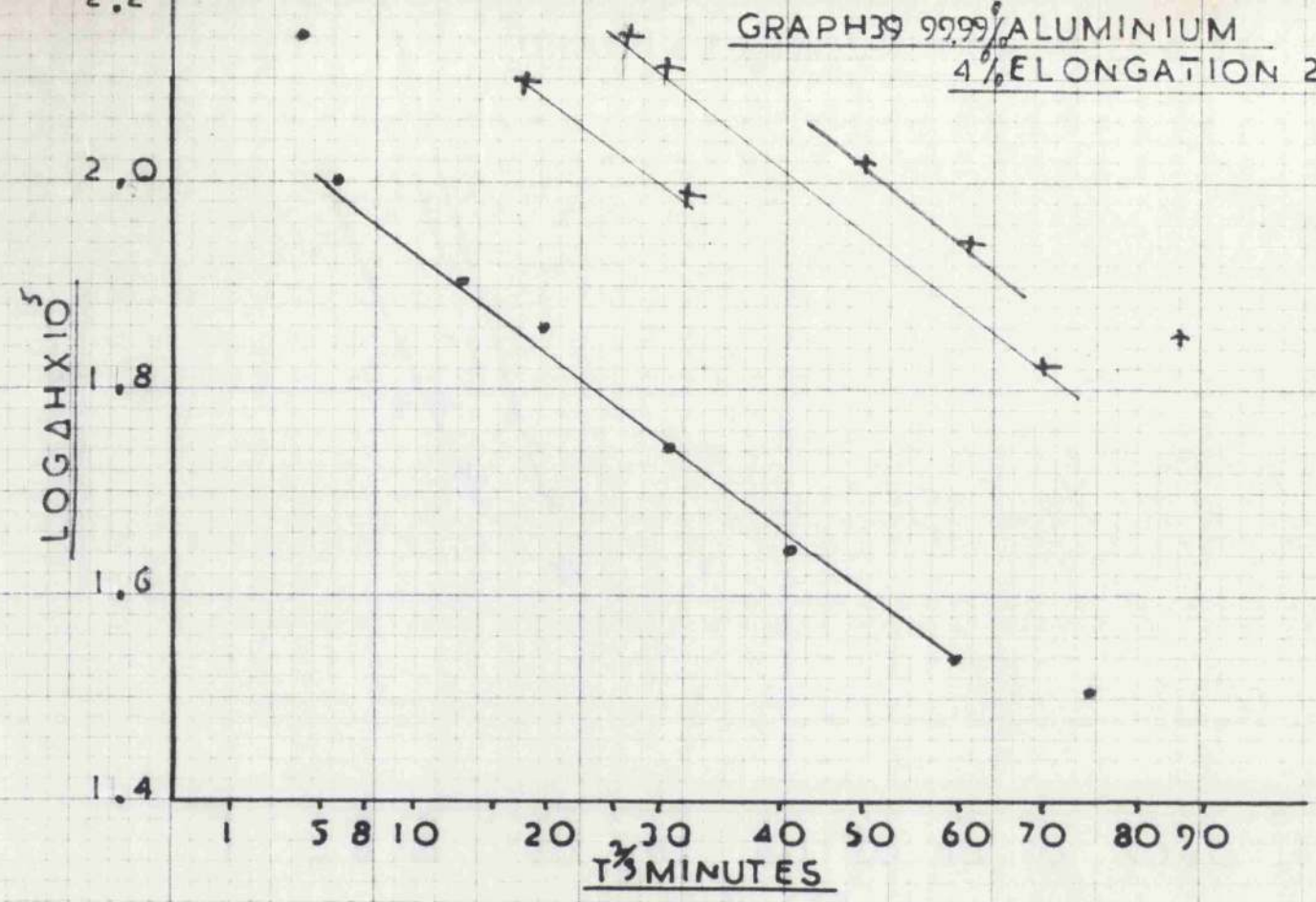

GRAPH 40 99.99% ALUMINIUM 4% EL 14.4°C

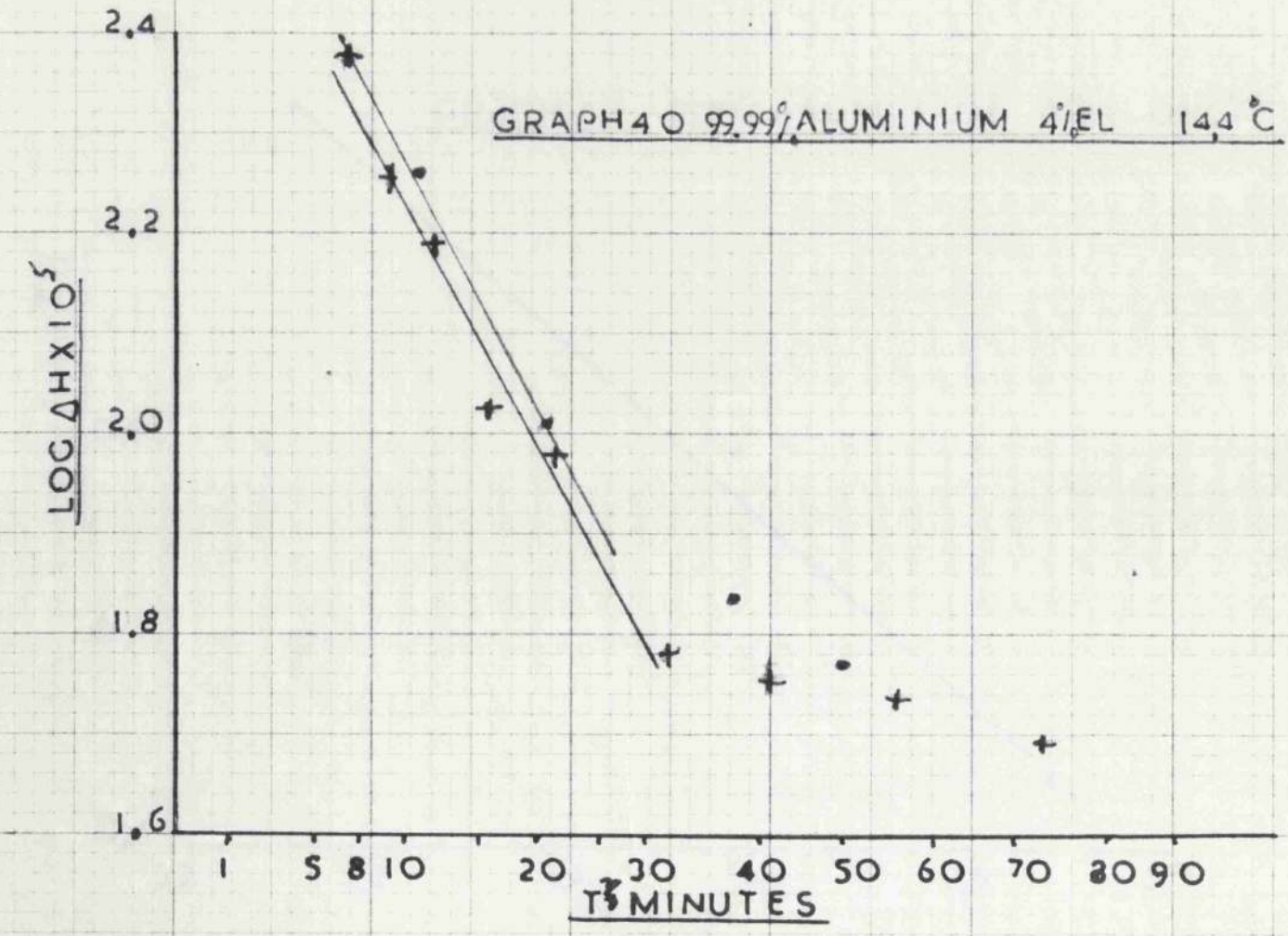

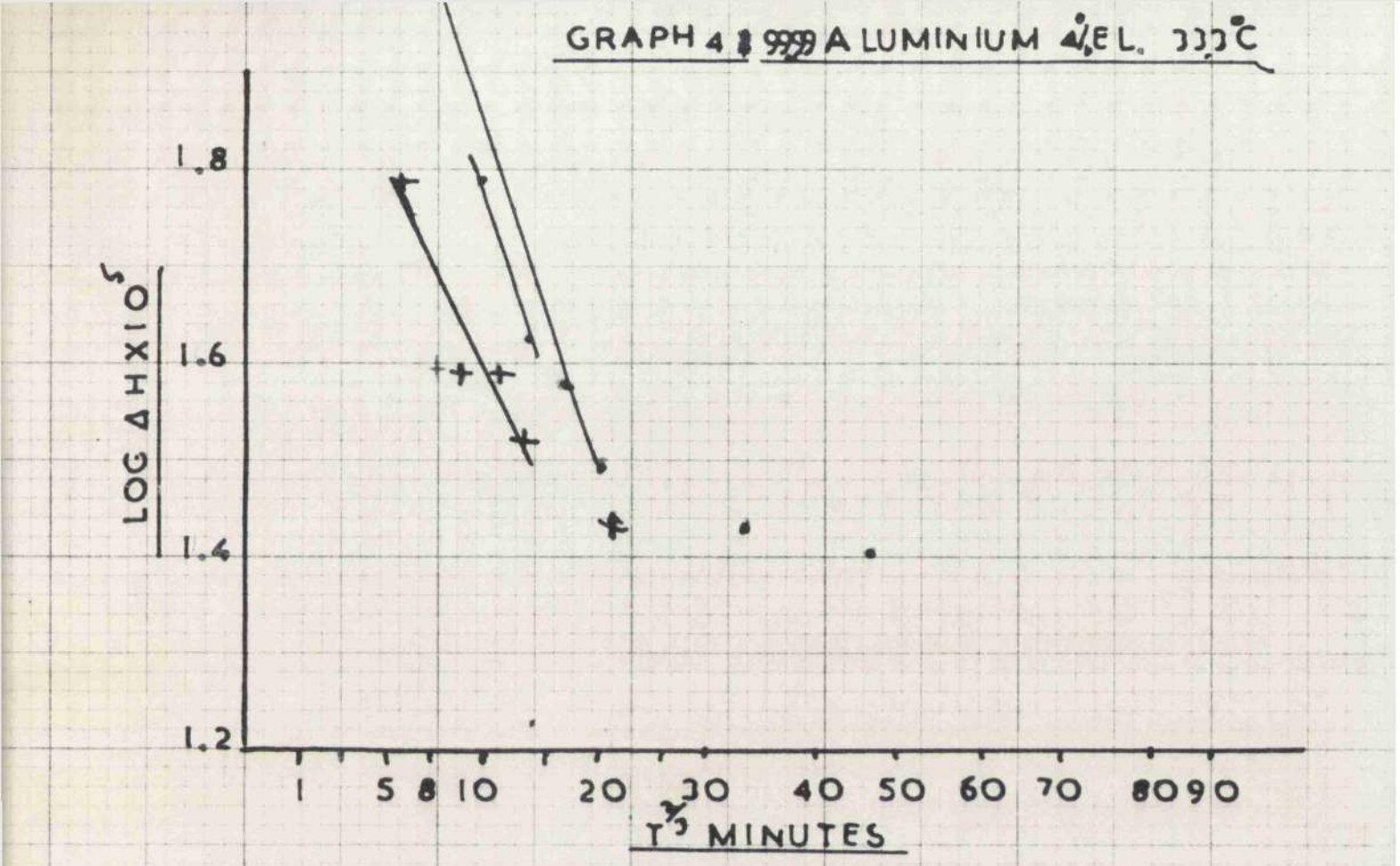
GRAPH 41 9999 ALUMINIUM 4% EL. 333°C
LOG ΔH X 10^5
1.8
1.6
1.4
1.2
1 5 8 10 20 30 40 50 60 70 80 90
T^2/3 MINUTES

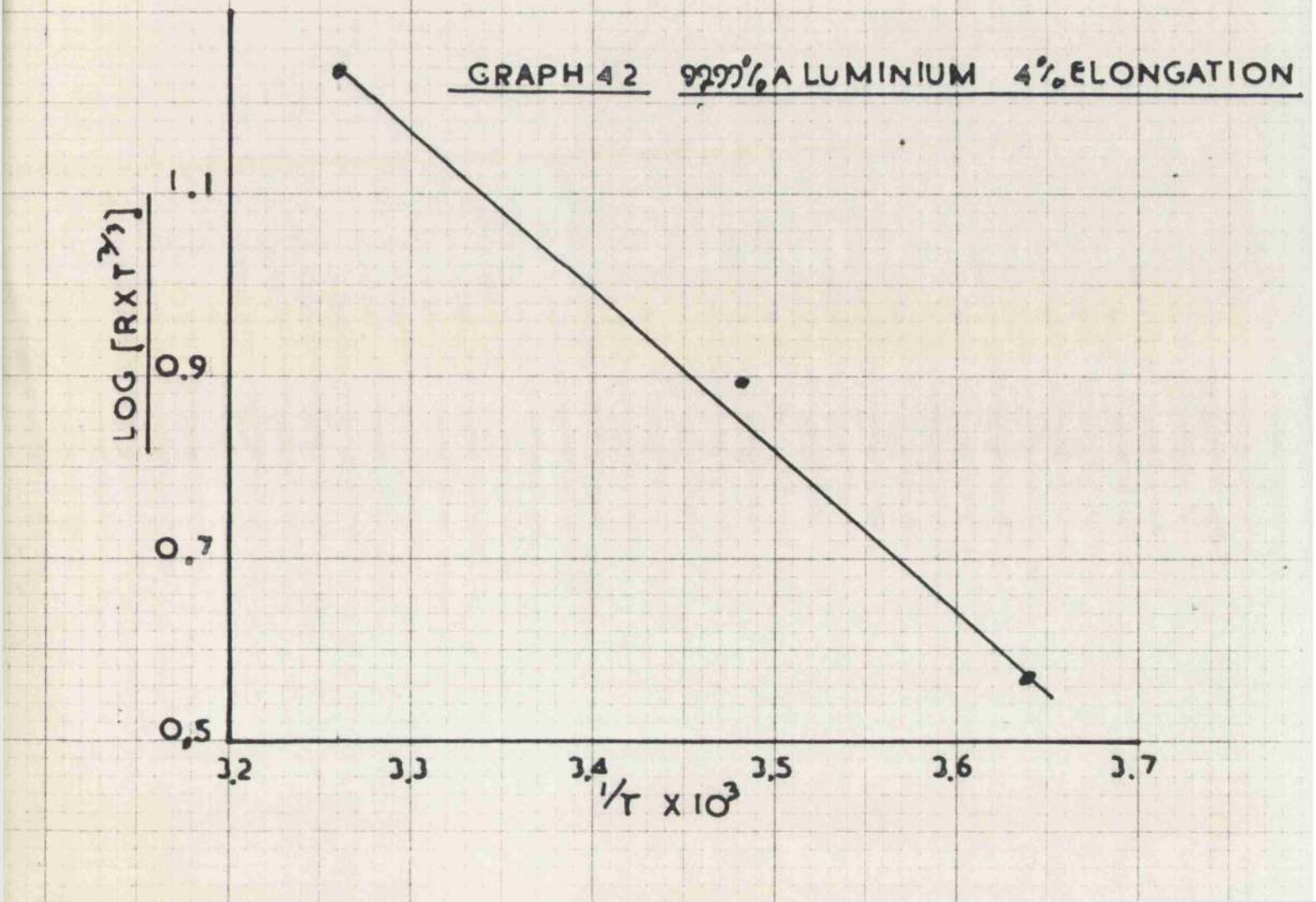
GRAPH 42 9999% ALUMINIUM 4% ELONGATION
LOG [R X T^2/3]
1.1
0.9
0.7
0.5
3.2 3.3 3.4 3.5 3.6 3.7
1/T X 10^3

GRAPH 43A 99.999% ALUMINIUM 4% EL -5.5C

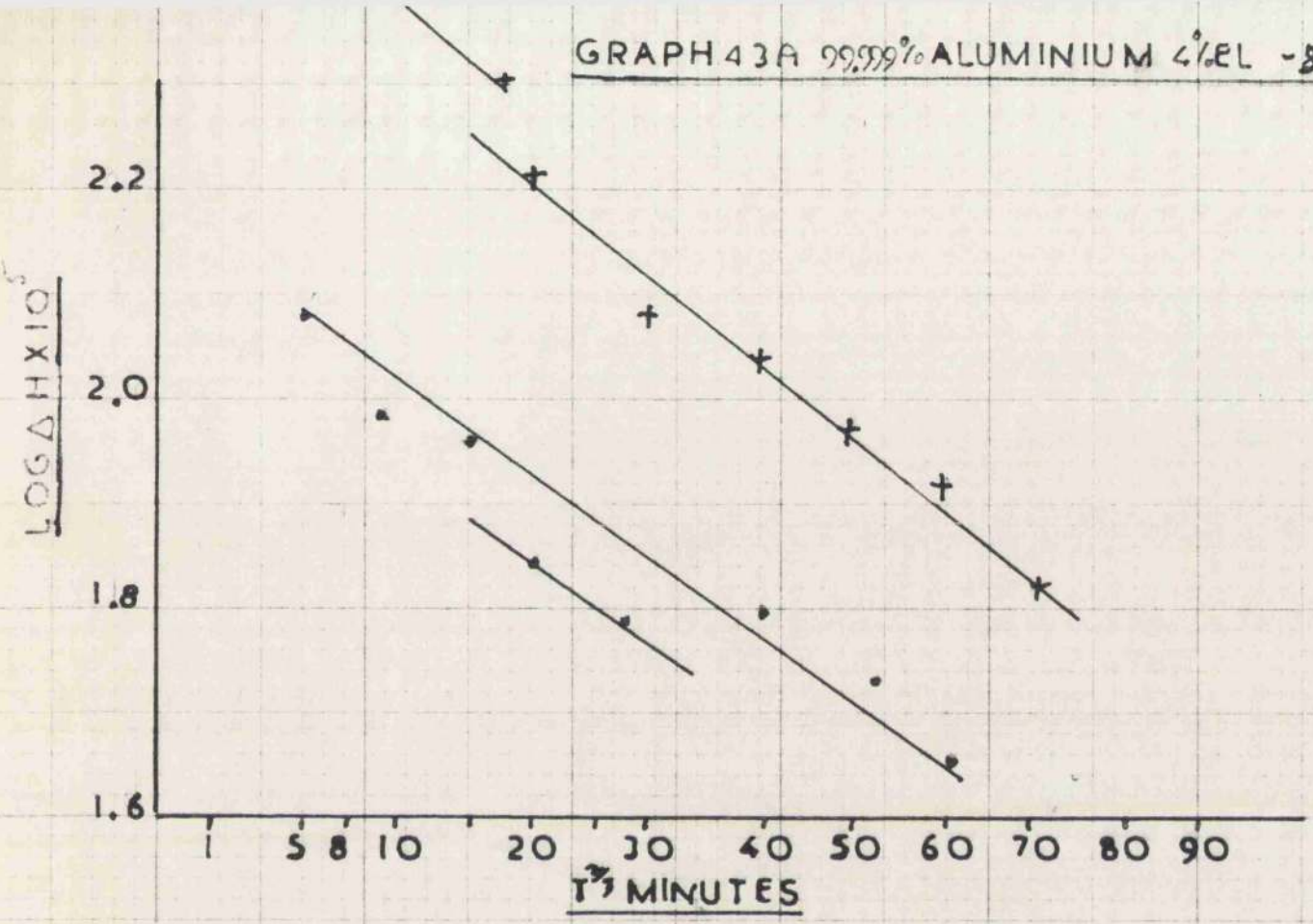

GRAPH 43 B 99.999% ALUMINIUM 4% EL 2.2°C

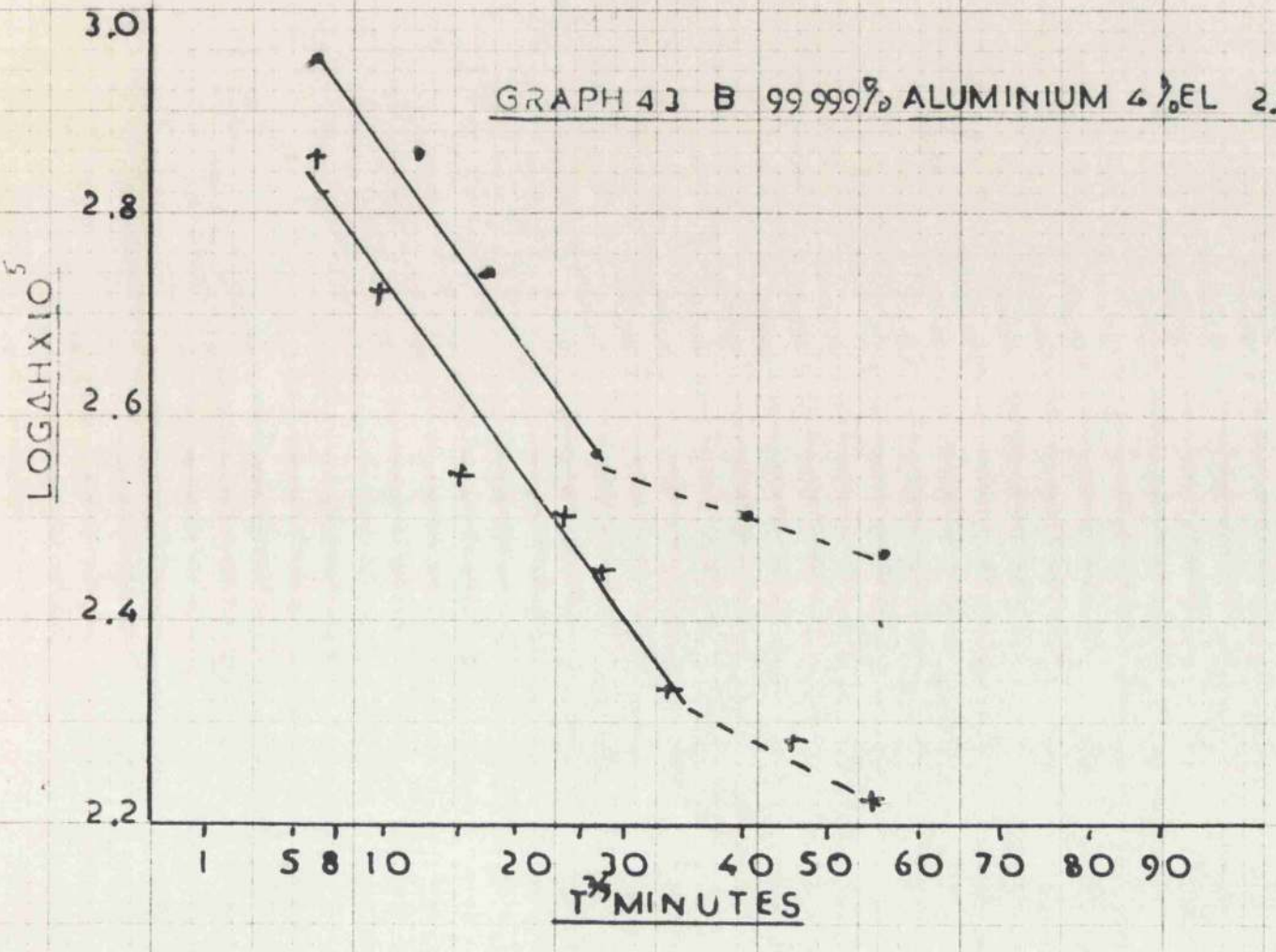

GRAPH 44 99.999% ALUMINIUM 4% EL 13.3 °C

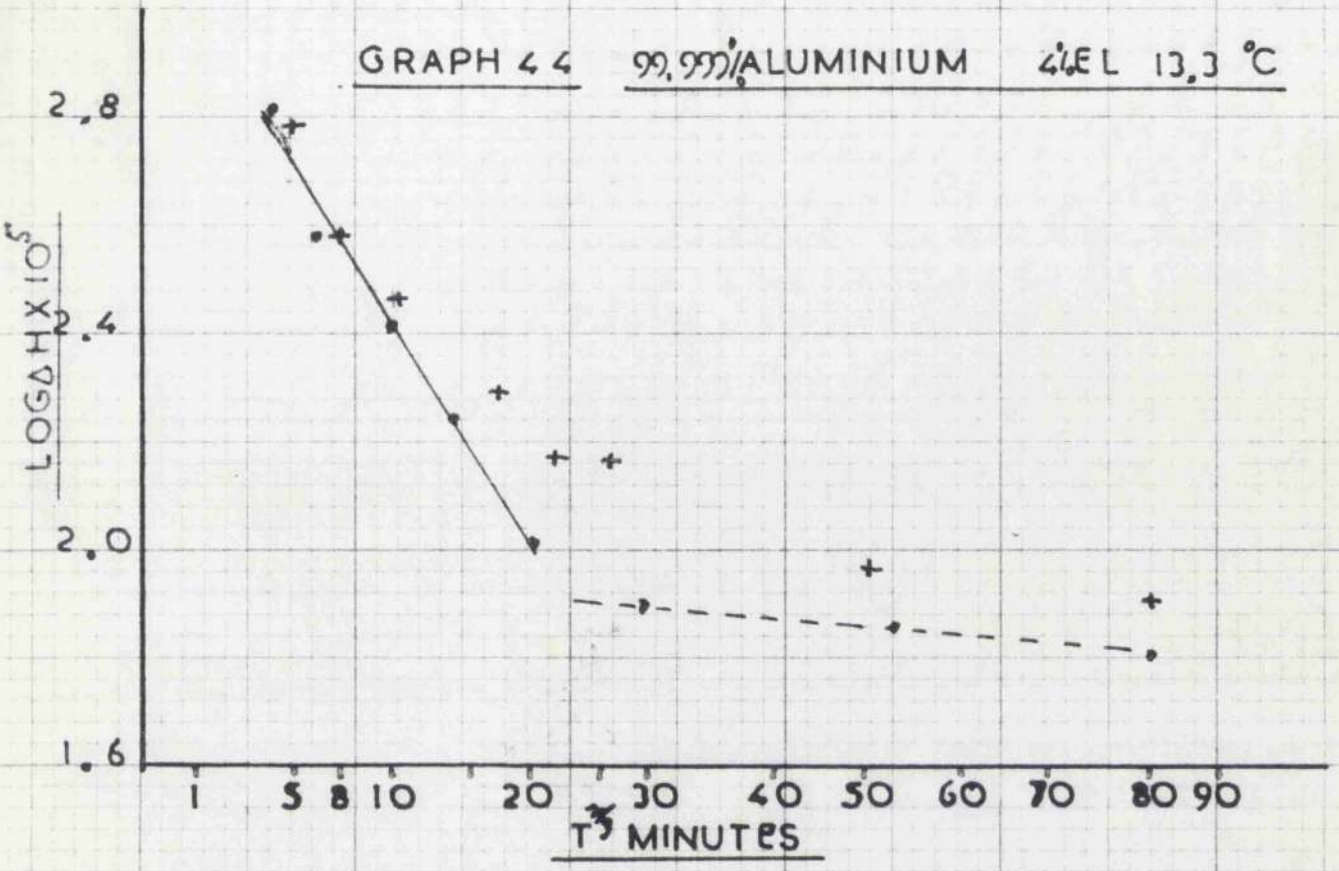

GRAPH 45 99.999% ALUMINIUM 4% ELONGATION

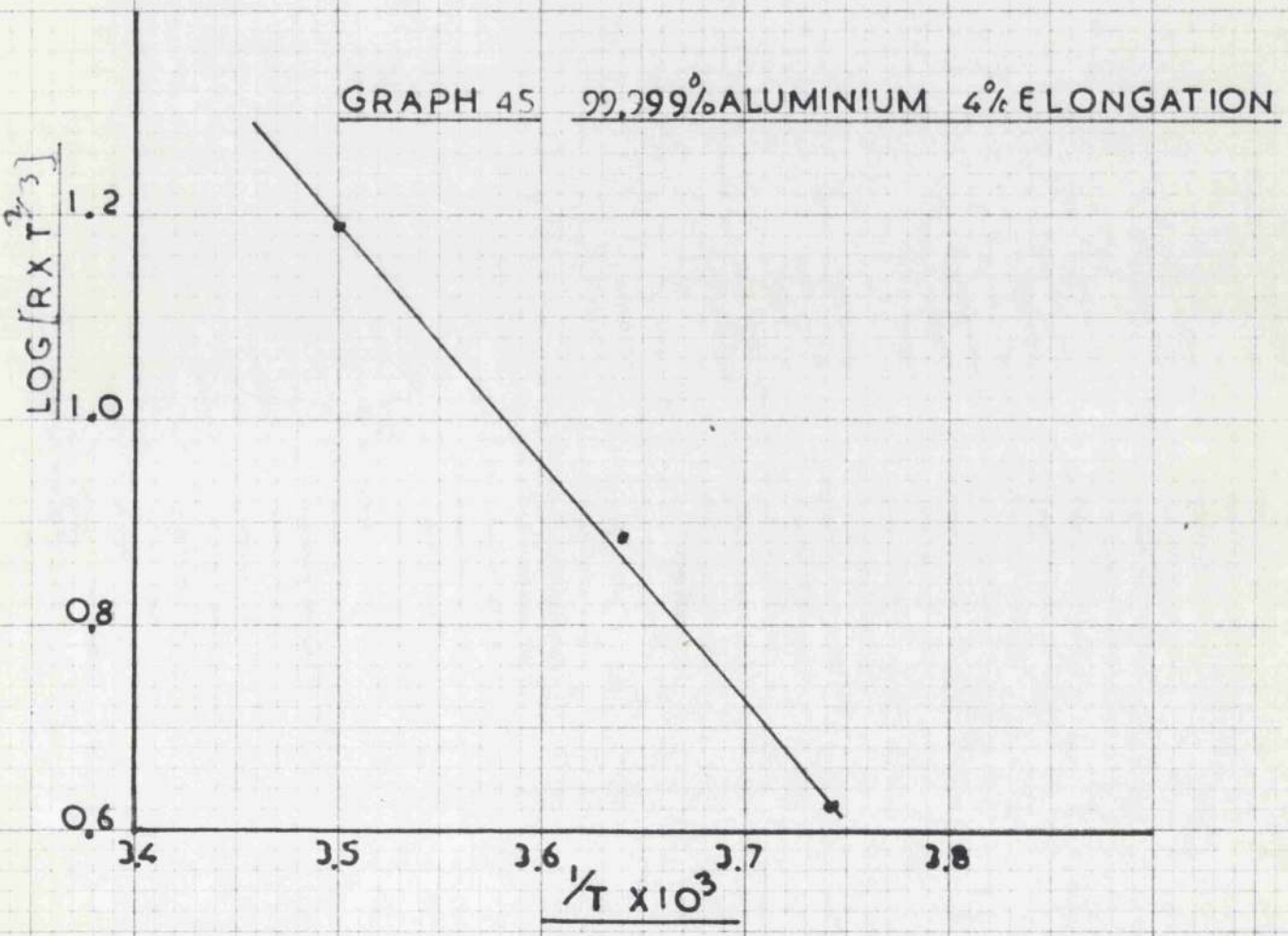

GRAPH 46 99.99% ALUMINIUM QUENCHED 570°C
4% ELONGATION -6.7°C

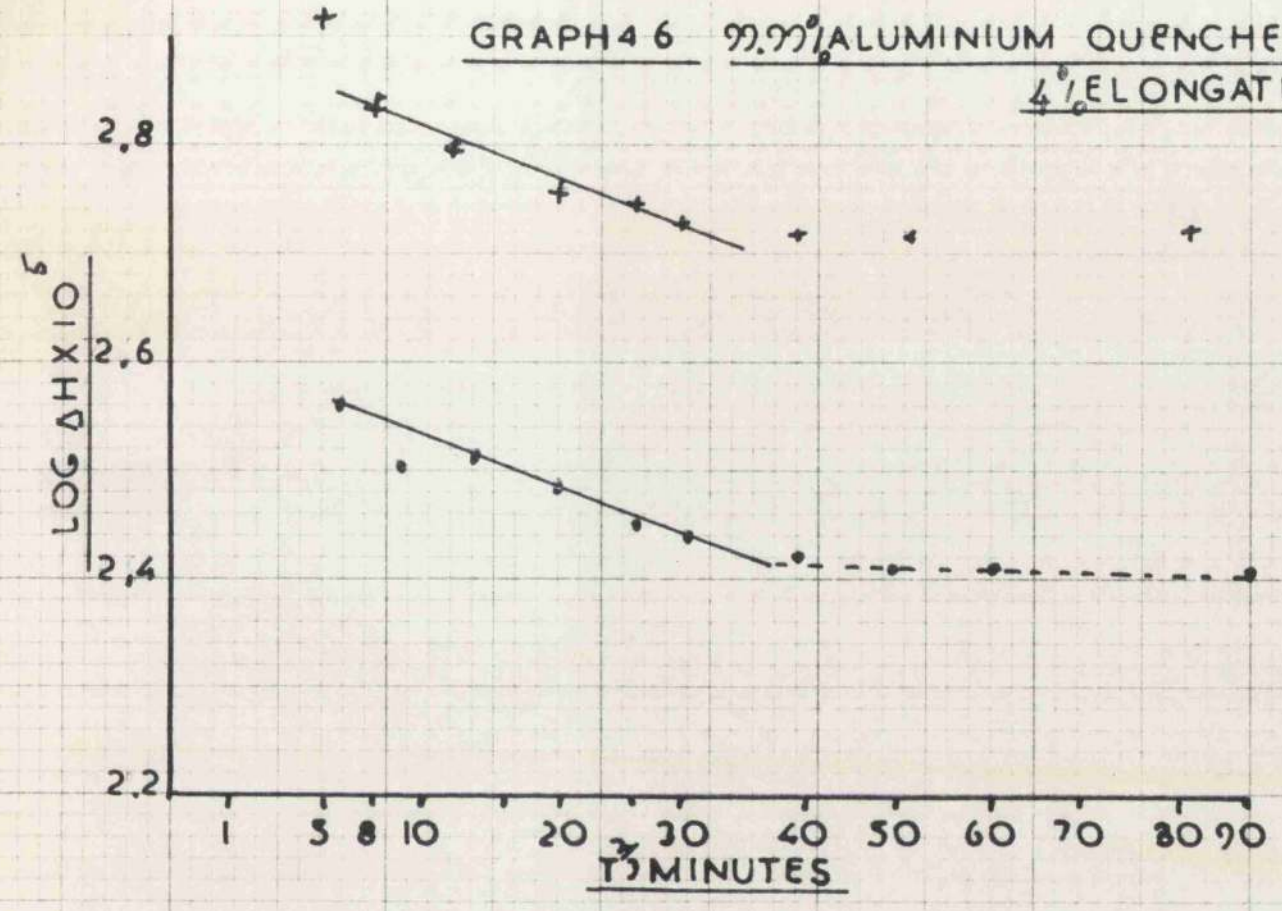

GRAPH 47 99.99% ALUMINIUM Q 570C 4% EL -2.2°C

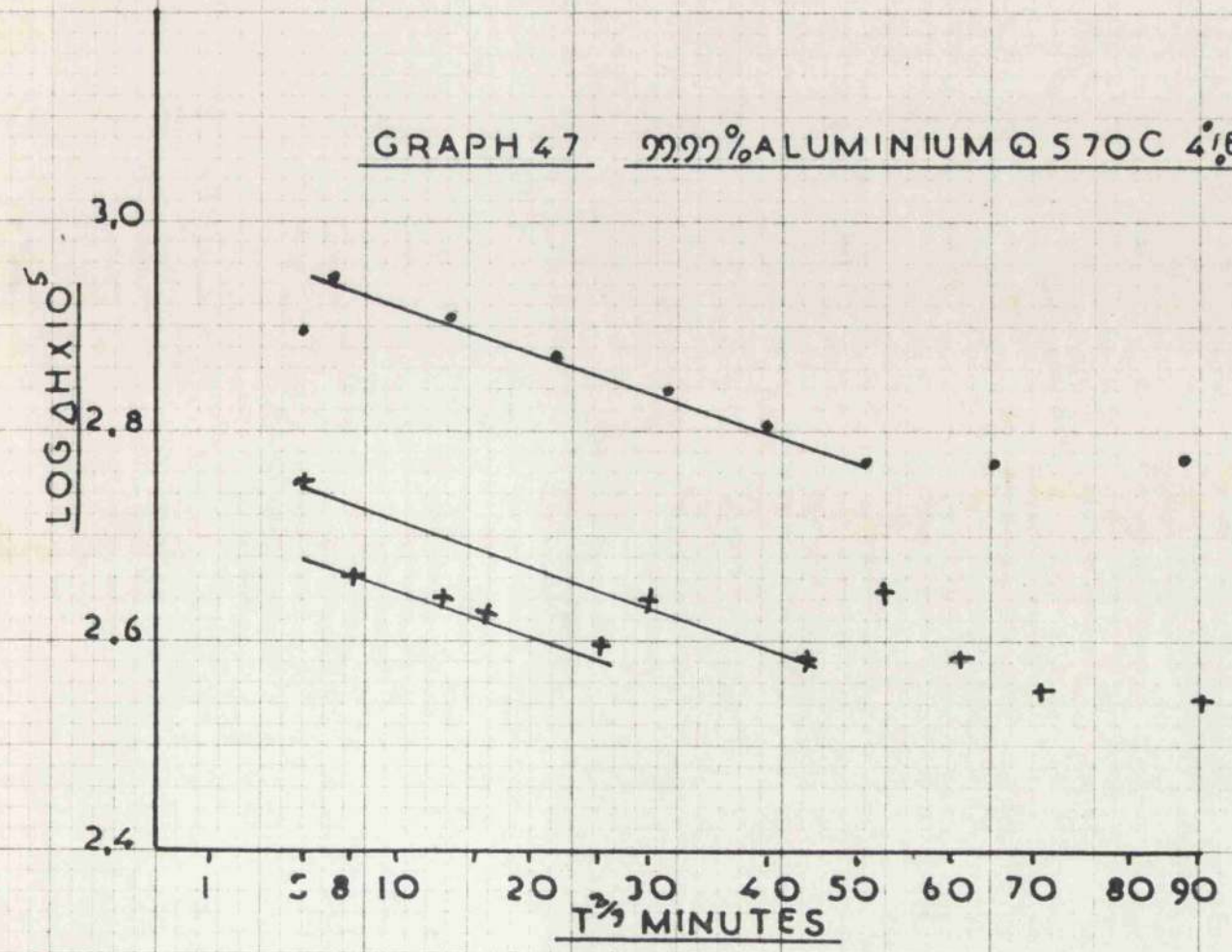

GRAPH 48 99.99% ALUMINIUM Q 570°C 4% EL

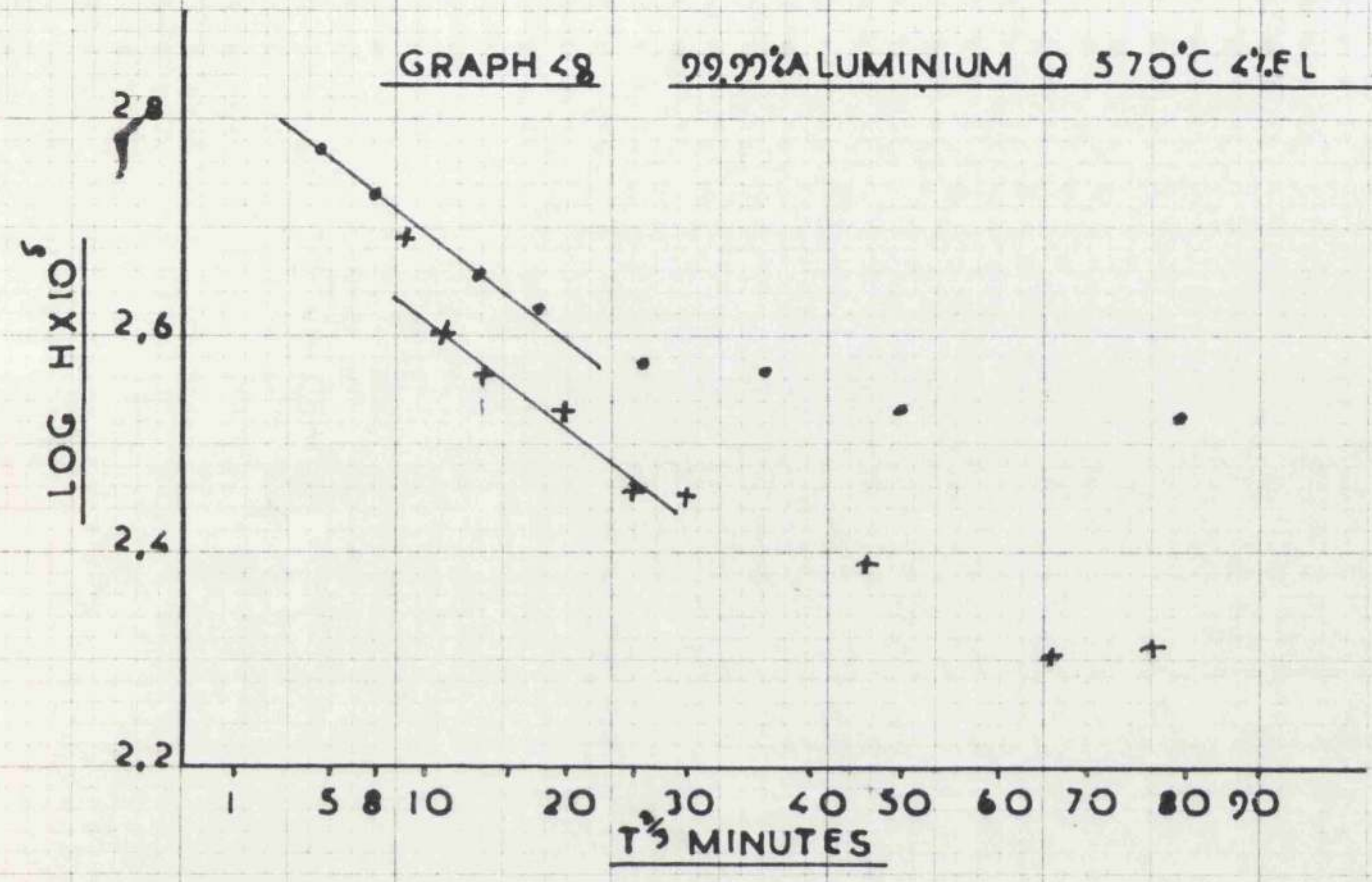

GRAPH 49 99.99% ALUMINIUM Q 570°C 4% EL

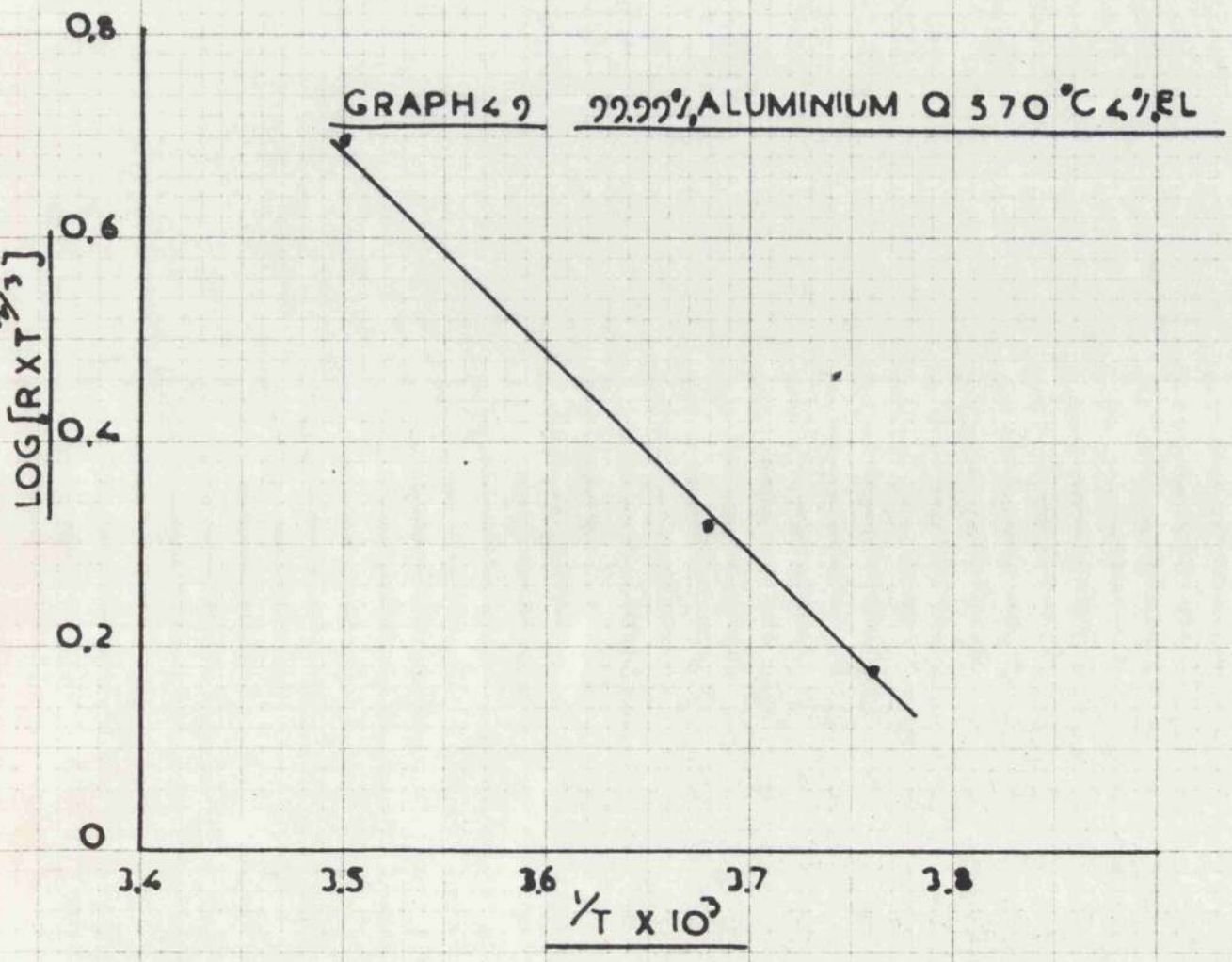

CHAPTER 5

THE EFFECT OF DEFORMATION ON NICKEL

(1) Recovery after Elongation

(2) Recover y after Fatigue

(3) Recovery after Quenching

The Effect of Deformation On Nickel

From the previous results it appears that while in aluminium the activation energy for vacancy diffusion is constant in copper it varies as a function of deformation. It is thus desirable to test a metal intermediate in character between copper and aluminium. It was felt that as copper was characterised by a low stacking fault energy and aluminium by a high energy (20 → 120 ev) it would be instructive to use a metal with an intermediate stacking fault energy. The available F.C.C. metal was nickel which was thought to have a stacking fault energy of 75 ev. However recently Seeger has cast some doubt on this value and the situation is at present rather obscure. The result obtained for the stacking fault energy seems to depend on the method used for its determination.

The material was supplied by the Mond Nickel Co., Ltd., in the form of 3/16" dia. rod of unknown purity. The initial measurements on annealed material were rather interesting, the internal friction was remarkably high and almost amplitude independent. The internal friction was about $7 - 8 \times 10^{-3}$ even at very low amplitude though naturally not much variation of amplitude could be obtained with a specimen of so high an internal friction.

Very high internal friction which is mainly amplitude independent can indicate either (1) a very pure (almost theoretically pure metal) which would exhibit this behaviour from the Granato and Luke equation; or (2) a material which contained a large volume of cracks.

When a little cold work was applied to a specimen it was found that its internal friction was reduced to 1/6th of its original value at once and to 1/18th after 24 hours. This indicated that the metal was quite pure originally. However, the situation was confused by the fact that very often intergranular failure was observed in specimens even before treatment. The conclusion reached was that the metal being very pure was susceptible to contamination and was embrittled at the grain boundaries. Efforts were made to determine the exact nature of any contamination but were quite unsuccessful. It was suggested by the manufacturers that sulphur was the most probable cause of this type of embrittlement.

The metal was softened in lengths of about one foot at 500°C under vacuum and then straightened. It was then cut to length and annealed under high vacuum at 1200°C for 1.1/2 hours. This resulted in the large grain size required for this work.

(1) Recovery after Elongation

The specimens were annealed as above in 15cm. lengths and stressed in the apparatus previously described. By experiment

it was found that the most useful recovery measurements could be made after 3% elongation which was equivalent to a stress of 9·05 Tons/in^2.

Measurements were made at stresses of $1{\cdot}6 \times 10^{-9}$ and 3×10^{-6} exactly as described previously. The results are shown in Graphs 50, 51 and 52. It can be seen that two recovery processes are active. the first, as before, is the faster, giving way after a time to the second. It can be seen that as the temperature was increased the shorter became the duration of the first stage. The results are by no means satisfactory, but it was possible to obtain the following data for the two stages.

Table 11 - Nickel 3% Elongation

°C	°K	$\frac{1}{T} \times 1000$	$T^{\frac{3}{2}}$	R/2·303	R	$T^{\frac{3}{2}}$ R	log [$T^{\frac{3}{2}}$ R]
First Stage							
18·3	291·3	3·435	44	0·0205	0·0472	2·08	0·318
37·8	310·5	3·215	45·8	0·393	0·905	4·15	0·418
52	325	3·07	47·1	0·0590	0·1355	6·38	0·805
Second Stage							
18·3	291·3	3·435	44	0·0013	0·00312	0·137	-0·88
37·8	310·5	3·215	45·8	0·00525	0·0122	0·506	-0·296
52	325	3·07	47·1	0·0119	0·0275	1·3	+0·114

These results plotted in Graph 53 gave the activation energies as 9·15 Kcals/mole for the first stage and 18·3 Kcals/mole for the second.

(2) Recovery after Fatigue

The specimens were 15 cm long and annealed as before. The fatigue machine was an Amsler High Frequency Vibrophore in push-pull stressing. A series of preliminary experiments to determine the most suitable stress for these experiments were made. Eventually a stress of $\pm$ 0·453 T/in^2 which gave a life of 2·8 x 10^6 cycles. The specimens were fatigued to 2·5 x 10^5 cycles, that is about 1/10th of their life measurement. As the speed of the fatigue machine was about 5500 c/s the fatigue process required a bout 45 minutes.

It was found that a small positive bias was necessary in the stress at the commencement of the fatigue run. This bias had however disappeared by the end of the test. A number of premature failures were found. These were either due to a faulty anneal or more probably the metal was contaminated when received. Freshly annealed material proved quite satisfactory. As before the specimens were cut to 10 cm. after fatigue and measured.

The results are shown in Graphs 54, 55, 56 and 57 and there appears to be only one recovery process active. The results show little scatter and the following table was obtained.

Table 12 - Nickel Fatigued

°C	°K	$\frac{1}{T} \times 1000$	$T^{\frac{2}{3}}$	R/2·303	R	$T^{\frac{2}{3}} R$	$\log[T^{\frac{2}{3}} R]$
16·7	289·7	3·45	44·0	0·0008	0·00184	0·084	-1·080
44·5	317·5	3·15	46·2	0·00525	0·0121	0·557	-0·354
58·5	331·5	3·02	47·7	0·01075	0·0167	0·795	-0·10
70	343	2·97	49·0	0·01385	0·0318	1·565	+0·195

These results from Graph 58 gave the activation energy for the process as 15·3 Kcals/mole.

(3) Recovery after Quenching

The apparatus used was the vacuum quenching unit previously described. As quite a high quenching temperature was required a platinum wound furnace was required. The vacuum obtained was not particularly good as the mullite furnace tube used was slightly porous at 1400°C and was of the order of 5×10^{-4} m.m. Owing to the large weight of the specimens and the small volume of oil the quench obtained was not particularly severe.

It was found that quenching from 1400°C did not give enough recovery for measurement by this method and it was decided to quench from 1410°C.

The results, shown in Graphs 59, 60 and 61, are rather scattered and unsatisfactory but the following results were obtained for two stages of recovery.

Table 13 - Nickel - Quenched from 1410°C

°C	°K	$\frac{1}{T}$x1000	$T^{\frac{1}{3}}$	R/2·303	R	$T^{\frac{1}{3}}R$	log $[T^{\frac{1}{3}}R]$
Fast rate of recovery							
17·2	290·2	3·45	43·6	0·0177	0·0317	1·38	0·14
35·0	308	3·24	45·2	0·280	0·064	2·87	0·458
51·0	324	3·08	47·1	0·0435	0·10	4·71	0·673
Slow rate of recovery							
17·2	290·2	3·45	43·6	0·000825	0·0010	0·0813	-1·02
35·0	308	3·24	45·2	0·0050	0·010	0·572	-0·242
51·0	324	3·08	47·1	0·0142	0·0328	1·55	+0·1779

From Graph 61 the activation energies for the process are 10·0 Kcals/mole for the fast process and 20·2 Kcals/mole for the slower.

It had been hoped to obtain a set of recovery results from quench aged and elongated specimens, however, it was found on stressing that the grain boundaries opened up. This was probably due to the attack of the specimen during annealing by the oil vapour from the quenching medium. However as this could not easily be prevented, no further experiments were carried out on nickel.

Discussion

It is quite clear from the results obtained that two processes are active. There can be little doubt that the values obtained refer to vacancy and divacancy movement. The actual values obtained on elongation and quenching are quite close to the value given by Nicholas[65] (0.98 ev) for a single vacancy. There seems from the results obtained that the activation energy obtained is lowered by the severity of deformation.

The value obtained after fatigue is rather hard to understand. It appears to refer to the movement of single vacancies only. From the recovery graphs it seems that there is little if any divacancy movement. It might possibly be expected that the divacancies produced during the fatigue would condense to the dislocation lines as the fatigue continued. However from the results of O'Hara this does not appear to happen. It may in fact be the case that the result obtained refers to divacancy recovery in which case it would be rather high when compared with the others.

With the exception of the fatigue result it would seem that as anticipated the dependance of Em on the vacancy concentration lies roughly between the effect in copper and aluminium.

GRAPH 50 NICKEL ∂ELONGATION 18.3 °C

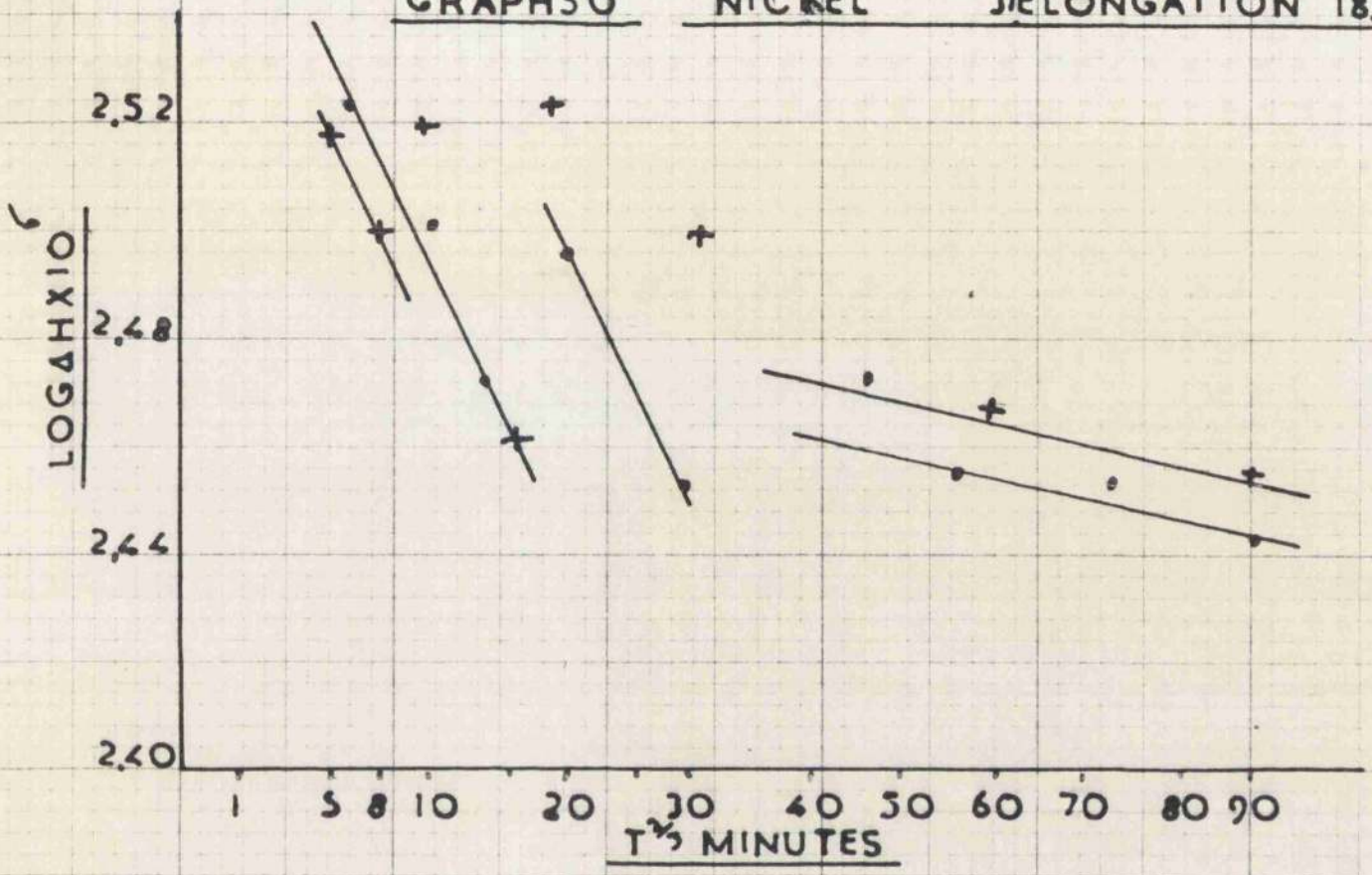

GRAPH 51 NICKEL ∂/EL 37.8 °C

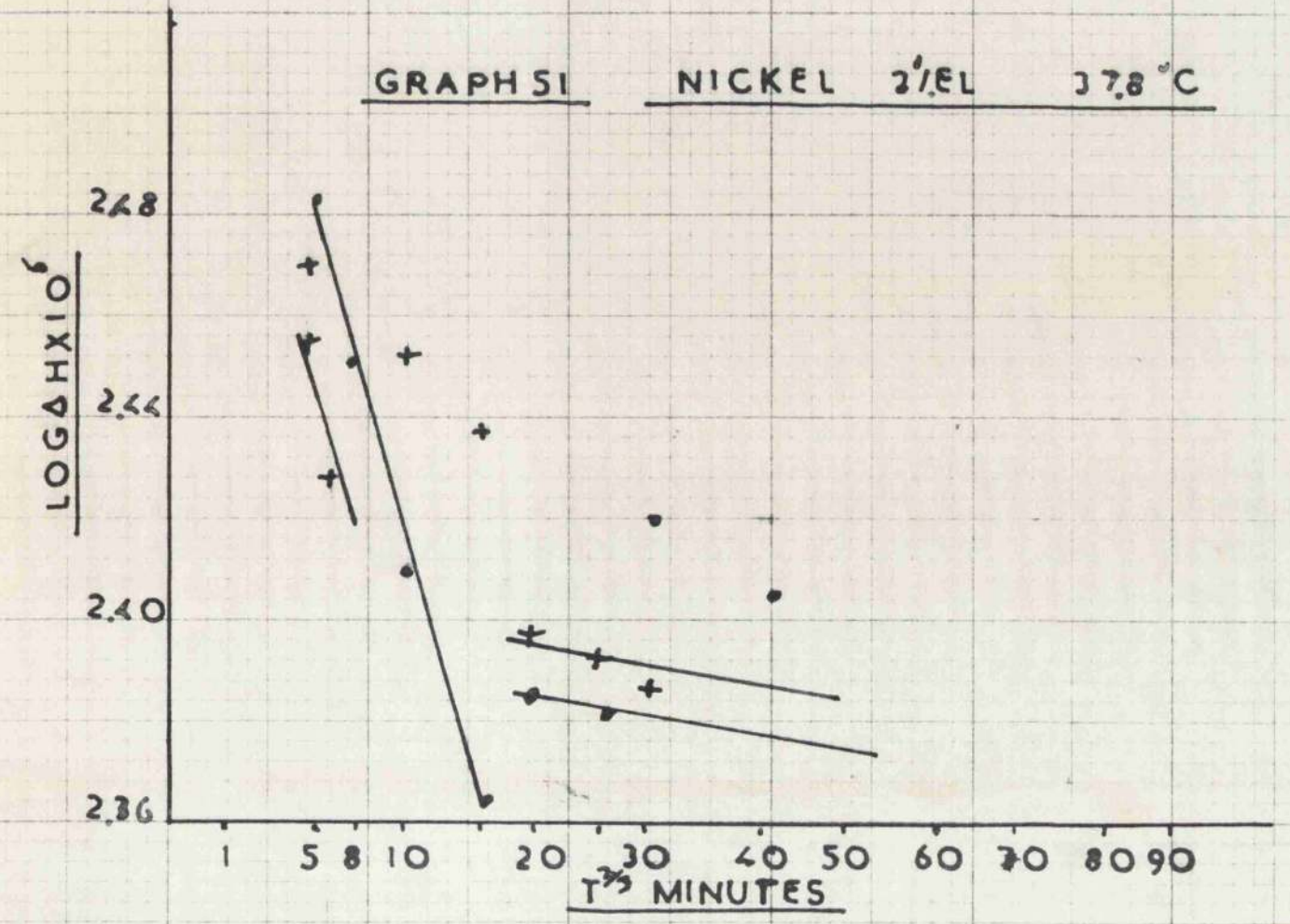

GRAPH 52 NICKEL 3% EL 52°C

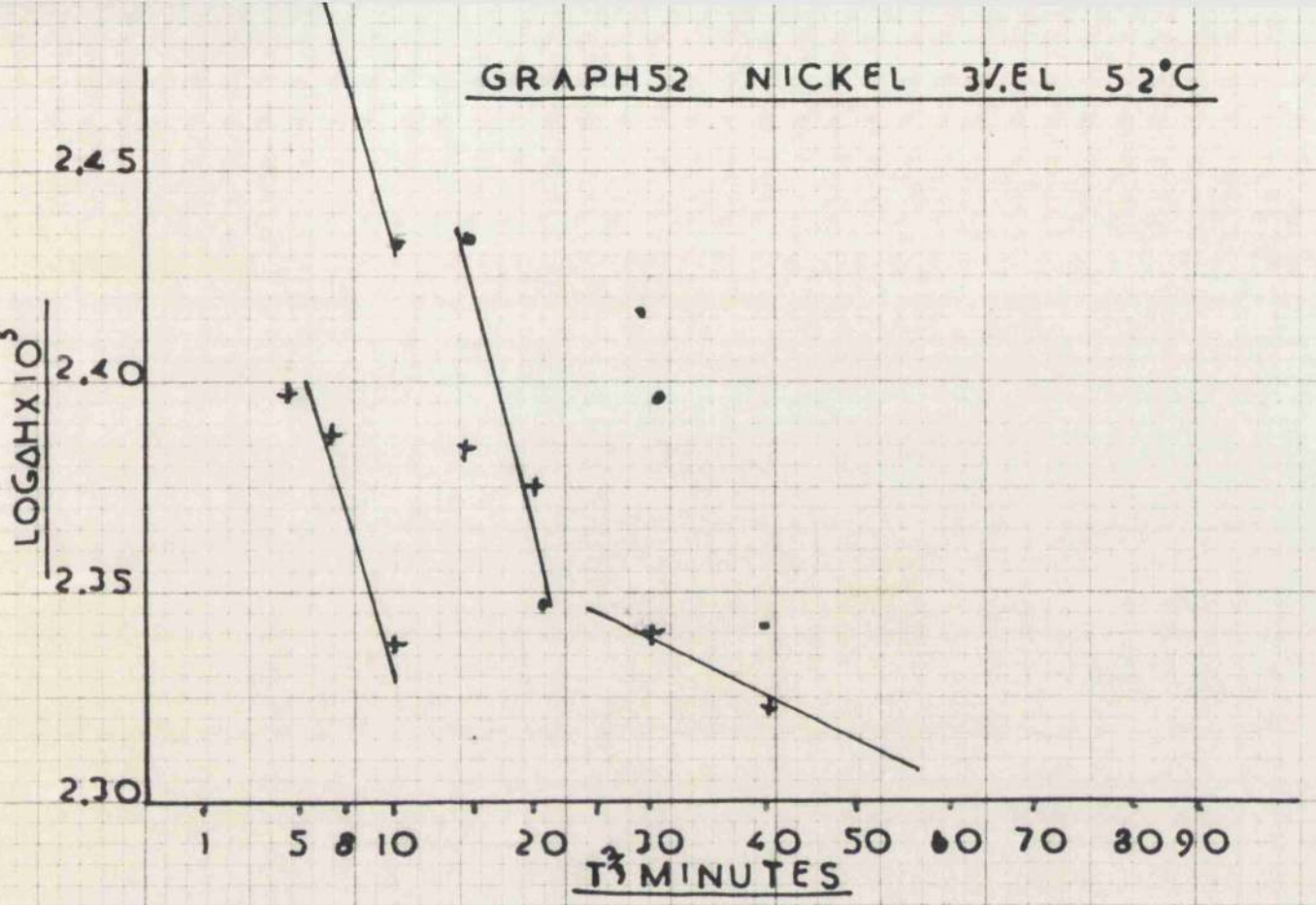

GRAPH 53 NICKEL 3% EL

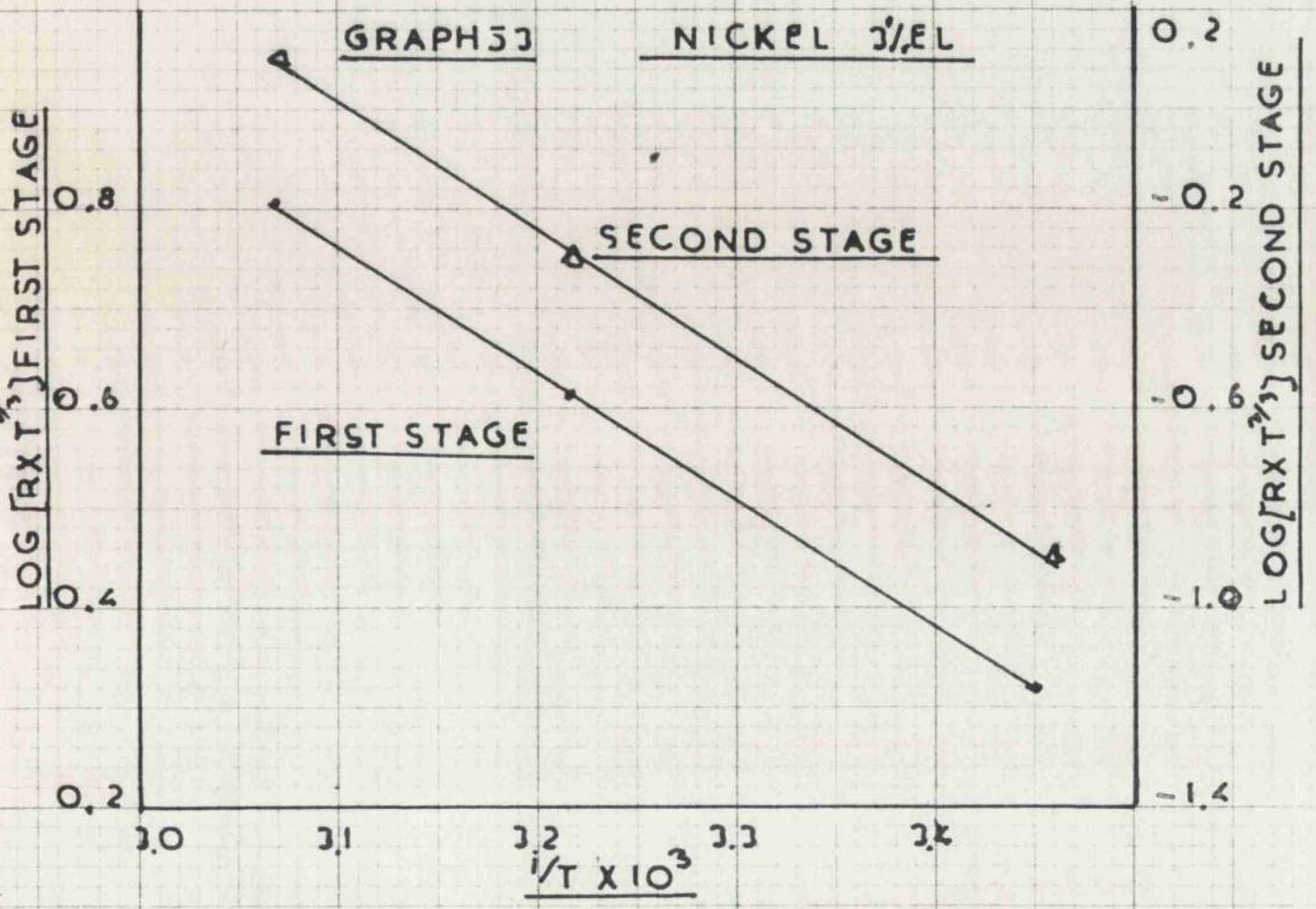

GRAPH 54 NICKEL FATIGUED 16.7 °C

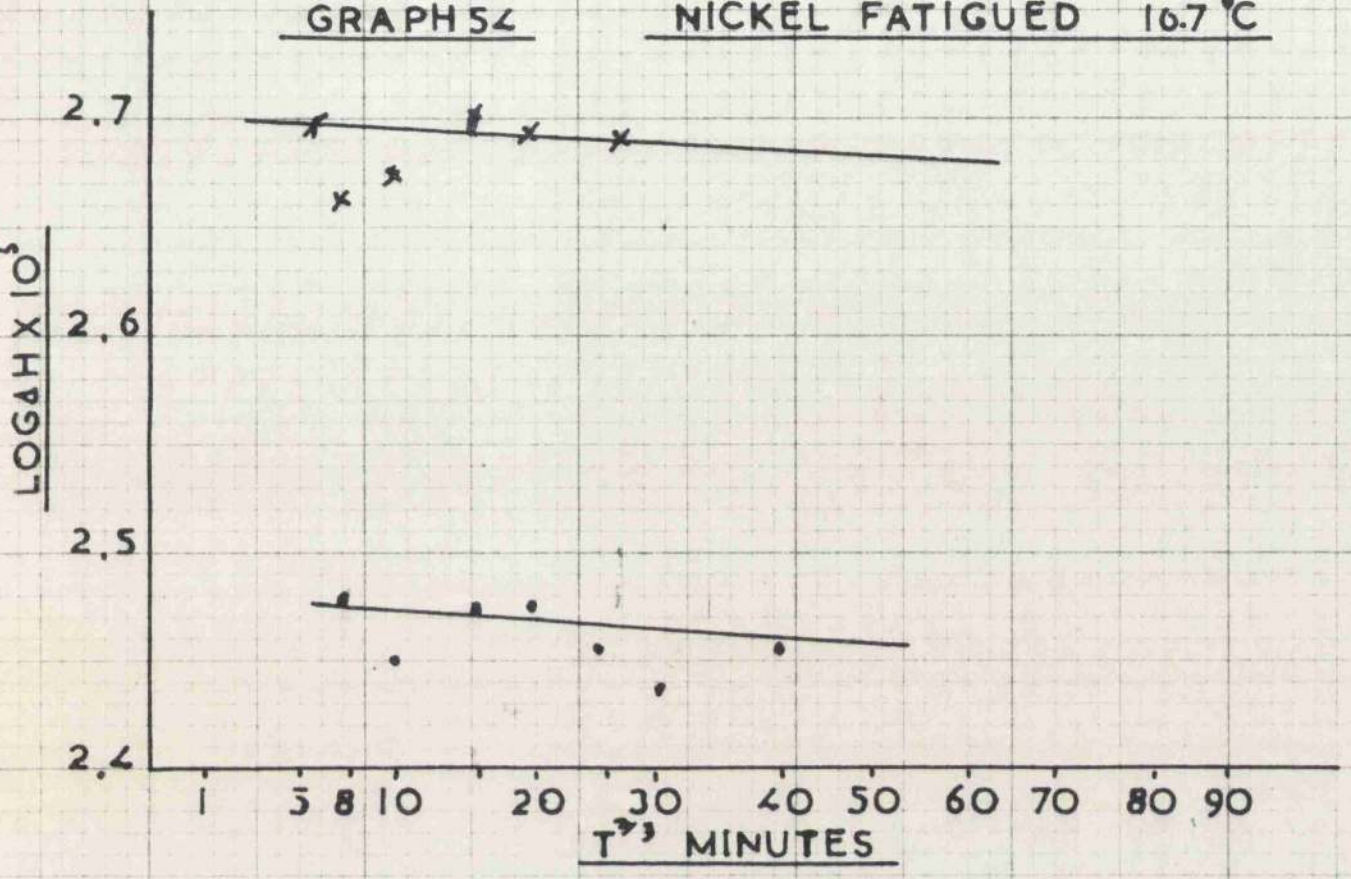

GRAPH 55 NICKEL FATIGUED 44.5°C

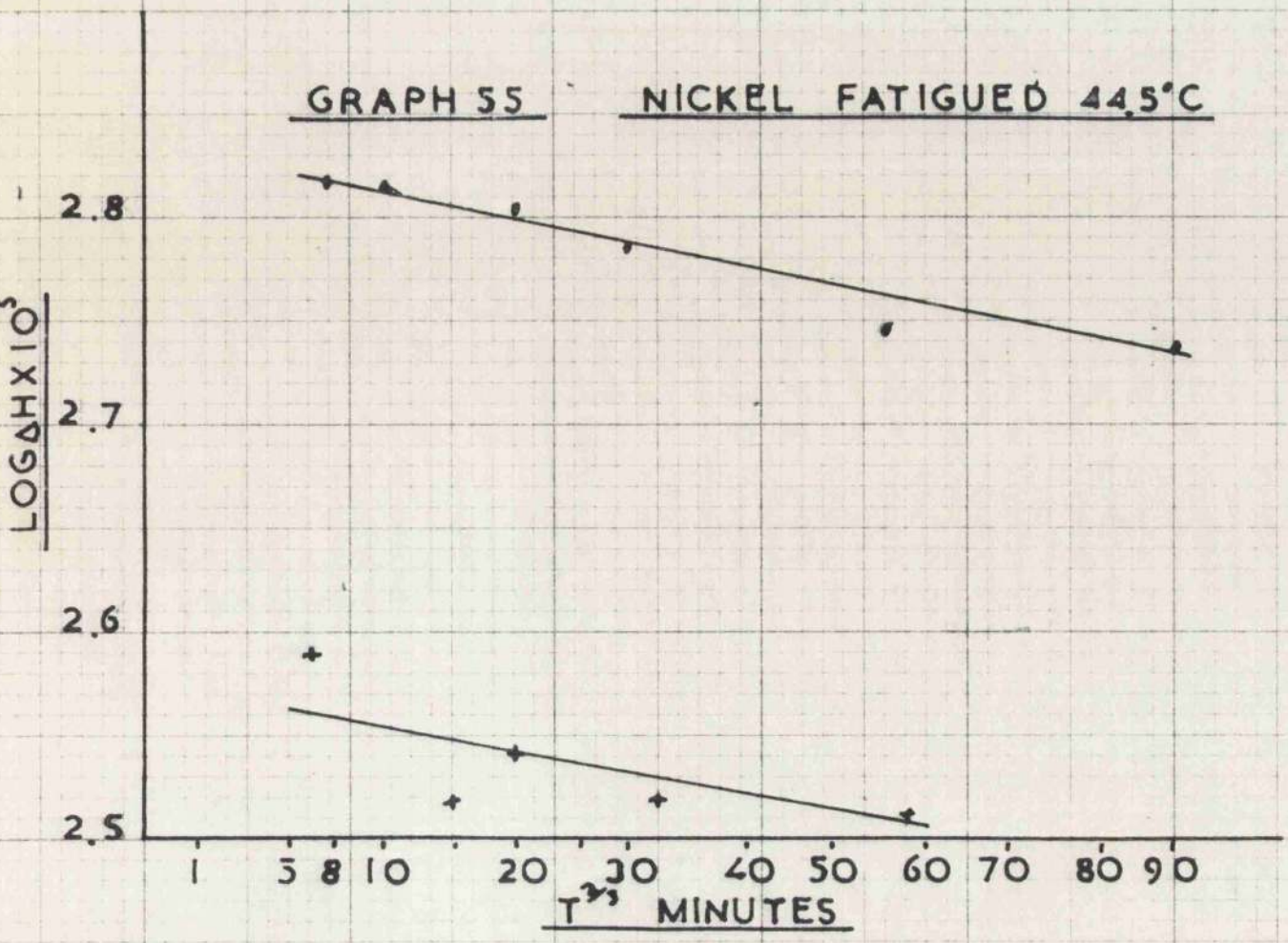

GRAPH 56 NICKEL FATIGUED 58.5 °C

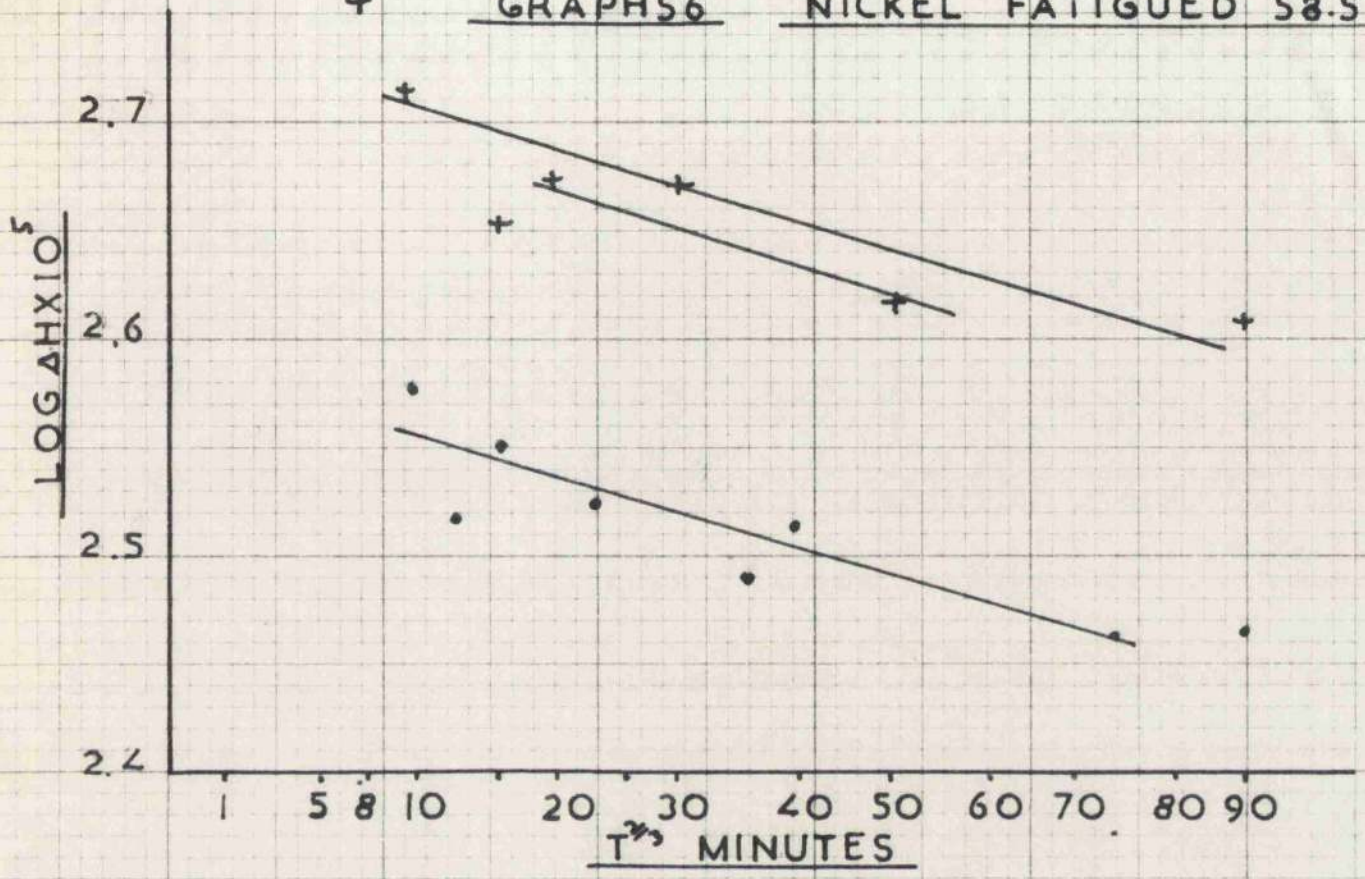

GRAPH 57 NICKEL FATIGUED 70 °C

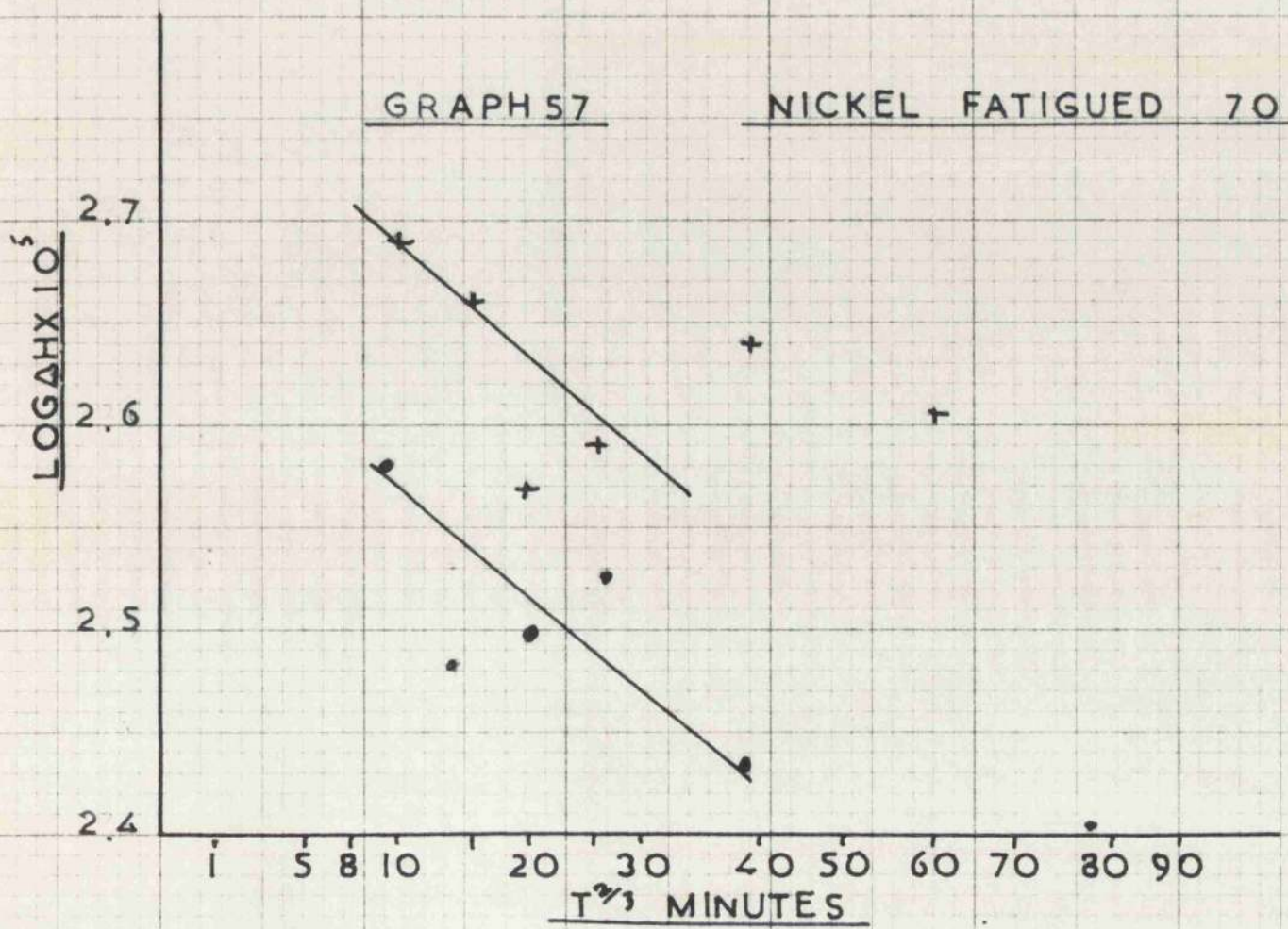

GRAPH 58 NICKEL FATIGED

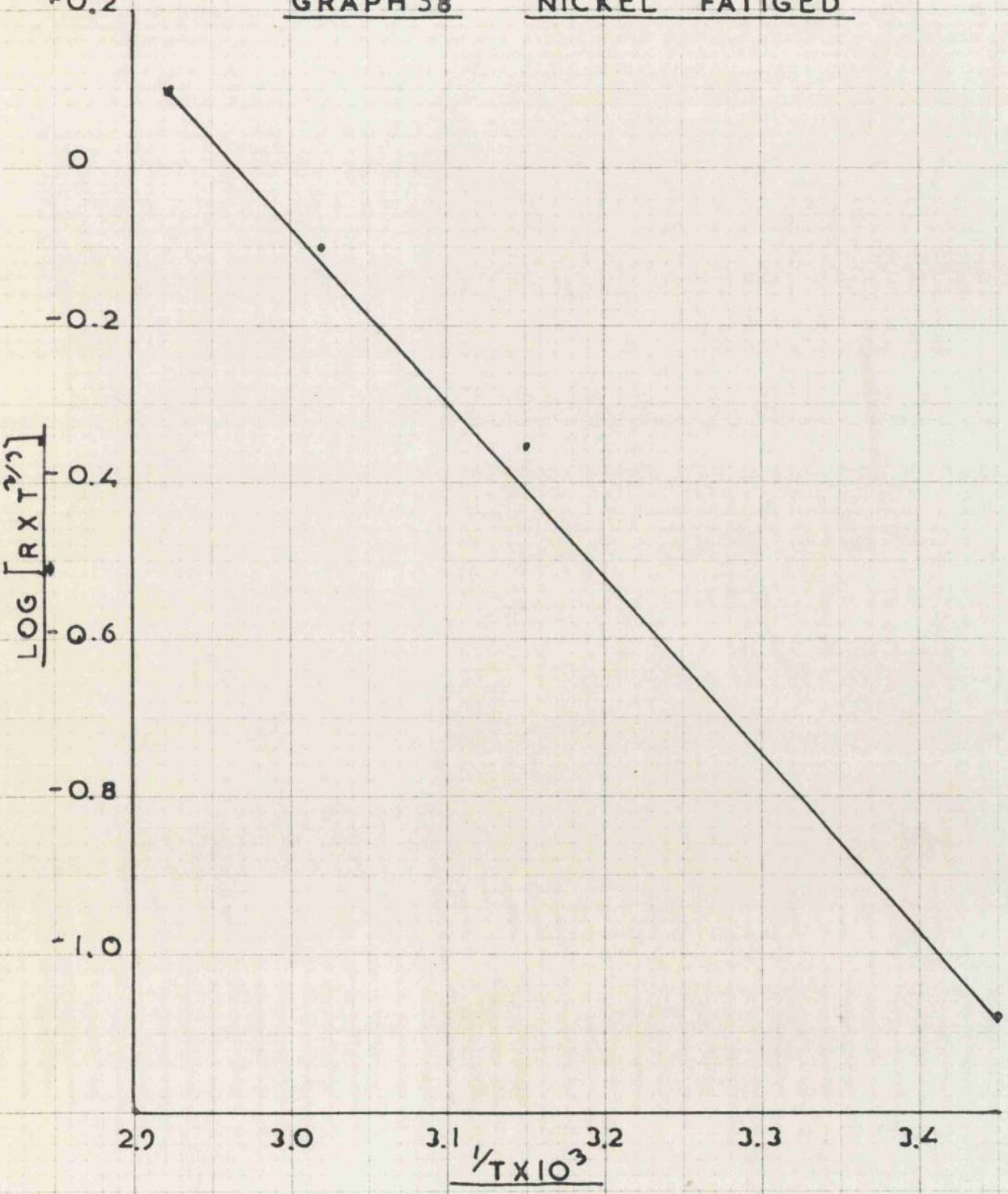

GRAPH 59 NICKEL QUENCHED 1410 °C 17.2 °C

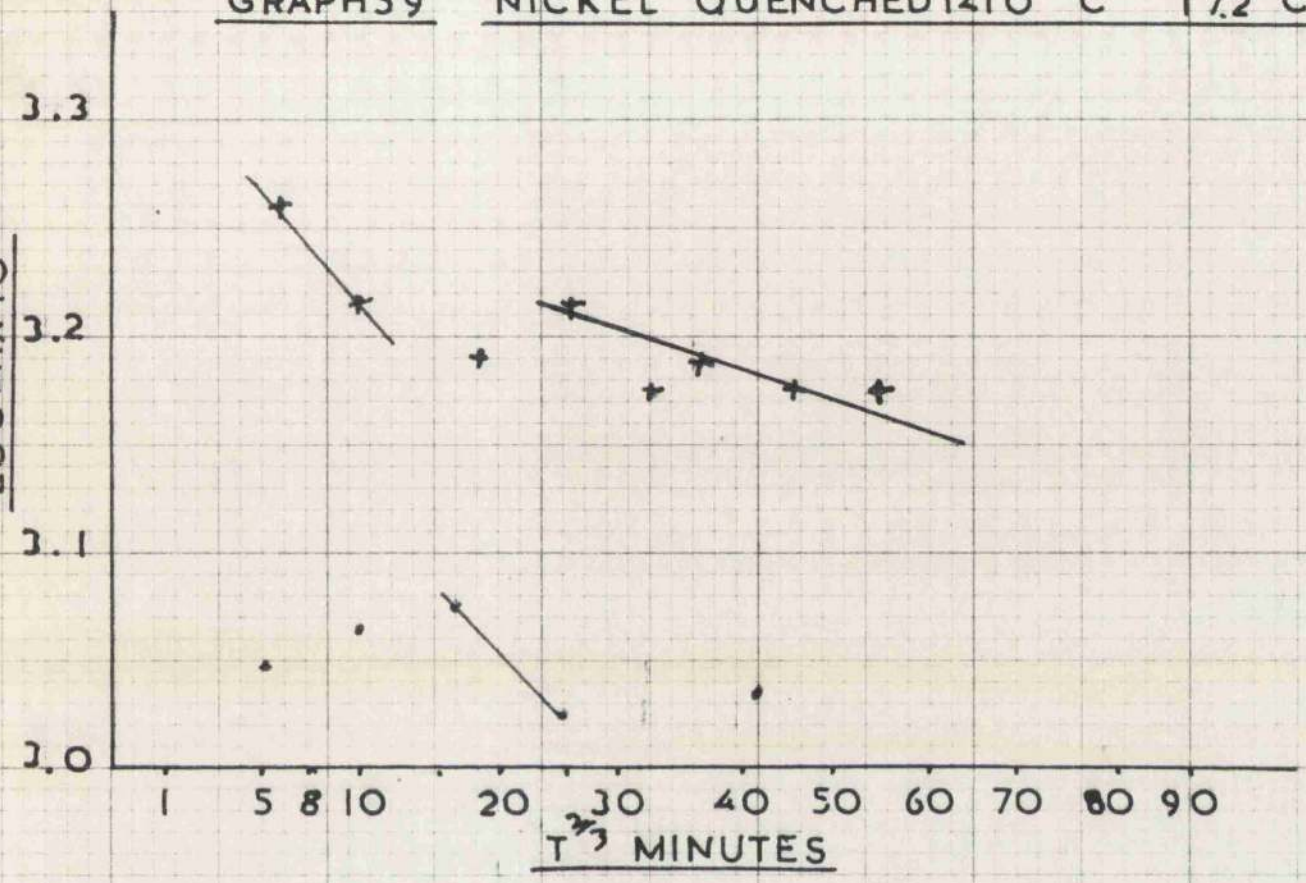

GRAPH 60 NICKEL QUENCHED 1410 °C 35 °C

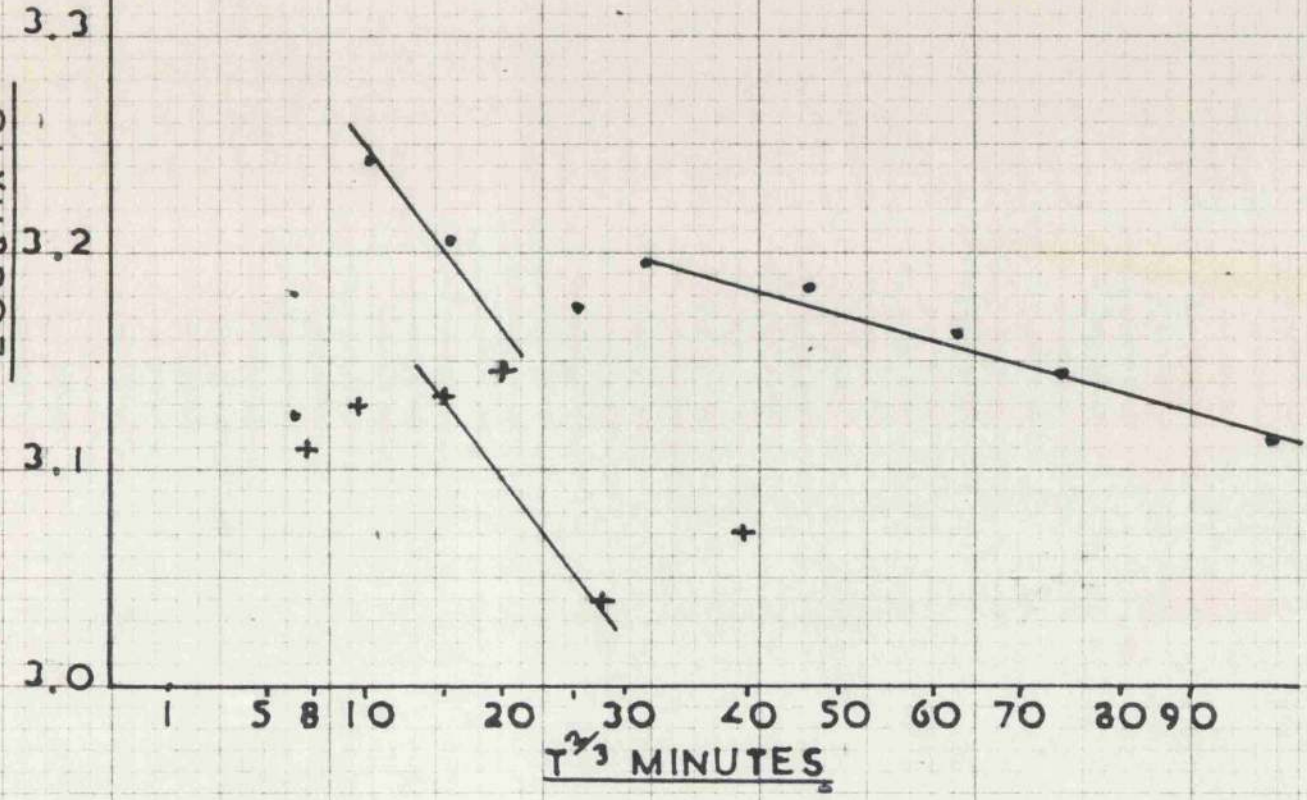

GRAPH 61 NICKEL QUENCHED 1410°C 51°C

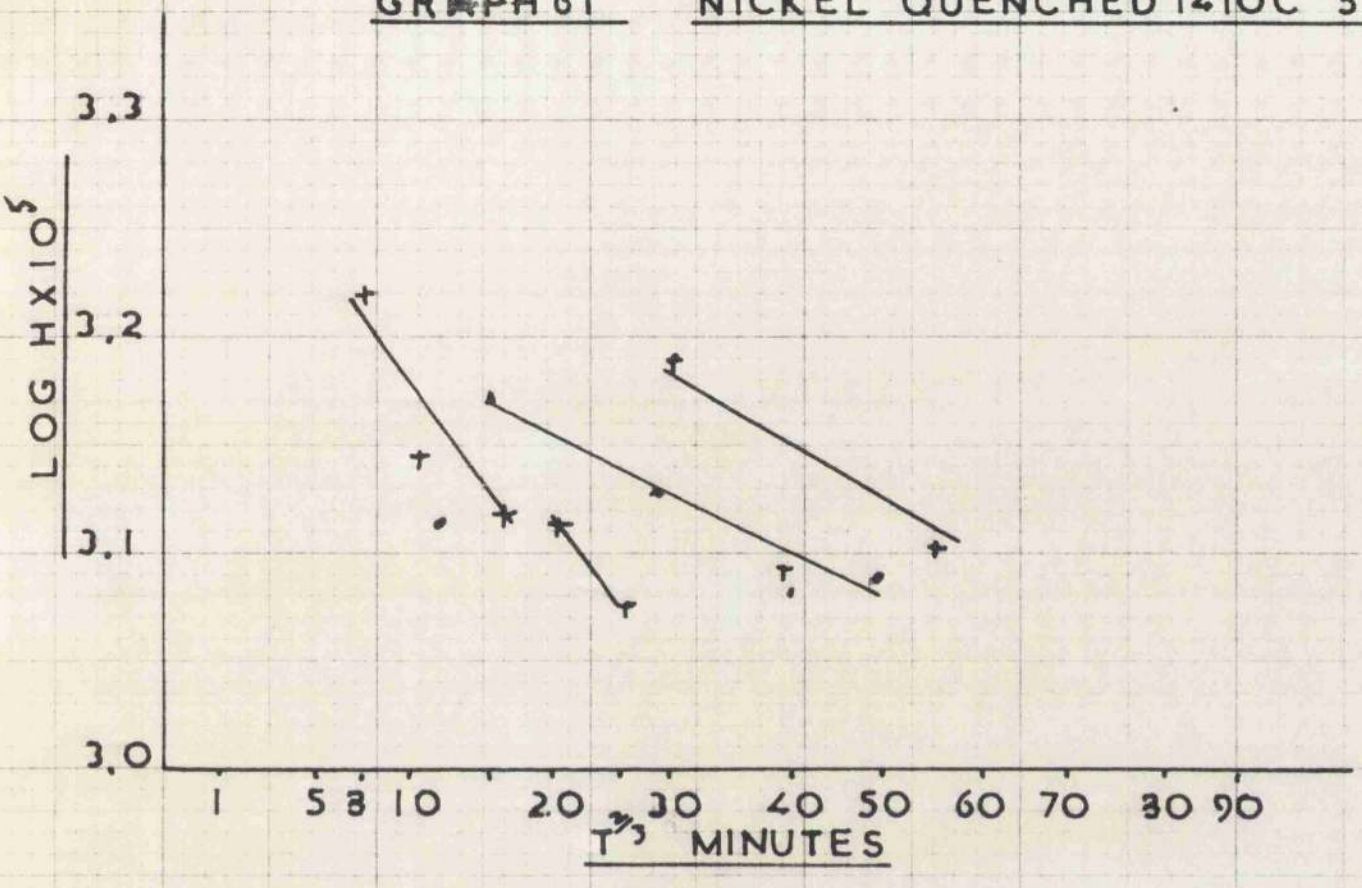

GRAPH 62 NICKEL QUENCHED 1410 °C

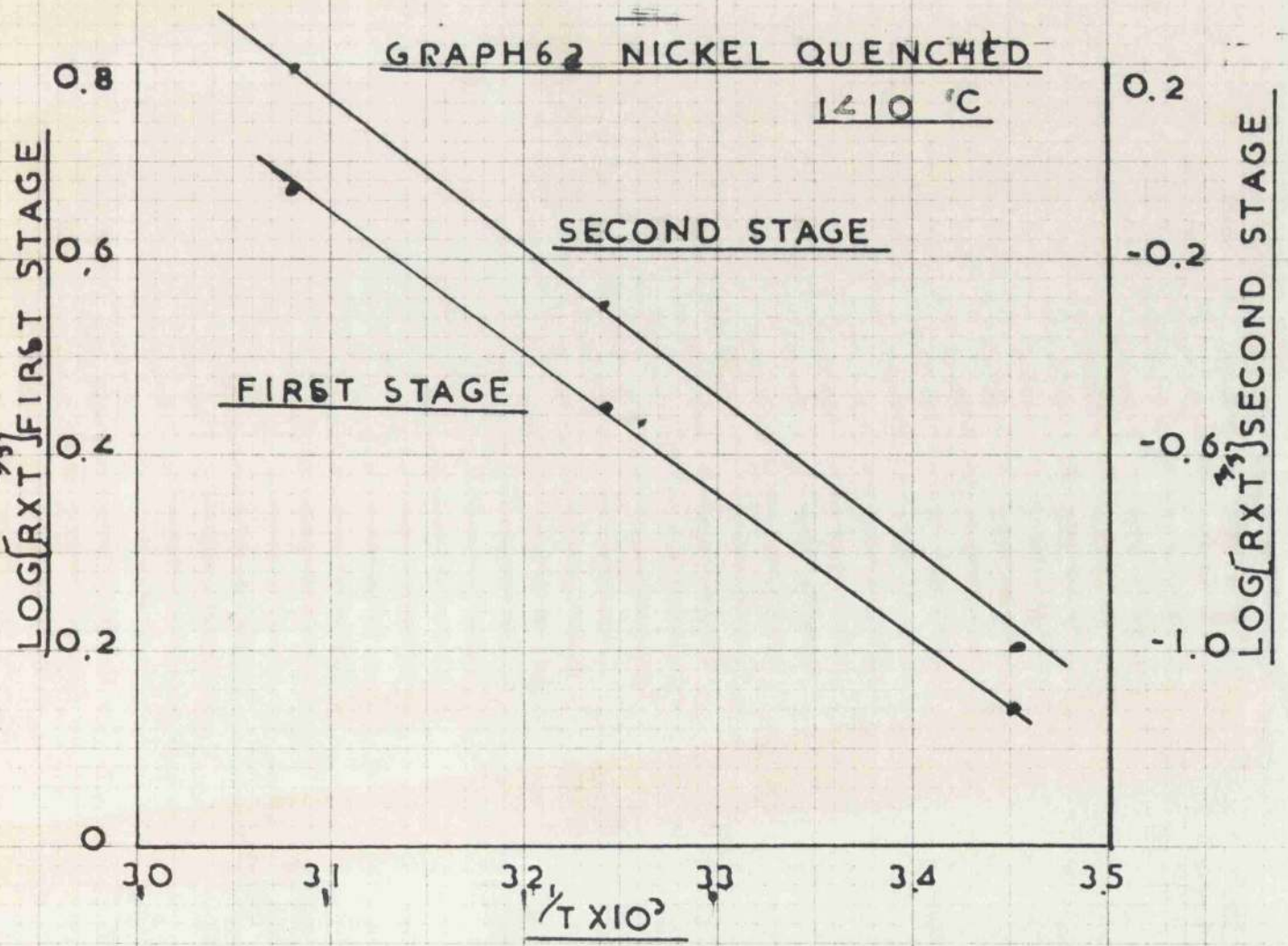

CHAPTER 6

SELF DIFFUSION IN SILVER

(a) Quenched from 810°C

(b) Quenched from 910°C

Discussion

Self Diffusion in Silver

It was thought desirable that the behaviour exhibited in the low stacking fault energy metal be checked on another metal of similar stacking fault energy. Silver was the most suitable metal available but owing to the expense involved, it was decided to carry out only quenching experiments.

Kimura et al[34] showed that two possible types of recovery are possible in noble metals. If the metal is quenched from below 800°C most of the observed recovery was due to single vacancies. If however the metal was quenched from above 800°C then most of the observed recovery was due to divacancy migration. It was also shown that the formation of vacancy clusters provided a sink for the quenched in point defects.

In veiw of the larger diameter of the specimens used in these experiments and the consequent rather milder quench the quenching temperatures used were 810°C and 910°C. The two temperatures chosen should provide both a range of vacancy concentrations and divacancies when quenched from the upper temperature.

The material used was Johnson Mathey fine silver, supplied as 3/16" diameter rod. This was cut to 10 cm. lengths and annealed at 900°C for 3 hours under vacuum. The specimens were quenched from an argon atmosphere into water after soaking at the

quenching temperature for one hour. The quenching medium used was water at room temperature and a glass wool cushion was used to reduce the shock of the impact.

(a) Quenched from 810°C

The silver was quenched as described above and measurements made at temperatures of -1·1, 4·4, and 15°C, the results being shown in graphs 62, 63 and 64. While the results obtained are only moderately satisfactory, it is evident that only one recovery process is active. The results are summarised in Table 14.

Table 14 - Silver quenched from 810°C

°C	°K	$\frac{1}{T}$ x 1000	$T^{\frac{2}{3}}$	R/2·303	R	$T^{\frac{2}{3}}$ R	log[$T^{\frac{2}{3}}$ R]
15	288	3·475	43·6	0·0252	0·058	2·53	0·43
4·4	277·2	3·65	42·2	0·00866	0·0199	0·84	- 0·075
-1·1	272	3·72	41·8	0·00653	0·0153	0·642	- 0·1925

When these results were plotted on Graph No. 65 the activation energy for the process was found to be 16·6 Kcals/mole.

(b) Quenched from 910°C

The procedure was the same as above and the recovery measurements made at the same temperature. The results shown in Graphs 66, 67 and 68 show two recovery processes. The data obtained is shown in Table 15.

Table 15 - Silver quenched from 910°C

°C	°K	$\frac{1}{T} \times 1000$	$T^{\frac{3}{2}}$	R/2·303	R	$T^{\frac{3}{2}} R$	log $[T^{\frac{3}{2}} R]$
Short Time Recovery							
15	288	3·475	43·6	0·052	0·119	5·22	0·718
14·4	277·2	3·65	42·2	0·0315	0·0726	3·07	0·482
-1·1	272	3·72	41·8	0·0282	0·066	2·72	0·442
Long Time Recovery							
15	288	3·475	43·6	0·0163	0·0375	1·69	0·218
14·4	277·2	3·65	42·2	0·0127	0·0291	1·23	0·09
-1·1	272	3·72	41·8	0·00466	0·0175	0·45	-0·3468

From Graph 69 the activation energies for the two processes were found to be

(1) Short time recovery Q = 7·82 Kcals/mole

(2) Long time recovery Q = 14·5 Kcals/mole

Discussion :

The results obtained above are of the correct order of magnitude and it appears that the recovery after the 810°C quench is due to the movement of single vacancies. The quenching temperature of 910°C gave two stages of recovery, the first of which is almost certainly due to the movement of divacancies. The second stage may with confidence be ascribed to single vacancies. The relative values of the activation energies for these two processes are about correct as the activation energy for divacancy movement should be about half that for vacancy movement.

While the results from quenching from 810°C were not entirely satisfactory, the activation energy for the process is certainly greater than 14·5 Kcals/mole. It would appear that the activation energy is reduced by a more severe quench. However, it will be seen from Tables 14 and 15 that the corresponding values of R for the higher quenching temperature are lower indicating that the vacancy concentration was lower. A possible explanation of this is found in Kimura's work where it is suggested that the point defects are retained mainly as divacancies after the high temperature quench.

It would seem, therefore, that the reduction in activation energy found is a function of the total number of point defects rather than the concentration of any one species. It is of some interest to note that the high concentration of divacancies reduced the value of Em for single vacancies even though they had condensed on to the dislocation lines. It might then be that the value of Em was connected with the lattice strain.

GRAPH62 SILVER QUENCHED 810 °C -1.1 °C

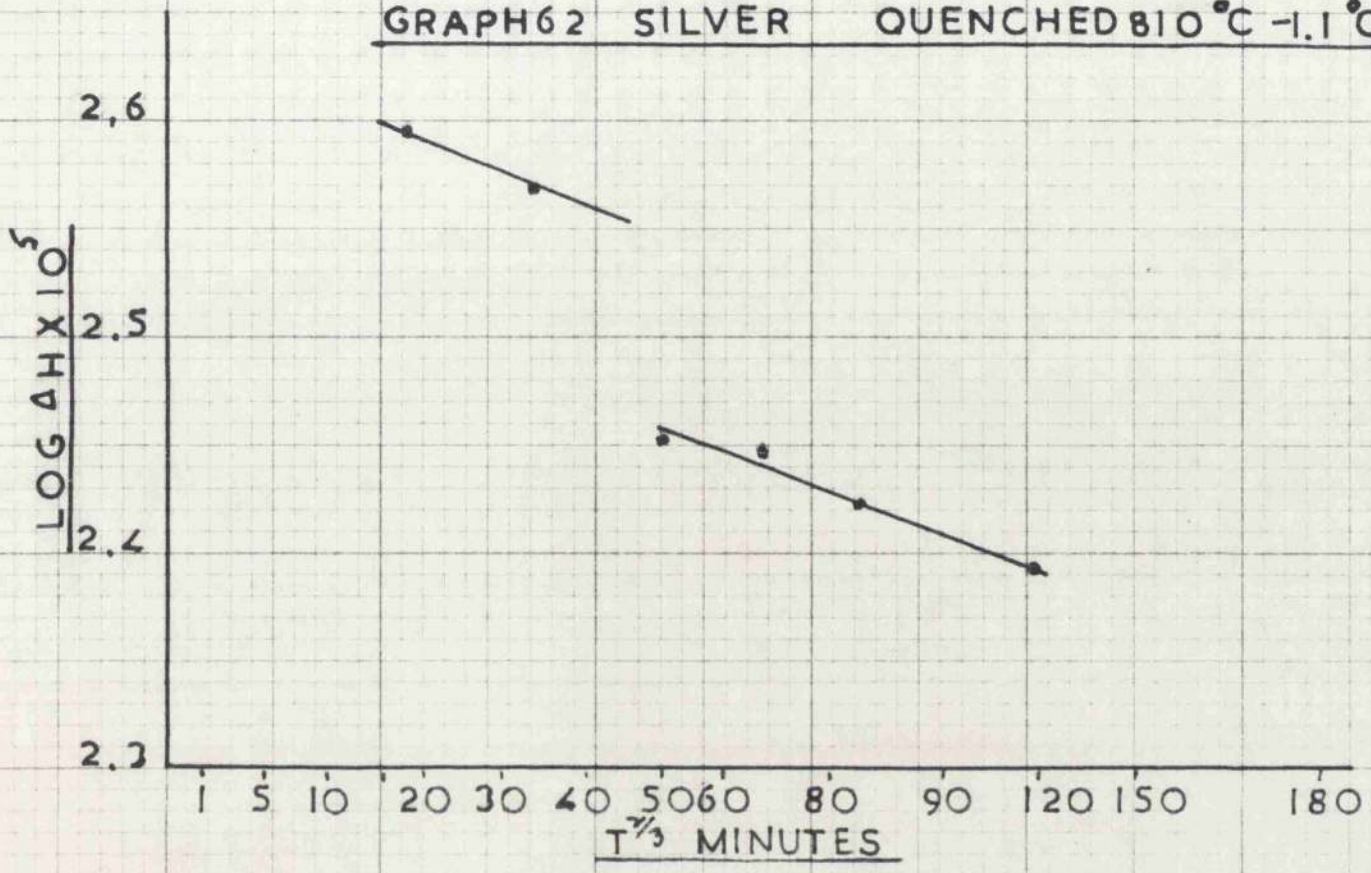

GRAPH63 SILVER QUENCHED 810°C 44°C

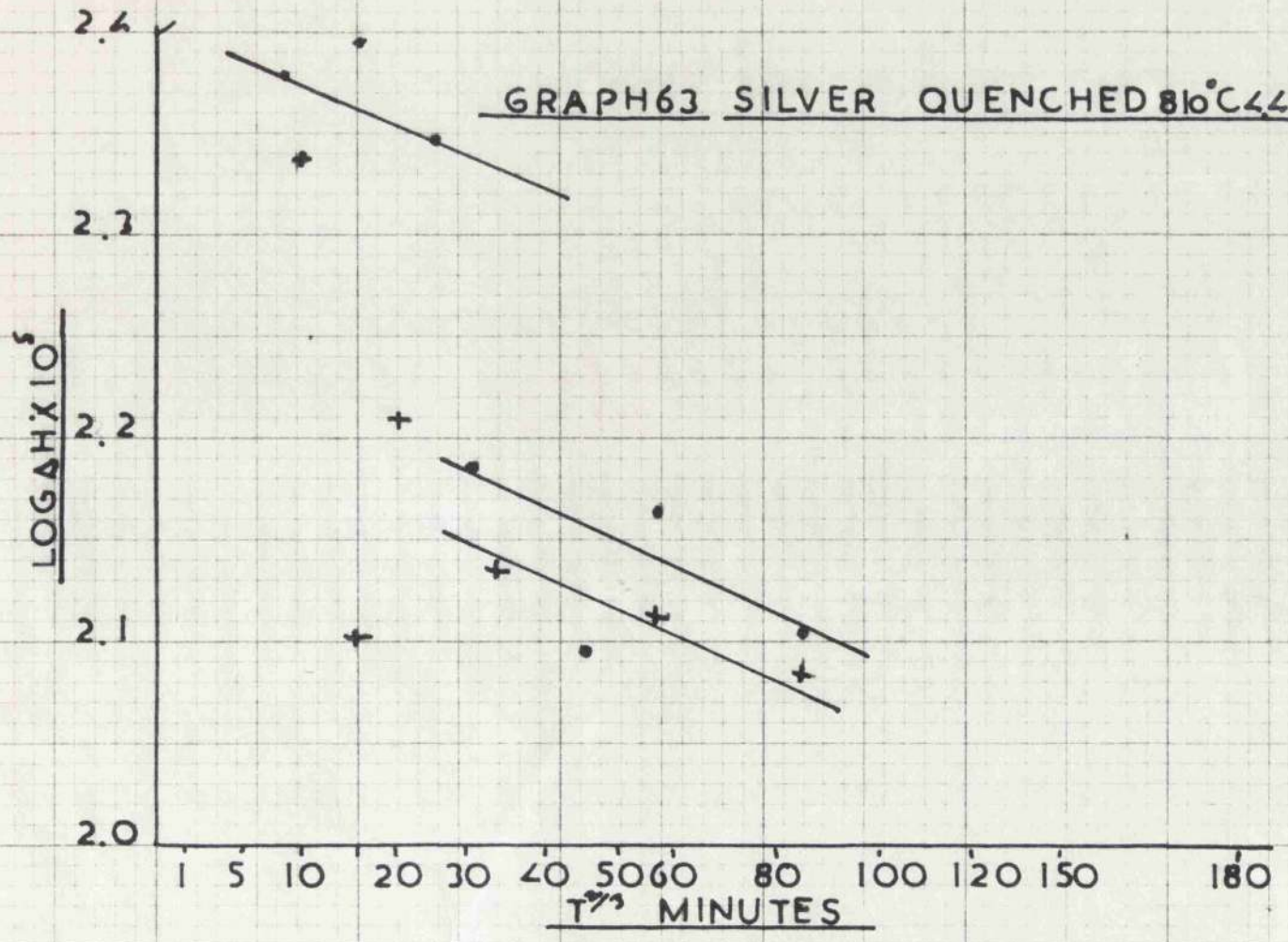

GRAPH 64 SILVER QUENCHED 810°C 15°C

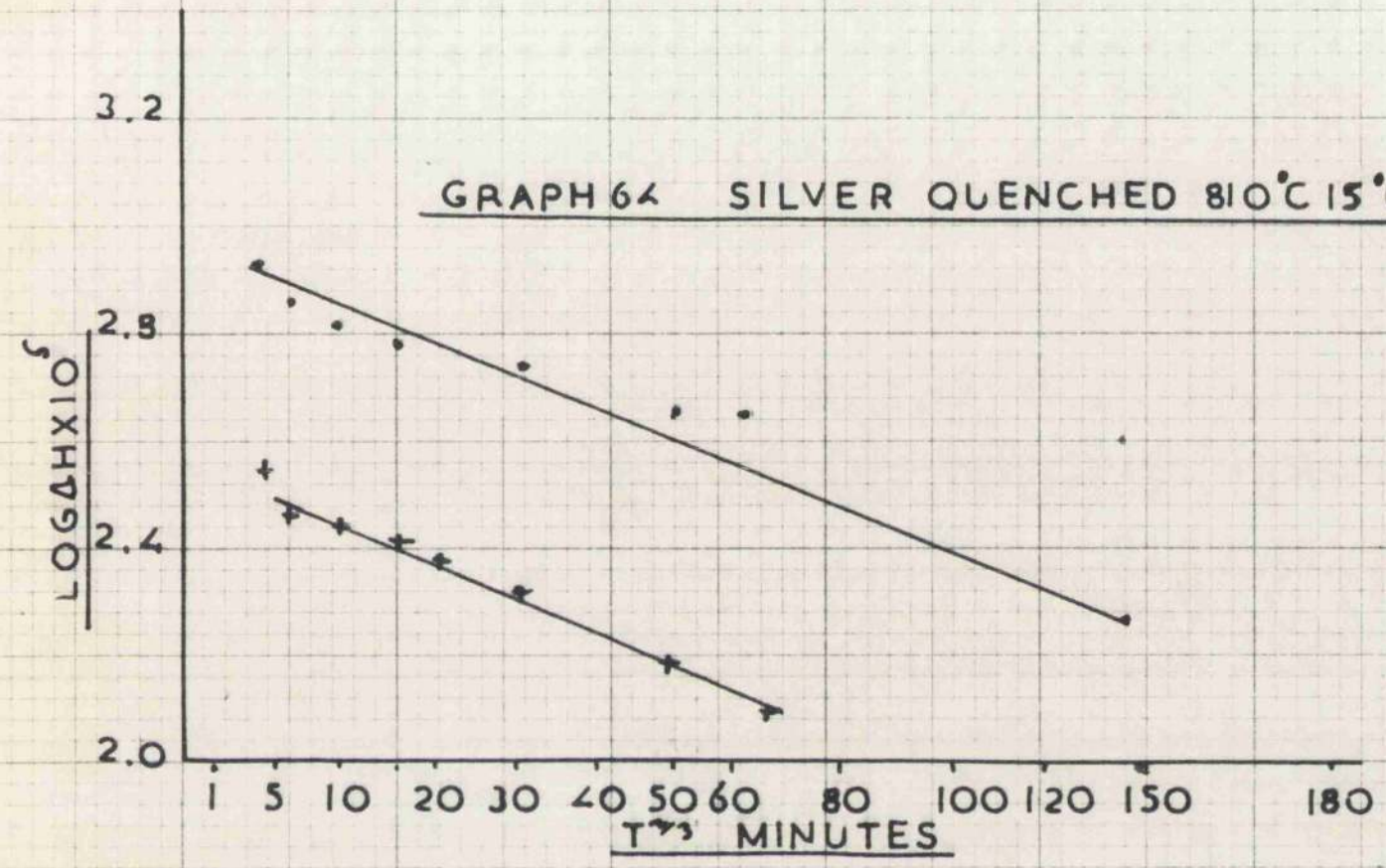

GRAPH 65 SILVER QUENCHED 810°C

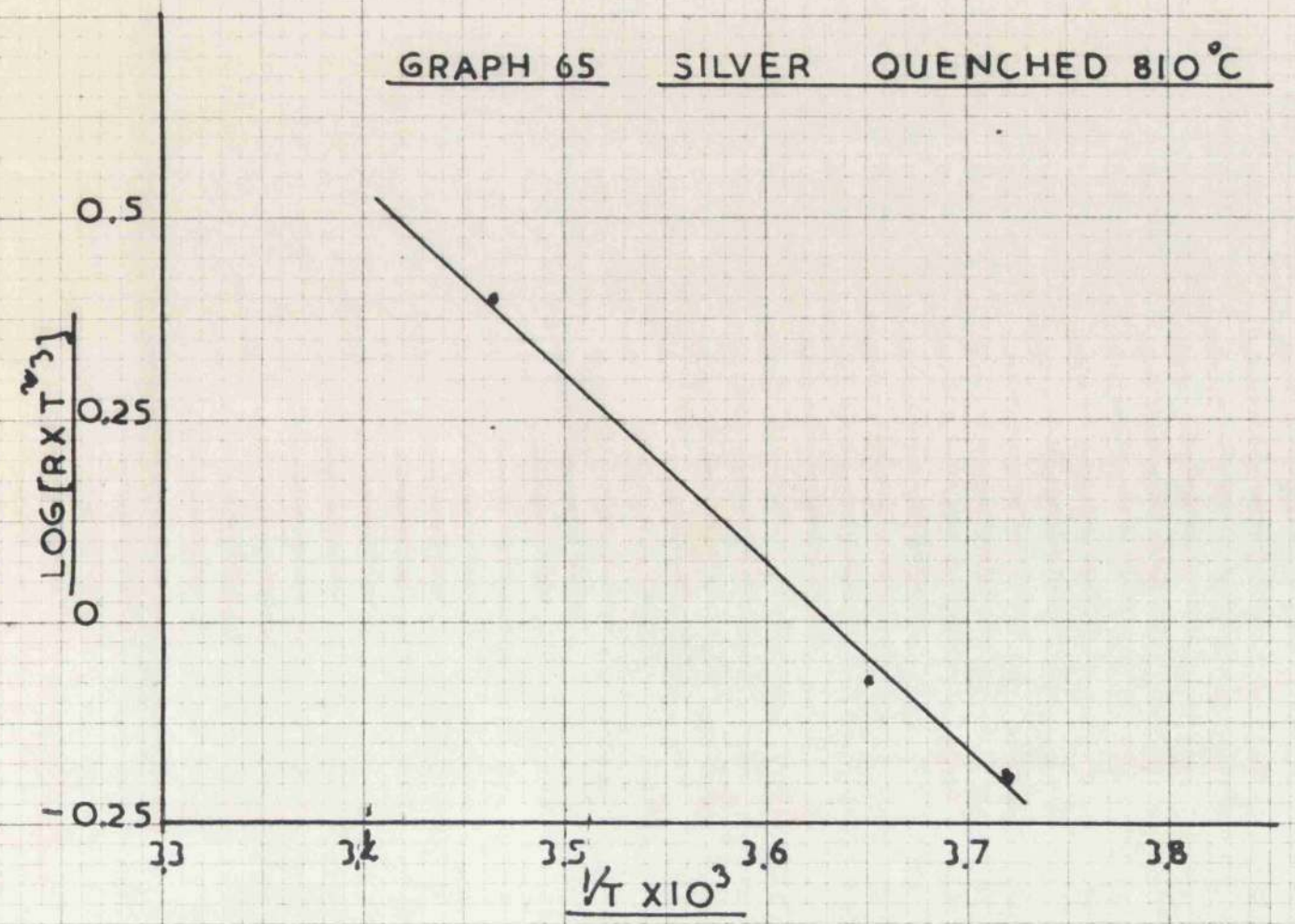

GRAPH 66 SILVER QUENCHED 910°C -1.1°C

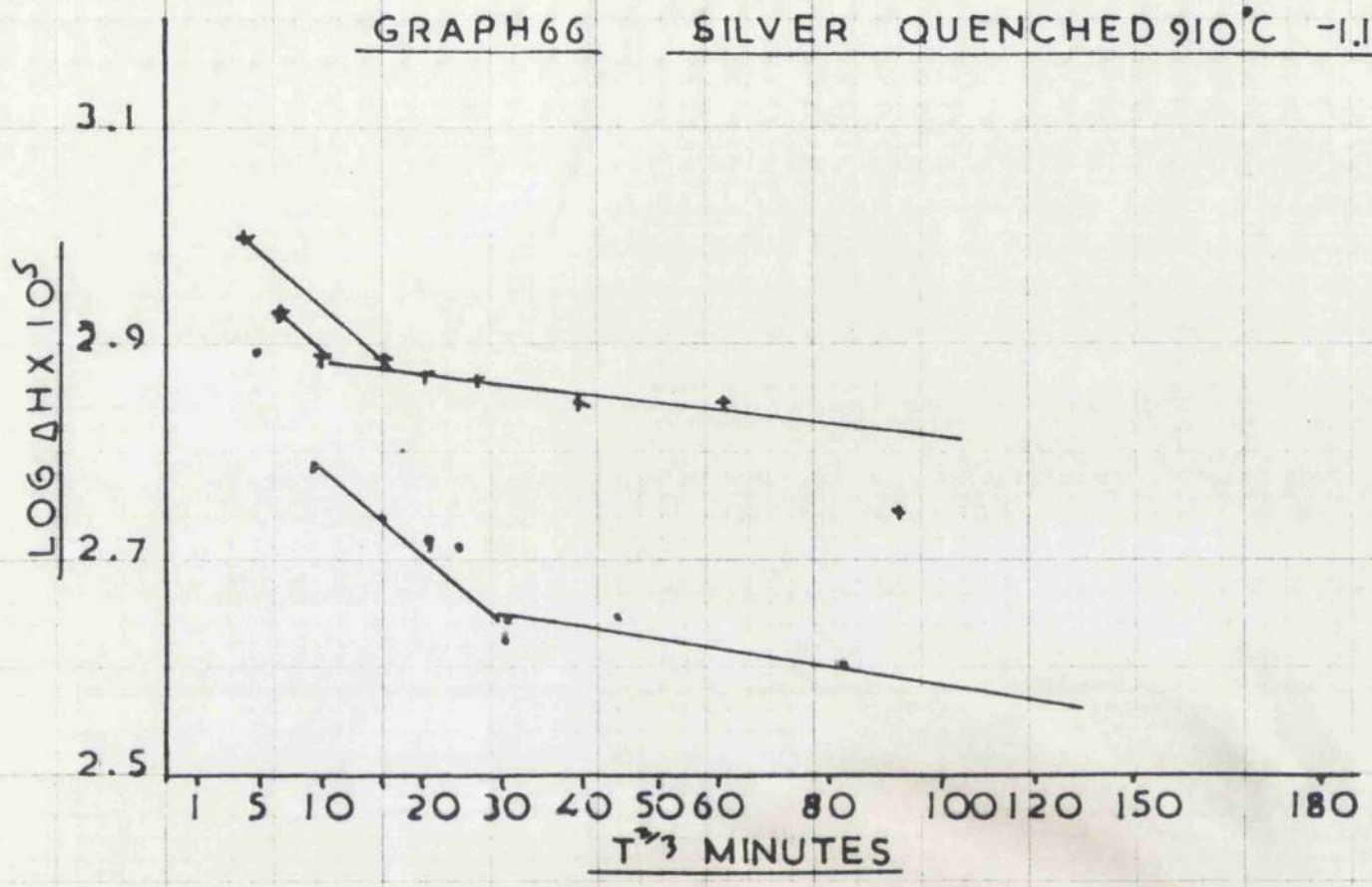

GRAPH 67 SILVER QUENCHED 910°C -4.4°C

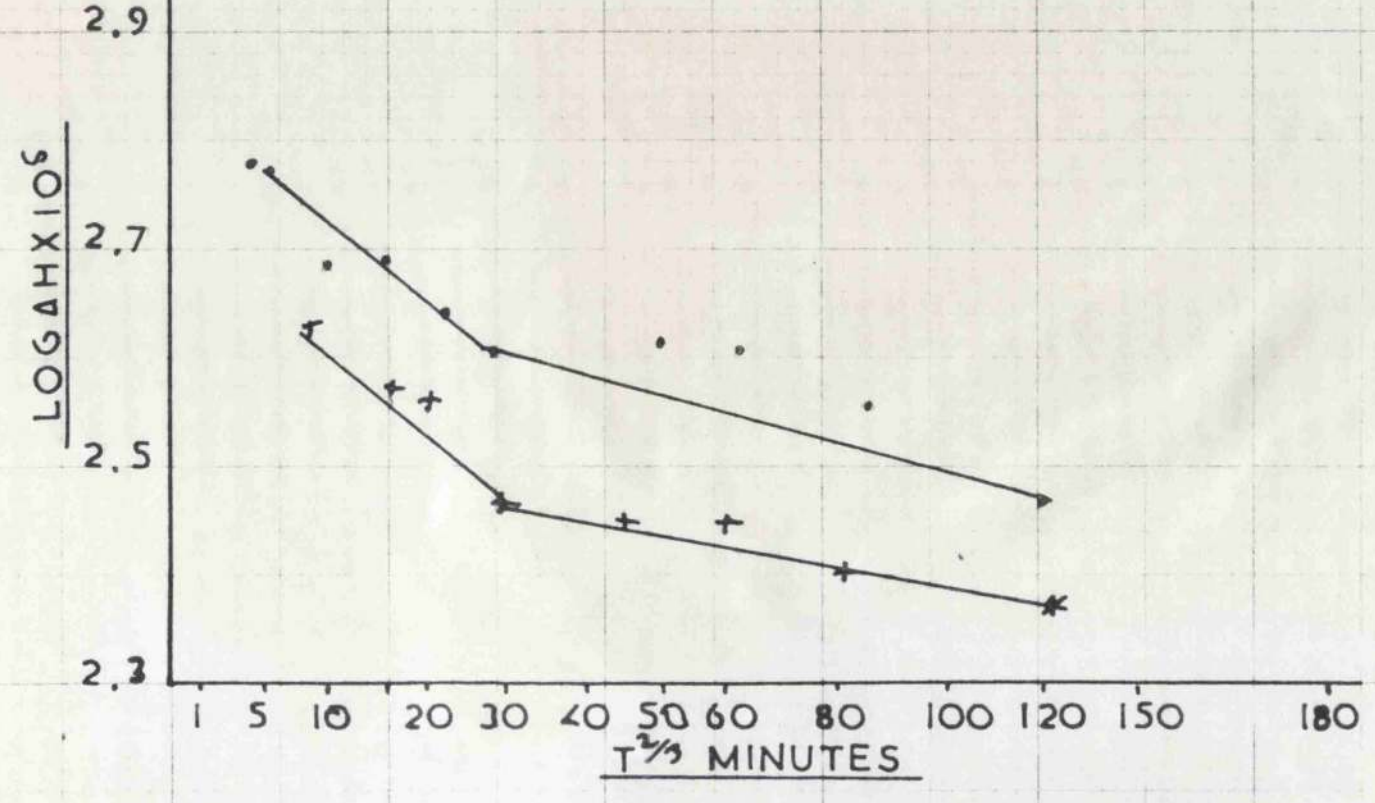

GRAPH 68 SILVER QUENCHED 910°C 15 °C

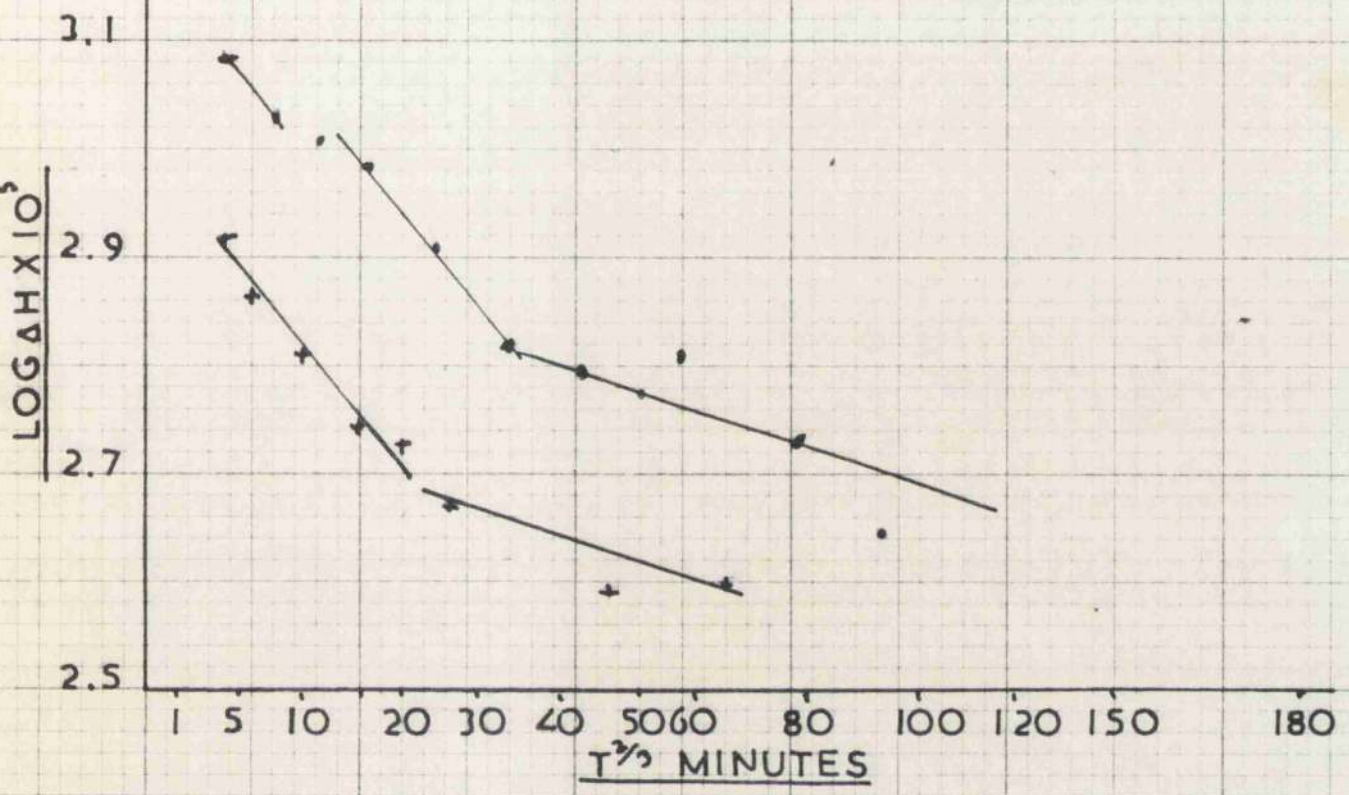

GRAPH 69 SILVER QUENCHED 910 °C

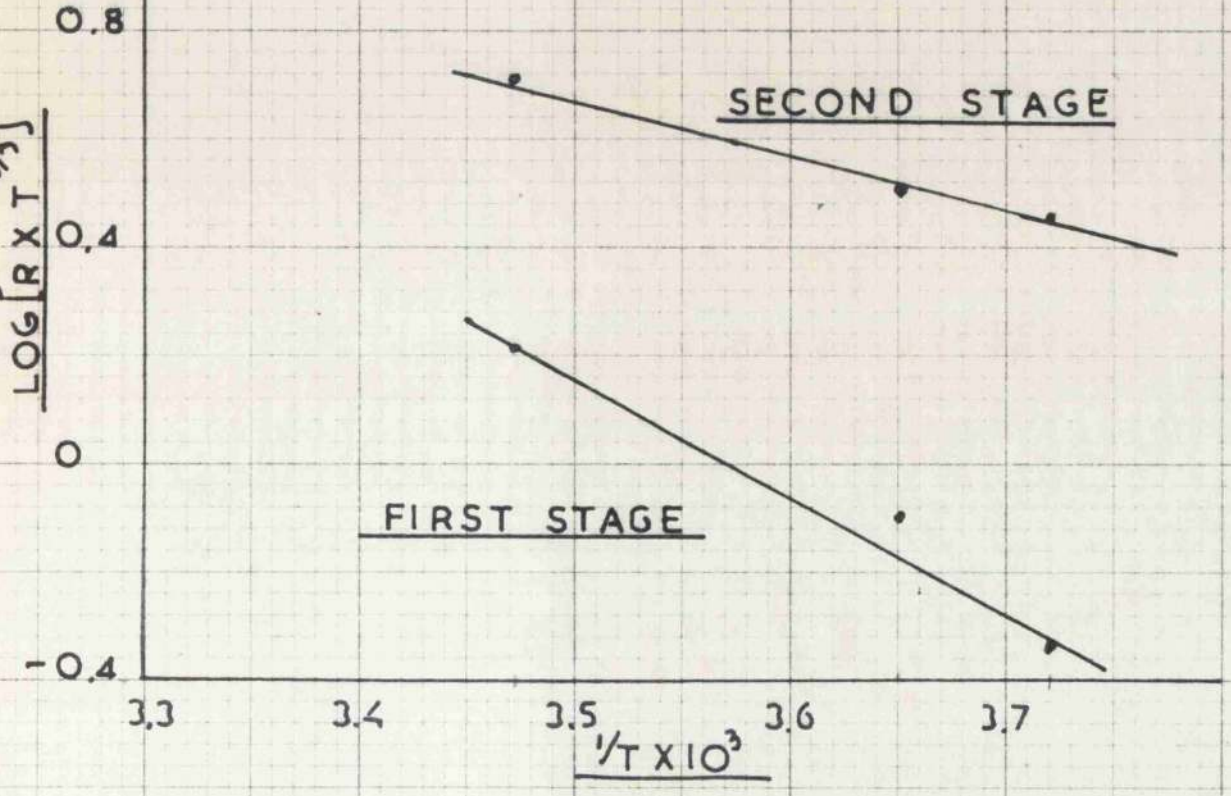

CHAPTER 7

ANALYSIS OF DIFFUSION RESULTS

Analysis of Diffusion Results

In the experimental work described above a selection of F.C.C. metals have been examined and a number of different effects illustrated.

In copper the activation energy obtained after 4% elongation (20·1 Kcals mole) could be related with confidence to the movement of single vacancies. This value of 20·1 K cals/mole is close to but rather lower than other reported values. The reason for this low value will become clear later. It was also shown that another recovery process was active with an activation energy of about half the above figure. This indicates that the process was due to the movement of divacancies which are thought to move with about this energy.

From the series of results shown in Table 7 it appears that the value obtained for the activation energy is lowered by the increasing severity of process used. It would also appear that this reduction in activation energy is a function of point defect concentration rather than of dislocation density.

As previously stated the value of 5·5 Kcals/mole obtained in the quench-aged-elongated specimen seems rather out of place. The value is close to the 0·25 ev estimated by Huntington[60] for the movement of a copper interstitial. However, as it requires 4 ev[63] to form an interstitial atom in copper compared to

1.3 ev[62] to form a divacancy, it is difficult to imagine a process where a high concentration of interstitials is formed. Cottrell[64] has illustrated that screw-screw ~~interstices~~ INTERSECTIONS will probably result in the production of interstitials. As this effect was only noted when a fully quench aged specimen was elongated, it would appear that the heavily jogged dislocation lines have a controlling function if in fact intersections are produced. The other possible process, i.e. the movement of jog segments alon g the dislocation lines does not seem very reasonable. Indeed it would appear that only rearrangement of jogs on a dislocation line would result in an increase in internal friction. Thus while no firm explanation can be given for this process, it may possibly be due to the movement of interstitial atoms produced by a rather unusual process as a result of prior quenching.

It can be said however that the decrease in activation energy predicted from the preliminary work was in fact substantiated over a fair range of deformations.

The results obtained with quenched silver showed that the Em value for single vacancies was affected by the concentration of point defects. From these results it appeared that the reduction in Em was occasioned by the total concentration of point

defects and not by any specific species. Again, a further type of recovery was noted and attributed to divacancies.

Nickel yielded two results for both vacancy and divacancy recovery. While the reduction in Em was present a rough comparison with the values obtained for copper and silver indicated that it was less in nickel for a similar change in deformation. The value of the activation energy after fatigue seems to be out of sequence and cannot be explained at present. The actual values obtained are quite close to the value given by Nicholas[65] (0·98 ev). In this respect nickel differs from the other metals used in that the value of Em is less than half the value of E_d (activation energy for self diffusion), which is about 2·7 ev[66].

The aluminium used gave results which were in very good agreement with those obtained by other methods. While only two stages of deformation were possible it appears that within the limits of experimental error no significant change in Em occurred. There is no doubt that the value obtained refers to the movement of single vacancies.

It now remains to find an explanation why these four rather similar metals should behave in these rather different ways. The only significant difference between the metals lies in the strength of atomic binding and this may be rationalised in terms of the stacking fault energy γ. The values of which

for the metals used are:

(1) Silver = 25 ergs/cm^2

(2) Copper = 40 ergs/cm^2

(3) Nickel = 120 ergs/cm^2

(4) Aluminium = 200 ergs/cm^2

It would now appear that the reduction in Em for both vacancies and divacancies is controlled in some way by the value of the stacking fault energy. Silver and copper showed a quite marked reduction in Em with increasing point defect concentration. Nickel showed a somewhat reduced effect and no significant decrease was noted in aluminium.

The most significant effect of the stacking fault energy in this type of process is the control it exercises over the size of dislocation pile ups. In a metal of low stacking fault energy the partial dislocations are widely separated, cross slip is difficult and large dislocation pile ups are possible. On the other hand, a high stacking fault energy means the partial dislocations are not greatly separated and cross-slip is quite easy. This prevents the build up of dislocation against a barrier.

The effect of the widely separated partial dislocations and large areas of dislocations concentrations is to provide a path of strained lattice in which the point defects can diffuse relatively easily. A high concentration of point defects will

contribute to the lattice strain and tend to make diffusion rather easier. It seems likely that divacancies will be more effective in this respect than single vacancies.

In a metal of high stacking fault energy there will be few areas of strained lattice in which easy diffusion is possible.

It is difficult to fully assess the significance of the data obtained here as the dislocations which contribute to the internal friction may not be the same as those governing the mechanical properties of the metal. It is true that the internal friction of a metal is greatly influenced by factors which seem scarecely to affect other mechanical properties. In this respect the measurements made here are very similar to data obtained by electrical resistivity measurements. When point defect ageing proceeds in a metal there is no doubt that the modulus of elasticity of the material is raised. This is indicated by a steady increase in the resonant frequency of the specimen. The yield strength and hardness of the material will also increase to a very limited extent but it is likely that these changes will be difficult to measure. Useful data was obtained on the different species of point defect produced by various kinds of deformations. This and the nature of the recovery process is useful in understanding the later stages in deformation leading up to fracture. However, it seems unlikely that any very much more extensive deformations could be employed with the method used here.

The experiments described in the previous sections have led to the following picture of the recovery of a metal after deformation. Immediately after deformation or quenching a large non-equilibrium number of point defects exists in the lattice. These point defects then migrate to the sinks available which may be either dislocation lines, grain boundaries, or free surfaces. Each species of point defect has its own distinct activation energy for movement and these have been shown to be about the values expected. A point of some interest is the large proportion of the recovery which is attributable to divacancies, even after quenching the number of divacancies retained was far greater than could have been expected.

The formation of vacancy clusters or sessile dislocation rings by condensation of point defects was indicated. This type of sink is rather complex in action owing to the fact that it expands as more vacancies condense on it and becomes a more potent sink.

CHAPTER 8

THE EFFECT OF INTERNAL OXIDATION ON COPPER ALLOYS

Experimental Methods and Results

Conclusions

The Effect of Internal Oxidation on Copper Alloys

The alloys used in these experiments were. Copper 0·2% silicon, copper 0·2% aluminium, copper 0·2% magnesium. and copper 0·15% titanium.

The first two alloys were supplied by Messrs. Thomas Bolton, Ltd., and the remaining two made in the department. The specimens were in rod form 3/16" diameter and cut to 10 cm. length. These were given a preliminary vacuum anneal at 950°C for 2 hours to ensure uniformity of grain size, ect. The internal oxidation was carried out using the cuprous oxide/copper powder method in an inert argon atmosphere. The specimens were supported on a porous refractory plaque which was grooved toprevent specimen movement. This plaque was placed above 50gsm. of the mixture of 50 mesh copper powder and 200 mesh cuprous oxide powder in a copper container. One end of the container was permanently closed by a copper disc and the other covered by a copper foil cap which was wired in place.

This container was heated in a closed end refractory tube in a furnace wound to have a long even hot zone. The furnace tube was evacuated and filled with argon to a slight positive pressure. This pressure was checked from time to time and any loss made good from an argon cylinder.

The time required for internal oxidation could be calculated from the equations and data given by Rhines[46] and it

was decided to check this data by deliberately incompletely internally oxidising some specimens and comparing the calculated and measured depths of penetration of the oxidation front. This was done by oxidising for 100 hours at 910°C and the results are as follows.

Copper 0·2% Si;	Depth of penetration	1·5 m.m.
	Calculated depth	1·8 m.m.
Copper 0·2% Al,	Depth of penetration	2·2 m.m.
	Calculated depth	1·9 m.m.

These results are fairly satisfactory and indicate that the data given by Rhines is quite reliable. In the case of the aluminium alloy it seems likely that some of the solute was already combined with oxygen in the metal and this reduced its effective concentration allowing the greater depth of penetration.

Complete oxidation was carried out at 960°C for 100 hours which was calculated to be more than sufficient for complete oxidation in any of the alloys used.

It is convenient to consider separately the silicon and aluminium alloys. These were oxidised as described above. Pure O.F.H.C. copper specimens were placed in the container for comparison. The specimens were measured before and after internal oxidation and then annealed in vacuum at 1020°C for 24 hours to remove oxygen dissolved in the metal and measured". The results are shown in Graphs 70, 71 and 72.

The pure copper shows marked amplitude dependence in the unoxidised state. After being saturated with oxygen the amplitude dependance was markedly reduced indicating that the oxygen in the metal was present to some extent on the dislocation lines. After another vacuum anneal the amplitude dependance returned partially. This indicates that before the first measurement the specimen had been slightly strained by handling.

In the unoxidised state the copper silicon alloy was completely amplitude independent as might be expected. After internal oxidation the internal friction was very high indeed and was reduced on annealing but was still greater than pure copper.

The copper aluminium alloy showed a similar effect but on a rather smaller scale. However it should be noted that the internal friction after annealing was reduced was less than was the case with the silicon alloy.

The copper magnesium and copper titanium alloys were unfortunately much less satisfactory. The alloys prepared contained a great deal of porosity and oxide inclusions and the analysis given do not represent the true condition of the alloy.

The average behaviour of the specimens was as shown in Table 15.

Table 15 -

	Internal Friction x 10^3	
Copper 2% Magnesium	Low Amplitude	High Amplitude
Originally	0.5	0.79
After internal oxidation	1.02	1.80
After anneal	0.65	1.24
Copper 1.5% Titanium		
Originally	0.57	0.74
After internal oxidation	1.12	2.20
After anneal	0.65	1.22

It will be seen that the specimens were slightly amplitude dependent before internal oxidation indicating that most of the alloying element was present as oxide inclusions. However, the same general effect on internal friction was observed.

In order to compare the results obtained after the anneal it was decided to divide the Δ H portion of the internal friction after annealing by the Δ H portion after internal oxidation(i.e. before annealing) It was felt that possibly the reduction in internal friction would be related to the thermodynamic stability of the oxide precipitate. For this reason the approximate Δ G values for oxide formation at 1000°C are given with the internal friction values.

Alloy	ΔG_{1000} °C(Kcals)	$\frac{\Delta H \text{ after anneal}}{\Delta H \text{ before anneal}}$
Copper silicon	-155	0·24
Copper titanium	-160	0·31
Copper aluminium	-200	0·36
Copper magnesium	-220	0·77

From this list it is clear that the reduction in internal friction is connected with the stability of the oxide precipitated. The most probable explanation is that the oxide precipitate decomposes under vacuum at high temperature, the oxygen leaving the system and the alloying element being redissolved in the copper. This does not, on first examination considering the thermodynamic data above, seem very probable but it must be remembered that in this system any oxygen evolved may be removed. This will allow the decomposition of the oxide to proceed even against the thermodynamic barrier. It is thought that the mechanism of decomposition is

$$MO \rightleftharpoons M + O + Cu_2 = Cu_2O\uparrow$$

The oxide is in thermodynamic equilibrium with solute and oxygen in the metal. Some oxygen is lost from the surface of the specimen either as free oxygen or more probable as Cu_2O which is reasonably volatile at 1000°C. The energy of formation of Cu_2O will aid the reaction by reducing the thermodynamic barrier. Once the

oxygen is free of the surface of the specimen it is pumped away and lost to the system. This allows the oxide to decompose slowly but steadily. The rate of decomposition will naturally be dependent upon the stability of the oxide and this is confirmed by the experimental results.

A point of some importance is the fact that after internal oxidation the damping in the alloyswas higher than in pure copper. Considering that the metal was loaded with oxygen this indicates that dislocations were quite free and suggests that the precipitates had deformed the metal on cooling. There is little doubt that the oxide particles formed in the lattice at 1000°C cause quite a considerable local strain in the metal on cooling due to the quite different coefficients of thermal expansion of the metal and oxide. This results in areas of local strain round the particles which raise the internal friction by freeing the dislocations in the metal.

The copper silicon alloy showed a more marked effect and it seems possible that this was due to the rather irregular contraction of silicon on cooling. The β-δ tridymite change causes a sudden shrinkage on cooling from 170°C. This shrinkage will relieve the compression round the particle and allow an increase in internal friction in the metal. As the other oxides formed do not show

this type of change this particular effect is not found in the other alloys. It should be remembered that the shape of the particle will also be important in the amount by which the internal friction is raised.

It might be thought that the reduction in internal friction on annealing could be due simply to the annealing of these areas of local stress. However, it must be remembered that in this case the particles would still be present in the lattice and would again stress the material on cooling. In any case no difference should be found between different alloy systems.

Microscopic examination was carried out on the internally oxidised material. The results were largely as expected and it was shown that the particle size increased towards the centre of the specimen. Preferential precipitation took place at the grain boundaries. As the precipitates were too small to be properly resolved in the light microscope, an electron microscope was used. The replica technique used was as follows:

1. A small piece of perspex (1" x 1/2" x 1/16") was washed in warm soapy water followed by distilled water and then clamped on to the surface to be examined at a pressure of a few lbs. per square inch.

2. The specimenand perspex plate were placed in an oven at 120°C for one hour. They were allowed to cool before unclamping.

3. A film of carbon was evaporated on to the perspex replica

in high vacuum.

4. A layer of nitrocellulose was spread over the surface to protect the thin carbon film - which formed the final replica - from a 2% solution in amyl acetate.

5. A specimen grid was placed over the area of interest using the light microscope to locate any special feature in the surface. A small disc of paper was placed on top of the grid, the diameter of the disc being slightly less than that of the grid so that the rim of the latter was clear.

6. A strip of gummed paper was then stuck on the entire surface of the perspex, covering the grid and holding everything in position.

7. The whole composite replica was placed overnight in chloroform. The perspex dissolved away but the gum on the paper was insoluble in chloroform and so held the grid and carbon film intact.

8. The grid was released from the brown paper and placed with carbon film uppermost in amyl acetate (using a wire mesh to support). This removed the protective layer of nitrocellulose.

9. The carbon replica was finally shadow-cast with gold/palladium before examination in the electron microscope.

This replica was then examined in a Metro-Vickers Em3 instrument.

The silica particles were shown to be almost perfectly spheroidal. The alumina particles were irregular and rather

angular and were deposited along preferred crystallographic planes. A point of some interest was the rather peculiar growths of some of the silica particles indicating that some decomposition had taken place. The specimen for this examination was polished chemically to prevent surface distortion. An attempt was made to use a bromine etch for dislocations, to show free dislocations perhaps in loops round the particles but the results were rather inconclusive.

Conclusions.

The particles deposited on internal oxidation can be various shapes governed by their chemical composition. The size of the precipitate increases towards the centre of the specimen. The rate of internal oxidation is very close to that predicted by Rhines.

On cooling from the internal oxidation temperature the particles set up stress in the material, due to the different coefficients of expansion of oxide and metal, which free the dislocations round the particle and increase the internal friction. Silica particles were shown to have a more pronounced effect and it is thought that this is due to the sudden contraction of silica on cooling below 170°C.

The oxide precipitate on further vacuum annealing can decompose with a consequent decrease in damping and a possible mechanism for this was discussed.

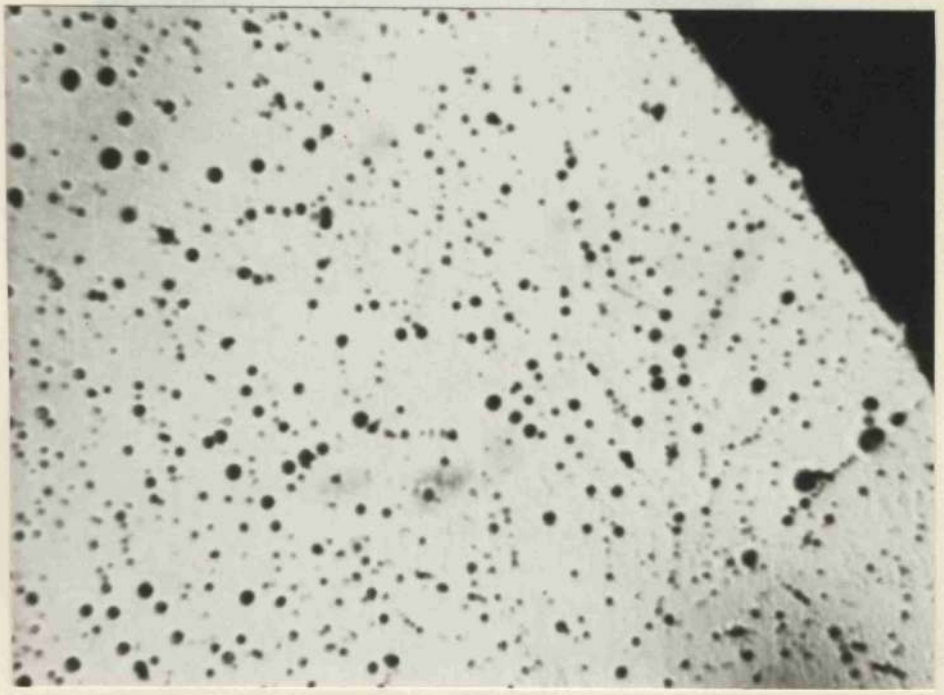

Precipitate in Internally Oxidised Cu., 0·2% Si ×500

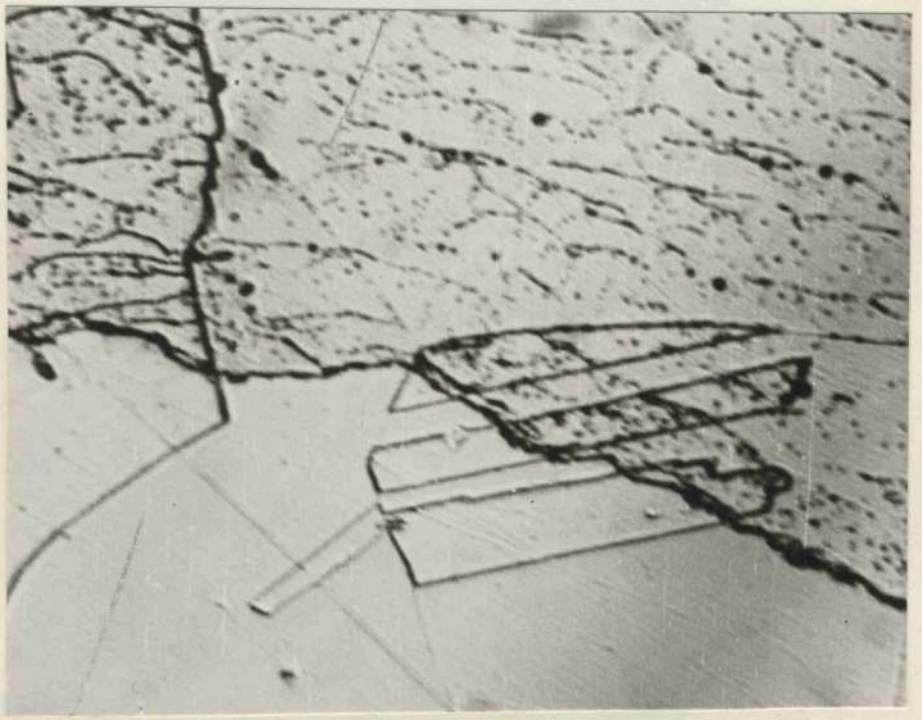

Precipitate Boundary in Cu 0·2% Si ×500

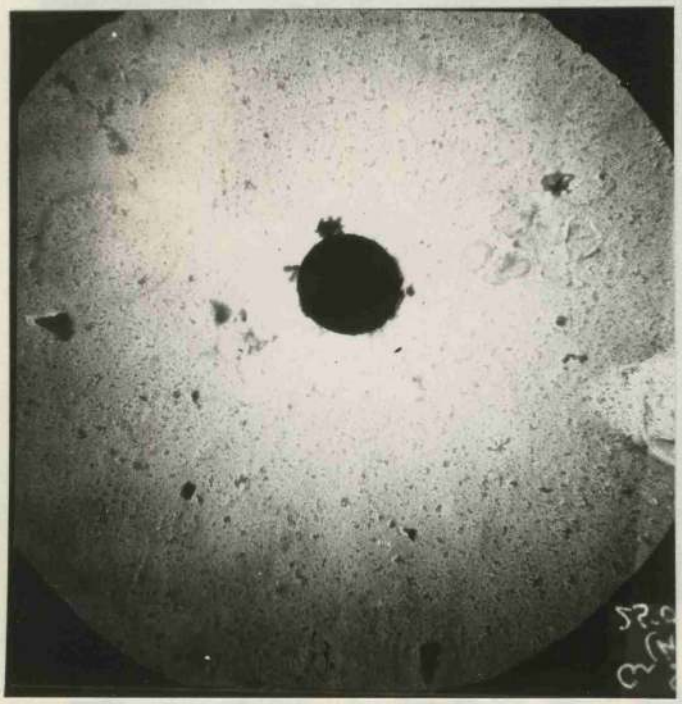

SiO_2 Particle 2500X

Grain Boundary in Cu 0·2% Si 2500X
Internally oxidised

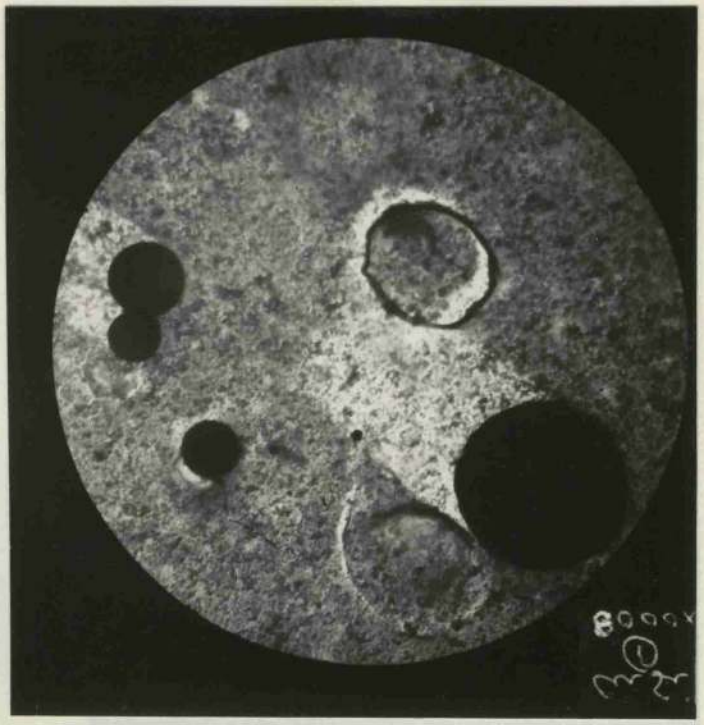

SiO_2 Particle in Cu 0·2% Si 8000X

SiO_2 Particle in Cu 0·2% Si 6000X

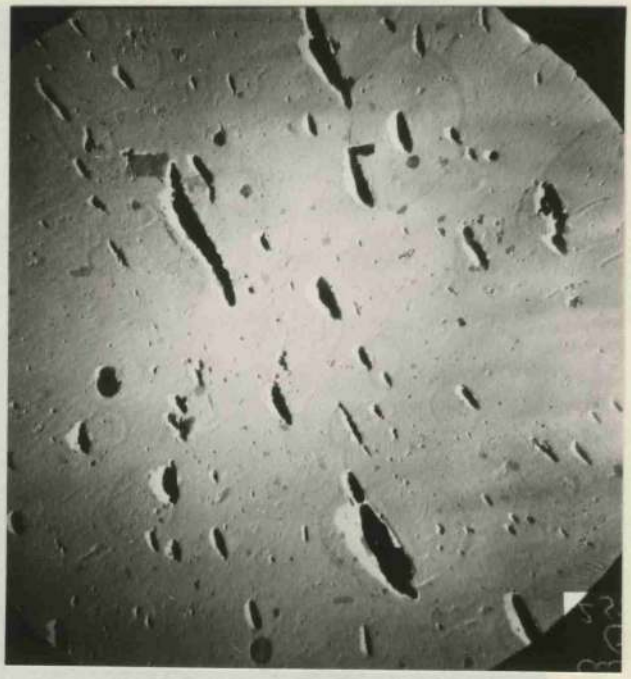

Al_2O_3 Particles in Cu 0·2% Al 2500X

Grain Boundary in Cu 0·2% Al 2500X
Internally oxidised

Al_2O_3 Particle 6000X

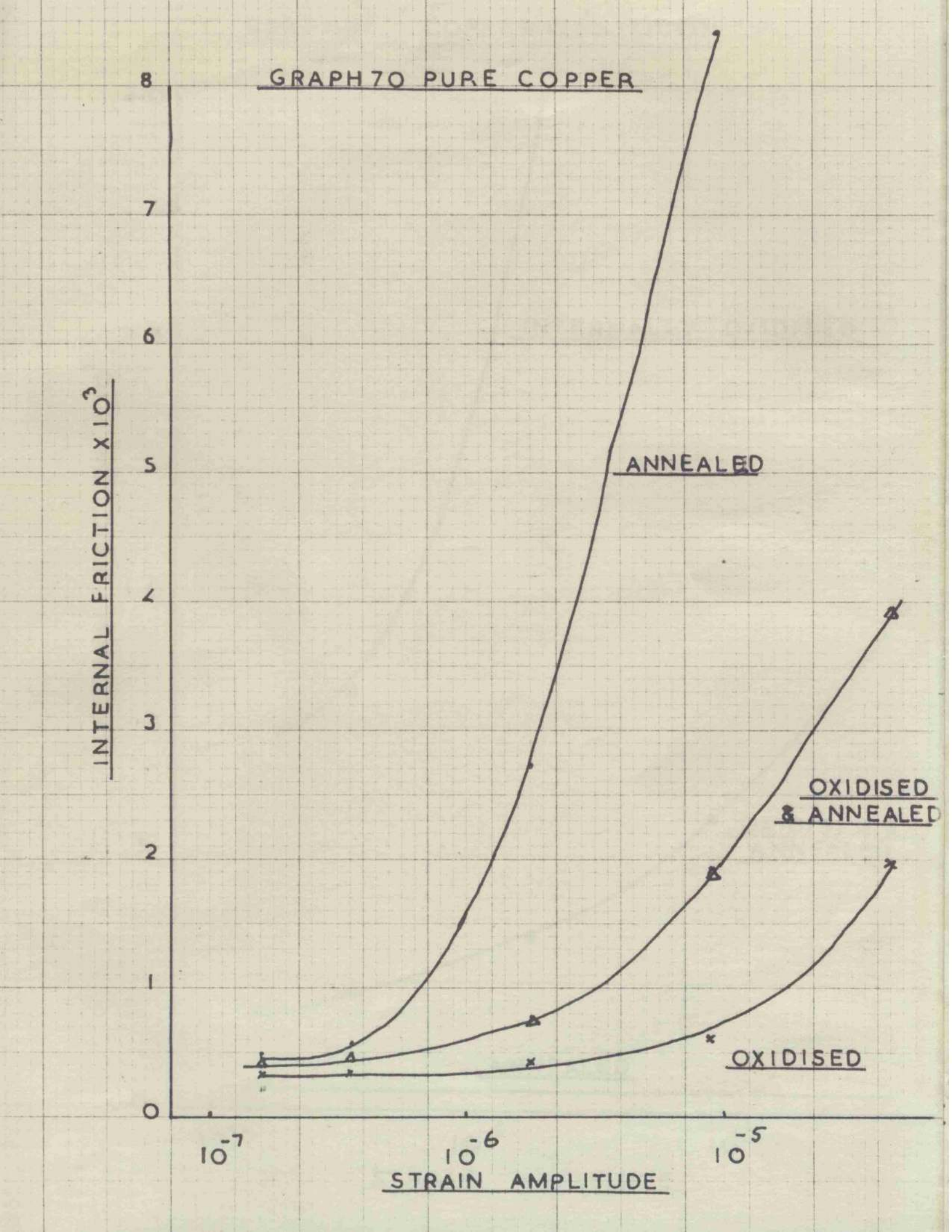
GRAPH 70 PURE COPPER
INTERNAL FRICTION X 10^3
8
7
6
5
4
3
2
1
0
ANNEALED
OXIDISED & ANNEALED
OXIDISED
10^-7
10^-6
10^-5
STRAIN AMPLITUDE

GRAPH 71 COPPER 0.2% SILICON

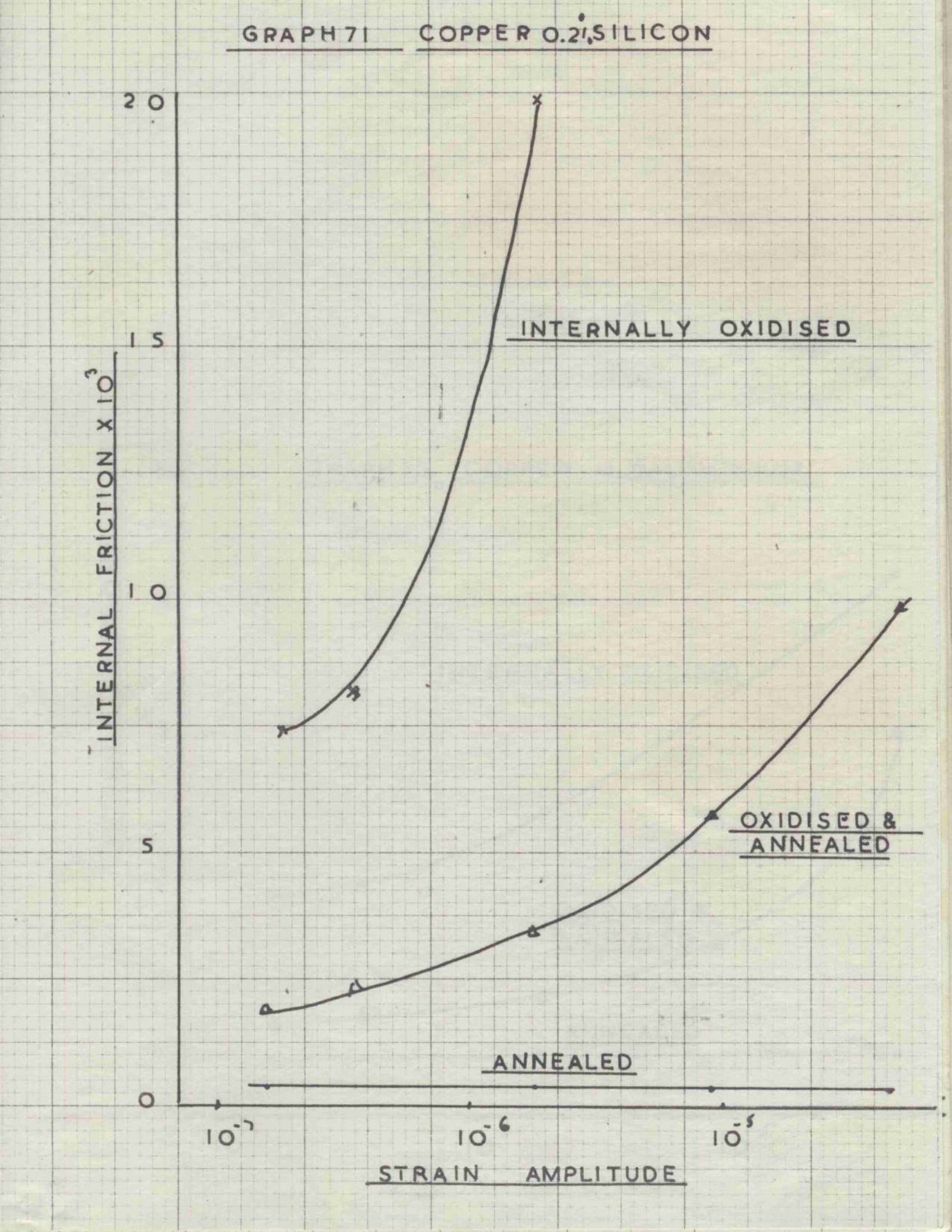

GRAPH 72 COPPER 0.2% ALUMINIUM

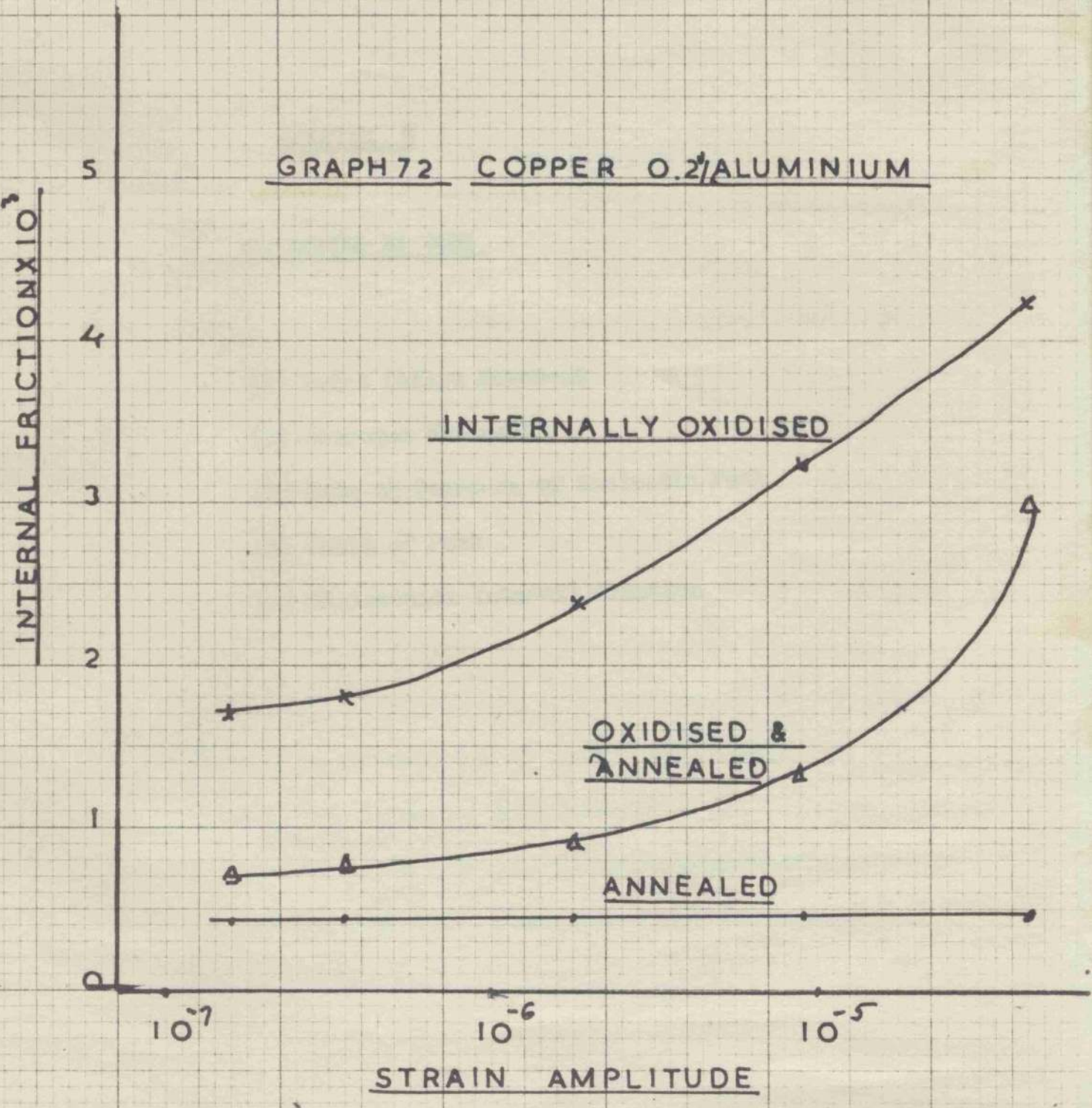

CHAPTER 9

MOVEMENTS IN IRON

(a) Point Defect Movement

(b) Nitrogen Movement

(1) Rate of Decrease of Anelastic Peak

(2) Shift of Peak

(3) Dislocation Internal Friction

Diffusion in Iron

A. Movement of Vacancies.

It had been hoped to obtain data for iron similar to that for the face centered metals. The metal used was Armco iron which was supplied in 1/2" diameter rod. These were drawn down to 0·169" by a wire drawing bench or rolled to rectangular specimen.

Some specimens were annealed at 1200°C for two hours under vacuum and on measurement were found to be slightly amplitude dependent. Specimens 15 cm. in length were then elongated as previously described and measurements made at about room temperature. However, it was found that the internal friction did not decrease appreciably. As the activation energy for self diffusion (Ed) in iron was known to be of the order of 80 Kcals/mole this did not seem unreasonable and the experiments were repeated using recovery temperatures of 70°C, but they were no more successful than before.

On a further temperature increase it became clear that the anelastic peaks due to carbon and nitrogen in the metal would cause an unduly high background ΔI in the internal friction results. In any case the deformation would probably free the interstitial atoms whose subsequent diffusion would

confuse any vacancy recovery. For these reasons it was decided to remove both carbon and nitrogen from the metal by a wet hydrogen treatment.

Hydrogen gas which had been bubbled through water at room temperature was passed over the specimens at 700°C. The time required for complete decarburisation of a 3/16" specimen was estimated to be about one week. After this time dry hydrogen was passed for an hour or so to remove moisture and the specimens cooled under argon.

By making use of the anelastic peaks in the material, the internal friction technique is a very sensitive and convenient method of analysis for carbon and nitrogen. The original specimens were cooled from 160°C and the internal friction measured as the temperature fell and is shown in Graph 73. There is a pronounced but rather irregular peak. This peak will be due to the combined effects of carbon and nitrogen. Some of the irregularities on the curve are very probably due to temperature fluctuations and variations in the bath. It is almost impossible to measure accurately the temperature of the specimen in changing conditions in this apparatus. After the wet hydrogen treatment the specimen was again tested and the peak had disappeared indicating that the impurities had been successfully removed.

The decarburised specimens were elongated as before and kept in an alcohol/CO_2 mixture at - 80°C until measurements could be made. However, it was found that when the specimen was placed in the apparatus very little amplitude dependence remained. It was thus concluded that all the vacancy recovery had taken place at - 80°C. This did not at first seem very likely but some information which became available as this work was being carried out suggested that vacancies diffused in iron with an activation energy of about 4 Kcals/mole. At this very low value it is quite possible that all the recovery could have taken place before measurements were made even when stored at - 80°C. The value of Em for vacancies is remarkably low compared with the Ed value but it seems quite probable that self diffusion is carried out mainly by another process than vacancy migration, perhaps a four ring diffusion mechanism.

It was decided to proceed no further with this investigation as the temperatures required were rather too low to be practicable. However, it is quite feasible that measurements could be made on this apparatus if one were prepared to work at liquid air temperatures. Low temperature work is made difficult by frost forming on the specimen.

B. Movement of Nitrogen

The initial measurements made on specimens containing

a little carbon and nitrogen had shown some recovery. This was presumably due to the movement of carbon and nitrogen atoms, freed by the deformation, to the dislocation lines. This suggested that the movement of interstitial atoms was likely to be very significant. In the recovery after deformation it probably plays a similar role to the movement of point defects in F.C.C. metals. For this reason it was decided to study the movement of nitrogen by this apparatus.

Specimens were nitrided in a horizontal furnace at 600°C for one week. The gas mixture used was 10%NH_3 + 90%H_2 passed with a flow rate of about 100c.c./minute. This was calculated to be sufficient to saturate the specimens at the temperature used. That is to give a nitrogen concentration of 0·1% in the iron. Naturally there will be a concentration gradient of nitrogen in the metal but it was hoped that this would not be very serious. It was found that the specimens would only absorb nitrogen if their surfaces were bright and it was necessary to cool them from the decarburising temperature under hydrogen.

After nitriding the specimens were stored in an alcohol/CO_2 mixture until required. They were then vacuum annealed at 600°C for one hour in the vertical quenching furnace and quenched into oil at room temperature. The vacuum

anneal removed the dissolved hydrogen and dissolved the nitrogen in the ferrite. The quench retained the nitrogen in supersaturated solution and it then diffused to the available sinks.

Normally this ageing of nitrogen is followed by measuring the decrease in the anelastic peak height. The height of the peak is thought to be directly proportional to the quantity of nitrogen in solution. This method has been widely used but naturally it is by no means certain that the nitrogen leaving the ferrite is condensing on the dislocation lines. Exactly similar results would be obtained if the nitrogen reached any other sink. The fact that it can be shown that the sink has about the same length as the dislocations are estimated to haveis a rather empirical confirmation.

It was decided to attempt to correlate the different methods of determining the activation energy for nitrogen diffusion with measurements made directly on the dislocation lines. This can best be done by using the dislocation internal friction methods previously described.

(1) Rate of Decrease of an Anelastic Peak

After quenching a specimen was placed in the apparatus with the bath at a temperature of 108°C and measured at a fairly low strain amplitude over a period of time. The temperature of 108°C while not exactly on the top of the nitrogen peak gave results which were perfectly representative of the peak behaviour. The results are shown in Graph 74.

In order to see if the ageing followed Harper's equation it was necessary to extrapolate the recovery line to zero time to obtain an estimate of the original nitrogen concentration. This is quite simply achieved by the fact that the height of the peak is proportional to the nitrogen in s olution. From Harper's equation

$$\log (1 - q) \propto t^{2/3}$$

where t is time and q is the fraction of the nitrogen precipitated.

Thus if the internal friction at time t is divided by the internal friction at time zero and plotted logarithmically against $t^{2/3}$ a straight line should be obtained. This was done in Graph 75 and as can be seen a fair time was obtained over most of the recovery. This indicates that Harper's equation holds true even at ageing temperatures at the relatively high temperature of 108°C. The deviation of line after about 30 minutes is to be expected as the equation is said to hold only for about 80% of the recovery. In order to obtain an activation energy by this method it is necessary to obtain the rate of recovery at at least two widely separated temperatures. As the temperature of the anelastic peak only changes slowly with respect to changes in frequency, a large change in frequency would be required. This did not seem practicable as the change in specimen size

would be too great and no higher harmonics could be used because because of the grain size thermoelastic effect at about 10,000 c/s. It is extremely important to note that results were obtained by this apparatus at a temperature above 100°C on peak ageing. It had been feared that the recovery would be too rapid to be followed.

(2) Temperature Shift with Changing Frequency

An alternative method of measuring the activation energy of nitrogen movement is to determine the change in the temperature of the anelastic PEAK as the frequency is changed. As previously described the activation energy for the shift of the peak is exactly the same as that for nitrogen diffusion.

The experiment was tried at first using circular specimens with 3/16" diameter and one which had been drawn down further. Unfortunately, the change in frequency was not sufficient to give an adequate change in peak temperature. Unfortunately, it was not possible to make use of the second harmonic at about 10 Kc/s owing to the presence of the grain size thermoelastic at that frequency.

It was decided then to use a rectangular specimen with one side about half the size of the other. The specimens were decarburised and nitrided as before. After quenching it was necessary that the specimen be stabilised by ageing before measurement. This was done by annealing it at 100°C. for an hour or so. Unfortunately, the height of the peak was reduced

by this process but sufficient nitrogen remained in the ferrite to allow measurement. The results are shown in Graph 76 in which the specimen had slowly been cooled through the peak while measurements were made at low strain amplitude. It is clear that the specimen had not been fully stabalised as the peak had reduced in size between measurements. The activation energy obtained by this method was 22·8 Kcals/mole but the accuracy is not very great as it is difficult to determine the actual temperature of the peak. Once again it is evident that there is difficulty in determining the temperature of the specimen while the bath is slowly changing its temperature.

(3) Determination by Dislocation Internal Friction Method

In order to use dislocation internal friction methods in iron it is first necessary to re-examine the relevant equations. The theories of Granato and Luke are are specifically for part diffusion in F.C.C. metals.

The problem is simplified by assuming that the nitrogen atoms are the only impurity mobile during the experiment. This is quite reasonable and is equivalent to Granato and Luke's assumption with regard to vacancies.

The next alteration necessary is in the number of atoms per unit cube, i.e. $a^3 = 2$ and not 4 as is the case

with F.C.C. metals. This appears in the β term which becomes

$$= \frac{C_N}{C_N + C_{20}} \cdot \frac{2\alpha}{a^2} \left(\frac{AD}{T\pi}\right)^{\frac{2}{3}}$$

where C_N is the concentration of nitrogen atoms.
The other terms are as before

Now

$$\Delta H = A \exp[-A_2 (C + C_{20})(1 + \beta t^{\frac{2}{3}})]$$

This by exactly the same process as previously described gives the activation energy. The factor of 2 in the β term does not appear in the final calculation which is just as for a F.C.C. metal.

The specimens were quenched from 600°C under vacuum into oil. It was found that a water quench gave a lower internal friction and it was concluded that some vacancies were present after by water quenching. This was probably due to the stresses set up on quenching rather than retention of vacancies from the quenching temperature. Again it was not possible to investigate this effect and oil quenching was used throughout these experiments.

It was found that if the upper measuring stress used was $9{\cdot}5 \times 10^{-6}$ inconsistent results were obtained and it seems that this strain is too high and tends to remove the nitrogen atoms from the dislocation line in the early stages of precipitation. The strain amplitude was lowered to 3×10^{-6} and it was found that reasonably satisfactory results could be obtained. At this low amplitude however the internal friction was not very high and

and the errors due to the apparatus were rather evident.

A series of results were obtained at various temperatures and are shown in Table 16.

Table 16 - Iron Nitrided, Quenched from 600°C

°C.	°K	$\frac{1}{T} \times 1000$	$T^{\frac{2}{3}}$	R/2·303	R	$T^{\frac{2}{3}}R$	Log[$T^{\frac{2}{3}}$ R]
15·6	288·2	3·46	43·2	0·00836	0·0192	0·83	-0·909
21	294	3·40	44·1	0·0157	0·0362	1·61	0·20
29	302	3·31	44·8	0·0286	0·066	2·96	0·47
37·8	310·8	3·22	45·6	0·0426	0·098	4·46	0·65
44·5	311·5	3·155	46·5	0·075	0·173	8·03	0·905

This data plotted in Graph 77 gives the activation energy for the process as 21·5 Kcals/mole. This result is in good agreement with those obtained by other methods and provides a satisfactory confirmation of the Cottrell-Bilby and Harper equations. It is a convincing verification that the nitrogen atoms do condense to the dislocations.

Conclusions.

It was found that data could not be obtained at about room temperature on vacancy diffusion in iron but it appears that the vacancies move with quite a low activation energy.

The movement of nitrogen in iron was investigated and it was shown that it was quite feasible to measure the decrease

in peak height even at frequencies of 2,000 c/s where the peak temperature is of the order of 120°C. It was shown that the ageing at this temperature obeyed Harper's equation. The shift of peak temperature as the frequency changed was quite a convenient method of determination but it would have been desirable to have some direct measure of the specimen temperature.

It was also shown that the dislocation internal friction theories could be adapted to the interpretation of nitrogen diffusion in iron. The experiment was carried out and satisfactory data obtained.

To obtain further data on iron either for vacancy or interstitial diffusion it would seem desirable that a modified apparatus be used. It would seem that a longitudinal type of vibration is best as the frequency can easily be changed by lengthening or shortening the specimen and a thermocouple could be directly attached to the node of the specimen. It would however be necessary to change the specimen temperature quickly and this would possibly be difficult under vacuum.

Longitudinal vibration cannot normally be made to have a very high amplitude and this would tend to preclude dislocation damping measurements. Transverse vibrations with the specimen supported at the nodes and electromagnetically driven and detected might be best if the supports were made to act as thermocouple wires allowing a fairly accurate measurement of the specimen temperature to be made.

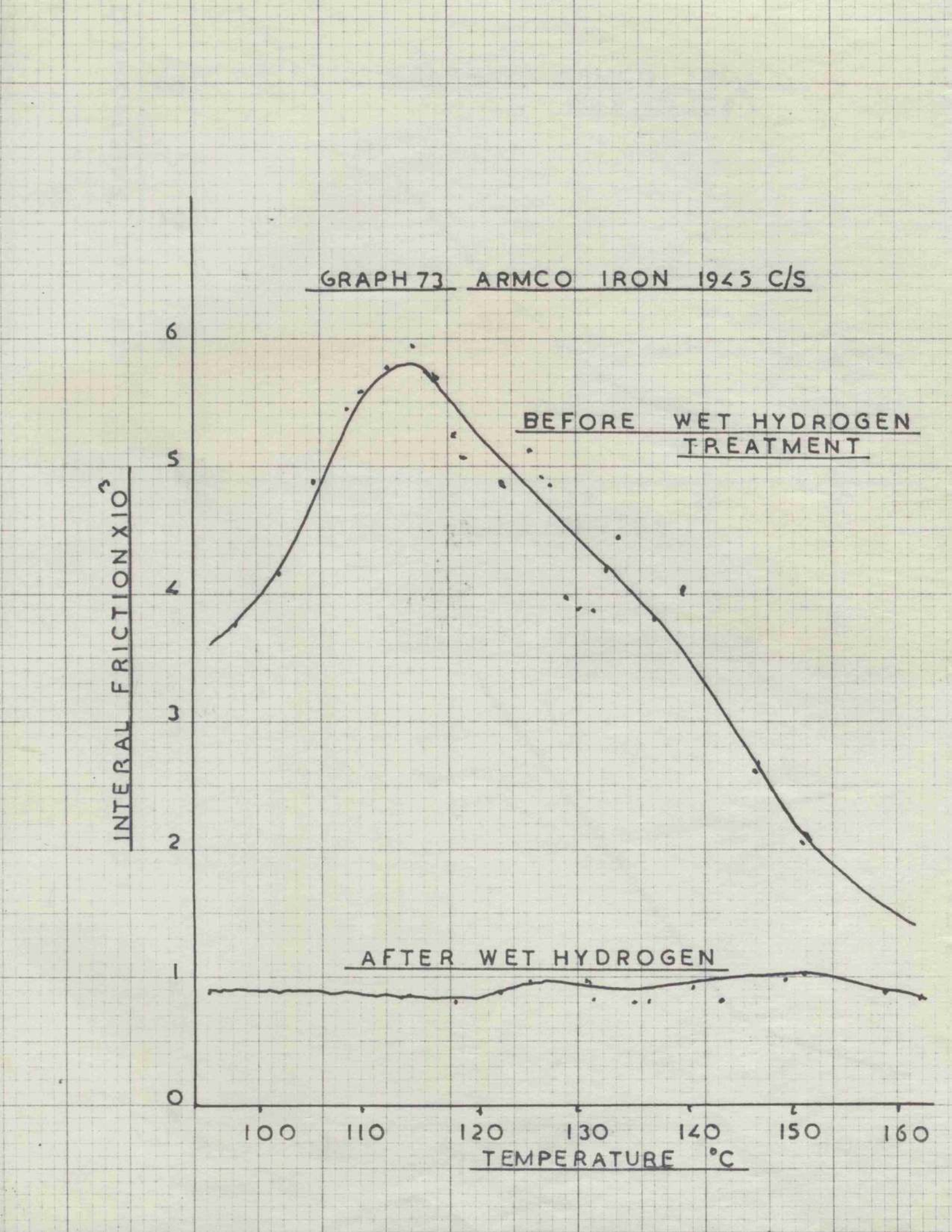
GRAPH 73 ARMCO IRON 1943 C/S
BEFORE WET HYDROGEN TREATMENT
AFTER WET HYDROGEN
INTERAL FRICTION X10³
6
5
4
3
2
1
0
100
110
120
130
140
150
160
TEMPERATURE °C

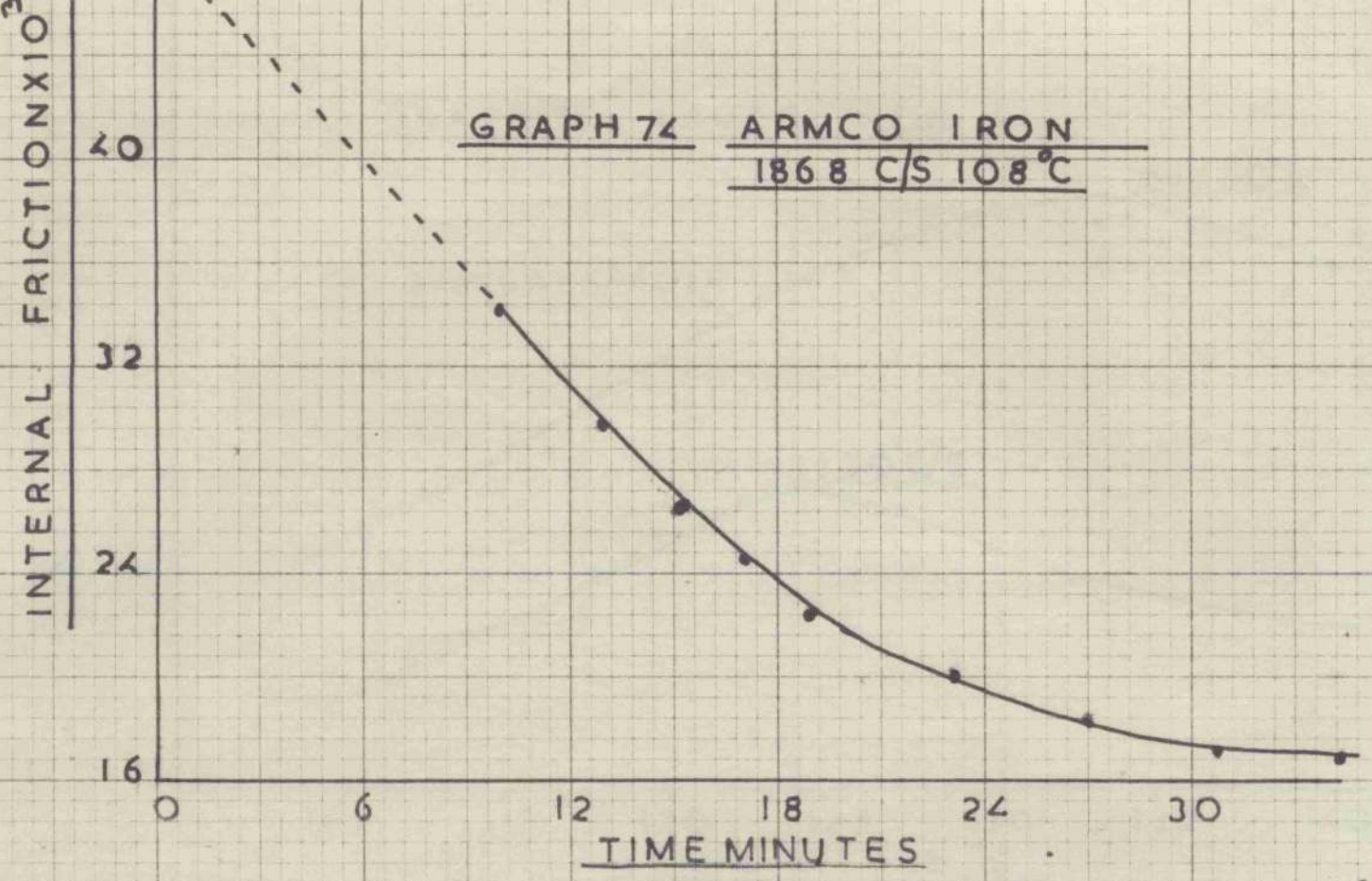
GRAPH 74 ARMCO IRON
1868 C/S 108°C
INTERNAL FRICTION X10³
40
32
24
16
0
6
12
18
24
30
TIME MINUTES

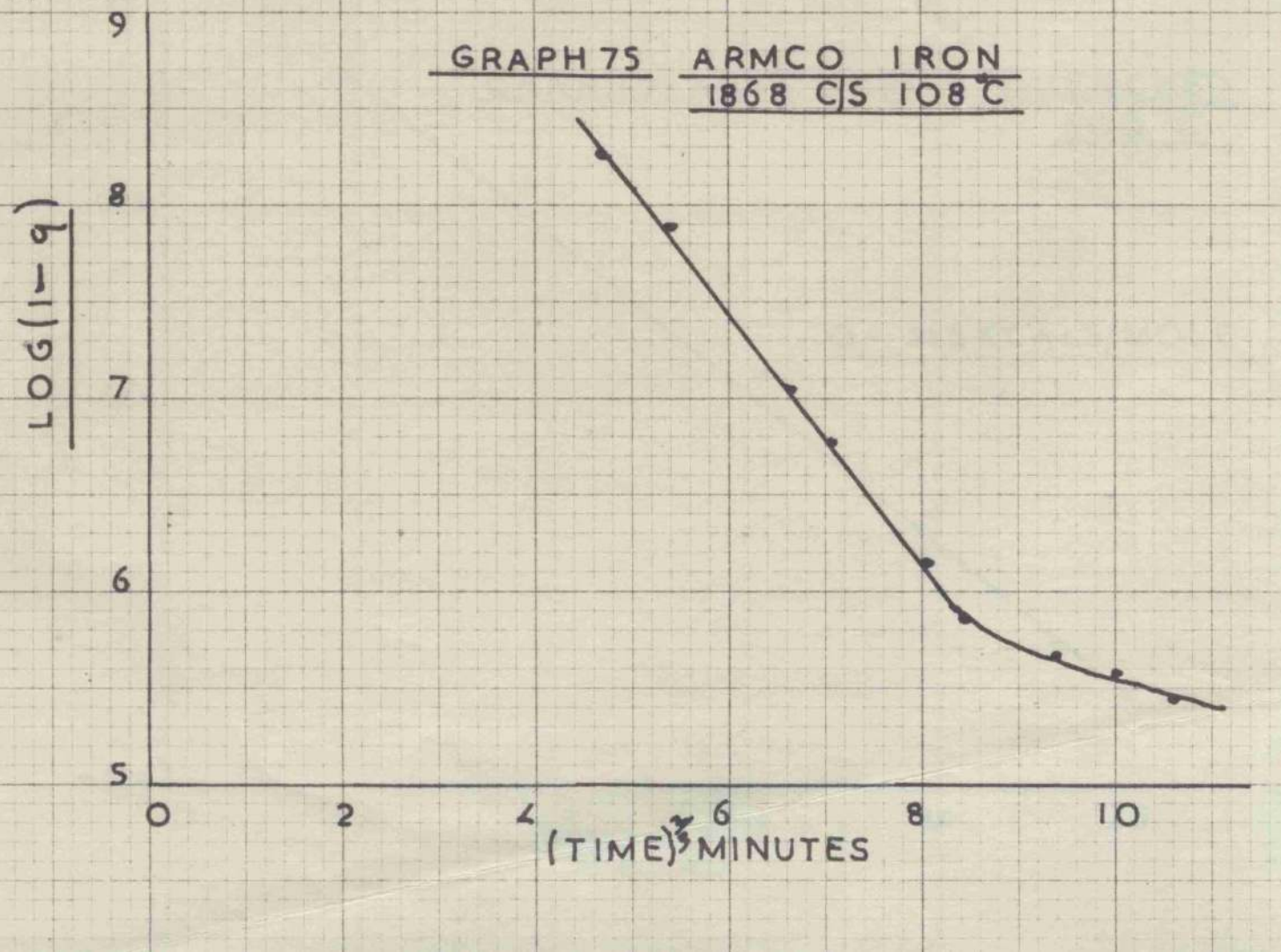
GRAPH 75 ARMCO IRON
1868 C/S 108°C
LOG(1-q)
9
8
7
6
5
0
2
4
6
8
10
(TIME)^½ MINUTES

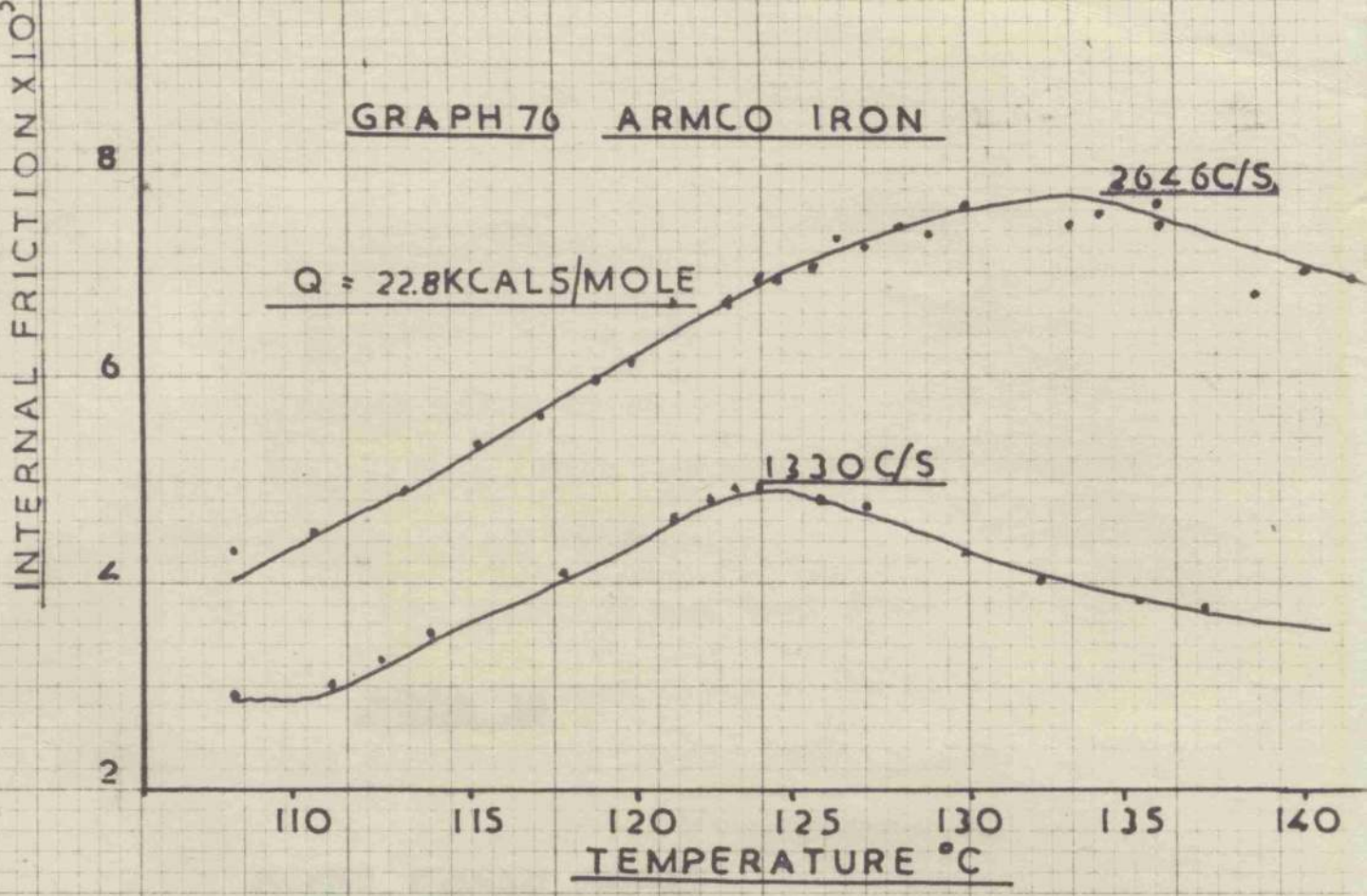
GRAPH 76 ARMCO IRON
INTERNAL FRICTION X10³
8
6
4
2
2646C/S
Q = 22.8KCALS/MOLE
1330C/S
110
115
120
125
130
135
140
TEMPERATURE °C

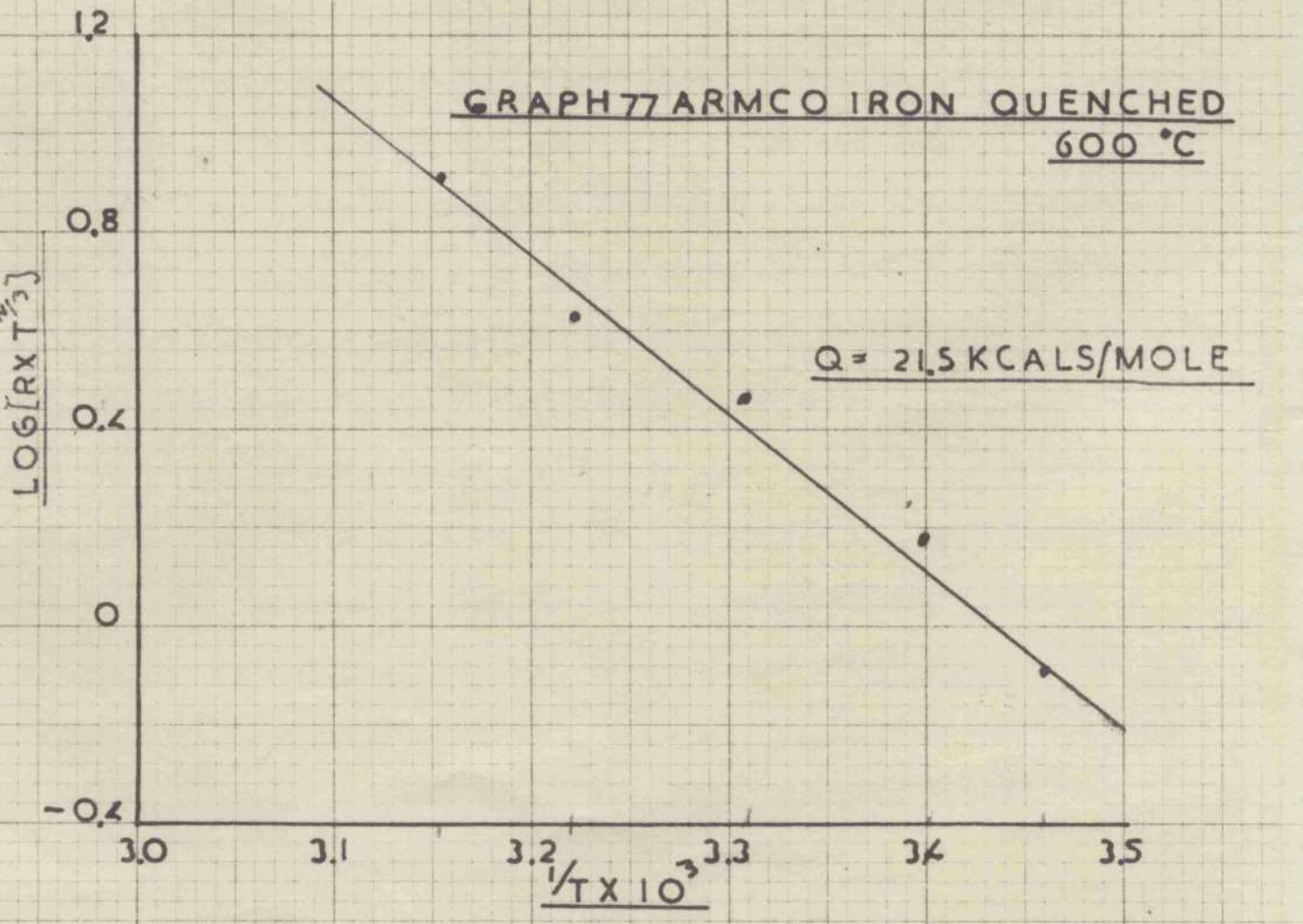
GRAPH 77 ARMCO IRON QUENCHED 600 °C
LOG[RX T^3/2]
1.2
0.8
0.4
0
-0.4
Q = 21.5 KCALS/MOLE
3.0
3.1
3.2
3.3
3.4
3.5
1/T X 10³

CHAPTER 10

TORSION PENDULUM RESULTS

Torsion Pendulum Results

The theory of Granato and Luke discussed earlier was stated by them to apply only to frequencies of the order of 10^4 c/s. However the results of Smith, which they used in their discussion, were obtained at about 700 c/s and O'Hara's and the present work indicates that the theory applies at much lower frequencies. It It was decided therefore to endeavour to see if the theory could be extended at least quantitatively to very low frequencies i.e. lc/s and it was thus necessary to construct a torsion pendulum. The type built was roughly that described by Ke. The specimen in the form of a wire was held in a fixed upper clamp and its lower end was attached to a swinging inertia bar. Below the inertia bar a pointed rod of brass protruded into a container of oil. This was used to reduce transverse vibration of the specimen assembly. Measurement of the amplitude of vibration was measured by deflection of a light spot by a mirror fixed on the cross beam inertia member. This spot of light was focused on a transparent screen. The vibration was ~~stored~~ STARTED in the specimen by electron magnets near the cross beam which were excited as required. The method used in these experiments was to excite the beam to give the maximum amplitude required. and to note the amplitude of vibration as it decayed every 10 cycles for 200 cycles. This resulted in virtually a complete record of the amplitude dependent ~~specimen~~ SPECTRUM of the internal friction. In this respect

the torsion pendulum is superior to the Forster method.

Both copper and aluminium wires were used in the torsion pendulum. The copper (0·036") specimens were annealed in a horizontal furnace at 600°C for one hour, and then carefully placed in the pendulum and annealed for a further four hours in situ. Measurements were made on the aanealed material and the material then lightly stressed in situ and remeasured as soon as possible, i.e. after about 15 minutes. The results are shown. GRAPH 78

The aluminium wire was measured immediately after an anneal at 400°C for 1/2 hour in situ. Testing was carried out after various times. GRAPH 79

Discussion of Results:

The results for the copper specimen show a very distinct change from the amplitude dependent range to the independent range. This rather precise break away of the dislocations from the pinning points allows a calculation of change in loop length due to stressing to be made.

From the Granato and Luke equation

$$\Delta_I = K L^4$$

If the background damping is subtracted from the measured values of Δ_I the reduction is found by

$$\frac{\Delta I_S}{\Delta I_A} = \frac{L_S^4 \text{ (STRESSED)}}{L_A^4 \text{ (ANNEALD)}}$$

If a value of 5×10^{-4} is taken as a reasonable value

and this gives

$$\frac{\delta(s)}{\delta(A)} = 1 \cdot 108$$

The stress at which breakaway occurs is given by

$$\varepsilon_c = \frac{k'}{\ell}$$

and this

$$\frac{\varepsilon_c(A)}{\varepsilon_c(s)} = \frac{\ell_s}{\ell_A}$$

amd using the value from the graph

$$\frac{\ell_s}{\ell_A} = 1 \cdot 140$$

The above results are in very good agreement with each other and if in fact the background damping of the apparatus was higher than 5×10^{-4} δ_s seems likely the agreement would be much better. The above is taken as a con vincing demonstration that the theory is sound at low frequencies.

The aluminium specimens on the other hand did not give any amplitude dependents internal friction in the stress range used but its recovery was measured and plotted according to the equation $\log A_{F1}/\log (1 + Bt^{\frac{1}{3}})$ using the value of B given by Granato and Luke. As can be seen a fair straight line was obtained. This is reasonable proof that the theory of recovery applied even at quite low frequencies. GRAPH 80

Conclusions. (1) It was shown that the theories of

Granto and Luke were applicable at low frequencies and the recovery stress was also sound at least for amplitude independent recovery.

(2) If the above theories are accepted a very convenient method of determining the background damping of a torsion pendulum is to determine the reduction of loop length before and after elongation.

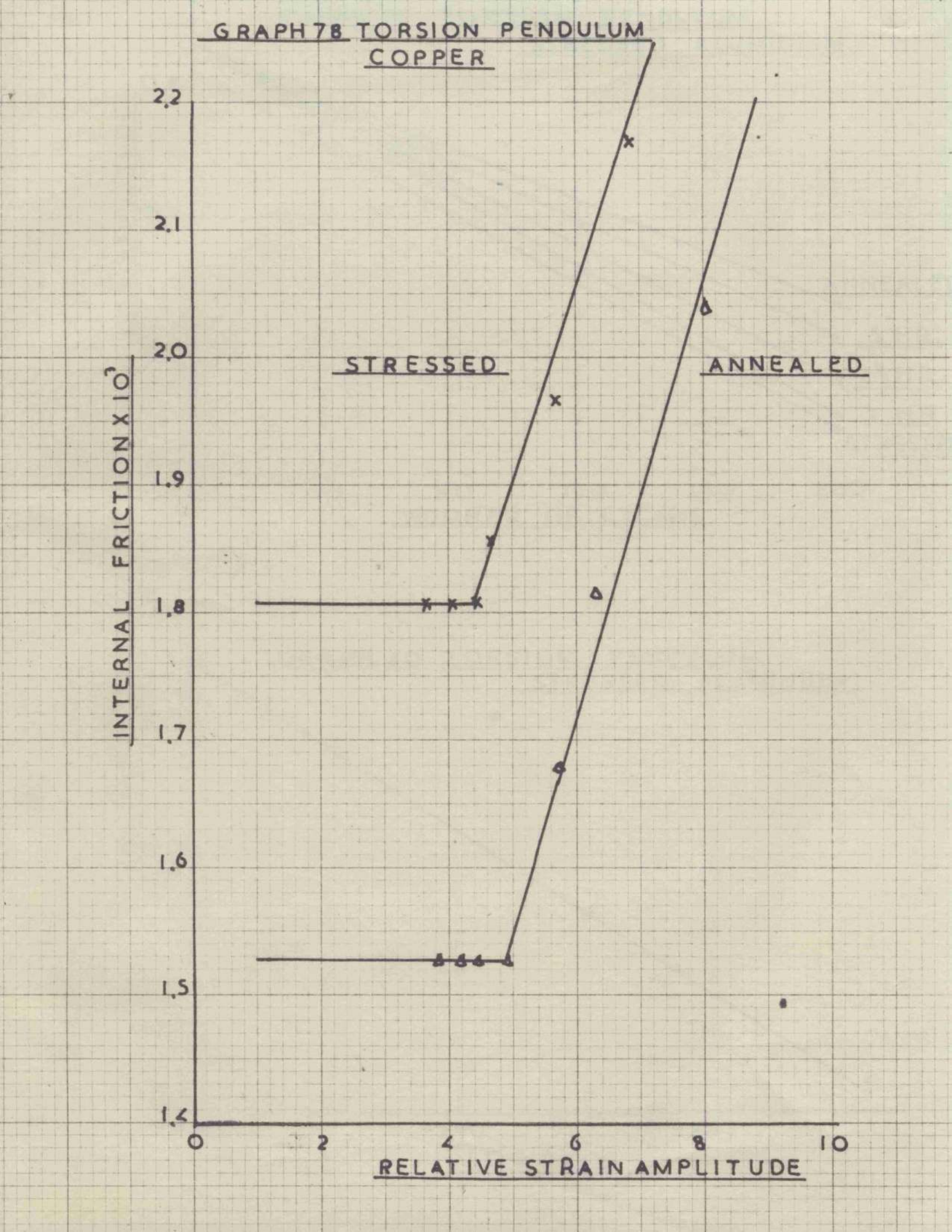
GRAPH 78 TORSION PENDULUM
COPPER
STRESSED
ANNEALED
INTERNAL FRICTION X 10³
2.2
2.1
2.0
1.9
1.8
1.7
1.6
1.5
1.4
0
2
4
6
8
10
RELATIVE STRAIN AMPLITUDE

GRAPH 79 TORSION PENDULUM
STRESSED ALUMINIUM

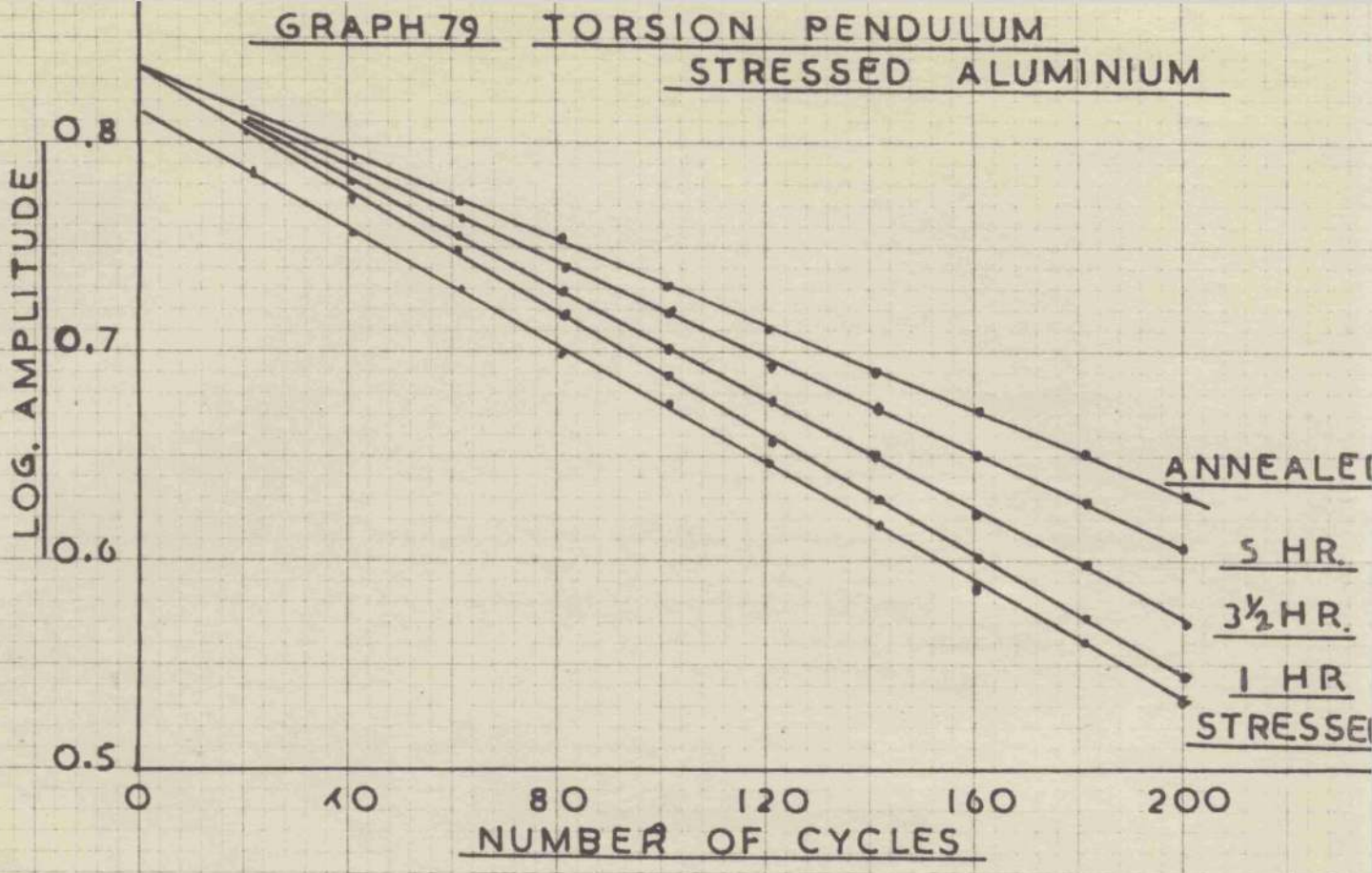

GRAPH 80 TORSION PENDULUM
STRESSED ALUMINIUM

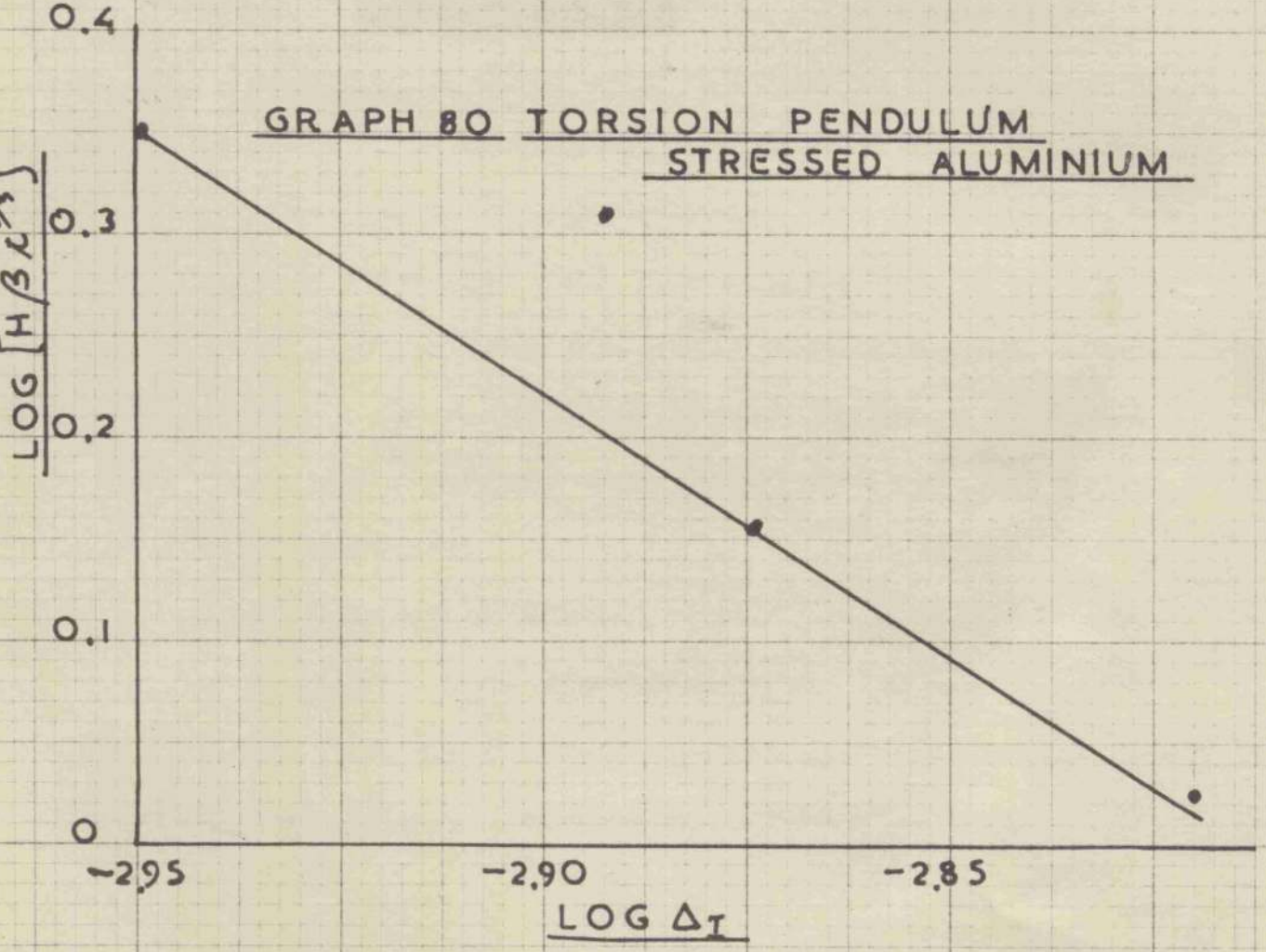

GENERAL CONCLUSIONS

GENERAL CONCLUSIONS

The existing apparatus was modified and improved. Measurements can now be made at much lower strain amplitudes with accuracy and it was found that direct measurements on the amplitude independent part of the internal friction could be made and this greatly facilitated the interpretation of recovery phenomenon. Errors arising from shortcomings in the apparatus were encountered and in the interpretation of recovery results it was necessary to allow for the errors of the oscillator. Some experience was necessary to do this and even then results could not always be successfully interpreted. This type of error could naturally be avoided if a frequency measuring device was put into the circuit; commercial instruments have quite adequate accuracy. But it means that the use of this instrument would slow down the rate of measurement and might make recovery measurement difficult under certain circumstances. If an oscillator without the errors mentioned above, some form of accurate sweep instrument, were used these errors would be avoided.

The recovery of internal friction in face centred cubic metals after various types of deformation was extensively investigated. It was found that various types of recovery mechanisms were active. Of these vacancy and divacancy

movement were identified and the activation energies of the process obtained. These were found to be generally in good agreement with those in the literature. It was shown that a decrease in the activation energy for point defect movement occurred as the concentration of point defects increased. It was indicated that the magnitude of this effect was dependent upon the stacking fault energy of the metal. The effect being greatest in metals of low stacking fault energy, it was suggested that the dislocation arrangement, which is controlled by the stacking fault energy, was responsible. The contribution of divacancies to the recovery after deformation was found to be unexpectedly large and indeed appears from the results to be of major importance.

The results from the internally oxidised alloys showed the effects of the different types of oxide particle. It was shown that in the case of silica particles the rise in internal friction after oxidation was emphasised by the phase change in silica below 200°C. The thermodynamic stability of the oxide was known to be of some importance as the oxide can decompose on annealing under vacuum. The results obtained by optical and electron microscopy largely confirmed published data.

Experiments were carried out on pure iron but it seemed that any vacancies produced ~~differed~~ DIFFUSED with quite a small activation energy. Nitrogen movement in iron was studied by a number of methods. The internal friction method was successfully used to measure the diffusion of nitrogen and gave confirmation to the theories current on nitrogen ageing.

REFERENCES

1. Zener, C. Elasticity and Anelasticity of Metals 1948
2. Ke, T.S. Phys. Rev. 71, 533, 1947
3. Norton, J. Rev. of Sc. Ints. 1939, 10, 77
4. Snoek, J. Physica 1939, 6, 591
5. Wert C. and Zener C. Phys. Rev. 1949
6. Cottrell A.H. and Beilby B.A. Proc. Phys. Soc. 62, 149, 19—
7. Mason, W.P. Phys. Rev. 98, 1136, 1958
8. Weertman J. and Koehler J.S. J. Appl. Phys. 24, 1953
9. Weertman J. and Salkovitz E.I. Acta.Met. 3, 1, 1956
10. Granato A. and Luke K. J. App. Phys. 27, 583, 1956
11. Beskers, D. J. Appl.Phys. 30, 252, 1959
12. Robinson, P.M. and Rawlings, R. Phil. Mag. 1959. 1959
13. Read, T.A. T.A.I.M.M.E. 148, 30, 1941
14. Thomson, D.O. and Holmes,P.K. J. Appl. Phys. 27, 713, 1956
15. Granato A. Hikato, A. and Luke, K. Acta Met. 1958, 6, 470
16. Boulanger, C. Rev. Met. 46, 1949, 321
17. Mason, W.P. Phys. Rev. 97, 557, 1955
18. Morse, R.W. Phys. Rev. 97, 1116, 1955
19. Nowick, A.S. Progress in Metal Physics.Vol. 4, 1953
20. Niblett, D.H. and Wilks,J. Advances in Physics Vol 7, Jan.1960 No.33
21. Quimby, S.L. Phys. Rev. 25, 558, 1925.
22. Bordoni, P-G. J. Accos. Soc. Amer. 26, 495, 1947
23. Wengel, R.L. and Walther, H. Physics 6, 141, 1935
24. Forster, F. Z. Metallh. 29, 109, 1937

25. Postnikov, V.Š. Fiz Met i Metalloved 4, 344, 1955

26. Powers,R.W. and Doyle, M.V. Acta Met. 4, 233, 1956

27. Smith, A.N.D. Phil. Mag. 44, 453, 1953

28. Hikata et al J. Appl. Phys. 27, 396, 1956

29. Zener, C. Imperfections in Nearly Perfect Crystals 19

30. Broom, T. and Ham R.K. Vacancies and Other Point Defects in Metals and Alloys Inst Met London

31. Friedel, F. Les Dislocations, 1956

32. Seitz, F. Advances in Physics 1, 43, 1952

33. Mott, N.F. Phil. Mag. 1952, 43, 1157

34. Van Buren and Jongenburger Nature 1955, 175, 544

35. Blewitt, T.H. Rep. Conf. Defects in Crystalline Solids 19

36. Zahamura, T. Metal Physics 1956, 3, 112

38. Koehler, J.S. Phys. Rev. 102, 1499, 1957

39. Kimura and Maddin, R. Acta Met. Vol. 7 195 9 145

40. Koehler, J.S. Dislocations and Mechanical Properties of Crystals, 1956

41. Huntington, H.B. and Seitz, F. Phys. Rev. 61, 325, 1942

42. Bartlett, J.H. and Dienes,G.J. Phys. Rev. 89, 848, 1953

43. Silcox, J.M. and Whelan Phil. Mag. 1, 1960

44. Washburn Phil. Mag. 1, 1960

45. Levey, M. and Metzger M. Phil. Mag. 1021, 46, 1955

46. Rhines et al T.A.I.M.M.E., 1942 P.205

47 Wood, D.L. T.A.I.M.M.E. Vol. 25, 1925, 1959

48. Mott, N.P. and Nabarro, F.R.N. Proc. Phys. Soc. 52, 86, 1940

49. Mott, N.F. and Nabarro F.R.N. Phys. Soc. Report 1948 P.1.

50. Crowan, E. J.O.M. Symposium Report No. 5, 1948, P.451.

51. Geisler, A.H. Phase Transformations in Solids N.Y.1951 P.381.

52. Martin, J.W. and Smith, G.C. J.I.M. 83, 1955, 153.

53. O'Hara, S. and Gibbons, T.B. Phil. Mag. Vol 5. P. 140 1960

54. Parnasis and Mitchell, W. Phil Mag. 4, 121 1959

55. Holden, J. Acta Met. 1959

56. Harper, S. Phys. Rev. 1951, 83, 209

57. Wilson, D.V. and Russel, B. Acta Met. 8, 1960, 468

58. O'Hara, S. Ph.D. Thesis Glasgow University, 1959

59. Bartlett, J.H. and Dienes Phys. Rev. 1953, 89, 848

60. Huntingdon, H.B. Phys. Rev. 1953, 91, 1092

61. Seitz, F. Discussions of the Faraday Soc.1949, 221

62. Seiger A. and Bross, H. Z. Physic, 1950, 145, 167

63. Lomer, W.M. Progress in Metal Physics, Vol. 4.

64. Cottrell, A.H. Dislocations and the Mechanical Properties of Crystals, 1950, P. 509

65, Nicholas J.F. Phil. Mag. 1955, 46, 87

66. Burgess, H. and Smoluckowski, R. J. App. Phys. 1955, 26, 492.

67. Wachtman, J.B. and Tefft, W.E. Rev. Sc. Ins. 1958, 6, 510.